University of Southampton

Faculty of Environmental and Life Sciences

School of Biological Sciences

Manipulation of Chloroplast Development to Enhance Photosynthesis and Nutritional Value of Tomato

by

Erick Ramon Gomes Oliveira

Thesis for the degree of Doctor of Philosophy in Biological Sciences

February 2026

University of Southampton

Abstract

Faculty of Environmental and Life Sciences

School of Biological Sciences

Thesis for the degree of Doctor of Philosophy

Manipulation of Chloroplast Development to Enhance Photosynthesis and Nutritional Value of Tomato

by

Erick Ramon Gomes Oliveira

Fruit chloroplasts convert light energy into chemical energy, contributing to fruit growth, development and the overall plant carbon budget. During ripening, the transition from chloroplasts to chromoplasts is associated with chlorophyll degradation and carotenoid accumulation. This study explores a novel strategy to enhance tomato (*Solanum lycopersicum*) fruit photosynthetic pigment content, photochemical capacity and nutritional value by the genetic manipulation of chloroplast development. Transgenic tomato lines were generated overexpressing *BpMADS*, a MADS-box gene from birch (*Betula platyphylla*), under the control of fruit-specific promoters to drive expression at both green and ripening stages. Additional lines were developed with two *Arabidopsis thaliana* GATA transcription factors, *AtCGA1* and *AtGNC*, involved in chloroplast biogenesis, and a double construct simultaneously overexpressing the plastid division components *AtPDV1* and *AtPDV2*, all driven by early fruit-specific promoters. Overexpression of *BpMADS* and *AtCGA1* significantly enhanced chloroplast coverage, chlorophyll content and photochemical capacity of green tomato fruit. Similarly, overexpression of *AtGNC* led to enhanced chlorophyll and carotenoid levels in green fruit. Additionally, both early and ripening expression of *BpMADS* were associated with higher levels of lycopene and β-carotene in red ripe fruits. By contrast, simultaneous overexpression of *AtPDV1/PDV2* had a limited effect on fruit photosynthesis. Taken together, the results indicate that the manipulation of chloroplast development via transcription factors can provide a practical route to improve photosynthetic function and nutritional content in tomato fruits. This work provides new insights into the contributions of chloroplast biogenesis to fruit metabolism and could be used in other fruit crops.

Table of Contents

Table of Tables

Table of Figures

Research Thesis: Declaration of Authorship

Print name: Erick Ramon Gomes Oliveira

Title of thesis: Manipulation of Chloroplast Development to Enhance Photosynthesis and Nutritional Value of Tomato

I declare that this thesis and the work presented in it are my own and have been generated by me as the result of my own original research.

I confirm that:

1. This work was done wholly or mainly while in candidature for a research degree at this University;
2. Where any part of this thesis has previously been submitted for a degree or any other qualification at this University or any other institution, this has been clearly stated;
3. Where I have consulted the published work of others, this is always clearly attributed;
4. Where I have quoted from the work of others, the source is always given. With the exception of such quotations, this thesis is entirely my own work;
5. I have acknowledged all main sources of help;
6. Where the thesis is based on work done by myself jointly with others, I have made clear exactly what was done by others and what I have contributed myself;
7. None of this work has been published before submission
8. Signature:
9. Date:

Acknowledgements

This thesis could not have been achieved without the help and support of many people, to whom I am deeply grateful.

First, I would like to thank my supervisors, Dr Andrew Simkin and Professor Matthew Terry, for their guidance, encouragement, and patience throughout my PhD. I am also grateful to Professor Tracy Lawson for her valuable support, which has been fundamental to the development of this work.

I would like to thank all those who have supported me in my research at NIAB East Malling, the University of Southampton, and the University of Essex. At Southampton, I would especially like to thank Mark Willett for his help and advice on microscopy. At Essex, I would like to thank Will Atkinson for his friendship and Phil Davey for his support with gas exchange measurements. I am also thankful to the SoCoBio Doctoral Training Partnership for providing the funding that made this research possible.

Finally, I would like to thank my family. Most of all, I am deeply grateful to my husband, Jonny, who moved cities and changed jobs so that I could pursue this PhD. Thank you for supporting me through the stressful days, celebrating the small victories, and tolerating countless conversations about tomatoes and chloroplasts. I am especially thankful to my mum, for always supporting me through every challenge, being there whenever I needed her, and surrounding me with love. I would also like to thank my parents-in-law, Karen and Chris, for their constant encouragement and support.

I love you all.

Definitions and Abbreviations

MADS-box	MADS-box transcription factor
GATA	GATA transcription factor
CGA1	*CYTOKININ GATA FACTOR 1*
GNC	*GATA TRANSCRIPTION FACTOR 21; GATA TRANSCRIPTION FACTOR, NITROGEN-INDUCED, CARBON METABOLISM RELATED*
ATP	Adenosine triphosphate
NADPH	Nicotinamide adenine dinucleotide phosphate
RuBisCO	Ribulose-1,5-bisphosphate carboxylase oxygenase
GLU1	*GLUTAMATE SYNTHASE 1*
PDV	PLASTID DIVISION
ARC	ACCUMULATION AND REPLICATION OF CHLOROPLASTS
FtsZ	Tubulin-like proteins involved in chloroplast division in Arabidopsis
GUN4	*GENOMES UNCOUPLED 4*
HEMA1	Encodes a protein with glutamyl-tRNA reductase (GluTR) activity
PIF	*PHYTOCHROME INTERACTING FACTOR*
AHK	Arabidopsis Histidine Kinase = AHK2/3/4 are cytokinin receptors
PHY	PHYTOCHROMES
AP1	*Apetala1*
PPFD	Photosynthetic Photon Flux Density
PAR	Photosynthetic Active Radiation
ΦPSII	Effective PSII quantum yield

Definitions and Abbreviations

F_v/F_m	Maximum quantum yield of PSII
qL	Coefficient of photochemical quenching
qN	Coefficient of non-photochemical quenching
Azygous	Null segregant

Chapter 1 Literature Review

1.1 General Background

As global population growth continues to pressure existing agricultural systems, developing higher-yielding crop varieties becomes ever more critical to achieving sustainable food security (Ray et al., 2013). This challenge is particularly acute in the developing world, where global population growth is expected to be higher, and underperforming agricultural systems exacerbate food insecurity (Alexandratos & Bruinsma, 2012). While traditional breeding and agronomic approaches have successfully delivered significant benefits to crop yield, their capacity to sustainably meet long-term demands is increasingly limited, requiring new technological solutions to develop higher yielding varieties (Jaggard et al., 2010; Ort et al., 2015; Simkin, 2019). One parameter that needs improvement is the conversion efficiency of photosynthesis (εc), which represents the amount of sunlight energy converted into biomass, making it a key determinant in enhancing crop productivity (Zhu et al., 2010). Designing plants with enhanced photosynthetic performance that can withstand a range of environmental conditions requires complex manipulation of the structure of the photosynthetic apparatus (Driever et al., 2017; Lefebvre et al., 2005; Simkin et al., 2015). To effectively address this issue, a large body of research has demonstrated that the genetic manipulation of carbon assimilation, photorespiration, and electron transport can enhance productivity and yield potential in both model and crop species (Simkin et al., 2017, 2015; Driever et al., 2017). Despite the gains in biomass achieved by altering these metabolic processes, such as key enzymes involved in the Calvin-Benson-Bassham cycle (CBB) and electron transport proteins, the conversion efficiency of photosynthesis has shown minimal improvements in crops, representing a significant opportunity to enhance photosynthetic efficiency further (Long et al., 2015). Traditionally, efforts to improve photosynthetic efficiency have focused on the leaves, with little attention given to non-foliar green organs such as fruits, stems, and seed pods. However, studies have shown that functional photosynthesis occurs in these tissues, providing an alternative localised source of photoassimilates (Blanke, 1989; Hetherington et al., 1998; Simkin et al., 2020; Aschan and Pfanz, 2003).

Fruit photosynthesis has been estimated to account for up to 15% of the total carbon stored in tomatoes (Tanaka et al., 1974). This could play an important role in supporting fruit growth and development by reducing reliance on resources imported from leaves and contributing to the overall plant carbon budget (Cocaliadis et al., 2014; Tanaka et al., 1974). Interestingly, in many fruit species, such as tomatoes, the process of photosynthesis is coupled with the differentiation of chloroplasts into chromoplasts during ripening, resulting in the accumulation of large amounts of carotenoids that affect the fruit's colour, flavour, and nutritional value (Simkin et al., 2020; Lytovchenko et al., 2011). Therefore, the genetic manipulation of fruit chloroplasts offers a novel strategy to simultaneously enhance photosynthetic efficiency during early fruit development and improve key quality traits, such as nutritional value, flavour, and colour in these organs.

Crop plants' ability to fix carbon is achieved through chloroplasts, essential organelles that convert sunlight into biochemical energy for plant growth and reproduction (Pyke, 2007). Recent studies have shown that the manipulation of chloroplast development and density can improve photosynthetic carbon fixation and pigment content (Dutta et al., 2017). The over-expression of a MADS-box gene from *Betula platyphylla* (*BpMADS*) in transgenic tobacco (*Nicotiana tabacum*) was shown to enhance chloroplast growth and division rates, resulting in increased numbers of chloroplasts, higher photosynthetic pigment content, and higher rates of photosynthesis by 2-fold in leaves (Qu et al., 2013). Similarly, transgenic tomato lines with increased plastid numbers in their fruits have the potential to accumulate up to 30% more carotenoids (Galpaz et al., 2008). These experiments suggest that manipulating chloroplast/plastid density could be a promising strategy for producing plants with higher pigment content and improved photosynthetic performance (Galpaz et al., 2008; Qu et al., 2013). Nevertheless, the extent to which increased plastid density in fruit tissues translates into improvements in whole-plant yield remains to be determined.

This project aims to manipulate different aspects of chloroplast development to produce tomato plants with higher pigment content, improved photosynthetic performance, and enhanced nutritional quality. By targeting fruit photosynthesis, this research aims to provide a novel approach to addressing the challenge of global food security while meeting the growing demand for higher-yielding and nutritionally enriched crop varieties.

1.2 Breaking Barriers to Global Food Security

1.2.1 Growing Populations, Growing Pressures

Global population growth poses a significant threat to achieving food security in the coming decades, pressuring existing agricultural systems to increase the yields of the most common crops (Ray et al., 2013). According to FAO (Food and Agriculture Organization of the United Nations), the world population is likely to reach 10 billion by 2050 (United Nations, 2019). Therefore, an increase of about 70% of available food for human consumption will be required to feed the world sustainably (Cole et al., 2018). However, in many regions of the world, the increase in the production of major crops has slowed significantly. This decline is caused by factors such as climate change, loss of soil fertility, and crops reaching their genetic yield potential, making current global yield rates insufficient to meet the growing demand for food (Ramankutty et al., 2018; Ray et al., 2013; Schauberger et al., 2018). Increasing yields is further complicated by the fact that most countries where population growth rates are expected to be higher have low incomes and already suffer from underperforming agricultural systems, along with limited access or capacity to import from other countries (Alexandratos & Bruinsma, 2012). Many of these countries also lack investment in technology to solve this problem. Although there is strong evidence that investing in new agricultural technologies could alleviate the rising global hunger, low-income countries spend only around 0.52% of their agricultural GDP on research and development, compared to over 3% in high-income countries (Tilman et al., 2002; Fuglie et al., 2019; Molotoks et al., 2021). Projections indicate that a 2.5-fold increase in global GDP could occur by 2050, likely driving a rise in per capita consumption, especially in developing countries (Alexandratos & Bruinsma, 2012). Moreover, the shift in diets expected to be observed in some of these countries towards more western-type livestock-based diets may contribute to the increase in agricultural demand, as they require large amounts of primary agricultural products (Alexandratos & Bruinsma, 2012). Finally, the allocation of crops to non-food uses, such as biofuels, also may contribute to the increase of agricultural aggregate demand and affect the amount of food available for human consumption (Alexandratos and Bruinsma, 2012; Long et al., 2015).

Significant global increases in crop yields were achieved in the last 50 years, keeping pace with rising global requirements. Between 1960 and 2010, global yields increased by 63% for cassava and 171% for wheat, while rice showed yield increases of about 36% between 1970 and 1980

(Long, 2014; Long et al., 2015; Long & Ort, 2010). However, improved technology will be essential to increase food production enough to meet the world's demand in the following decades (Jaggard et al., 2010; Long et al., 2015). In addition to crop yields, it is imperative to focus on increasing nutritional quality as most advances in production in the last decades were achieved in calorie-dense crops, providing a short-term solution to the problem of hunger. However, yields of micronutrient-dense crops have not improved even though globally, over 2 billion people suffer from undernourishment (FAO, 2021; Simkin, 2019). Traditionally, less attention has been given to non-staple crops such as fruit and vegetables, ultimately reducing their availability, which, coupled with rising demands, affects these products' prices and contributes to hidden hunger (Johns and Eyzaguirre, 2007; Sharma et al., 2017).

Biofortification is the process of enhancing a plant's natural ability to produce essential nutrients through traditional breeding or modern biotechnology. It has the potential to increase the bioavailability of key micronutrients in crops. Biofortification, therefore, offers a sustainable strategy to improve human nutrition and combat undernutrition (Mayer et al., 2008; Bouis et al., 2011; Johns and Eyzaguirre, 2007). Economic gains are also associated with nutritionally improved crops, as they can be grown at no additional cost to farmers. Estimates suggest that a saving of up to $17 could be achieved for every dollar initially invested in developing biofortified crops. As a result, biofortification represents a more cost-effective alternative for supplementing micronutrients to large populations compared to current methods, such as adding them to food after processing, which requires continual funding support (Simkin, 2019; Bouis and Saltzman, 2017). Genetic engineering and biofortification have already shown promising results in enhancing the nutrient content of crops such as fruits and vegetables. Studies manipulating the expression levels of genes for provitamin A (Fraser et al., 2002; Römer et al., 2000), folate (Díaz De La Garza et al., 2004; De La Garza et al., 2007) and vitamin C metabolism (C. Zhang et al., 2011), have led to an increase in these micronutrients. Combining these manipulations could result in a multivitamin corn with positive effects on human health (Naqvi et al., 2009). Biofortified crops particularly benefit remote communities with limited access to diverse diets (Simkin, 2019). The integration between synthetic biology into crop improvement strategies enables precise modifications. These advancements have made genetic engineering a viable solution to addressing food security challenges while aligning with broader sustainability goals (Long et al., 2015; Zhu et al., 2010).

1.2.2 Climate Change

Climate change represents a major obstacle to increasing crop yields, with an expected mean global temperature rise of 2°C by 2050. These changes will be accompanied by an expected increase in atmospheric CO_2 levels, which are projected to rise from 426 ppm to 550 ppm by 2050 (Field & Barros, 2014; Jaggard et al., 2010). Although several reports have shown that elevated atmospheric CO_2 has the potential to increase photosynthesis and biomass in a wide range of plant species, including fruiting crops such as tomatoes and peppers, this potential benefit will be hindered by the increased frequency and severity of droughts and heatwaves (Ainsworth & Long, 2005, 2021; Gray et al., 2016). These climatic changes are anticipated to affect many physical and biological systems, including water uptake, nutrient assimilation, and reproductive development, which can negatively impact crop growth and productivity (Jaggard et al., 2010; Intergovernmental Panel on Climate Change (IPCC), 2022). Elevated atmospheric CO_2 levels may also lead to increased carbon but decreased nitrogen concentrations within the leaf, particularly in C_3 crops (Taub & Wang, 2008; Walsh et al., 2024).

Evidence from Free Air CO_2 Enrichment (FACE) research, a technique used as a proxy to explore how field-grown plants respond to growth in atmospheric CO_2, has shown that carbon assimilation increases total fruit yield and biomass (Poorter et al., 2016). Increased CO_2 enhances the substrate for RuBisCO, the enzyme responsible for carbon fixation during photosynthesis, improving carbon fixation and reducing losses to photorespiration, which occurs when RuBisCO fixes O_2 instead of CO_2 (Gannon et al., 2014; Parry et al., 2013). In addition, a higher concentration of CO_2 could allow plants to use water more efficiently. The stomata, small pores on the surface of the leaves that control evapotranspiration, are able to partially close at high CO_2 concentrations, reducing water loss whilst still allowing CO_2 uptake (Iizumi et al., 2018). Enhanced photosynthesis in carbon-rich environments has been previously observed in tomatoes, sweet peppers, and chilli peppers, contributing to increased yields. For instance, in carbon-enriched greenhouses, tomatoes' fruit yield increased by 30% (Islam et al., 1996), 38% (F. Li et al., 2007) and 83.61% (Khan et al., 2013), with CO_2 ranging from 450 ppm to 1200 ppm. In sweet and chilli pepper, yield increases of 12.9% - 370.2% and 43.8% - 142% were observed, respectively (Garruña-Hernández et al., 2013; Milhet and Costes, 1975).

The increase in photosynthesis and crop yield observed in FACE studies raised hopes that rising atmospheric CO_2 levels could counteract yield losses due to climate change. However, crop yields are heavily impacted by several components of the Earth's changing climate, such as rising

temperatures, changing precipitation, and extreme weather events, including floods and droughts (Yang et al., 2024; Gray et al., 2016). The negative impacts of climate change on yields have been well documented by several studies. The 6th assessment report from the Intergovernmental Panel on Climate Change (IPCC) highlighted that the effects of global climate change typically led to yield reductions in many regions worldwide over the last decades (Intergovernmental Panel on Climate Change (IPCC), 2022). Recent studies also indicate that the advantages of elevated CO_2 are eliminated with the intensification of heatwaves and drought conditions (Doddrell et al., 2023; Gray et al., 2016). Higher temperatures, for instance, are associated with an increased rate of evapotranspiration, which neutralises the benefits of elevated CO_2 to water use, causing decreases in yield (Jaggard, Qi and Ober, 2010). Altered rainfall patterns can also cause yields to decrease. Between 1983 and 2009, approximately 75% of global agricultural areas suffered yield losses caused by drought events (Kim et al., 2019; Yang et al., 2024). These negative impacts of climate change on agriculture are further demonstrated by research combining the effects of elevated atmospheric CO_2, rising temperatures, and drought on the yield of key staple crops. For instance, studies have shown that higher levels of atmospheric CO_2, along with increasing temperatures and drought, correlate with decreased productivity in major crops like maize and soybean, which have seen net reductions of 4.1% and 4.5%, respectively (Iizumi et al., 2018). This is further supported by studies on C_3 crops exposed to elevated CO_2 levels, along with heat and drought stresses, which resulted in significant decreases in grain yield. The results indicated that drought reduced cereal grain yield by 70%, while elevated temperatures led to a reduction of approximately 24.85% (Mariem et al., 2021). Moreover, climate variations could lead to increases in pests and disease outbreaks, which could challenge not only increasing crop yields but also existing pest control strategies (Munaweera et al., 2022).

As the global population continues to grow, the interaction of increased CO_2 levels, climate fluctuations, and agricultural production represents a significant threat to food security, which is particularly alarming in areas that are already vulnerable to agricultural failures and environmental stresses (Jaggard et al., 2010; Mirzabaev et al., 2023; Mariem et al., 2021). The expected increases in atmospheric CO_2 cannot be considered the only alternative to counteract the negative impact of climate change. Exploring new advancements in biotechnological alternatives, such as genetic engineering and genome editing, are some of the tools with the potential to enhance current agricultural practices, allowing us to reduce the environmental

impacts of agriculture and tackle the future challenges of sustainable food security (S. B. Gray et al., 2016; Yang et al., 2024).

1.2.3 Land Availability for Crop Cultivation

The global trend of urbanisation is a dominant force affecting the amount of land available for agriculture. Rapid urbanisation and population growth are frequently linked to the rise of overcrowded cities and the demand for industrial and infrastructure development, such as water management and transportation systems, which puts pressure on natural resources (Mccarl et al., 2022). Since the 1980s, the Global South (comprising Africa, Latin America, and Asia, excluding high-income countries in East Asia) has experienced significant growth in agriculture, fuelled by a rising population, changes in food demand, and technological advancements. In 2020, it was estimated that the Global South accounted for 73% of global agricultural production (Fuglie et al., 2024). This growth has raised concerns, as it has been estimated that 80% of new croplands resulted from deforestation (Foley et al., 2011). In addition, many countries in these tropical regions have also primarily relied on ongoing agricultural intensification to increase productivity, as historically, their yields have been lower compared to those in temperate regions (Foley et al., 2011).

Agricultural intensification, associated with increased use of irrigation, fertilizers and mechanization, has significantly contributed to the depletion of critical ecosystem services (Foley et al., 2011). Agriculture is estimated to be responsible for over a fifth (22%) of global greenhouse gas emissions (Burney et al., 2010). Agricultural production accounts for 64% of global freshwater withdrawals (Döll et al., 2014). In addition, agriculture has significantly impacted soil fertility, with around 15% of the world's soil being degraded by agricultural activity by the 1990s (Ramankutty et al., 2018). The integration between agriculture and the energy market and the diversification of diets in the developing world has shifted agricultural products away from food uses. By 2050, it is expected that 56% of global feed use of coarse grains will be to supply the demand for animal feed. The growing use of crops in biofuel production also represents a potentially disruptive force in the future, increasing price vulnerability and intensifying competition for arable land (Alexandratos & Bruinsma, 2012). Agriculture is undoubtedly a major consumer of arable land, and although there is potential to explore new areas for crop production, clearing forests or other natural ecosystems into new agricultural areas would represent extensive deforestation and biodiversity loss. Furthermore, the best land

suited for farming has already been cropped, and newly available areas are of poor quality and marginally suitable for crop production, requiring extensive external inputs (Smil, 2001).

As a driving force behind environmental threats, reducing agriculture's environmental footprint is imperative. Although reducing the area available for croplands could help minimise the environmental impacts caused by agriculture in the coming decades, a truly effective solution requires an integrated strategy combining new biotechnological tools with conservation efforts (Leclère et al., 2020). A potential solution to address this problem would be to focus on the resilience and efficiency of food systems in order to maximise agriculture's yield, developmental performance, and environmental sustainability. Investments in crop genetics provide a pathway to overcome this challenge through the introduction of novel foreign genes that have the potential to enhance crop productivity. These advancements could improve agricultural efficiency while minimising the impact on natural ecosystems (Foley et al., 2011; Jaggard et al., 2010).

1.3 Tomato Is One of the Most Valuable Crops in the World

Originally from western South America, the tomato (*Solanum lycopersicum*) was first introduced to Europe in the 16th century. The vast diversity of habitats in the Andes, such as desert areas and the sea level pacific coast, might explain wild tomatoes' large genetic, morphological, and physiological diversity (Bergougnoux, 2014). However, the genetic diversity of modern cultivated tomato is much smaller than its wild relatives (Bai & Lindhout, 2007; Bergougnoux, 2014). This narrow diversity has been attributed, in part, to the selection of preferred genotypes for the tomato industry, which has resulted in predominantly in breeding species (Bai & Lindhout, 2007).

The tomato is extensively consumed worldwide. It is one of the world's major fresh and processed fruits, estimated at circa 192 million tons of fruits produced on over 5 million ha every year (FAO, 2023). The tomato is an economically attractive crop due to its relatively short duration and high yield. The global production of tomatoes has enormously increased in the last decades, and that trend looks set to continue, given the investments made in the processing sector and research programmes (Costa & Heuvelink, 2018). Apart from the organoleptic qualities that make the tomato an attractive crop, such as colour and flavour, tomatoes contain many health-promoting compounds as they are a source of vitamins, minerals, and antioxidants (Costa and Heuvelink, 2018). Tomatoes are the primary dietary source of lycopene, a natural antioxidant associated with reduced heart attack rates, certain types of cancer and some age-related diseases (Nasir et al.,

2015). Tomato also contains significant amounts of β-carotene, which functions as a precursor to the formation of vitamin A (Nasir et al., 2015; Davuluri et al., 2005).

Tomatoes are widely available and broadly accepted, which, coupled with their high cost-effectiveness, have made them an important research tool in horticulture (Nasir et al., 2015). The tomato is also considered the most important plant for studying fleshy fruit ripening and, among many varieties, the miniature cv. Micro-Tom has been established as a model system in tomato research, compared to Arabidopsis (*Arabidopsis thaliana*) (Shikata & Ezura, 2016). The entire tomato genome has been sequenced, marking a major milestone for the study of the complex and highly coordinated process of maturation in fleshy fruits (The Tomato Genome Consortium, 2012). The tomato was also one of the first crops to be successfully transformed via *Agrobacterium tumefaciens* (Smith and Townsend, 1907), thus being a powerful genomic resource and providing bases to understand the links between photosynthesis, yield, and the quality of the fruit (Klee & Giovannoni, 2011; Quinet et al., 2019).

In addition to being a valuable plant for genetic engineering, the tomato was in many countries the first transgenic food crop approved for commercialisation, with several nations worldwide currently reviewing and modifying their legal frameworks and biosafety protocols to accommodate the use of GM technology (Conner, 1997; Verma, 2022). It is estimated that around 74% of the world's tomato production is located in Africa and Asia, making an important dietary contribution to their population (FAO, 2023). These continents, which are the ones most commonly suffering from agricultural failures and extreme weather events, are also predicted to experience intense population growth in the next decades (Alexandratos & Bruinsma, 2012).

Ensuring sustainable tomato production has become increasingly crucial to guarantee the vital dietary contribution that tomatoes can offer to the world's growing population. Traditionally, the challenges in harmonizing quality traits with the interests of the tomato business have made commercial growers opt to favour yield over flavour. Engineering tomato fruits represents, therefore, an opportunity in tomato research, with the enhancement of fruit plastids rising as a potential avenue to improve both flavour and nutrition (Klee and Resende, 2020; Cocaliadis et al., 2014).

1.4 The Components of Photosynthesis

Plants can efficiently exploit sunlight as an energy source to support their growth and development. Photosynthesis is the primary process used by plants to transform sunlight energy into the biochemical energy that is used to synthesise a usable form of carbon (sugar) from carbon dioxide and water, which is subsequently used in all cell activities (J. R. Evans, 2013; Sudhakar & Mamat, 2019). Photosynthesis consists of two main processes. The first involves light-dependent reactions in light-harvesting pigment-protein complexes (LHCs) embedded in the thylakoid membranes of chloroplasts. The second is the conversion of atmospheric CO_2 into biomass via the Calvin-Benson-Bassham Cycle (CBB) in the chloroplast stroma (Bassham & Calvin, 1960; Nelson & Yocum, 2006; Taiz et al., 2015). The light-harvesting complexes of the photosystems initially absorb sunlight, and its energy is transferred to a chlorophyll molecule in the reaction centre, where it excites electrons to a high energy level. These excited electrons travel through a series of electron carriers in the electron transport chain, creating a proton gradient that allows the generation of chemical energy (ATP) and reducing power (NADPH) with O_2 released as a byproduct (Mirkovic et al., 2017; Nelson and Yocum, 2006). In the Calvin-Benson-Bassham Cycle (CBB), atmospheric CO_2 is fixed by ribulose-1,5-bisphosphate carboxylase/oxygenase (RuBisCO) to produce carbon intermediates that can be utilised to generate biomass. This process is driven by ATP and NADPH from the light reactions. The fixed carbon takes the form of triose phosphates, glyceraldehyde-3-phosphate (G3P) and dihydroxyacetone phosphate (DHAP), which are converted to starch in the chloroplast or exported to other parts of the plant as sucrose, which is then used to sustain growth and development (Bassham & Calvin, 1960; Taiz et al., 2015).

Photosynthesis is highly sensitive to changes in environmental conditions. A balance is required between absorbing light and using the biochemical energy in metabolic pathways. Many factors tightly regulate the efficiency of photosystems, including light availability, atmospheric CO_2, and nutrient uptake. Light intensity, for instance, is one of the most dynamic components affecting photosystems (Murchie & Ruban, 2020). Reduced availability of photosynthetically active radiation (PAR) reduces the quantity of light absorbed, thereby reducing electron transfer and ATP/NADPH production. When light intensity increases after a phase of darkness or prolonged low light, the photosynthetic rate gradually increases in a process known as the induction of photosynthesis, during which the enzymatic reactions related to light harvesting and electron transport become activated (Yamori, 2016). Electron transport rates in the photosystems

respond to fluctuations in irradiance, which requires regulatory mechanisms to prevent over-reduction or over-oxidation of key steps. A pivotal process during this transition is the dissipation of excess energy as heat, a process known as non-photochemical quenching (NPQ), ensuring photochemistry while maintaining the photosystem's integrity (Murchie & Ruban, 2020). Moreover, one key protective mechanism of the photosynthetic membrane is its ability to self-repair, allowing it to cope with damage caused by high light intensities and environmental fluctuations (Albertsson, 2001). Photosynthetic organisms have evolved to regulate the repair of damaged PSII, in which the reaction centre protein D1 is a primary target of photooxidative damage. The sensitivity of the D1 protein to photodamage has been suggested to enhance PSII functionality, as it is easier to focus on repairing one protein rather than the many subunits of PSII (Kato et al., 2012; Kirchhoff, 2019).

The rate of carbon assimilation in foliar photosynthesis is directly impacted by CO_2 concentrations. Under conditions of low internal atmospheric CO_2, RuBisCO becomes the rate-limiting factor due to reduced substrate availability and its affinity to oxygen, leading to the competitive photorespiration reaction, which reduces photosynthetic efficiency. However, under high atmospheric CO_2, the rate of regeneration of the carbon acceptor molecule ribulose-1,5-bisphosphate (RuBP) becomes the rate-limiting step in the Calvin-Benson-Bassham cycle (CBB) (Yamori et al., 2010). Nitrogen uptake is also directly linked to photosynthetic activity and the overall carbon status of the plant. Most of the nitrogen absorbed by leaves is allocated to chloroplasts to enhance photosynthesis (Bassham & Calvin, 1960; Y. Li et al., 2013; Poorter & Evans, 1998). An increased nitrogen supply, therefore, increases the number of photosynthesis-related proteins and, subsequently, sugar production, promoting plant growth and development (Hudson et al., 2011). In summary, the photosynthetic membrane is responsible for generating the currency molecule ATP and the reductive force NADPH for carbon fixation and has been described as the most abundant biological membrane on earth, housing RuBisCO, the most abundant protein (Albertsson, 2001; Sauer, 1978).

1.5 Genetic Approaches to Increase Photosynthetic Efficiency

The potential yield of a crop is described as that achieved under ideal conditions, in the absence of biotic and abiotic stresses (Evans & Fisher, 1999). This maximum yield is determined by the incident solar radiation over a crop, the efficiency of light capture, the efficiency of conversion of

the intercepted light, and the harvest index (Long et al., 2006). More specifically, the yield equation is described as follows:

$Pn = St \cdot \varepsilon i \cdot \varepsilon c / k$

$Yp = \eta \cdot Pn$

where Yp defines the yield potential in function of η (harvest index) and Pn (primary production of biomass); St defines the annual incident solar radiation over a crop; εi defines the efficiency of light interception by the crop; εc defines the efficiency of conversion of intercepted light into biomass; K defines the energy content of the harvestable biomass (Long et al., 2006).

Increases in agricultural production in the last decades have been achieved mainly by advances in agricultural practices and the improved breeding of new varieties (Zhu et al., 2010). The large scope of factors contributing to enhanced light interception (εi) and harvest index (η), which include the selection of genotypes with increased leaf area or with a greater partition of biomass into the harvested product, has allowed traditional breeding to deliver considerable benefits to crop yield. On the other hand, the mechanism of photosynthesis is overall very conserved among different groups of plants (Long et al., 2015). As a result, the conversion efficiency (εc) is the one parameter that has shown minimal improvements in crops (Zhu et al., 2010). Whilst the harvest index almost doubled over the last 50 years and light interception, similarly, reached 0.8-0.9 for modern crop genotypes, levels close to their biological limits with slight potential for further increases, the conversion efficiency remained at only about 0.02, which represents around 20% of the theoretical maximum for C_3 crops (Long et al., 2015). The advance in the knowledge of photosynthesis, with the characterisation of critical genes involved in the process, coupled with the advent of synthetic biology, has made improving photosynthetic efficiency a suitable target for achieving higher yields whilst protecting diverse environments and maintaining food resources for the 21st century (Long et al., 2015; Zhu et al., 2010).

Evidence from elevated CO_2 research has shown that increases in carbon assimilation result in total fruit yield and biomass increase in horticultural crops, providing a direct correlation between photosynthesis and yield (Wohlfahrt et al., 2018). Photosynthetic energy transduction is, however, affected by many losses. To start, the leaves of healthy crops can only absorb specific wavelengths of visible light, which account for approximately 90% of the photosynthetically active radiation (400-700 nm). Furthermore, photochemical inefficiency limits the available energy to synthesise carbohydrates (Sudhakar & Mamat, 2019). As a result, the maximum

theoretical efficiency of photosynthesis is reduced to approximately 5% in C_3 crops, with the rest being lost due to respiration, reflection, and thermodynamic limitations (Zhu et al., 2010). Photosynthesis at low levels (< 100 μmol m^{-2} s^{-1}) and under optimum conditions has been shown to operate close to the theoretical efficiency, as 80% of the energy absorbed can be utilised (Long et al., 1994). As the light intensity increases, plants become light-saturated, and the efficiency of radiance use decreases. At half of full sunlight (approximately 1000 μmol m^{-2} s^{-1}) only around 25% of the absorbed quanta are used, and at full sunlight, this value drops to approximately 10%, resulting in energy waste and photodamage (Long et al., 1994).

A significant body of research has been presented with opportunities to tackle this problem effectively by increasing maximum εc in crop plants. The over-expression of target genes associated with light harvesting and the CBB cycle provides further evidence supporting the primary role of photosynthesis in increasing yields (Simkin, 2019; Simkin et al., 2019). Recent work with tobacco overexpressing the CBB cycle enzyme SBPase developed transgenic plants with increased CO_2 assimilation rates and biomass yield (Lefebvre et al., 2005; Simkin et al., 2015). Similarly, the modulation of the expression of key enzymes within the electron transport rate has shown positive effects on biomass and yield in transgenic Arabidopsis (Chida et al., 2007; Simkin et al., 2017), tobacco (Heyno et al., 2022) and sorghum (Ermakova et al., 2023).

Re-engineering the photosystems to optimise the use of light is another alternative with the potential to raise the maximum efficiency of photosynthesis. Reducing the antenna size by optimising the balance between pigment concentration would reduce the overexcitation of chlorophyll molecules and the potential for photodamage, as well as allow a greater light distribution into lower layers of the crop canopy (Zhu, Long and Ort, 2010). Therefore, a fine-tuned antenna size has been identified as a strategy to improve light capture and assimilation. Downregulation of a gene responsible for Chl *a* to Chl *b* conversion (chlorophyllide *a* oxygenase (CAO)) developed transgenic *Camelina* plants with a moderate reduction in antenna size, which could, in turn, enhance high light use efficiency, avoiding photodamage and improving biomass production in plants by 40% (Friedland et al., 2019; Simkin et al., 2022). The potential for partially reducing chl *b* levels has also been described in the green alga *Chlamydomonas reinhardtii*, where it led to a two-fold increase in photosynthetic rates at high light intensities (Perrine et al., 2012).

Photosynthesis in C_3 crop plants is also largely limited by the maximum RuBisCO activity and the capacity for regeneration of the acceptor molecule of CO_2, ribulose biphosphate (RuBP). It has

been suggested that the theoretical εc may be increased by improving the maximum capacity for regeneration of RuBP and higher rates of carboxylation of RuBP. Kinetic models show that higher rates of carboxylation catalysis can bring εc closer to the theoretical maximum of 0.02 (Long, Humphries and Falkowski, 1994). Moreover, increasing the specificity of RuBisCO for CO_2 relative to O_2 could potentially decrease photorespiration due to RuBP oxygenation, although a higher specificity to CO_2 is associated with lower catalytic rates of carboxylation. Increasing specificity at the expense of catalytic rates is not intuitive, as it also depends on the CO_2 uptake by the crop canopy. Higher CO_2 specificity could benefit light-limited photosynthesis, but the decrease in the rates of carboxylation would imply a detrimental effect on light-saturated photosynthesis, revealing that a fine balance between specificity and catalytic rates is necessary to ensure optimum RuBisCO performance (Long et al., 2004). Efforts to improve photosynthesis would be more effective if combined with strategies that also focus on enhancing carbon availability around RuBisCO. A promising strategy is redesigning C_3 crops with C_4 carbon concentrating mechanisms (CCMs), which have also been the focus of many research projects around the world, including the C_4 Rice Project (Ermakova et al., 2020; Hernández-Verdeja & Lundgren, 2024). Moreover, recent work by Hanson et al. (2016) suggested that improving the concentration of CO_2 near the RuBisCO site could be achieved by engineering faster forms of RuBisCO enzymes, such as Cyanobacterial RuBisCO. Although considered highly challenging, this approach could provide an avenue to improved carboxylation rates in C_3 plants (Hanson et al., 2016).

When plants are exposed to high levels of light, the additional energy exceeds the capacity of the photosystems to operate and can lead to the production of oxygen radicals that are harmful to the photosynthetic apparatus (Simkin et al., 2022; Takahashi and Badger, 2011). Therefore, when the absorption of light is higher than the photosynthetic capacity, the xanthophyll cycle is activated with the conversion of violaxanthin to zeaxanthin and of lutein epoxide to lutein, which dissipates the excess energy as heat via NPQ (Eberhard et al., 2008; Zhu et al., 2010). Although this thermal dissipation mechanism protects the photosystems against photooxidative damage in high light, it limits photosynthesis under low light conditions. The delay in the photoprotection recovery can account for up to a 17% decrease in photosynthesis at 30 °C and 32% at 10 °C. Therefore, significant gains in εc can be achieved by decreasing this lag in photoprotection relaxation (Long et al., 2006). Work developed with rice has shown a direct correlation between a rapid recovery from the photoprotective state and biomass. This further suggests that engineering photosynthesis to speed up NPQ activation and recovery is a feasible approach to reducing losses in εc (Wang et al., 2002; Long et al., 2006).

Genetic engineering to improve photosynthesis has been at the cutting edge of agricultural science in recent years, as traditional agronomical approaches have delivered very small improvements to conversion efficiency. Single and multigene manipulation of photosynthetic processes can provide an important avenue to increase both yield and nutrient content, with the potential to produce targeted changes without pleiotropic effects, making photosynthesis a suitable target to tackle the increasing demands for food whilst addressing the challenge of the "hidden hunger" in at-risk populations (Long et al., 2006; Simkin et al., 2019).

1.6 The Mechanisms of Chloroplast Development

Plastids are cellular organelles derived from proplastids, progenitor plastids found in meristem cells (Pyke, 2007). The origin of plastids in plant cells is attributed to an endosymbiotic event in which a photosynthetic prokaryotic organism, such as a *Cyanobacterium*, was engulfed by an ancestral eukaryotic cell (Gray, 1989). Plastids are essential to many plants' biological processes as they harbour numerous functions. As they divide, they differentiate into specialized cells for photosynthesis (chloroplasts) found in all green tissues, pigment accumulation (chromoplasts) present in flowers and fruits, starch storage (amyloplasts), which accumulate in seeds, roots, and tubers and, finally, lipid storage (elaioplasts) (K. Pyke, 2007). Plastids also have the ability to interconvert into different forms in response to environmental cues, hormonal signalling and cellular developmental processes (Figure 1.1) (Lopez-Juez & Pyke, 2005; Pyke, 2007).

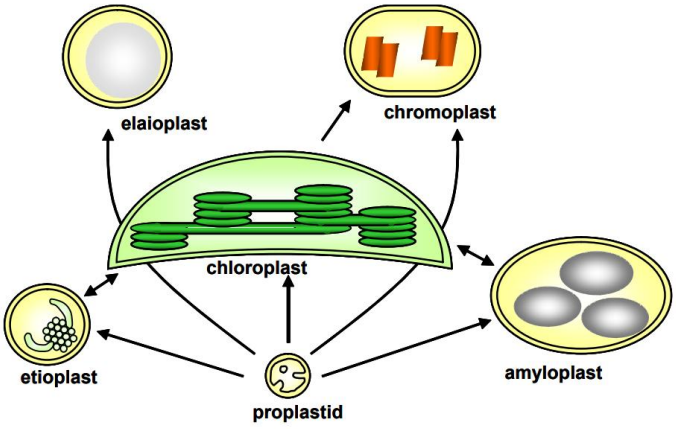

Figure 1.1. A general model for plastid interconversion. In the centre is the representation of a chloroplast, the most prominent form of plastid. Although various routes for plastid interconversion are

possible, the most extensively studied is the differentiation of chloroplasts into chromoplasts. Reproduced from Jarvis & López-Juez (2013).

Among plastids, chloroplasts are remarkable for hosting the photosynthetic apparatus, enabling photosynthetic carbon fixation (de Boer and Weisbeek, 1991). They measure around 5 to 10µm in diameter, and the presence of a protein-pigment transmembrane allows photosynthetic light capture (de Boer & Weisbeek, 1991). Besides photosynthesis, chloroplasts also perform other processes associated with plant metabolism, such as the synthesis of amino acids, lipids, and several phytohormones (Cackett et al., 2022). They are central in plastid-based research as the focus of studies and provide crucial knowledge in plastid biology (Pyke, 2007).

Chloroplasts harbour their own genome, comprised of around 120 to 130 genes encoding 80 proteins. However, most chloroplast proteins are nuclear-encoded, translated in the cytoplasm and transported to the organelle (Jarvis & López-Juez, 2013). Like all plastids, chloroplasts are bounded by a double membrane, which functions as a permeability barrier, isolating the plastid stroma from the cytosol. The envelope membranes contain specific transport complexes that control the import and export of metabolites and integrate the plastid metabolism within the cell. The plastid envelope membranes are also essential in the interaction between the organelle and nucleus, coordinating nuclear gene expression of chloroplast target proteins and ensuring chloroplast biogenesis and homeostasis (Block et al., 2007). A major structural component of chloroplasts is the internal membrane of thylakoid discs, functional units where the photosystems (PSI and PSII) are located (Sakamoto et al., 2008).

The thylakoid discs are fused as stacks resembling fan blades, a structure named grana, connected by stromal lamellae, non-stacked regions. This complex morphology provides a larger surface area, enabling higher light capture and electron transport in the chloroplasts (K. Pyke, 2007). The Photosystem I (PSI) and Photosystem II (PSII), embedded in the photosynthetic thylakoid membrane, consist of protein-pigment complex that includes the reaction centre and the antenna system, which is the light-harvesting complex I (LHCI) for PSI and light-harvesting complex II (LHCII) for PSII (Dekker and Boekema, 2005; Albertsson, 2001; Gao et al., 2018). At the centre of the light-harvesting complexes lie photosynthetic pigments, primarily chlorophylls and carotenoids, which are responsible for light-harvesting and energy transfer to the reaction centre, where a special pair of chlorophylls excites electrons to a high-energy state level (Mirkovic et al., 2017; Sakamoto et al., 2008; Krause and Weis, 1991). These excited electrons travel through a series of electron carriers in the electron transport chain, generating a proton gradient that drives

the production of ATP and NADPH (Mirkovic et al., 2017; Sakamoto et al., 2008). It has been suggested that approximately 10% more chlorophyll is associated with PSI than with PSII, consistent with previous studies showing that PSI absorbs about 20% more photons than PSII (Nelson & Yocum, 2006). Another study suggests that the excess chlorophyll in PSI compared to PSII ranges between 14-20%, enabling it to absorb approximately 40% more quanta than PSII (Albertsson, 2001). The light-independent reaction of photosynthesis, CBB, is located in the stroma, where ATP and NADPH produced in the light reactions are used to reduce CO_2 to carbohydrates (Raines, 2003; Gurrieri et al., 2021; Sharkey, 2019).

In addition, their crucial role in the biosynthesis of many essential molecules for the viability of plants makes the control of the expression of nuclear and chloroplast genes a critical process to maintain chloroplast integrity and adjust its function at optimal levels in response to metabolic and environmental conditions (Cackett et al., 2022; Mielecki et al., 2020). Many metabolic pathways have been described as possible sources for retrograde signals, including chloroplast gene expression, tetrapyrrole signalling, chloroplast redox status and reactive oxygen species (ROS) (Chi et al., 2015; Chan et al., 2016; Gurrieri et al., 2021; Cackett et al., 2022; Jarvis and López-Juez, 2013). Moreover, chloroplast signalling regulates numerous developmental, biogenic, and operational processes in plants, such as nuclear alternative splicing (Petrillo et al., 2014), flowering (Feng et al., 2016) and heat stress responses (Sun & Guo, 2016). Regardless of the source of the signal, communication between the chloroplast and nucleus is crucial for chloroplast biogenesis and homeostasis, with perturbations to these signals causing metabolic imbalances that can affect the plant's development, growth and stress responses (Mielecki et al., 2020; Cackett et al., 2022).

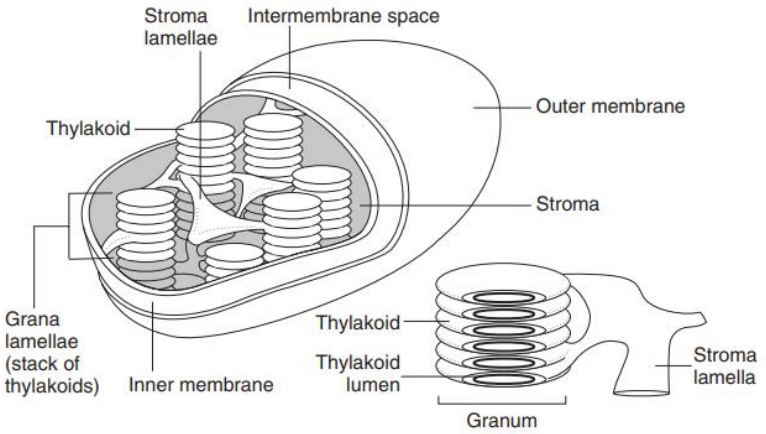

Figure 1.2. A schematic drawing of a chloroplast. Chloroplast structure showing stacked thylakoid discs (grana), stromal lamellae (unstacked regions), and the inner and outer chloroplast membranes. Reproduced from Blankenship (2008).

The thylakoid discs are fused as stacks resembling fan blades, a structure named grana, connected by stromal lamellae, non-stacked regions. This complex morphology provides a larger surface area, enabling higher light capture and electron transport in the chloroplasts (Pyke, 2007). The Photosystem I (PSI) and Photosystem II (PSII), embedded in the photosynthetic thylakoid membrane, consist of protein-pigment complex that includes the reaction centre and the antenna system, which is the light-harvesting complex I (LHCI) for PSI and light-harvesting complex II (LHCII) for PSII.

Chlorophylls and carotenoid pigments embedded in the thylakoid membrane of chloroplasts are essential for the functioning of the photosynthetic apparatus. They contain a cyclic tetrapyrrole ring linked to a central atom of magnesium in a structure that resembles haemoglobin. The main difference is that chlorophyll contains a chlorin ring with magnesium instead of an iron-centred porphyrin ring, like heme. This structure allows efficient photon capturing, water oxidation and electron mediation (Senge et al., 2014). The chlorophyll biosynthetic pathway consists of at least 17 steps, with the first 6 diverting general metabolic precursors into the production of the first cyclic tetrapyrrole, protoporphyrin IX, shared with the biosynthesis of other tetrapyrroles. The latter stages are chlorophyll-specific and involve magnesium insertion and the formation of the characteristic chlorin ring structure, enabling chlorophyll to efficiently capture light at specific wavelengths (Beale, 1999).

The chlorophyll family harvests light energy in the photosynthetic reaction centre, which is then conserved in ATP and NADPH (Simkin et al., 2022). Chlorophyll *a* and chlorophyll *b* are the only forms of chlorophyll possessed by terrestrial plants and play a key role in allowing photosynthetic organisms to adapt to both high and low light conditions, with plants adjusting their Chl *a*/*b* ratios to ensure maximum photosynthetic performance (Friedland et al., 2019; Simkin et al., 2022). In high light, plants develop a smaller antennae size with a higher proportion of chlorophyll a relative to chlorophyll *b*, while in low light, there is an increase in the antennae size cross-section associated with a reduction in PSII efficiency from approximately 91% to 84% (Mirkovic et al., 2017).

Chlorophyll *a* is the core pigment located at both the reaction centre and antennae of the light-harvesting structure. In contrast, chlorophyll b is only present in the antennae and is critical in harvesting light at lower intensities (Simkin et al., 2022). Reaction centre chlorophylls alone are not sufficient to drive photosynthesis since they don't absorb light fast enough to sustain the downstream electron transport process. Therefore, an antenna system comprised of 100-800 associate chlorophyll molecules is required to ensure an effective energy-collecting system (Mirkovic et al., 2017). Chloroplasts also accumulate high levels of carotenoids in the thylakoid membrane, essential pigments functioning in the stabilisation of lipid membranes, photosynthetic light harvesting and photoprotection against reactive oxygen species (ROS), with lutein, β-carotene, violaxanthin, and neoxanthin being the main chloroplast carotenoids (Li & Yuan, 2013; Nisar et al., 2015; Simkin, 2021).

After chloroplast remodelling into chromoplasts during the ripening stage, compounds such as lycopene and β-carotene, besides their protective function from oxidative stress, provide precursors of key molecules such as flavour and aroma compounds, abscisic acid and Provitamin A. Moreover, their antioxidant activity is associated with health benefits, preventing the incidence of some chronic diseases, such as cardiovascular diseases and cancers (Simkin, 2021; Sun et al., 2018).

1.7 Chloroplast Biogenesis

The modulation of chloroplast development in the cell allows the optimisation of the chloroplast compartment size for photosynthesis. This process depends on balancing chloroplast biogenesis and division (Cackett et al., 2022). The assembly of chloroplasts is triggered through exposure to

light, which is a key signal for the activation of phytohormones involved in the regulation of chloroplast development, notably cytokinin, and expression of photosynthetic-related genes (Cackett et al., 2022; Hills et al., 2015). Chloroplast biogenesis from proplastids requires the coordinated transcriptional regulation of nuclear and chloroplast-encoded genes, with the paralogou GATA transcription factors *CGA1* and *GNC* positively regulating this process (Hudson et al., 2011). The GATA family of transcription factors are a family of zinc-finger DNA-binding proteins, which have been reported to integrate these hormonal and environmental cues to coordinate chloroplast development (Bi et al., 2005). They recognise the DNA sequence A/T-GATA-A/G with the zinc motif serving in DNA binding, protein folding, and stabilisation. In the case of plants, GATA members have also been found to interact with other proteins, however, further research is needed to elucidate that (Behringer & Schwechheimer, 2015). In the Arabidopsis and rice genomes, there are approximately 30 encoded GATA factors divided into four different categories, based on their zinc finger domain characteristics. The paralogs *CGA1* and *GNC* are members of the B-class of plant GATA factors, which contain additional domains. These additional domains lack a fully functional characterisation but may serve for interactions with other proteins (Behringer and Schwechheimer, 2015; Bi et al., 2005).

Among the factors contributing to the expression of *CGA1* and *GNC*, their response to nitrogen uptake is a key factor. They were first identified based on their induction by nitrogen (Wang et al., 2003; Price et al., 2004; Bi et al., 2005; Chiang et al., 2012). In addition, cytokinin (which is stimulated by nitrate uptake) is also known to induce *CGA1*/*GNC* expression (Miyawaki et al., 2004; Takei et al., 2001; Chiang et al., 2012). Light and hormonal cues have been proposed to be master regulators of the expression of *CGA1*/*GNC* (Chiang et al., 2012; Hudson et al., 2011). It has been proposed that the activation of the *GCA1*/*GNC* family acts to bypass other factors repressing chloroplast development (Hudson, 2010; Hudson et al., 2011). *PIF3* expression, for instance, is negatively correlated with the expression of *GUN4* and *HEMA1* (Stephenson et al., 2009). By contrast, *CGA1*/*GNC* have shown opposite expression to *PIF3*, counteracting its action to positively control the activation of essential chlorophyll biosynthesis and carotenoid genes (Chiang et al., 2012). *CGA1* and *GNC* act downstream of light and cytokinin, exhibiting partially redundant roles in modulating the expression of chloroplast-localised *GLU1*, involved in chloroplast nitrogen assimilation and the chlorophyll biosynthesis genes *HEMA1* and *GUN4* (Chiang et al., 2012). Previous research has shown that the *cga1* and *gnc* mutants develop smaller chloroplasts with a 10-30% decrease in chlorophyll content. In contrast, overexpression of either *CGA1* or *GNC* was shown to enhance chloroplast growth and division rates in

Arabidopsis, with transgenic plants exhibiting increased numbers of chloroplasts, higher chlorophyll content and starch levels (Cackett et al., 2022). By modulating the expression of *GLU1*, both *CGA1* and *GNC* enhance nitrogen assimilation rates in the chloroplast, increasing the Glutamate pool, an essential molecule required to produce amino acids, chlorophyll, and nucleic acids. Moreover, the expression of *HEMA1* and *GUN4* directs the flow of nitrogen towards chlorophyll biosynthesis (Hudson et al., 2011).

In summary, it appears that the *CGA1/GNC* family is an important regulator of chloroplast development and has a key role in integrating light and cytokinin pathways to promote chlorophyll biosynthesis and chloroplast biogenesis, which makes them a suitable target to engineer plants with enhanced chloroplast development and photosynthesis (Cortleven & Schmülling, 2015).

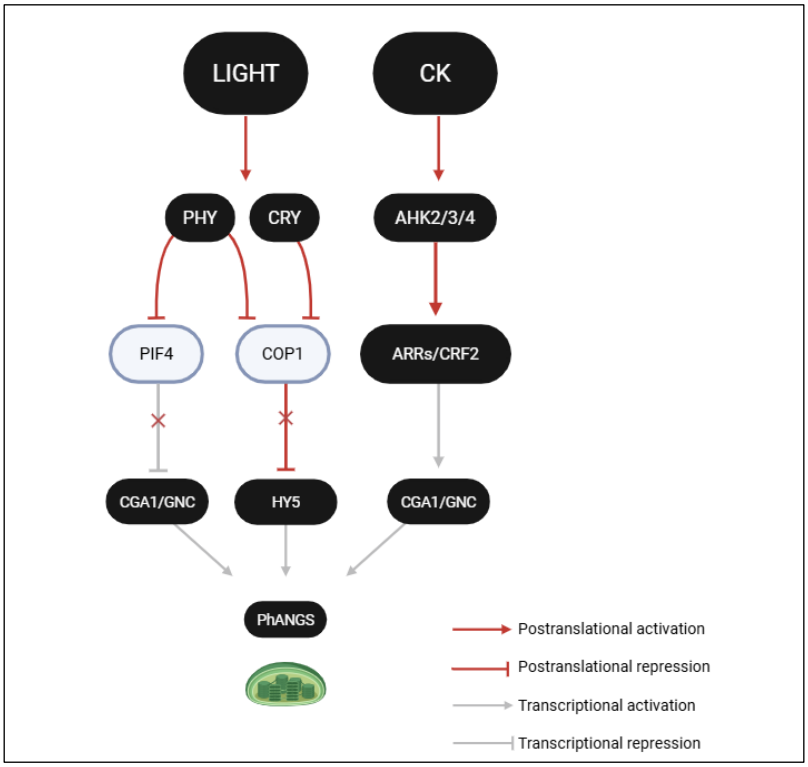

Figure 1.3. A simplified model for the activity of *CGA1* and *GNC*. Light and cytokinin play separate but interrelated roles in regulating *CGA1* and *GNC* expression. Whilst both light and cytokinin upregulate the expression of *CGA1/GNC*, light can also modulate the levels of cytokinin. Light signals are transmitted by phytochromes (PHYA/B) and cryptochromes, while cytokinin signals pass through receptors (AHK2/3) and response regulators (ARRs). Light can also influence cytokinin levels, linking the two pathways. Together, *CGA1* and *GNC* promote chlorophyll biosynthesis and chloroplast development. Adapted from Cackett et al. (2022).

1.8 Chloroplast Division

Like their bacterial ancestors, chloroplasts replicate by binary fission from pre-existing proplastids in the cytosol, maintaining the appropriate population size during cell development and assuring the photosynthetic competence of mature cells (Juniper & Clowes, 1965). Molecular genetic studies in Arabidopsis have established a class of nuclear-encoded proteins involved in chloroplast division in photosynthetic eukaryotes (Marrison et al., 1999). The chloroplast replication mechanism requires the activity of two protein complexes on both the inner and outer envelope membranes. This process starts with the arrival of FtsZ to the division site, a group of tubulin-related cytoskeletal proteins. This initial event takes place on the stromal face of the chloroplast inner membrane, and it is controlled by two FtsZ gene families, FtsZ1 and FtsZ2, a process similar to the bacterial cell division apparatus (M. Zhang et al., 2013). It has been shown that the functionality of the Z Ring is dependent on the levels of either FtsZ1-1 or FtsZ2-1, with the antisense expression of these proteins being associated with severe phenotypes (Osteryoung et al., 1998). This process is mediated by the interaction with division-site regulators, including a stromal factor MinE1, ARC6 and ARC3. The combined action of these proteins is believed to be required for the mid-cell placement and stabilisation of the Z-ring protofilaments (Maple & Møller, 2007).

More recently, new components of plastid division have been identified on the outer envelope membrane, comprising the cytosolic division machinery. The envelope–spanning proteins PDV1 and PDV2 are recruited to the division site through direct interaction with ARC6. To accomplish the final scission, PDV1 and PDV2 localise to ring-like structures on the membrane outer envelope and recruit ARC5, which is essential in the final stages of chloroplast division. Studies with Arabidopsis have suggested that PDV proteins have a crucial effect on chloroplast size and number, enabling plants to adapt to varying cell differentiation conditions (Okazaki et al., 2009). These studies indicate that these nuclear-encoded proteins play a key role in plastid division, performing different but coordinated activities and providing the contractile force separating the chloroplast into two daughter organelles (Miyagishima et al., 2006).

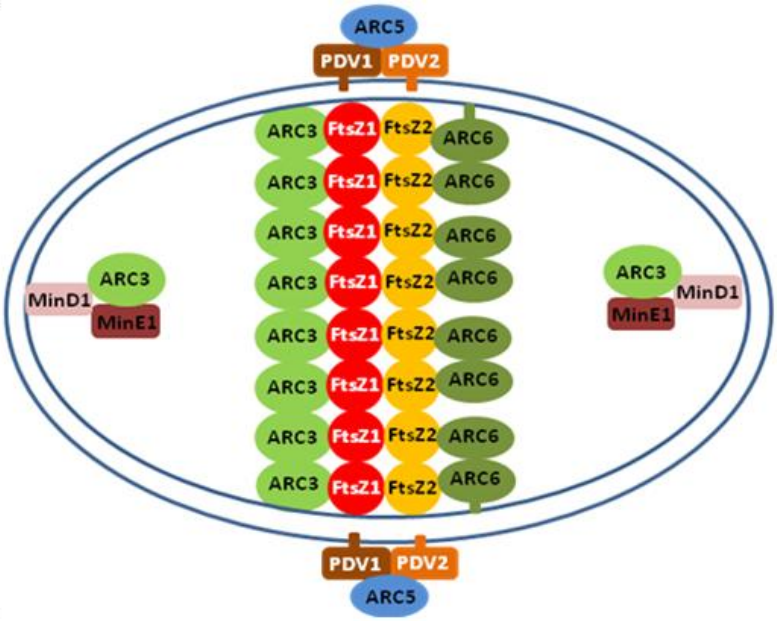

Figure 1.4. Stromal and cytosolic machineries of the plastid division mechanism. At the first step of stromal division, FtsZ1-1 and FtsZ2-1 form a Z-ring at the centre of chloroplasts. The accessory proteins ARC6, ARC3, MinE1 and MinD1 are recruited to the Z-ring. PDV1 and PDV2 localize to ring-like structures on the cytosolic surface of the outer envelope membrane and recruit ARC5 to the division site to constitute the cytosolic division machinery (modified from Maple & Møller (2007).

The isolation of several *arc* (accumulation and replication of chloroplasts) mutants in Arabidopsis, which has provided a pathway to elucidate the function of chloroplast division genes in plant development. These mutants present alterations in chloroplast size and number due to the altered expression of division genes. They are a well-suited tool to better understand the importance of chloroplast density and morphology in photosynthesis (Pyke & Leech, 1992). Mutants with larger chloroplasts differ significantly from the wild type, exhibiting impaired photosynthetic performance and increased photodamage. The abnormal chloroplast morphology has been associated with an altered thylakoid architecture, reduction in PSII quantum efficiency, and diminished chloroplast movement under different light conditions, a feature related to the loss of ability to perceive/respond to changing light intensities (Austin II and Webber, 2005; Dutta et al., 2017). A mutation in *ARC6* leads to an inhibition of plastid division, with mutants developing only two enlarged chloroplasts per mesophyll cell, compared to wild-type, which generally has over 100 chloroplasts per cell (Pyke et al., 1994). Equally, a mutation in *ARC3* has been associated with a low copy number of large-sized chloroplast and a reduction in

photosynthetic capacity. Finally, a mutation in *ARC5* reveals that the increase in chloroplast size, and consequently maintenance of chloroplast to mesophyll cell volume, is not enough to maintain photosynthetic performance (Austin II and Webber, 2005).

1.9 Understanding the Significance of Fruit Photosynthesis

Improving photosynthetic efficiency to increase yields has traditionally focused on leaf tissues, with less attention given to the contribution of photosynthesis in non-foliar green organs to plant growth and development (Blanke, 1992; Laval-Martin, 1977; Simkin et al., 2020; Cocaliadis et al., 2014; Blanke, 1989). Although leaves are often regarded as the powerhouse of plants, producing photoassimilates that will be used for the growth and metabolism of other parts of the plant, photosynthesis is not restricted to these tissues (Cocaliadis et al., 2014). There is significant evidence that functional photosynthesis takes place in other parts of the plant, such as the fruit (Blanke, 1989; Carrara et al., 2001), petiole and stems (Hibberd & Quick, 2002) and seeds (Ruuska et al., 2004) and they may be an important factor contributing to crop growth and yield. Recent transcriptomic analyses have demonstrated a high level of expression of photosynthetic genes in tomato fruit cells (Simkin et al., 2020; Wang et al., 2009). Further, proteomic studies have shown that all the chloroplast complexes associated with light harvesting, electron transport and the CBB cycle are present at the protein level in the tomato fruit (Barsan et al., 2010, 2012).

Fruit photosynthesis has been estimated to account for up to 15% of the total carbon stored in these organs, with all stages of development contributing to final sugar accumulation (Tanaka et al., 1974; Cocaliadis et al., 2014). Work with developing tomato fruit reported 41% of the photosynthetic electron transport capacity of leaf tissues and functional activity of RuBisCO, demonstrating photosynthetic function (Piechulla et al., 1987). Although absolute photosynthetic rates are reduced in fruits, chloroplast density is also considerably lower in fruit tissues when compared to leaves (Blanke, 1989). Photosynthesis in fruit tissues measured on a unit chlorophyll level is comparable to the photosynthesis performed in the leaves (Smillie, 1992; Williams et al., 1985; Aschan and Pfanz, 2003). Work with young tomato fruit revealed that the carboxylation activity of RuBisCO was observed at similar levels to those recorded in leaf tissues, declining as the fruit ripens (Carrara et al., 2001). Furthermore, the presence of a photochemical apparatus and effective electron transport provides evidence that fruits can process energy for photosynthesis, which has been confirmed by chlorophyll fluorescence measurements in tomato fruits (Aschan & Pfanz, 2003; Carrara et al., 2001).

Photosynthesis in fruits is particularly interesting as in fruit tissues, stomata are present in generally lower numbers compared to those on the leaves. It has been reported that, overall, stomata density in fruits represents only between 1-10% of leaves in most crops, with their significance being currently not fully understood and their functionality mainly associated with evaporative cooling down (Sánchez et al., 2013; Simkin et al., 2020). In the case of tomato fruit, stomata are virtually absent, which has been confirmed microscopically (Vogg et al., 2004). The normal activity levels of RuBisCO, whilst in the absence of stomata, and the detection of an efficient phosphoenolpyruvate carboxylase (PEPC), strongly indicate that the main supply of carbon in tomato fruit photosynthesis is internal CO_2 recycling, refixing CO_2 generated by mitochondrial respiration. This process not only re-utilises carbon that would otherwise be lost but may also supply an important fraction of the total fruit's carbon requirement (Vogg et al., 2004; Aschan and Pfanz, 2003). Interestingly, work with tomato fruit revealed that PEPC activity was considerably higher than RuBisCO, increasing the efficiency of carbon refixation by creating a significant carbon pool (Carrara et al., 2001). This is reinforced by the high levels malic enzyme (ME) and malate dehydrogenase (MDH) in fruit tissue, compared to leaves, indicating that CO_2 is fixed by PEPC into oxaloacetate (OAA), which is then reduced to malate via NAD-dependent malate dehydrogenase (MDH) (Willmer & Johnston, 1976). Malate can then be translocated to the chloroplasts, where NADP-malic enzyme (NADP-ME) performs its decarboxylation into CO_2 and pyruvate, the first being re-fixed by RuBisCO via CBB cycle, while the latter can be converted back into phosphoenolpyruvate (PEP) by pyruvate phosphate dikinase (PPDK) (Garrido et al., 2023). The proposed mechanism supports photosynthetic carbon assimilation in fruits, despite having negative assimilation rates (Blanke, 1989; Garrido et al., 2023; Willmer and Johnston, 1976). Several factors affect fruit gas exchange, including incident photosynthetically active radiation (PPFD), chlorophyll content, and the availability of CO_2. Light is key for chlorophyll biosynthesis and the activation of photosynthetic pathways. However, light penetration is often limited due to the thickness and morphology of fruit tissues (Garrido et al., 2023).

In fruits, a remarkable feature of the process of photosynthesis is the fact that in many species, such as tomato, the process of ripening is associated with the differentiation of chloroplasts into chromoplasts. The ripening developmental programme is responsible for the regression of the thylakoid structures, moving from photosynthetic (or partially photosynthetic) to a completely heterotrophic metabolism (Büker et al., 1998; Kahlau and Bock, 2008). Nuclear regulation controls the differentiation of chloroplasts into chromoplasts, in which degradative enzymes like chlorophyllase and proteases break down chlorophyll and lead to the dismantling of the

photosynthetic machinery (Bian et al., 2011; Camara et al., 1995; Egea et al., 2010). This process is coupled with a decline in the expression of photosynthesis-related genes and enzymatic activity associated with chloroplast development and chlorophyll biosynthesis (Kahlau & Bock, 2008; Steinhauser et al., 2010). Evidence shows that the levels of mRNA encoding chloroplast proteins reduce dramatically on the onset of ripening, whilst a significant rise is observed in transcripts associated with carotenoid accumulation, ethylene biosynthesis and cell wall metabolism (Bian et al., 2011; Egea et al., 2010; Gray et al., 1992).

1.10 Tomato Fruit Development and Ripening

Tomato fruit set and development are highly coordinated processes that involve cross-talk between auxins, cytokinins, and gibberellins. These important phytohormones are involved in different aspects of cell division and expansion and have combined action to promote the expression of the genes that will determine fruit size, weight and shape (Quinet et al., 2019). The ripening stage is mainly influenced by a balance between ethylene and abscisic acid (ABA), with ABA being an important regulator of the primary metabolism, whilst ethylene is essential in the transition from primary to secondary metabolism (J. Gray et al., 1992; Quinet et al., 2019). In tomato and other climacteric fruit, a respiratory peak during ripening has been proposed to fuel the metabolic changes typical of the ripening programme, such as colour change and softening of the fruit, making it attractive to dispersers and facilitating seed release (Alexander & Grierson, 2002; Seymour et al., 2013). This increase in respiration is stimulated by ethylene, which modulates the expression of several ripening-related genes, including cell wall hydrolases and carotenoid biosynthesis (Hoeberichts et al., 2002; Seymour et al., 2013; Alexander & Grierson, 2002).

Another key developmental feature associated with ripening is the biosynthesis of large amounts of carotenoids in the newly differentiated plastid. Thylakoid disassembly is accompanied by the synthesis of new membrane complexes that enable carotenoid biosynthesis and storage. It has been reported that the levels of MFP1, a thylakoid-associated DNA-binding protein, are dramatically reduced during tomato fruit ripening, in accordance with the loss of photosynthetic competence (Egea et al., 2010; Li & Yuan, 2013). In tomato, mainly lycopene and β-carotene accumulate in the fruit chromoplast, which has a major influence on the fruit's colour and nutrition (Klee & Giovannoni, 2011). Chromoplast differentiation starts at the breaker stage, where most genes involved in photosynthesis are down-regulated, and lycopene, the red pigment

that gives the tomato its characteristic colour, begins to accumulate (Bian et al., 2011; Quinet et al., 2019). It has been reported that the levels of lycopene increase by about 10 to 14-fold during ripening, accumulating as the fruit reaches maturity (Quinet et al., 2019). Data provided by confocal microscopy showed a mixed population of both chloroplasts and chromoplasts at the breaker stage, as well as intermediate plastids containing both chlorophyll and carotenoids. As the fruit ripens, all chloroplasts are degraded and only fully developed chromoplasts are present in the fully ripe fruit (Egea et al., 2010).

Several ripening-related transcription factors are proposed to drive carotenoid accumulation in tomato fruits. However, to date, the only identified gene controlling chromoplast biogenesis is the *Or* gene, isolated from cauliflower, which triggers the formation of carotenoid-sequestering structures (Li & Yuan, 2013; Lu et al., 2006; Sun et al., 2018). Evidence shows that the overexpression of *Or* has led to enhanced carotenoid levels in transgenic tomato (Yazdani et al., 2019), potato tubers (Lopez et al., 2008) and sweet potato (Park et al., 2016), revealing the key role of *Or* in regulating carotenoid accumulation and potential use as a genetic tool in the nutritional biofortification of crop plants. The carotenoid biosynthetic pathway is affected by both the levels of production and degradation, with the enzyme Phytoene synthase (PSY) being considered the rate-limiting step affecting the carotenoid pool. The PSY-catalysed product, phytoene, is therefore, the first carotenoid formed in the pathway (Lu & Li, 2008). Expression of *PSY* is highly associated with carotenoid source and sink metabolisms, representing a key factor controlling carotenoid metabolic flux (Li & Yuan, 2013).

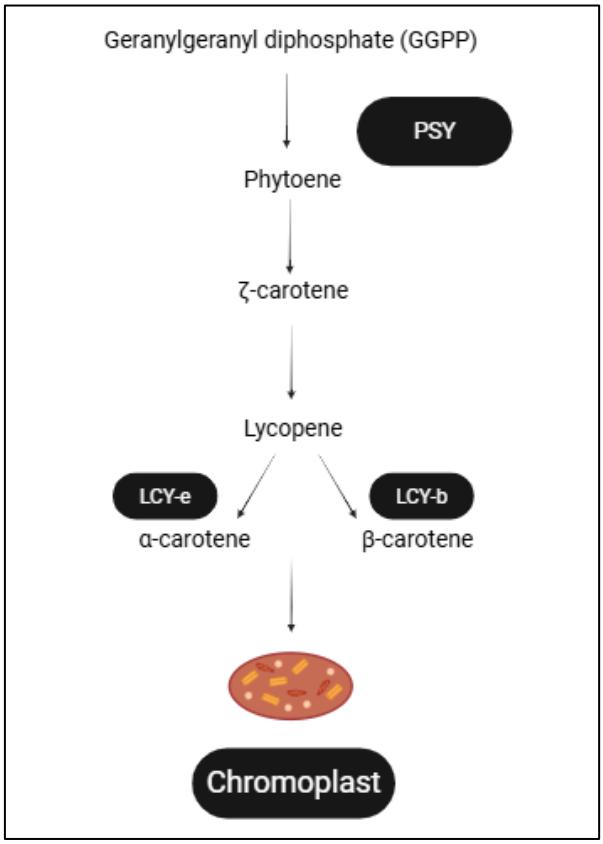

Figure 1.5. Simplified carotenoid biosynthesis pathway. Carotenoid accumulation is determined by the rate of biosynthesis, turnover, and stable storage in plastid sink structures. Phytoene synthase (PSY) catalyses the committed step and is a major determinant of total carotenoid content. Phytoene undergoes sequential desaturation, first forming ζ-carotene and ultimately lycopene. Lycopene ε-cyclase (LCY-e) and lycopene β-cyclase (LCY-b) direct flux into the α-carotene and β-carotene branches. Adapted from Li & Yuan (2013).

Different approaches have been attempted to enhance carotenoid content in tomatoes. Evidence shows that an increased chromoplast compartment size strongly correlates with a higher carotenoid biosynthesis and storage capacity (Li & Yuan, 2013; Simkin, 2021). The ABA-deficient *high pigment 3* (*hp3*) tomato mutant displayed plastids 30% larger and with 30% more carotenoids in the mature fruit (Galpaz et al., 2008). In addition, overexpression of a transcription factor related to the *ARABIDOPSIS PSEUDO RESPONSE REGULATOR2-LIKE* gene (*APRR2-like*) in tomato developed transgenic plants with increased plastid area by 50%, plastid number by 20% and increased carotenoid content by 20% at the ripe stage (Pan et al., 2013). As the levels of carotenoid biosynthesis in plant cells have been proposed to be a balance between the rate of biosynthesis and storage capacity, it is not surprising that enlarged plastids at the green stage display higher chlorophyll and chloroplast-carotenoid levels and as the fruit ripens higher

lycopene levels in the mature tissue (Galpaz et al., 2008). All of these studies further indicate that chloroplast/chromoplast fortification may result in fruits with better nutrient quality.

Fruits have a consistent photochemical activity, and the ability to internally assimilate endogenously produced CO_2 may supply a significant fraction of the fruit's own carbohydrate requirement and contribute to the whole plant's carbon economy, which could, in turn, offset the costs of reproduction (Aschan & Pfanz, 2003). The last stages of fruit development are also associated with the degradation of the starch stored in the chloroplasts into soluble sugars. As the content of soluble carbohydrates in the ripe stage of the fruit has been correlated with the level of transient starch in immature and mature green fruits, fruit chloroplasts are suggested to have an active role in the supply of sugars in red fruit (Cocaliadis et al., 2014). Transgenic tomato plants developed to display an increased chloroplast content and more grana per cell were shown to accumulate greater amounts of starch in green tissues and higher amounts of sugar in the mature fruit (Sagar et al., 2013). Therefore, the links between photosynthesis in developing fruit and desirable traits in the ripe stage, such as flavour, nutrient content, and aroma, make fruit photosynthesis an attractive target for improving fruit quality, and potentially enhancing whole-plant productivity (Sagar et al., 2013; Pan et al., 2013).

1.11 Target Genes for The Manipulation of Chloroplast Development

The manipulation of different aspects of chloroplast development has emerged as a promising alternative to enhance fruit photosynthetic capacity. Changes in the amount of cellular space allocated to chloroplasts, pigment biosynthesis and components of the photosynthetic apparatus could have direct implications on fruit photosynthetic efficiency (Hu et al., 2024; Larkin et al., 2016; Pan et al., 2013; Powell et al., 2012; Shi et al., 2021). Many genes have been reported to affect the amount of cellular space allocated to plastids or pigment biosynthesis. Genes such as *SlAPRR2-Like*, *SlREC*, *SlZHD17* and *SlMYB72* have been associated with pigment metabolism, pericarp development, and plastid cellular compartment size. Overexpression of *SlAPRR2*-Like has been shown to increase both chloroplast number and size, resulting in fruits with more chlorophyll at the green stage and carotenoids at the ripe stage (Pan et al., 2013). Moreover, *SlZHD17* has been shown to suppress chlorophyll and carotenoid metabolism (Shi et al., 2021). The authors reported that the downregulation of *SlZHD17* led to transgenic plants with larger chloroplasts and increased chlorophyll content. Work on the *SlREC* genes has demonstrated their role in determining the amount of cellular space allocated to chloroplasts, a key, but poorly

understood determinant of fruit photosynthetic potential (Hu et al., 2024). All these studies provide evidence that plastid size and pigment biosynthesis can be influenced not only by the expression of structural genes but also by various transcription factors that integrate different pathways, including chloroplast biogenesis, division and pigment activity during fruit development (Cookson et al., 2003; Galpaz et al., 2008; Powell et al., 2012; Shi et al., 2021).

Designing plants with enhanced photosynthetic performance that remain robust across diverse environmental conditions requires complex manipulation of the photosynthetic apparatus at the genetic level. The table below summarises key genes from the literature that have been selected for their potential roles in improving photosynthetic efficiency.

Table 1.1. Overexpression of relevant genes targeted as an alternative to improve chloroplast development.

Species	**Gene**	**Function**	**Effect on leaf tissue**	**Reference**
Tobacco (*Nicotiana tabacum*)	*BpMADS* (ortholog of *AP1* in Arabidopsis)	Required for sepal and petal development in *Betula platyphylla*	Bigger and more abundant chloroplasts than wild type; A 2-fold higher photosynthetic rate.	(Qu et al., 2013)
Arabidopsis (*Arabidopsis thaliana*)	*AtCGA1*/*AtGNC*	Required for the expression of photosynthesis and chloroplast-related genes	10-20% increase over chloroplast numbers; Increased overall chlorophyll biosynthesis.	(Hudson, 2010); (Hudson et al., 2011)
Poplar (*Populus trichocarpa*)	*PdGNC*	Required for the expression of photosynthesis and chloroplast-related genes	25–30% faster growth, 20–28% higher biomass accumulation, and ~25% increase in chlorophyll content, photosynthetic rate, and plant height.	(An, Y, 2020)

Rice (*Oryza sativa*)	*OsCGA1*/*OsGNC*	Required for the expression of photosynthesis and chloroplast-related genes	*OsGATA16* (*GNC*) and *OsGATA11* (CGA1) mild over-expression plants exhibited an increase in both biomass and yield.	(Hudson, 2010)
Arabidopsis (*Arabidopsis thaliana*)	*AtPDV1*/*AtPDV2*	Membrane constriction at the chloroplast division site	Overexpression of both *PDV1* and *PDV2* leads to a larger number of smaller chloroplasts.	(Okazaki, 2009)

1.11.1 Overexpression of the *Betula platyphylla* MADS-Box Gene *BpMADS* Enhances Chloroplast Growth and Division in Tobacco

The MADS-box motif is a conserved 56-amino-acid region within the DNA-binding domain in MADS-box eukaryotic transcription factors, which are fundamental to numerous biological activities in eukaryotic organisms (Shore & Sharrocks, 1995). In Arabidopsis, the most extensively studied model plant, 107 MADS-box genes have been identified (Pařenicová et al., 2003). These genes regulate various developmental programmes, including controlling flowering time, flower formation, and vegetative development (Ng & Yanofsky, 2001). In flowering plants, the most extensively characterised MADS-box genes are involved in floral development, including the development of reproductive structures (Shore & Sharrocks, 1995). The ABC model of flower organ development, applicable to most plant species, states that three classes of homeotic genes are involved in flower development, forming multi-component regulatory complexes to specify the formation of the flower organ (Ng & Yanofsky, 2001). In Arabidopsis, the transition from the vegetative to the reproductive stage is mediated by the action of floral-identity transcription factors, such as the MADS-box *APETALA1* (*AP1*), which has an A-class homeotic function, with a pivotal role in the development of sepals and petals in flowers (Irish, 2017). *AP1* acts in the process of converting shoot meristems into floral meristems, with its overexpression reported to enhance endogenous flowering-related genes, considerably reducing the flowering time (Mandel & Yanofsky, 1995). In the tomato genome, *MACROCALYX* (*MADS-MC*) has been

shown to be closely related to the Arabidopsis *APETALA1* (*AP1*) gene and is thought to share conserved *AP1*-like functions. *MACROCALYX* plays a crucial role in sepal development and is essential for the transition to flowering and the regulation of floral meristem identity (Burko et al., 2013; Vrebalov et al., 2002). Expression of *MADS-MC* has been detected in the flower, floral pedicel, and in fruit-associated tissues such as the sepal and pedicel, consistent with its regulatory role in tomato fruit abscission (Nakano et al., 2012).

The name MADS-box comes from the first four identified members of the family, the *MINICHROMOSOME MAINTENANCE 1* (*MCM1*) in yeast, *AGAMOUS* (*AG*) in Arabidopsis, *DEFICIENS* (*DEF*) in *Antirrhinum* and serum-response factor (*SRF*) in humans (Ng & Yanofsky, 2001; Riechmann & Meyerowitz, 1997). MADS-box transcription factors are classified into two main types: Type I and Type II, which differ in structure and function. Type I MADS-box genes encode shorter proteins that consist only of the conserved MADS-box domain. Gene expression studies have indicated that they are primarily involved in seed and embryo development (Grimplet et al., 2016; Zhang et al., 2024). In contrast, type II MADS-box in plants, known as MIKC-type genes, features additional domains that include not only the MADS-box but also the weakly conserved Intervening (I) domain, the conserved Keratin-like (K) domain and the highly variable C-terminal (C) domain (Figure 1.6) (Grimplet et al., 2016; Ng & Yanofsky, 2001). Research indicates that the I and K domains play a role in protein-protein interactions, creating complexes that fine-tune the expression of downstream target genes. While the K-domain promotes dimerisation with other K-domain MADS-box proteins, the I domain affects the specificity of dimer formation, whether homo or heterodimer. The C region may play a role in stabilising these interactions (Grimplet et al., 2016; Zhang et al., 2024). MADS-box proteins primarily target the consensus sequence $CC(A/T)_6GG$, known as CArG-box. Protein dimerisation allows them to specifically recruit other transcription factors into multi-component regulatory complexes (Shore & Sharrocks, 1995).

Figure 1.6. MIKC Domain Structure of MADS-Box Proteins. The MADS-box domain targets the consensus sequence $CC(A/T)_6GG$, known as CArG-box. The Intervening (I) domain and Keratin-like (K) domain mediate protein interaction specificity and dimerization, allowing the formation of multiprotein complexes. The C-terminal (C) domain is involved in the transcriptional activation of target genes, regulating downstream gene expression. Adapted from Ng & Yanofsky (2001).

Several MADS-box genes expressed during the first stages of fruit development have been identified as candidates for the regulation of fruit set and development post-anthesis. In tomato fruit *TDR4*, *TAGL2*, *TAGL11* and *TAGL1* have been suggested to start this new developmental programme, being upregulated in response to positive signals perceived by the plant (Nezhdanova et al., 2021; Busi et al., 2003). Different dimers form part of larger transcriptional complexes that regulate gene expression during early fruit development (Busi et al., 2003). Moreover, the effects of downregulation and overexpression of MADS-box in fruit development have been previously characterised. For instance, in *tagl1* plants, fruit ripening was inhibited, whereas its overexpression led to homeotic changes (stamens converted to carpel-like structures, fleshy sepals) (Molesini et al., 2020).

MADS-box transcription factors have also been associated with fruit ripening. For instance, *rin* mutants failed to accumulate lycopene and soften (Li et al., 2023) . Similarly, suppression of *FUL1* and *FUL2* led to lower carotenoid content in tomato fruit (S. Wang et al., 2014). Finally, it has been demonstrated that *TAGL1* is associated with ethylene production, with its downregulation leading to fruits with very low lycopene levels (Giménez et al., 2010; Vrebalov et al., 2009). Together, these studies indicate that MADS-box transcription factors act as core components of processes underlying fruit ripening, including pigment biosynthesis and ethylene-mediated developmental changes.

Interactions with other proteins allow MADS-box to initiate a cascade of gene expression, with the activation or repression of downstream target genes to ensure precise regulation of key

developmental processes, including floral organ identity, fruit development, and responses to environmental cues (Shore & Sharrocks, 1995). More specifically, regarding fruit development, the studies presented here provide evidence that tomato MADS-box factors are part of interconnected gene regulatory networks that coordinate correct fruit set and development. They integrate hormonal and developmental signals to either repress or promote the initiation of fruit growth and pigment accumulation (Molesini et al., 2020; Giménez et al., 2010; Vrebalov et al., 2009; Busi et al., 2003).

Recently, the overexpression of the MADS-box gene *BpMADS* from *Betula platyphylla* (Birch) in tomato in transgenic tobacco was shown to enhance chloroplast growth and division rates (Qu et al., 2013). The BpMADS protein is an orthologue of AP1 in Arabidopsis with a high level of similarity (73%), and in tomato, it shares high similarity with MACRO-CALYX (MADS-MC) (85%). The transgenic tobacco plants exhibit an increased number of chloroplasts, higher photosynthetic pigment content, and higher rates of photosynthesis (Qu et al., 2013). In addition, the overexpression of the MADS-domain transcription factors *SOC1* and novel *SOC1-like* in *Petunia hybrida* under heat stress has been associated with the expression of chlorophyll biosynthesis-related genes and chloroplast biogenesis (Z. Wang et al., 2019). These findings, coupled with the expression of several MADS-box transcription factors at early stages of fruit development, further strengthen the link between MADS-box and the regulation of key developmental processes occurring after fruit set. These results suggest a wider role for this gene family beyond floral identity and reproductive development. The ability of Type II MADS-box proteins to bind to DNA as dimers enables them to generate complex intrafamily interaction networks. While the relationship between chloroplast division and the MADS-box family remains unclear, it has been proposed that the increased chloroplast content in transgenic plants overexpressing *BpMADS* is a by-product of the complex interactions performed by these transcription factors as they specifically recruit other transcription factors to regulate a cascade of gene expression (Qu et al., 2013; Shore & Sharrocks, 1995). Taken together, the studies of transgenic lines with increased plastid numbers suggest that improvements in photochemical capacity and pigment content may be achieved by manipulating chloroplast development in tomato and that the MADS-box transcription factors may represent a suitable target to improve fruit yield and quality (Galpaz et al., 2008; Qu et al., 2013; Z. Wang et al., 2019).

1.11.2 Overexpression of *CGA1* and *GNC* Has Been Shown to Enhance Chlorophyll Levels in Arabidopsis

Chloroplast and plant development are two processes deeply connected to light and cytokinin signalling, key components in the transcriptional activation of chloroplast and photosynthesis-related genes (Hudson et al., 2011). Based on their roles in integrating environmental and internal stimuli in chloroplast development, the *CGA1*/*GNC* family have also been identified as a promising target for engineering crops with improved photosynthesis (Cackett et al., 2022; Naito et al., 2007). *CGA1* and *GNC* have been suggested to enhance nitrogen use efficiency and direct its flow towards chlorophyll production by directly targeting transcription factor genes, such as *GLU1*, the primary gene involved in nitrogen assimilation, and pivotal chlorophyll biosynthesis genes, such as *GUN4* and *HEMA1* (Chiang et al., 2012). The expression of GATA in rice enhanced chloroplast development and photosynthetic pigment content, with mutant plants exhibiting reduced chlorophyll levels (G. Lu et al., 2017). In Arabidopsis, overexpression of both *CGA1* and *GNC* has been shown to enhance chlorophyll levels, chloroplast number and leaf starch, accelerating greening and promoting chloroplast development in non-green tissues, such as roots and leaf epidermis, as well as improving photosynthetic rates (Chiang et al., 2012; Hudson, 2010; Ohnishi et al., 2018). In Poplar, transgenic plants overexpressing *GNC* exhibited accelerated plant growth, chlorophyll accumulation and higher photosynthetic rates, whereas CRISPR mutants showed retarded development and reduced biomass (An et al., 2020). Moreover, the use of tissue-specific promoters to express the GATA genes has the potential to deliver desirable traits to crops, whilst avoiding detrimental phenotypes from constitutive expression (Hudson, 2010). These studies all suggest that improvements in photosynthetic carbon fixation and pigment content may be achieved by engineering the photosynthesis gene regulatory network with the GATA transcription factors *CGA1* and *GNC* performing partially redundant roles in integrating light, nitrogen and cytokinin pathways in chloroplast development, showing potential for making crop improvements (Chiang et al., 2012; Hudson et al., 2011). Because these genes are highly conserved in the plant kingdom, their application is expected to increase plant productivity across many crop species (Hudson, 2010).

A large body of experimental data supports the role of fruit photosynthesis as a genetic tool for enhancing not only fruit size but also their composition and nutritional value, which in turn could have major implications for crop development and improve crop yields and postharvest quality (Cocaliadis et al., 2014; Simkin et al., 2020; Tanaka et al., 1974). Besides the increase in

photosynthetic parameters, a higher level of active chloroplasts at the green stage could also develop ripe tomatoes with more active chromoplasts, resulting in higher amounts of secondary metabolites (Galpaz et al., 2008). Therefore, altered plastid compartment have a direct impact on pigment concentration and fruit nutrient quality. These results, together with the work developed with *arc* mutants suggest that chloroplasts are a suitable target for the manipulation of photosynthesis in tomato fruit (Cocaliadis et al., 2014; Wang et al., 2008).

1.11.3 Overexpression of *PDV1* and *PDV2* in Arabidopsis Leads to the Accumulation of Smaller and More Numerous Plastids

The evaluation of *arc* mutants in Arabidopsis demonstrated that mutants with larger chloroplasts differ significantly from the wild type, with both chloroplast movement and photosynthesis being compromised (Pyke & Leech, 1992). Among the components involved in chloroplast division, the Plastid Division proteins (PDV) have been shown to be the rate-limiting step in the process, controlling the extent of chloroplast division in land plants. Overexpression of *PDV1* and *PDV2* in Arabidopsis developed plants with smaller and more numerous chloroplasts. Moreover, simultaneous overexpression of both genes led to a further increase in the number of plastids and a reduction in size compared to single-overexpressed plants (Okazaki et al., 2009). A large population of smaller chloroplasts has been shown to benefit photosynthetic efficiency as small chloroplasts can rapidly adapt to changing irradiance, which can minimise photodamage under excess light conditions (Xiong et al., 2017). Chloroplast movement has been described as an important strategy adopted by plants to maximise light use efficiency, with chloroplasts positioning to the side walls of cells when exposed to high light and along walls perpendicular to the light direction under low light conditions (Kasahara et al., 2002; Weise et al., 2015). In addition, it has been demonstrated that in leaves, chloroplast number and shape strongly affect mesophyll conductance, which is a key factor reducing the availability of CO_2 at the site of RuBisCO, being estimated to account for a 40% loss of atmospheric CO_2 (Weise et al., 2015). Moreover, a large population of smaller chloroplasts is associated with an enhanced photosynthetic nitrogen use efficiency (PNUE). Because nitrogen is largely invested in photosynthetic proteins, such as RuBisCO, several studies have revealed a direct correlation between nitrogen content and CO_2 fixation in green tissues (Xiong et al., 2017). In addition, PNUE, which refers to the photosynthetic capacity per leaf nitrogen content, has been described as an important factor to characterise the photosynthetic activity and the overall carbon status of the plant (Zhong et al., 2019). These findings suggest that the Plastid Division components of the

chloroplast division machinery *PDV1* and *PDV2* could have a significant impact on photosynthesis by improving chloroplast plasticity and reducing photodamage, as well as improving nitrogen use efficiency, which may be an important factor contributing to fruit yield, particularly under variable environmental conditions (Okazaki et al., 2009; Xiong et al., 2017).

1.12 Concluding Remarks

Improving photosynthetic efficiency is recognised as an important avenue to increase yield potential in crop plants (Zhu et al., 2010). Several components of both the cytosolic and stromal plastid division machinery have been identified, allowing the study of the role of plastid number and size on photosynthetic parameters. Recently, the MADS-Box gene *BpMADS* from Birch family has been identified as a target for the manipulation of chloroplast development (Qu et al., 2013). Furthermore, various transcription factors expressed in Arabidopsis have been shown to increase leaf chlorophyll content (Chiang et al., 2012; Hudson et al., 2011). Finally, the components of the plastid division machinery *PDV1* and *PDV2* have been identified as a target to enhance chloroplast movement and photoprotection (Okazaki et al., 2009).The overall aim of this project is to manipulate chloroplast development to produce fruit with higher pigment content, enhanced photosynthetic performance, and nutritional quality. The secondary aim of this project is to determine the role of the plastid compartment in fruit organic compound sequestration.

Chapter 2 Materials and Methods

2.1 Construct Generation

Golden Gate cloning technology was used to generate overexpression constructs from basic standard parts. The assembly method is based on Type SII restriction enzyme activity, *BsaI* and *BbsI*, in which the cleavage of DNA occurs at a different location than the DNA restriction site, allowing for defined overhangs to be produced and directional assembly of multiple fragments (Weber et al., 2011). Level 0 modules were synthesised and provided by NBS Biologicals (NBS Biologicals, UK). Level 1 destination vectors, the assembled kanamycin resistance level 1 module and the level 2 linkers were provided by the University of Essex (University of Essex, UK). All plasmid expression vectors with corresponding antibiotic resistance are detailed in Table 2.1.

Table 2.1. Plasmid vectors and appropriate resistance.

Plasmid	Resistance	Concentration	Supplier
Level 0 modules	Kanamycin	100 µg mL^{-1}	NBS Biologicals, UK
Level 1 destination vector	Ampicillin	100 µg mL^{-1}	University of Essex
Level 2 destination vector	Kanamycin	100 µg mL^{-1}	NIAB

2.1.1 Level 1 Assembly

Level 0 modules consist of standardised parts which constitute a transcription unit, such as promoter, coding sequence and terminator. The initial step in the assembly of the multigene was to generate level 1 modules from the appropriate combination of compatible level 0 modules using the *BsaI* Golden Gate reaction. All level 1 destination vectors confer ampicillin resistance and encode a *lacZ* fragment, producing a blue phenotype in the presence of X-GAL and IPTG. Level 1 destination vectors were synthesised to provide a specific position and orientation for transcription units. Tables 2.2 and 2.3 represent information on the Golden Gate reaction components and setup.

Table 2.2. Golden Gate reaction components.

Component	Volume
Vector (100 µg mL^{-1})	1 µL
Insert or plasmid (100 µg mL^{-1})	1 µL of each
T4 ligase buffer	1.5 µL
Restriction enzyme	1 µL
T4 Ligase	1 µL
ddH_2O	6 µL

Table 2.3. Golden Gate reaction setup.

Temperature	Time	Cycles
37° C	3 min	25
16° C	4 min	
50° C	5 min	1
80° C	5 min	1
22° C	∞	1

2.1.2 Transformation of *E. coli* Competent Cells

The *Escherichia coli* strain used for plasmid transformation in this study was either TOP10 (Thermo Fisher Scientific, US) or in-house-made DH5α cells. Chemically competent *E. coli* cells were transformed with each Golden Gate module using the heat shock method of transformation (Sambrook & Russell, 2001). 4 µL of the plasmid DNA was added to 50 µL of *E. coli* competent cells. Then, this reaction mixture was gently mixed and incubated on ice for 1 minute. Heat shock was performed in a water bath at 42 ˚C for 45 seconds and then placed immediately on ice for 1 minute. After that, 300 µL of Luria-Bertani broth (LB) media was added to the cells and incubated at 37 ˚C for 1h. Lastly, an aliquot of 100 µL of the cells was spread on selective media containing ampicillin (100 µg mL^{-1}), supplemented with X-gal and IPTG (1.5 µL mL^{-1}) to allow blue/white selection of successfully transformed colonies and incubated at 37 ˚C overnight.

2.1.3 Plasmid DNA Preparation

NucleoSpin® plasmid kit (Machery-Nagel, Düren, Germany) kit was used to extract high-purity plasmid DNA from *E. coli* cells. For this, 5 mL of LB media containing ampicillin (100 µg mL $^{-1}$) and a single colony selected from a plate were grown overnight at 37 ˚C. After the incubation period, 5 mL of saturated *E. coli* LB culture was spun down and the cells were resuspended in 250 µL of resuspension Buffer A1. After that, 250 µL of lysis Buffer A2 was added, and the solution was gently mixed by inverting the tube 6-8 times and incubated at room temperature for 5 mins. Following this, 350 µL of neutralisation Buffer A3 was added, and the solution was vigorously mixed by inverting the tube 6-8 times. The tube was then centrifuged for 5 minutes at 11,000 x *g*, and the supernatant was decanted into a NucleoSpin column. The column was spun down for 1 minute at 11,000 x *g*, and the flowthrough was discarded. 500 µL of Buffer A4 was then added, and the column was again spun down for 1 minute at 11,000 x *g*. The flowthrough was discarded, and the column was put back in the empty collection tube. The column was then centrifuged for 2 minutes at 11,000 x *g*, transferred into a clean 1.5 mL Eppendorf tube, and added 50 µL of water nuclease-free. After 1 minute of centrifugation at 11,000 x *g*, the purified plasmid DNA was stored at -20 ˚C. The purity and concentration of isolated plasmids were measured using the Nanodrop 1000 (ThermoFisher Scientific).

2.1.4 Restriction Enzyme Digest and DNA Sequencing

The confirmation of the level 1 constructs was conducted either by restriction enzyme digest or Sanger sequencing (Eurofins Genomics, Ebersberg, Germany). The level 1 vectors contain the restriction site CACNNNGTG for *DraIII* digestion. For this 1.7 µg of genomic DNA was cleaved by 34 units of restriction endonuclease *DraIII* for 1 hour at 37 °C. Samples were run on a 1% agarose gel at 160 volts for 1 hour. For Sanger Sequencing, templates consisted of 5 µL purified plasmid with concentrations of 100 ng µL^{-1}. 5 µL of selected primer with a concentration of 5 µM was added to the tube to make a final volume of 10 µL. The isolated plasmids were sent to Eurofins Genomics using the primers listed in Table 2.4.

Table 2.4. Primers used in the Golden Gate level 1 construct sequencing.

Primer name	Sequence (5’ – 3’)	Target
L1-F	CGGATAAACCTTTTCACGCCC	Level 1 vector backbone

L1-R	GTACTGGGGTGGATGCAGTG	Level 1 vector backbone

2.1.5 Level 2 Assembly

Following the level 1 assembly, separate level 1 modules (functional transcriptional units) were assembled into level 2 modules as described in the level 1 assembly section using the Golden Gate reaction *BbsI*. After Golden Gate assembly, competent *E. coli* cells (Top10 Thermo Fisher Scientific or in-house-made DH5α cells) were transformed with 4 µL of each level 2 assembly as described previously. Level 2 destination vectors confer resistance to kanamycin and encode a canthaxanthin biosynthesis operon for the red/white selection. Cells were then plated onto agar plates containing kanamycin (100 µg mL^{-1}) and incubated overnight at 37 °C. Successful transformation of level 2 modules leads to the appearance of white colonies due to the replacement of the canthaxanthin operon by the integration of the level 1 modules (Weber et al., 2011). After *E. coli* transformation, plasmid DNA preparation is carried out following the protocol described previously. To confirm the construction of level 2 modules, Sanger sequencing (Eurofins Genomics) was performed. All primers used for the multigene constructs sequencing are detailed in Table 2.5. For the visualisation of construct maps and sequencing data, SnapGene® software was used.

Table 2.5. Primers used in the Golden Gate level 2 construct sequencing.

Primer name	**Sequence (5' – 3')**	**Target**
L2-F	TGGCACATACAAATGGACGAACGG	Level 2 vector backbone
L2-R	ATGGGCTGCCTGTATCGAGTGG	Level 2 vector backbone
pTFM F3	AAGTTAGGTTTGGAGCCGTATGG	*SlTFM7* promoter
pFIB F1	ATGGCTCCTTGTCCTCTAGCC	*CaFIB* promoter
pAFF F2	TTTGTCACGGTATTCCTACC	*SlAFF* promoter
MAD F2	AGACGTAACGAGCTTGAACTGACC	*BpMADS*
CGA1 F1	TTATTACCACCAGCGACAGCAGC	*AtCGA1*
GNC F1	AACGTCTTGACCAGAAAGACCACG	*AtGNC*
PDV F1	TTGCTCGGCTTGAACAGAGCAGG	*AtPDV1*
PDV2 F1	AACGGAGGATCTGGAGGTTCG	*AtPDV2*

tOCS F1	AGCATGTGTAGCTCAGATCCTTACC	*OCS* terminator
tHSP F1	TTGGCTTGTTGTGTTATGAATTTGTGGC	*HSP* terminator
L1-R-KAN1	AACTGTTCGCCAGGCTCAAGG	*nptII*

2.2 *Agrobacterium*-mediated Genetic Transformation of Tomato

2.2.1 Transformation of *Agrobacterium Tumefaciens*

To perform the transformation, the *Agrobacterium tumefaciens* strain EHA105 was used. First, the *A. tumefaciens* competent cells stored in 25% glycerol were thawed on ice. Following that, 1 µL of the plasmid of interest (100 ng mL^{-1}) was added to thawed bacteria. Then, the tube was flash-frozen in liquid nitrogen for 5 minutes and flash-thawed in a water bath at 37 °C for 5 minutes. After that, 700 µL of low salt LB media was added to the cells and incubated at 28 ˚C for 2 hours. After the transformation, the cells were spun down for 1 minute at 8,000 x *g* for 2 minutes. 600 µL of the low salt LB broth was decanted and discarded, and cells were re-suspended in the remaining 100 µL of media. Lastly, cells were plated on low salt agar plates containing rifampicin (50 µg mL^{-1}) and the selectable marker (kanamycin 100 µg mL^{-1}) and left to grow at 28 °C for a minimum of 48 hours. One day before inoculation, *A. tumefaciens* strain EHA105 harbouring the binary vector was then grown overnight in a shaker at 28 °C and 180 rpm as a preculture in low salt LB broth with markers (5 mL, rifampicin 50 µg mL^{-1} and kanamycin 100 µg mL^{-1}). Following the preculture, the bacteria were spun down at 3,000 x *g* for 4 minutes and re-suspended in MS liquid medium supplemented with Gamborg's Vitamin Solution (1 ml L^{-1}), 2,4-dichlorophenoxyacetic acid (0.2 mg L^{-1}), kinetin (0.1 mg L^{-1}) and acetosyringone (0.1 mM) to OD_{600} 0.1-0.2.

2.2.2 Plant Material, Seed Sterilisation and Germination

Seeds of tomato (*Solanum lycopersicum*) cv. Micro-Tom were sterilised in a 50 ml 15 % bleach solution containing 10 drops of 0.1 % Tween20, inverting/swirling occasionally, for 10 min, then rinsed five times with sterile water. The seeds were germinated in honey jars with 50 mL of MS medium (Murashige and Skoog) medium supplemented with sucrose (15 g L^{-1}), Gamborg's

Vitamin Solution (1 ml L^{-1}), 6-benzylaminopurine (8.9 µM) and agar (8 g L^{-1}). The pH was adjusted to 5.8 before autoclaving. Approximately 20 seeds were planted per jar. The cultures were incubated in the dark at 25 °C for 4 days and then maintained at 25 °C under a 16 h light/8 h dark cycle provided by fluorescent lamps (colour reference 835, colour temperature 3500K).

2.2.3 Transformation and Regeneration of Transgenic Plants

Transformation of tomato (*Solanum lycopersicum*) cv. Micro-Tom followed the Fraser Lab Tomato Transformation protocol (Royal Holloway, University of London) with minor amendments (Dan et al., 2006; H. J. Sun et al., 2006). To generate transgenic tomato plants, cotyledons of 2-week-old seedlings were cut at both ends in sterile condition to generate explants of about 5 mm and placed with the abaxial side down on a co-cultivation medium consisting of MS supplemented with Gamborg's Vitamin Solution (1 ml L^{-1}), 2,4-dichlorophenoxyacetic acid (0.2 mg L^{-1}), kinetin (0.1 mg L^{-1}), acetosyringone (0.1mM) and agar (8 g L^{-1}) and incubated for 24 hours at 25 °C in the dark. After the preculture period, the explants were co-cultivated with the *A. tumefaciens* suspension for 20 minutes at 28 °C and 50 rpm in the dark. Following the inoculation, the Agrobacterium solution was removed with a sterile pipette, and the explants were blotted dry with a sterile filter paper. The cotyledons were then co-cultured for 4 days at 25 °C in the dark. Four days after co-cultivation, the cotyledons were subcultured on to 2-Zeatin regeneration medium containing trans-zeatin-riboside (2.0 mg L^{-1}), Nitsch vitamin (x1000) (1.0 ml L^{-1}), indole-3-acetic acid (IAA) (0.1 mg L^{-1}), ticarcillin disodium/clavulanate potassium (300 mg L^{-1}) and kanamycin (50 mg L^{-1}). After 2 weeks on 2-Zeatin regeneration medium, explants were transferred to a second shoot induction medium, named 1-Zeatin regeneration medium, the same medium with different concentrations of trans-zeatin-riboside (1.0 mg L^{-1}) and kanamycin (100 mg L^{-1}). Explants were then subcultured to fresh media every 2 weeks. Approximately 4 to 6 weeks after transformation, cotyledons started forming shoots, which were individually removed and transferred to shoot elongation medium containing trans-zeatin-riboside (0.5 mg L^{-1}), Nitsch vitamin (x1000) (1 ml L^{-1}), ticarcillin disodium/clavulanate potassium (300 mg L^{-1}) and kanamycin (100 mg L^{-1}). After shoot elongation, shoots of 2-3 cm were then excised from the callus and transferred to rooting media containing IAA (1 mg L^{-1}), Nitsch vitamin (x1000) (1 ml L^{-1}), ticarcillin disodium/clavulanate potassium (300 mg L^{-1}) and kanamycin (50 mg L^{-1}) for 1 month without changing medium or until root developed. Rooted plantlets were gently washed with water to remove the remaining media and transferred to pots containing a mixture of compost and vermiculite (3:1) using Levington F2+S compost (The Scotts Company, Ipswich, UK) and vermiculite (Sinclair Pro, 2.0–5.0 mm; Cheshire, UK) and transferred to

covered propagators to ensure a high-humidity environment. Covers were progressively removed to allow acclimatisation to outer humidity (Cruz-Mendívil et al., 2011). Hardened transformants (T0 generation) were kept in greenhouse conditions at NIAB East Malling (day temperature 23 °C, night temperature 18 °C, 200 µmol m^{-2} s^{-1}).

2.3 Confirmation of Transgene Insertion By PCR

2.3.1 Genomic DNA Extraction

Genomic DNA of well-rooted tomato plants was extracted according to a method adapted from Edwards et al. (1991). For this, leaf samples were placed inside a sterile Eppendorf tube and macerated using a disposable grinder. Next, 400 µL of extraction buffer (200 mM Tris HCl, pH 7.5, 250 mM NaCl, 25 mM EDTA, 0.5% SDS) was added to the sample, and the tube was vortexed for 5 seconds. The extracts were centrifuged at 13,000 x *g* for 1 minute, and 300 µL of the supernatant was transferred to a fresh Eppendorf tube. The supernatant was then mixed with 300 µL isopropanol and incubated for 5 minutes at -20 °C. After 1 minute of centrifugation at 13,000 x *g*, the flowthrough was discarded, and 1 mL ethanol 70% was added. Centrifugation was repeated, and the ethanol was removed. The DNA pellet was then air-dried before 50 µL of sterile water was added to solubilise the gDNA.

2.3.2 PCR Verification of Transgene Insertion

PCR reactions using forward (KanF1-AAGATGGATTGCACGCAGGTTCTCC) and reverse (KanR1-AACGCTATGTCCTGATAGCGGTCC) primers for the kanamycin resistance gene present in all Level 2 constructs were performed to confirm transgene insertion. Primers were designed using NCBI Primer-Blast. PCR analysis was performed using BioMix™ Red (Meridian Bioscience, OH, USA). Samples consisted of 12.5 µL BioMix, 2.5 µL cDNA template, 9 µL dH2O, and 1.5 µL primer mix. The PCR reaction was as follows: 1x (95 °C for 5 min), 35x (95 °C for 30 sec, 60 °C for 30 sec, 72 °C for 30 sec) and 1x (72 °C for 5 mins). The PCR products were run for 60 minutes at 100V on a 1.5% agarose gel.

2.4 Quantification of Transgene Expression by qPCR

2.4.1 RNA Extraction

Three mature green fruits were collected for each plant, and pericarp tissue was ground to a powder in liquid nitrogen using a prechilled pestle and mortar. Samples were then stored at -80 °C until RNA extraction. Total RNA was isolated using the NucleoSpin® RNA kit (Macherey-Nagel, Düren, Germany) following the manufacturer's protocol. Briefly, up to 30 mg of pericarp tissue was lysed by adding 350 µL of Buffer RA1 and 3.5 µL of β-mercaptoethanol (β-ME) and vortexed vigorously to ensure complete disruption of cells. Cell debris was removed, and the lysate was cleared by centrifuging it at 11,000 × *g* for 1 minute using a NucleoSpin® Filter placed in a 2 mL collection tube. The flowthrough was transferred to a new 1.5 mL microcentrifuge tube, and 350 µL of 70% ethanol was added, mixed thoroughly by pipetting up and down, and then loaded onto a NucleoSpin® RNA column placed in a new collection tube. The column was centrifuged at 11,000 × *g* for 30 seconds, and the flowthrough was discarded. 350 µL of Membrane Desalting Buffer (MDB) was then added to improve RNA purity. To remove genomic gDNA contamination, 95 µL of DNase reaction mixture (10 µL rDNase in 90 µL reaction buffer) was then loaded directly onto the column and incubated at room temperature for 15 minutes. The membrane was washed in three steps:

1. 200 µL of Buffer RAW2 was added to the column and centrifuged at 11,000 × *g* for 30 seconds.
2. 600 µL of Buffer RA3 was added to the column and centrifuged at 11,000 × *g* for 30 seconds.
3. 250 µL of Buffer RA3 was added to the column and centrifuged at 11,000 × *g* for 2 minutes to ensure complete drying of the membrane, avoiding buffer remnants that could affect RNA quality.

RNA was eluted in 60 µL of RNase-free water, and the column was centrifuged at 11,000 × *g* for 1 minute. The RNA concentration and purity were assessed using a Nanodrop 1000 spectrophotometer (ThermoFisher Scientific), and the samples were stored at -80 °C for further analysis.

2.4.2 cDNA Synthesis

cDNA was synthesised using the UltraScript™ cDNA Synthesis Kit (PCR Biosystems, London, UK) following manual instructions. To do that, a master mix was prepared with 5x cDNA Synthesis Mix (4 µL), 20x UltraScript® Reverse transcriptase (RTase) for cDNA Synthesis (1 µL), 1,000 ng of total RNA, and dH_2O, adjusted to a final reaction volume of 20 µL. After that, the reaction was incubated at 42 °C for 15-30 minutes. Finally, RTase inactivation was performed at 85 °C for 10 minutes. cDNA was diluted 5x before use.

2.4.3 qPCR Analysis of Transgene Expression

Quantitative PCR (qPCR) was performed using 2x qPCRBIO SyGreen (Blue) Mix (PCR Biosystems, London, UK). Each qPCR reaction was prepared in a final volume of 20 µL, following the reaction set-up described in Table 2.6. Samples consisted of 10 µL 2x SyGreen Mix, 1.6 µL primer mix, 1 µL cDNA template, and 7.4 µL dH_2O. As a negative control, dH_2O alone was used. Reactions were performed using white half skirt 96-well plates (Sarstedt, Germany) and conducted using a Step One Plus Real Time PCR System (Thermo Fisher Scientific, USA). A melting curve was generated for each sample to ensure no unspecific products were amplified.

Table 2.6. qPCR Reaction setup.

Temperature	Time	Cycles
95° C	2 min	1
95° C	15 sec	40
60° C	30 sec	
60° C	1 min	1
95° C	15 sec	1

Primers for qPCR were designed using NCBI Primer-Blast (Table 2.7). Transgene primers were designed to span the region between the coding sequence and the terminator, ensuring primer specificity. For the design of tomato endogenous gene primers, both tomato (endogenous) and Arabidopsis (transgene) sequences were aligned, and primers were selected to target regions with low sequence similarity (up to 10 base pairs), ensuring endogenous gene specificity. *GAPDH* was selected as a housekeeping gene (Choi et al., 2018). Primers generated amplicons ranging

from 170 to 204 bp. Two complementary analyses were performed for transgene expression. First, transgene expression was quantified by qPCR and normalised to the housekeeping gene *GAPDH*. Relative levels were calculated using the $2^{-\Delta Ct}$ method and expressed as a percentage of *GAPDH* expression. This approach was used to confirm that transgene expression was detected in transgenic lines, whereas wild-type fruits showed no signal. In the second approach, expression values were further normalised to the wild-type endogenous gene (set to 1) using the ΔΔCt method and expressed as fold-change relative to endogenous wild-type.

Table 2.7. Primer sequences for qPCR.

Primer name	Sequence	Target	Species	Length
BpMADS qF BpMADS qR	CCACAACCTCTCCCGTGTTT GCGATCATAGGCTTCTCGCA	*BpMADS*	*Betula platyphylla*	*190 bp*
AtCGA1 qF AtCGA1 qR	TTACTGTTGAGCAAAAGTTCAGC CAAACTTAAGCACACAAGCTTTTTA	*AtCGA1*	*Arabidopsis thaliana*	*170 bp*
AtGNC qF AtGNC qR	CAAATTTTGCTTCGATGATTTGACA GCACACAAGCTTTTTATTTGACACA	*AtGNC*	*Arabidopsis thaliana*	*186 bp*
AtPDV1 qF AtPDV1 qR	GGCTACTAGTGAACATCATCTGC CACAAGCTTTTTATTTGACACACCA	*AtPDV1*	*Arabidopsis thaliana*	*191 bp*
AtPDV2 qF AtPDV2 qR	GCGATCATAGGCTTCTCGCA CCTACACCTGCTCCTCGTGT	*AtPDV2*	*Arabidopsis thaliana*	*180 bp*
SlGATA22 qF SlGATA22 qR	CCTACACCTGCTCCTCGTGT ATTGCTGCTTCCTTCTCATCCT	*SlGATA22*	*Solanum lycopersicum*	*170 bp*
SlGATA16 qF SlGATA16 qR	TGAGATGGAAGCAGCAATCCT ATTTCGTGACTCAACTTACTCTCA	*SlGATA16*	*Solanum lycopersicum*	*170 bp*
SlPDV1 qF SlPDV1 qR	CTGAGGGGTCATCATCCAGC ACTTGGTTTTCCCACCTCGG	*SlGATA21*	*Solanum lycopersicum*	*191 bp*
SlPDV2 qF SlPDV2 qR	TCCCCGTGGTTGAAAATGGT TTGTCAGGCCACACAGAGTT	*SlPDV2*	*Solanum lycopersicum*	*189 bp*
GAPDH qF GAPDH qR	GGCTGCAATCAAGGAGGAA AAATCAATCACACGGGAACTG	*GAPDH*	*Solanum lycopersicum*	*204 bp*

2.4.4 Copy Number

Transgene copy number was determined by AttoDNA (Norwich, UK) using real-time PCR assaying the presence of the kanamycin resistance gene.

2.5 Plant Growth Conditions

Following *agrobacterium*-mediated transformation (see section 2.2.3), T0 plants were grown in a controlled-environment growth chamber at NIAB at a photosynthetic photon flux density of 200 µmol m^{-2} s^{-1}, under a 16/8 h light/dark photoperiod, at 23 °C during the day and 18 °C at night, with 50% relative humidity. Selected independent tomato lines (T1 and T2 generation) were grown in a controlled-environment growth chamber at the University of Southampton under a 16/8 h light/dark photoperiod, at 23 °C during the day and 18 °C at night, with 50% relative humidity, and a photosynthetic photon flux density of 200 µmol m^{-2} s^{-1}. Tomato seeds were sown into 6 cm diameter pots containing a mixture of compost and vermiculite (3:1) using Levington F2+S compost (The Scotts Company, Ipswich, UK) and vermiculite (Sinclair Pro, 2.0–5.0 mm; Cheshire, UK). After two weeks, seedlings were transferred to 2 L pots containing Levington M3 compost (The Scotts Company, Ipswich, UK).

For the analysis of gas exchange, a T2 generation was grown at the University of Essex in a controlled-environment growth chamber under a 16/8 h light/dark photoperiod, at 25 °C, with 65% relative humidity, and a photosynthetic photon flux density of 250 µmol m^{-2} s^{-1} and ambient CO_2.

Flowers were marked at anthesis for fruit classification. Fruits were defined as immature green (IG, 7-10 days post-anthesis), mature green (MG, 20-23 days post-anthesis), and ripe (breaker +7-10 days), following Lupi et al. (2019), with minor adaptations. To minimise potential differences in development stage between genotypes, fruits were sampled across this defined developmental window rather than at a single fixed day. Sampling was randomised across wild-type, azygous, and transgenic lines, with fruits selected based on comparable developmental and visual maturity to ensure equivalent stage comparisons.

2.6 Microscopy Analysis

Mature green (MG) fruits were excised with a sterile razor blade (5 × 5 mm pericarp). Cells were then fixed in 3.5% glutaraldehyde solution for 1 hour in the dark. Fruit tissue was disrupted as follows: heat-treated at 65 °C in a solution of disodium EDTA (EDTA-Na_2; 0.1 M, pH 9.0) for 10 min, followed by maceration with clean forceps on glass microscope slides (Forth & Pyke, 2006; Pan et al., 2013). Samples were imaged using a Leica STELLARIS confocal laser scanning microscope mounted on a Leica DMi8 inverted microscope (Leica Microsystems, Germany), using Leica Application Suite X (LAS X) software v4.8.2.29567 (Pan et al., 2013; Shi et al., 2021). The emitted fluorescence of chloroplasts was collected at 650-750 nm using the following settings: 448-nm argon ion laser line, a 40×/1.25 glycerol-immersion objective, 1,024 x 1,024 resolution. To complement the fluorescence analysis, transmitted light images were simultaneously acquired using the same confocal settings (Pei et al., 2025). The images were then exported, and the size and number of the chloroplasts were analysed using Fiji/ImageJ (ImageJ v1.54f). Chloroplast number, chloroplast plan area, chloroplast coverage and chloroplast density were quantified. The chloroplast plan area was obtained by drawing around and measuring the outlines of clearly defined chloroplasts. Chloroplast coverage was calculated as the total plastid area divided by the cell plan area. Chloroplast density was calculated as the number of chloroplasts divided by the cell plan area (Pyke, 2011; Pyke & Leech, 1991). For each independent line, 10 chloroplasts were measured per cell, with at least six cells analysed from a minimum of three biological replicates.

2.7 Determination of Chlorophyll and Carotenoid Content in Green Fruit

Chlorophyll and carotenoids were extracted from both immature green (IG) and mature green (MG) fruits at the equatorial region of the pericarp (Hu et al., 2024; Lupi et al., 2019; Porra et al., 1989; Rangani et al., 2019). For the extraction, 200 mg of fresh tissue was extracted in 2 ml of pre-chilled N,N-dimethylformamide (DMF) and left incubating in the dark overnight at 4 °C. Undissolved debris was removed by centrifugation at 15,000 × *g* for 15 min at 4 °C. Measurements were performed using a VWR® P4 UV/Visible Spectrophotometer (Avantor, UK).

For chlorophyll, spectrophotometer measurements were performed at 664 and 647 nm and chlorophyll content were determined as:

$$\boldsymbol{Chlorophyll\ a}\ (\mu g/g) = [(12 * Abs664) - (3.11 * Abs647)] * (V / W)$$

$$\boldsymbol{Chlorophyll\ b}\ (\mu g/g) = [(20.78 * Abs647) - (4.88 * Abs664)] * (V / W)$$

Where V = volume of the extract (mL) and W = weight of fruit material (g). Total chlorophyll was then obtained by adding the obtained values (Lupi et al., 2019).

For carotenoids, spectrophotometer measurements were performed at 664 and 461 nm and total carotenoid content was determined as:

$$\boldsymbol{Carotenoids}\ (\mu g/g) = [Abs461 - (0.046 * Abs664)] * 4 * (V / W)$$

Where V = volume of the extract (mL) and W = weight of fruit material (g) (Chamovitz et al., 1993).

2.8 Determination of Lycopene and β-carotene Content in Ripe Fruit

Lycopene and β-carotene measurements were extracted from ripe fruits at the equatorial region of the pericarp (Pan et al., 2013). Lycopene and β-carotene content were measured according to the method proposed by Anthon & Barrett (2007). For the extraction, 100 mg of the sample was ground in liquid nitrogen. Then, 8 mL of a hexane/ethanol/acetone mixture (2:1:1, v/v/v) was added to the homogenised samples. The mixture was vortexed and incubated at room temperature in the dark for one hour. Next, 1 mL of distilled water was added, followed by vortexing and a 10-minute incubation at room temperature in the dark. Spectrophotometer measurements were performed at 503 and 444 nm. The contents of lycopene and β-carotene were determined as:

$$\boldsymbol{Lycopene}\ (\mu g/g) = (6.95 * Abs503 - 1.59 * Abs444) * 0.55 * 537 * V / W$$

$$\boldsymbol{\beta - carotene}\ (\mu g/g) = (9.38 * Abs444 - 6.70 * Abs503) * 0.55 * 537 * V / W$$

Where V = volume of the extract (mL), W = weight of fruit material (g) and 537 = the molecular weights of lycopene and β-carotene (g/mole). The ratio of the final hexane layer volume to the volume of mixed solvents added is 0.55 for hexane/ethanol/acetone (2:1:1).

2.9 Chlorophyll Fluorescence Measurements

Immature green (IG) and mature green (MG) fruits were harvested from tomato plants grown at the University of Southampton and transported to the University of Essex for chlorophyll fluorescence analysis. Analyses were performed on the same day, with fruits maintained in darkness during transport to minimise light-induced physiological changes. Photosynthetic activity was assessed using a HEXAGON-IMAGING-PAM system (Walz, Germany). For measurements, fruits were placed inverted (bottom facing upward) on a black, non-fluorescent background within the imaging chamber and dark-adapted for 30 min prior to measurement. An initial baseline fluorescence (F_o) and maximum fluorescence (F_m) were recorded using a saturating pulse following dark adaptation. Light response curves were subsequently performed with the samples being exposed to a sequence of increasing actinic light intensities (100-1416 µmol m^{-2} s^{-1}). Each light step was maintained for approximately 2 minutes (until steady-state fluorescence (F') was reached), with a saturating pulse applied at the end of each step. Fluorescence parameters measured included the maximum quantum yield of PSII (F_v/F_m), effective quantum yield of PSII (ΦPSII), electron transport rate (ETR), the coefficient of photochemical quenching (qL), and the coefficient of non-photochemical quenching (qN). All fluorescence parameters were calculated automatically using the ImagingWin software v2.57.q30, and values were exported for subsequent statistical analysis. At least four biological replicates were analysed per genotype, with two fruits sampled from each plant. Fluorescence measurements were obtained from individual fruits, and the total number of fruits analysed therefore varied between experiments. For a list of chlorophyll fluorescence parameters to be studied, see Table 2.8.

Table 2.8. Chlorophyll fluorescence parameters. Descriptions of key parameters measured, including their calculation where applicable.

Parameter	Calculation	Definition
F_O	Measured	Baseline fluorescence of dark-adapted tissue with all reaction centres open
F_m	Measured	Total fluorescence after saturating light pulse for dark-adapted plants
F’	Measured	Baseline fluorescence of the system under actinic light

F_m'	Measured	Total fluorescence after saturating light pulse for plants exposed to actinic light
F_v	$F_m - F_O$	Change in fluorescence caused by closing of all reaction centres in dark-adapted plants
F_q'	$F_m' - F'$	Change in fluorescence caused by closing of reaction centres in plants exposed to actinic light
F_O'	Can be measured. Calculated as: $F_O/[(F_v/F_m) + F_o/F_m']$	Baseline fluorescence of light-adapted leaves with all reaction centres open
F_v'	$F_m' - F_O'$	Change in fluorescence caused by the closing of all reaction centres in light-adapted plants
F_v/F_m	N/A	Maximum quantum yield of PSII
F_v'/F_m'	N/A	Maximum operating efficiency of PSII efficiency in the light with all reaction centres open
ΦPSII	F_q'/F_m'	Effective PSII quantum yield
qP	F_q'/F_v'	Coefficient of photochemical quenching, qP
qL	$qP \times (F_O'/F)$	Coefficient of photochemical quenching, qL
qN	$1 - (F_v' / F_v)$	Coefficient of non-photochemical quenching, qN
ETR	$0.5 \times \Phi PSII \times P\ AR \times 0.84$	Electron transport rate

2.10 Gas Exchange Analysis

Gas exchange analysis was performed on mature green (MG) fruits of T2 generation plants grown at the University of Essex. Gas exchange was recorded with a portable infrared gas analyser (LI-6400, LI-COR Biosciences) equipped with a custom chamber for non-foliar tissues. The chamber block temperature was set to 23 °C, airflow was maintained at 500 µmol s^{-1}, and a vapour pressure deficit (VPD) of 1.15 ± 0.05 kPa. Measurements were performed in two phases:

Light-response curves (A/Q):

1. Reference CO_2 concentration (Ca) fixed at 400 µmol mol^{-1}.
2. Actinic light (PPFD) sequentially stepped to 200, 500, and 800 µmol m^{-2} s^{-1}.

3. At each step, net CO_2 assimilation (A) was recorded after stabilisation, which typically required approximately 10 minutes per measurement.

CO_2 response curves (A/Ci):

1. Saturating irradiance fixed at 800 µmol m^{-2} s^{-1}.
2. Reference CO_2 (Ca) sequentially set to 200, 400, and 1500 µmol mol^{-1}.
3. At each step, net CO_2 assimilation (A) was recorded after stabilisation, which typically required approximately 10 minutes per measurement

Four biological replicates, each consisting of three fruits, were used per genotype. Data were initially normalised to both fruit surface area and weight, with no differences observed between the two approaches. Thus, fruit weight was selected as the basis for normalisation in subsequent experiments.

2.11 Phylogenetic Analysis

Amino acid sequences were derived from coding DNA sequences using the ExPASy Translate tool (https://web.expasy.org/translate/), accessed in July 2025. The predicted BpMADS protein sequence was used as a query in BLASTP searches against the NCBI protein database to identify putative homologous MADS-box proteins, including tomato sequences. Representative proteins were selected as the top-scoring BLASTP hit per species. Where multiple high-scoring hits were identified within a single species, only the highest-scoring sequence was retained. Sequence alignments were generated using the MUSCLE algorithm with default parameters in MEGA version 11.0.13. Phylogenetic trees were constructed using the maximum likelihood method with 1000 bootstrap replicates and are presented as unrooted phylograms, as no outgroup was specified (Du et al., 2022).

2.12 Statistical Analyses

All statistical analyses were conducted in R (version 4.3.1; R Core Team, 2023) using RStudio (Posit Software, PBC). Data were inspected for normality and homogeneity of variance before hypothesis testing. Where assumptions of normality were met, comparisons between groups under a single experimental factor were performed using one-way analysis of variance (ANOVA) followed by Duncan's Multiple Range test (Hu et al., 2024). Where assumptions were violated,

Kruskal-Wallis was applied, followed by Dunn's post hoc test (Liu, 2015). For microscopy parameters involving a single experimental factor, a nested one-way ANOVA was employed to test for an overall genotype-type effect while accounting for line-to-line variation within each genotype type. For pigment content and chlorophyll fluorescence parameters, where developmental stage was also considered, a two-way nested ANOVA was performed. Developmental stage (immature green vs mature green) and genotype type (control vs transgenic) were treated as fixed factors, with genotype (line) nested within genotype type, for the analysis of main effects and interaction between stage and genotype. Model fitting for the relationship between chloroplast coverage and chlorophyll content was performed using linear regression (lm) in R, based on genotype mean values. Coefficients of determination (R^2) and p-values associated with the regression slope were calculated.

Chapter 3 Genetic Transformation of Tomato cv. Micro-Tom

3.1 Introduction

To comprehensively study the role of fruit photosynthesis in fruit development and the plant's carbon economy, a range of transgenic plants overexpressing key genes involved in chloroplast biogenesis and division were developed for the study. A MADS-box gene *(BpMADS)* from Birch was selected due to its potential to produce plants with enhanced chloroplast growth, chlorophyll content and higher photosynthetic rates (Qu et al., 2013). In addition, the GATA transcription factors *CGA1/GNC* (An et al., 2020; Chiang et al., 2012; Hudson et al., 2011), which regulates chlorophyll biosynthesis and the Plastid Division components *PDV1*/*PDV2* (Miyagishima et al., 2006; Sun et al., 2020), were selected to investigate the role of fruit chloroplast development on the fruit's photochemical capacity and nutritional quality. The aim of this chapter is to detail the work undertaken to assemble the overexpression constructs and transform tomato with the selected genes of interest. Notable challenges and methods of troubleshooting are also explored.

3.2 Results

3.2.1 Construct Assembly

3.2.1.1 Level 1 Modules

The initial step in assembling the constructs was to generate level 1 modules from the appropriate combination of compatible level 0 parts using the *BsaI* Golden Gate reaction (Weber et al., 2011). The full-length coding sequences of *Betula platyphylla* (Birch) *BpMADS* (GenBank No. EE284583), *Arabidopsis thaliana* (Arabidopsis) *AtCGA1* (AT4G26150), *AtGNC* (AT5G56860), *AtPDV1* (AT5G53280) and *AtPDV2* (AT2G16070) were used to generate six level 1 modules. All constructs were driven by fruit-specific promoters: *SlTFM7* (Santino et al., 1997), an early-specific promoter, used for *BpMADS*, *AtCGA1*, *AtPDV1*; *LesAffx.6852.1.S1_at* (hereafter *SlAFF*) (Hiwasa-Tanase et

al., 2012), an early-specific promoter, used for *AtGNC* and *AtPDV2*; *CaFIB* (Kuntz et al., 1998), a ripening-specific promoter, used for a second *BpMADS* construct.

The level 1 destination vector contains flanking *DraIII* digestion sites, providing predictable digestion bands to screen for the correct assembled constructs. After assembly and transformation into *E. coli*, the constructs were screened for the presence of the recombinant plasmid using the blue-white selection method (Engler & Marillonnet, 2014) (Figure 3.1).

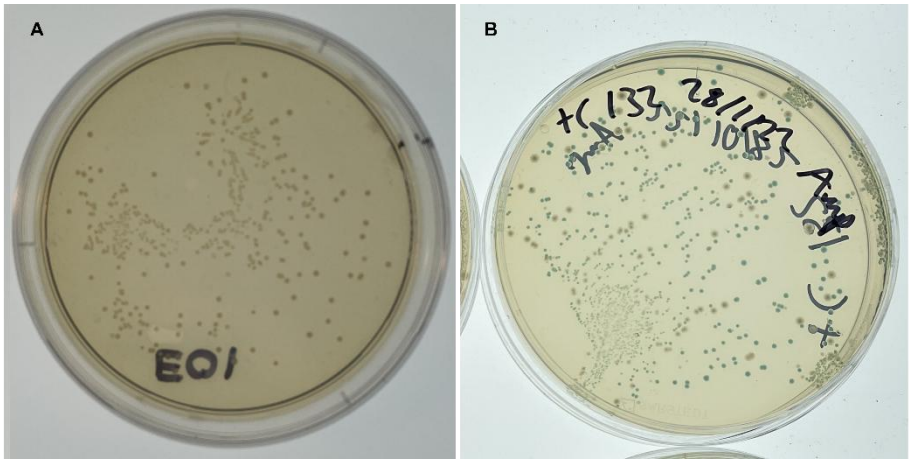

Figure 3.1. Identification of transformed *E. coli* competent cells in level 1 constructs. The blue-white selection method was used**.** Level 1 destination vector contains a *lacZα* fragment to allow the selection of correctly assembled constructs. (A) The colonies formed by non-recombinant cells, therefore, appear blue, while the recombinant cells appear white. (B) Blue colonies containing the Level 1 destination vector, which still contains the intact Lac operon.

Independent white colonies containing the desired plasmid were isolated and subject to plasmid extraction for the putative correctly assembled level 1 module. The presence of the insertion was confirmed either via *DraIII* restriction digestion (Figure 3.2), as the level 1 destination vector harbours its respective restriction sites flanking the Golden Gate insertion site, thus producing predictable banding patterns for correctly assembled modules, or by sequencing and analysis using SnapGene® software.

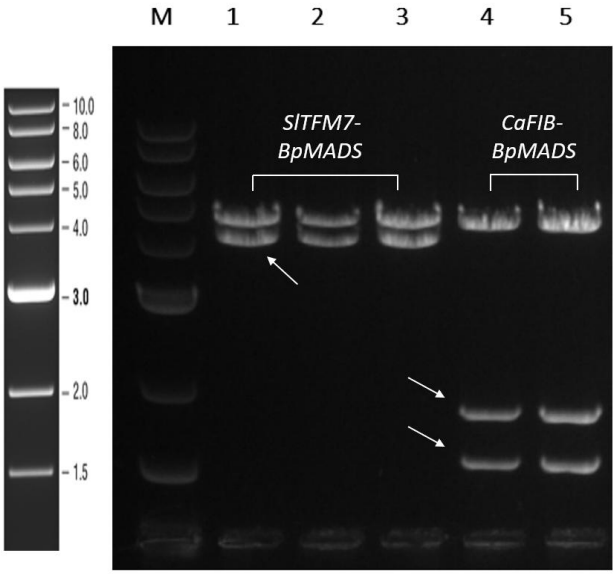

Figure 3.2. Restriction analysis of purified plasmids. *BpMADS* constructs under transcriptional control of *SlTFM7* early fruit-specific promoter and *CaFIB* ripening fruit-specific promoter**.** Digestion generated the expected 4.3-kb bands for the vector. Lanes 1, 2 and 3: DraIII activity generated 3.8-kb for the *SlTFM7-BpMADS* early fruit-specific. Lanes 4 and 5: DraIII activity generated two bands of 1.8 Kb and 1.5 Kb for the *CaFIB-BpMADS* ripening fruit-specific. The arrows highlight the corresponding bands from the digestion for each construct. Lane M: 10-kb DNA Ladder.

3.2.1.2 Level 2 Modules

The recombinant plasmids encoding the overexpression cassette of the genes of interest were then assembled into level 2 constructs via *BbsI* activity. For that, the kanamycin resistance level 1 module and the recombinant plasmids were cloned into a level 2 destination vector, followed by the appropriate end-linker. After transformation into *E. coli* competent cells, the two constructs were screened for the presence of the recombinant plasmid using the red-white selection method (Figure 3.3). Efficiency levels were higher in the level 1 assembly, with plates displaying fewer non-transformed colonies.

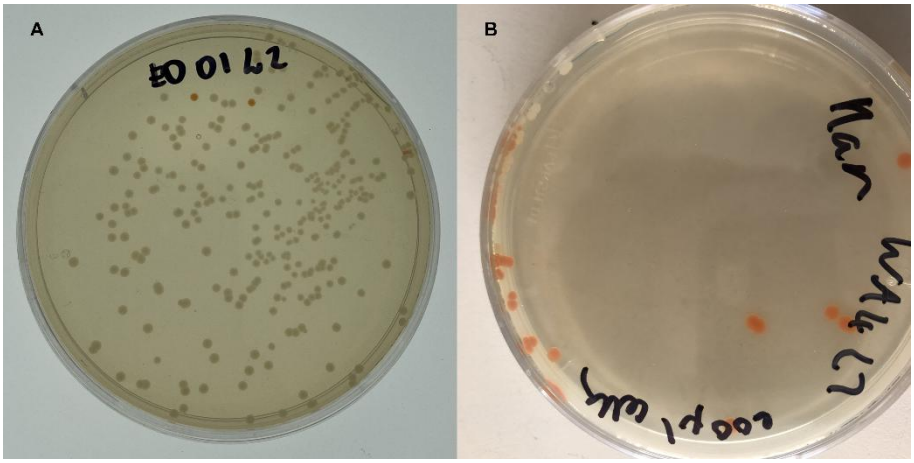

Figure 3.3. **Identification of transformed *E. coli* competent cells with the level 2 constructs.** The red-white selection method was used**.** (A) Level 2 destination vectors contain a red selectable marker (a bacterial operon for canthaxanthin production). Therefore, the colonies formed by non-recombinant cells appear red while the recombinant cells appear white. (B) Colonies formed by non-recombinant cells.

3.2.1.3 Construct Maps

All level 2 constructs were verified by sequencing (primers described in Chapter 2, Section 2.1.5, Table 2.5) and analysed using SnapGene® software. Two different constructs were designed for *BpMADS*, each driven by a promoter activated at a different developmental stage: *SlTFM7* targeting early fruit development and *CaFIB* targeting ripening tomato fruit. In tomato, the *SlTFM7* promoter acts predominantly during early fruit development, with weak expression in the ripe fruit and very weak/undetectable in leaves (Conner, 1997; Santino et al., 1997). The *CaFIB* promoter is expressed at high levels at the onset of fruit ripening (Kuntz et al., 1998; Smirnova & Kochetov, 2020). Both constructs included an *octopine synthase* (*OCS*) terminator and the *nptII* gene, conferring kanamycin resistance as a selective marker. Constructs will be referred to as e-*BpMADS* and r-*BpMADS* to differentiate between early and ripening expression. Construct maps are shown in Figures 3.4 and 3.5.

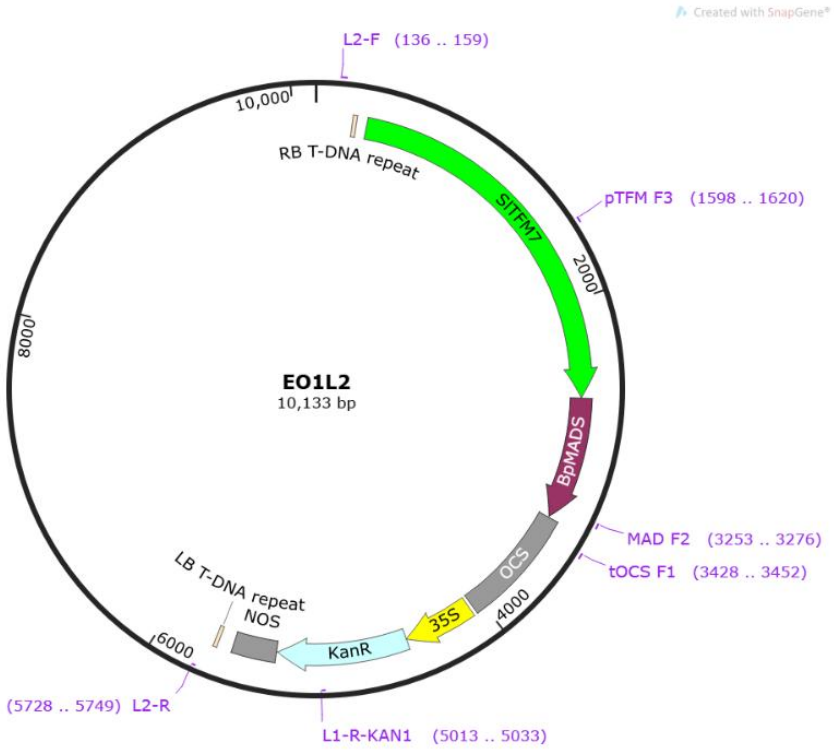

Figure 3.4. Map of the *BpMADS* early fruit-specific overexpression construct. Map of the MADS-box overexpression construct comprising the *BpMADS* overexpression cassette under the control of *SlTFM7* early fruit-specific promoter (e-*BpMADS*) and the kanamycin resistance module under the control of *CaMV35S* constitutive promoter. The DNA situated between the right border (RB) and left border (LB) T-DNA repeat was randomly inserted into the plant genome. Locations of primers used for sequencing are shown in purple.

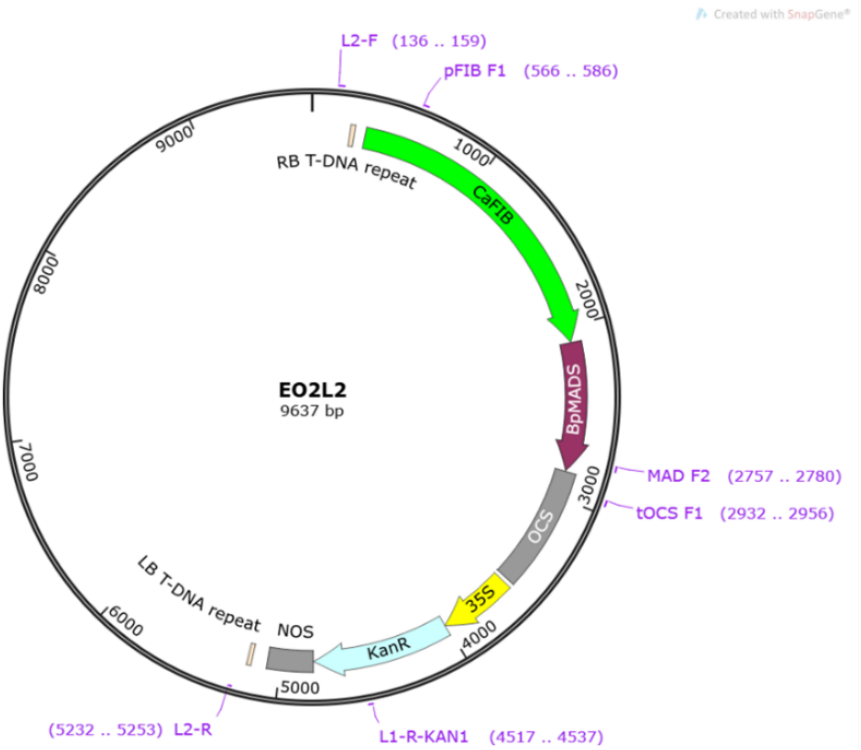

Figure 3.5. Map of the *BpMADS* ripening fruit-specific overexpression construct. Map of the MADS-box overexpression construct comprising the *BpMADS* overexpression cassette under the control of *CaFIB* ripening fruit-specific promoter (r-*BpMADS*) and the kanamycin resistance module under the control of the *CaMV35S* constitutive promoter. The DNA situated between the right border (RB) and left border (LB) T-DNA repeat was randomly inserted into the plant genome. Locations of primers used for sequencing are shown in purple.

The *AtCGA1* overexpression cassette was driven by the *SlTFM7* early fruit-specific promoter and the *AtGNC* by the *SlAFF* early fruit-specific promoter. In tomato, *SlAFF* has been reported to be strongly expressed in green fruit, with mild expression in red fruit, weak in the flower and undetectable in other tissues (Hiwasa-Tanase et al., 2012). Both constructs included a *heat shock protein 18.2* (*HSP*) terminator (Nagaya et al., 2010) and the *nptII* gene. Constructs will be referred to as e-*AtCGA1* and e-*AtGNC*. Construct maps are shown in Figures 3.6 and 3.7.

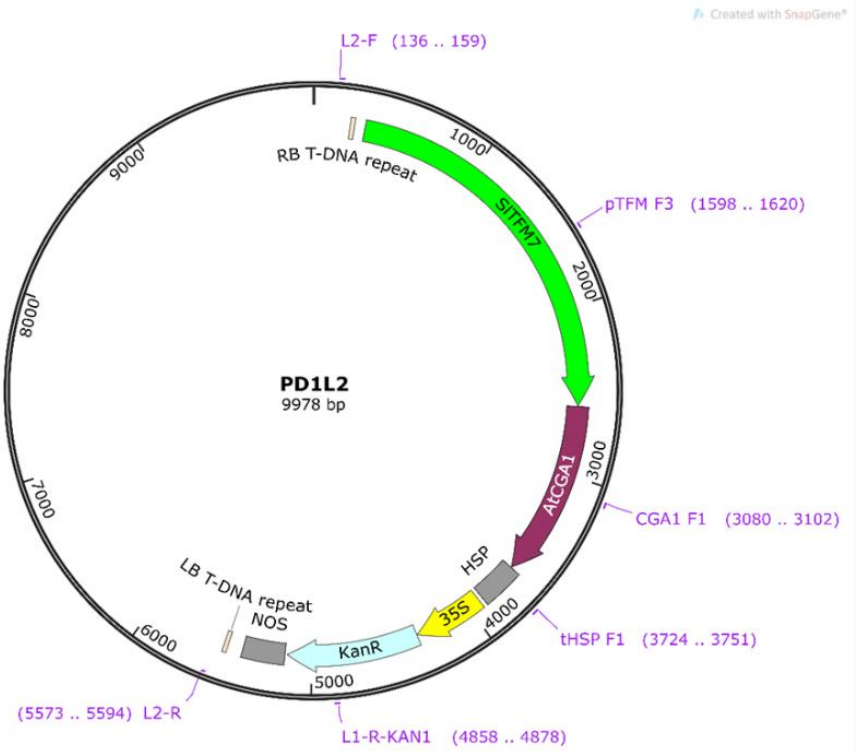

Figure 3.6. Map of the *AtCGA1* early fruit-specific overexpression construct. Map of the GATA overexpression construct comprising the *AtCGA1* overexpression cassette under the control of the *Solanum lycopersicum SlTFM7* early fruit-specific promoter (e-*AtCGA1*) and the kanamycin resistance cassette under the control of *CaMV35S* constitutive promoter. The DNA situated between the right border (RB) and left border (LB) T-DNA repeat was randomly inserted into the plant genome. Locations of primers used for sequencing are shown in purple.

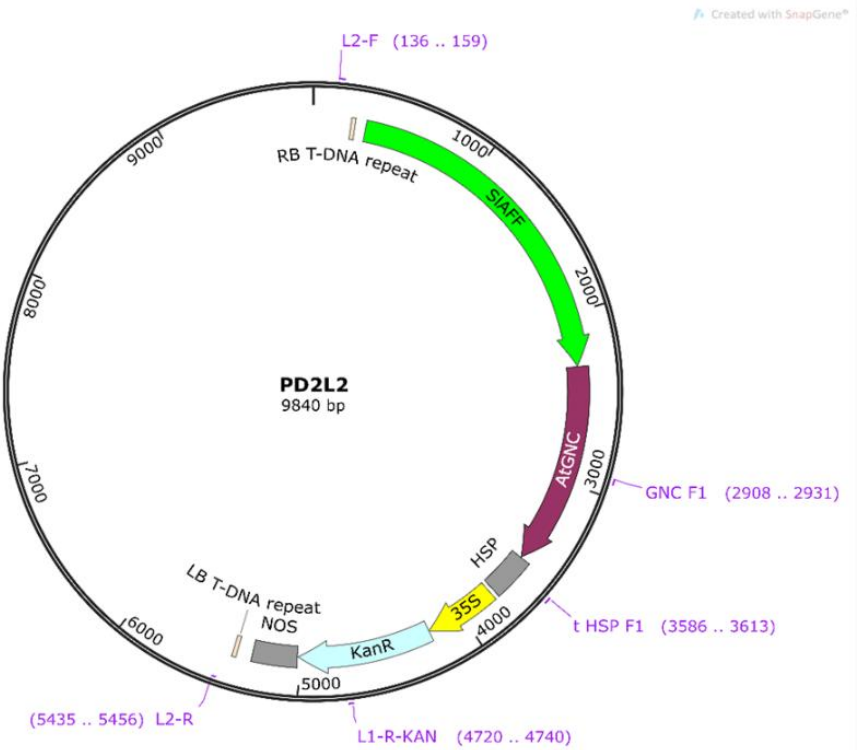

Figure 3.7. Map of the *AtGNC* early fruit-specific overexpression construct. Map of the GATA overexpression construct comprising the *AtGNC* overexpression cassette under the control of *SlAFF* early fruit-specific promoter (e-*AtGNC*) and the kanamycin resistance module under the control of *CaMV35S* constitutive promoter. The DNA situated between the right border (RB) and left border (LB) T-DNA repeat was randomly inserted into the plant genome. Locations of primers used for sequencing are shown in purple.

The plastid division overexpression constructs were assembled using the full-length coding sequence of *AtPDV1* under the control of the *SlTFM7* early fruit-specific promoter and *AtPDV2* driven by the *SlAFF* early fruit-specific promoter (e-*AtPDV1/PDV2*). The construct also included a *heat shock protein 18.2* (*HSP18.2*) terminator for *AtPDV1* and a *nopaline synthase* (*NOS*) terminator for *AtPDV2* and the *nptII* gene. Construct will be referred to as e-*AtPDV1/PDV2*. The construct map is shown in Figure 3.8.

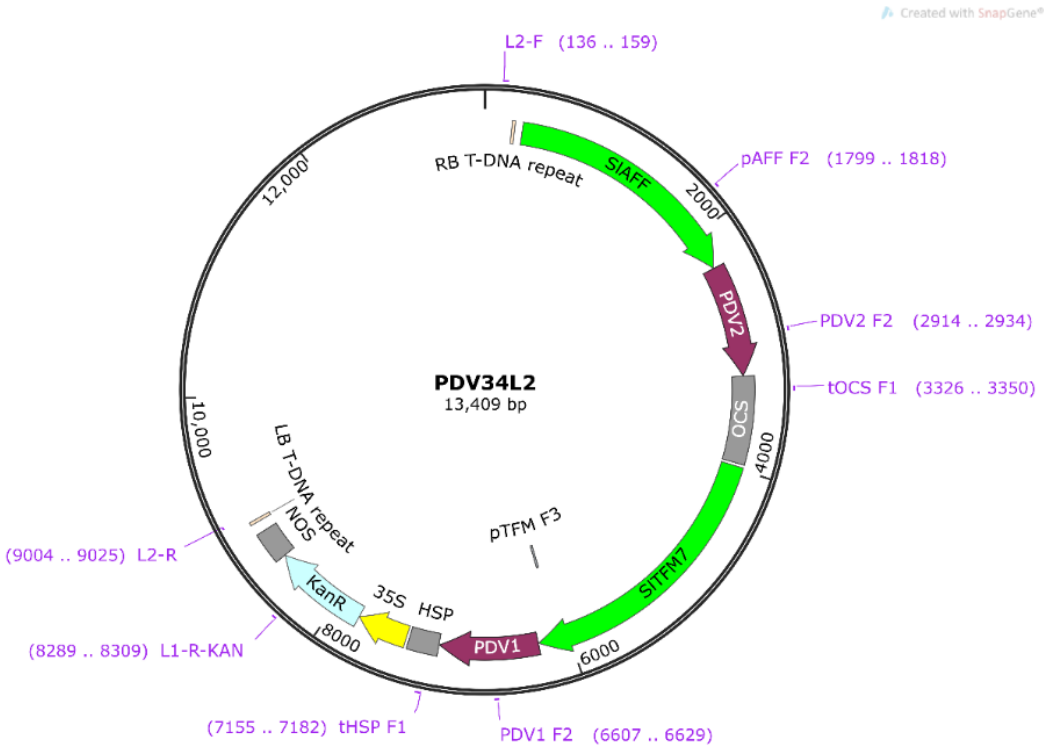

Figure 3.8. Map of the *AtPDV1/PDV2* early fruit-specific overexpression construct. Map of the plastid division overexpression construct comprising the *AtPDV1* overexpression cassette under the control of *SlTFM7* early fruit-specific promoter, *AtPDV2* under the control of *SlAFF* early fruit-specific promoter (e-*AtPDV1/PDV2*) and the kanamycin resistance module under the control of *CaMV35S* constitutive promoter. The DNA situated between the right border (RB) and left border (LB) T-DNA repeat was randomly inserted into the plant genome. Locations of primers used for sequencing are shown in purple.

3.2.2 *Agrobacterium*-mediated Genetic Transformation of Tomato

The *Agrobacterium tumefaciens* strain EHA105 was transformed with the binary vector containing the genes of interest and the *nptII* gene, which confers kanamycin resistance (Figure 3.9A). After selection on Luria-Bertani (LB) low salt medium containing kanamycin and rifampicin, *Agrobacterium* from a single colony harbouring the plasmid of interest was grown overnight. The bacterial culture was then used for the inoculation of the explants. Cotyledons of 2-week-old seedlings were infected with the bacterial suspension and co-cultivated for four days (Figure 3.9B). The kanamycin selective pressure was applied immediately after co-cultivation. It was observed that transformed explants developed calluses in the selection medium (Figure 3.9C). In contrast, non-transformed cells failed to regenerate and gradually lost their green colour, dying after a few weeks. Approximately 4 to 6 weeks after transformation, cotyledons started forming shoots (Figure 3.9D).

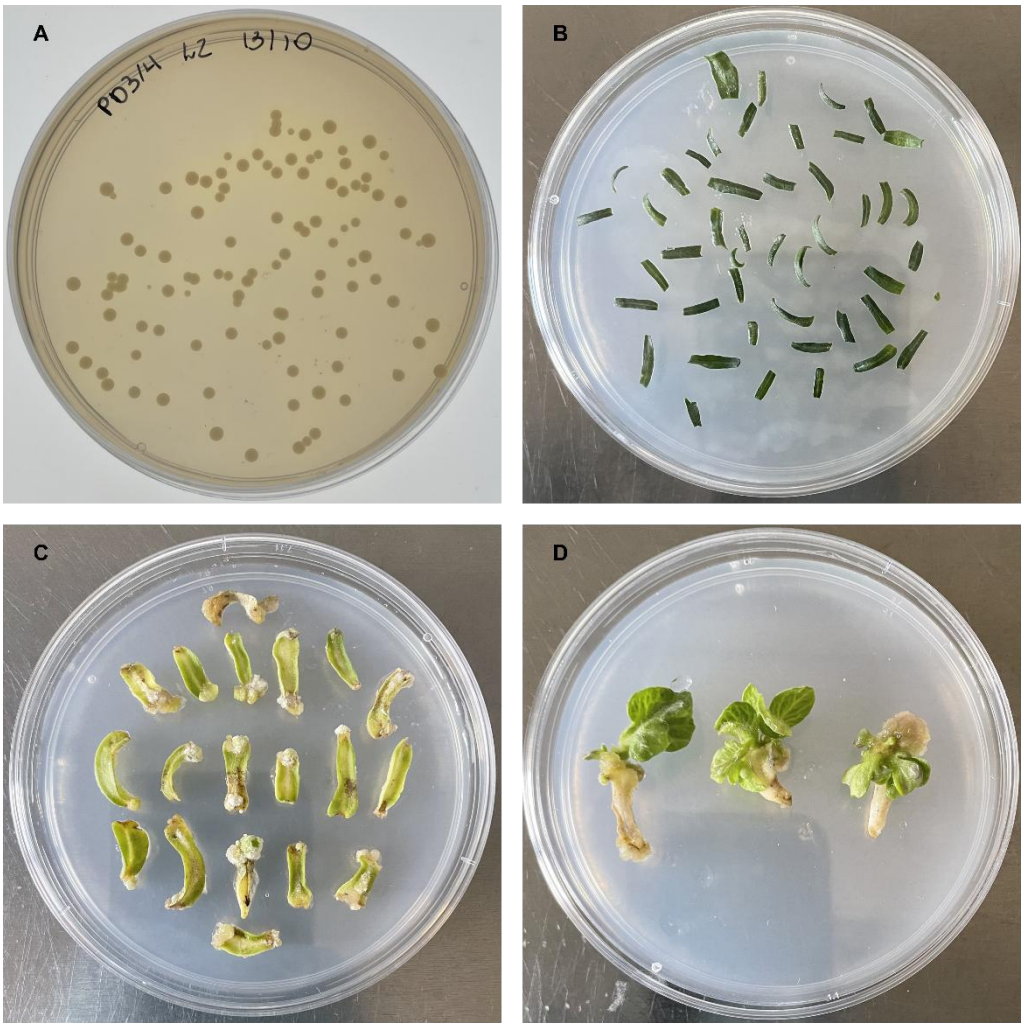

Figure 3.9. Transformation of wild-type tomato (*Solanum lycopersicum*) cv. Micro-Tom. (A) Successfully transformed *Agrobacterium tumefaciens* strain EHA105. (B) 2-week-old cotyledons on co-cultivation medium. (C) Explants on callus induction medium four weeks after inoculation. (D) Shoot formation after six weeks.

Individual shoots were removed and transferred to a shoot elongation medium (Figure 3.10A). Shoot elongation took approximately four to six weeks, and the shoots that survived the kanamycin selection were then subjected to a final selection stage consisting of a rooting medium. Development of roots and new leaves was observed after four weeks (Figure 3.10B). Independent tomato lines were then transplanted into soil and acclimatised. Hardened plants were kept in greenhouse conditions.

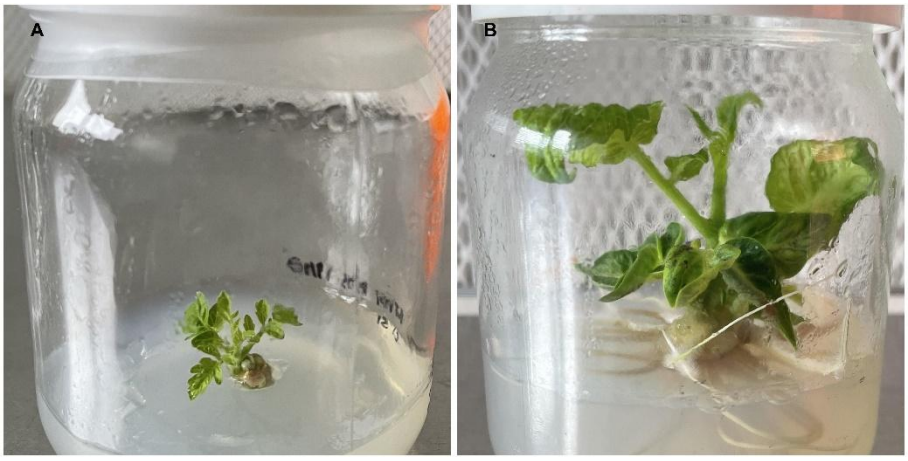

Figure 3.10. Transformation of wild-type tomato (*Solanum lycopersicum*) cv. Micro-Tom. (A) Shoots were individually removed and transferred to a shoot elongation medium. (B) Root induction 16 weeks after inoculation.

3.2.3 Confirmation of Transgene Insertion

DNA was extracted from a single leaf of well-rooted tomato plantlets to screen the transgene insertion. PCR reactions were performed using a set of primers for the kanamycin resistance gene (described in Chapter 2, Section 2.3.2, Table 2.6). The primers were designed to amplify a band only when a copy of the transgene is present in the sample. Based on this, PCR analysis of the WT plant did not yield a band, while the transgenic plants produced a fragment of around 650 base pairs (Figure 3.11)

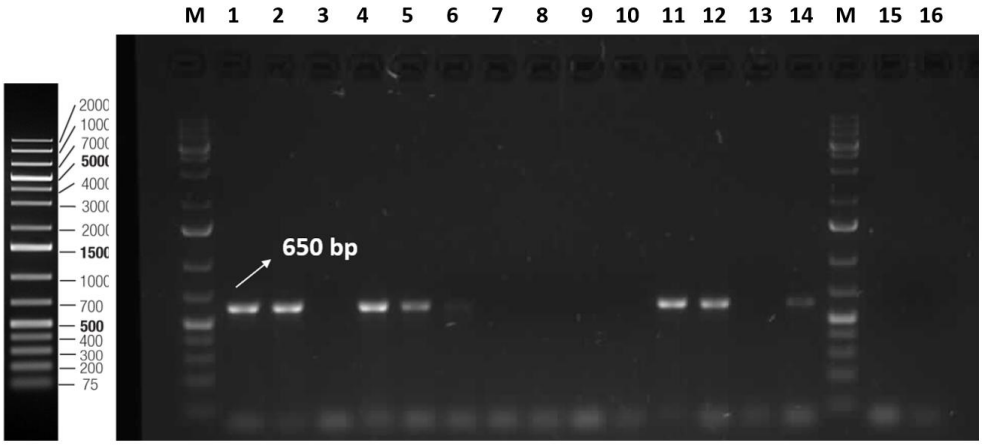

Figure 3.11. PCR amplification of the kanamycin resistance gene. Positive results from transgenic plants displayed a banding pattern of around 650 bp. Two negative controls were used, DNA extracted from leaves of wild-type tomato (*Solanum lycopersicum*) cv. Micro-Tom (lane 15), and water (lane 16). Lane M: 1-kb Plus DNA Ladder (Invitrogen, UK).

3.2.4 Confirmation of Transgene Expression

To analyse the expression of the transgene, total RNA was extracted from three tomato fruits from each independent line, and cDNA was amplified using qPCR. Green fruits were used for e-*BpMADS, e-AtCGA1, e-AtGNC, and e-AtPDV1/PDV2,* and ripe fruits for r-*BpMADS*. All qPCR results were normalised using *GAPDH* as a housekeeping gene, as *GAPDH* has been previously described as a stable and reliable internal control system to profile gene expression throughout fruit development (Choi et al., 2018). Two complementary analyses were performed for transgene expression. First, transgene expression was quantified by qPCR and normalised to the housekeeping gene *GAPDH* (expressed as % of *GAPDH*). This approach was used to confirm that transgene expression was detected in independent lines, whereas wild-type fruits showed no amplification. Second, expression values were further normalised to the wild-type endogenous gene (set to 1), using the ΔΔCt method, reported as fold-change relative to wild-type endogenous gene. For *BpMADS*, only the first approach was applied, as its closest tomato homologue is not expressed in fruit tissue. Transgene expression was used to support the selection of independent lines, ensuring that the transgene was being expressed. It is important to note that the selection of lines was also subjected to overall plant health and seed viability.

3.2.4.1 *BpMADS* Expression

The highest expression driven by *SlTFM7* was observed in e-*BpMADS* 27 and 34, with transcript levels equivalent to approximately 259% and 131% of *GAPDH*, respectively. In contrast, lines 1, 20, and 43 exhibited lower levels, less than 1% relative to the housekeeping gene (Figure 3.12A). These results reveal substantial variability in transgene expression across independent lines and support the selection of genotypes with a range of expression levels for downstream phenotypic characterisation. For instance, e-*BpMADS* 12 exhibited expression at around 6.72 ± 1.02% of *GAPDH*, while e-*BpMADS* 21 showed expression at 9.71 ± 1.20%. Relative expression was 28.3 ± 1.76% in e-*BpMADS* 10 and 71.1 ± 11.1% in e-*BpMADS* 25. A similar range was observed in the ripening-specific lines: r-*BpMADS* 16 showed relatively lower expression (6.28 ± 0.57%) compared to r-*BpMADS* 25, which exhibited 30.0 ± 12.4%. In contrast, r-*BpMADS* 8 exhibited the highest expression among all lines, corresponding to approximately 360% of *GAPDH* (Figure 3.12B).

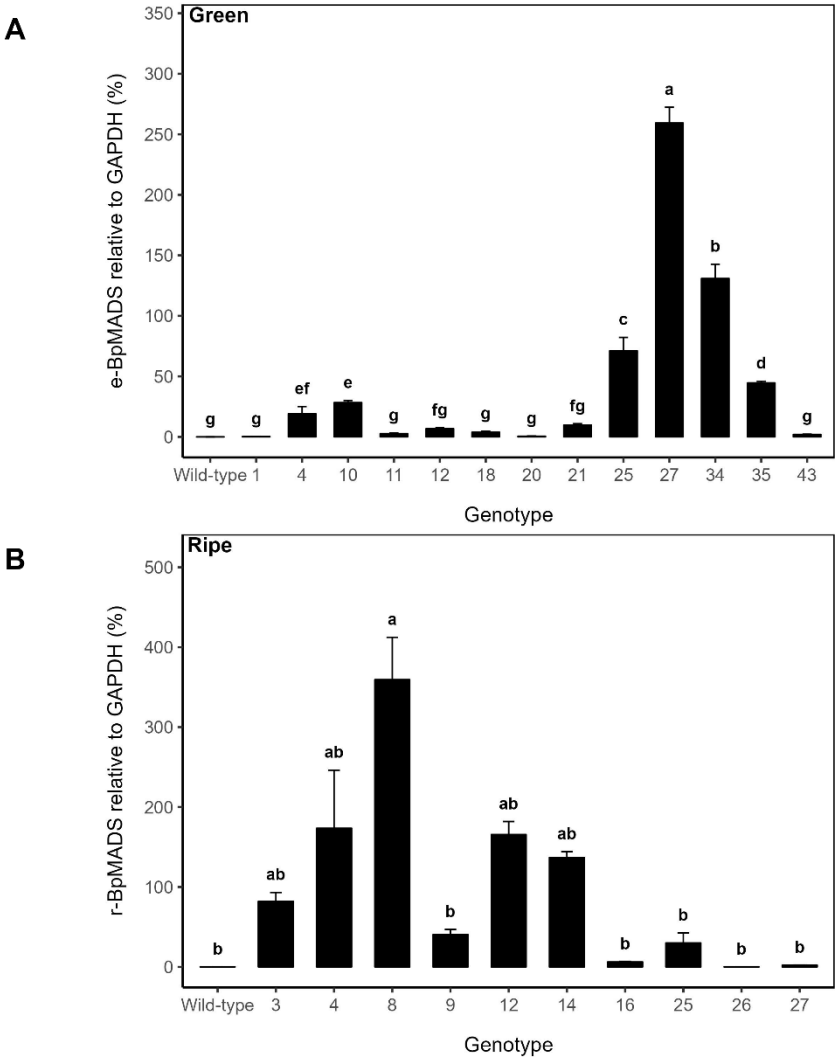

Figure 3.12. Relative *BpMADS* expression in transgenic Micro-Tom tomato genotypes. Bar charts show relative transcript levels of *BpMADS* in independent transgenic lines, quantified by qPCR and normalised to the housekeeping gene *GAPDH*. (A) *BpMADS* expression driven by *SlTFM7* early fruit-specific promoter (e-*BpMADS*). (B) *BpMADS* expression driven by *CaFIB* ripening fruit-specific promoter (r-*BpMADS*). All values represent means ± SE from three biological replicates per genotype, each analysed in three technical replicates. Statistically significant differences were determined using a 1-way ANOVA followed by Duncan's multiple range test. Different letters indicate statistically significant differences ($P<0.05$).

One limitation is that this approach assumes consistent PCR amplification efficiency across all samples and stable expression of the reference gene. However, it is important to note that *GAPDH* is one of the most abundantly and stably expressed housekeeping genes in tomato and is commonly used as a reference for gene expression studies (Wieczorek et al., 2013). Lines were selected to represent a range from low to high expression, and their transgene copy number was subsequently assessed (Tables 3.1 and 3.2).

Table 3.1. Transgene copy number in e-*BpMADS*. *BpMADS* genotypes driven by *SlTFM7* early fruit-specific promoter.

Genotype	Copy Number
21	1
25	3
4	4
35	4
12	7
10	12

Table 3.2. Transgene copy number in r-*BpMADS*. *BpMADS* genotypes driven by *CaFIB* ripening fruit-specific promoter (r-*BpMADS*).

Genotype	Copy Number
16	1
4	2
8	2
25	2
27	2

Transgenic lines e-*BpMADS* 10, 12, 21, and 25 were selected for biochemical and physiological analysis of early-specific *BpMADS* expression (e-*BpMADS*), while r-*BpMADS* 8, 16, and 25 were chosen for ripening-specific *BpMADS* expression (r-*BpMADS*), alongside azygous plants (null segregants).

3.2.4.2 *AtCGA1* and *AtGNC*

In the early-specific e-*AtCGA1* lines, e-*AtCGA1* 27 exhibited the highest relative expression, reaching approximately 126% of *GAPDH*. Other lines exhibited moderate relative levels, such as e-*AtCGA1* 17 (33.9 ± 3.3%), e-*AtCGA1* 21 (31.7 ± 3.81%), and e-*AtCGA1* 14 (16.3 ± 4.58%). In

contrast, e-*AtCGA1* 8 (14.1 ± 1.30%) and e-*AtCGA1* 23 (8.55 ± 3.69%) exhibited lower relative expression (Figure 3.13A). To complement this analysis, qPCR was used to compare the expression of the *AtCGA1* transgene in overexpression lines with the expression of its closest tomato homologue measured in the wild-type plants. *SlGATA22* (name here *CGA1-Like*) was chosen for *AtCGA1* due to its sequence similarity and because *CGA1* is also known in databases as GATA transcription factor 22. Expression of the transgene relative to *SlGATA22* in wild-type ranged from reduced levels in lines 24 and 26 to substantial increases, with line 27 showing the highest expression (24.4 ± 5.01-fold), followed by line 17 (6.58 ± 0.640-fold). Lines 14 and 23 showed moderate increases of 3.17 ± 0.889-fold and 1.11 ± 0.538-fold, respectively (Figure 3.13B).

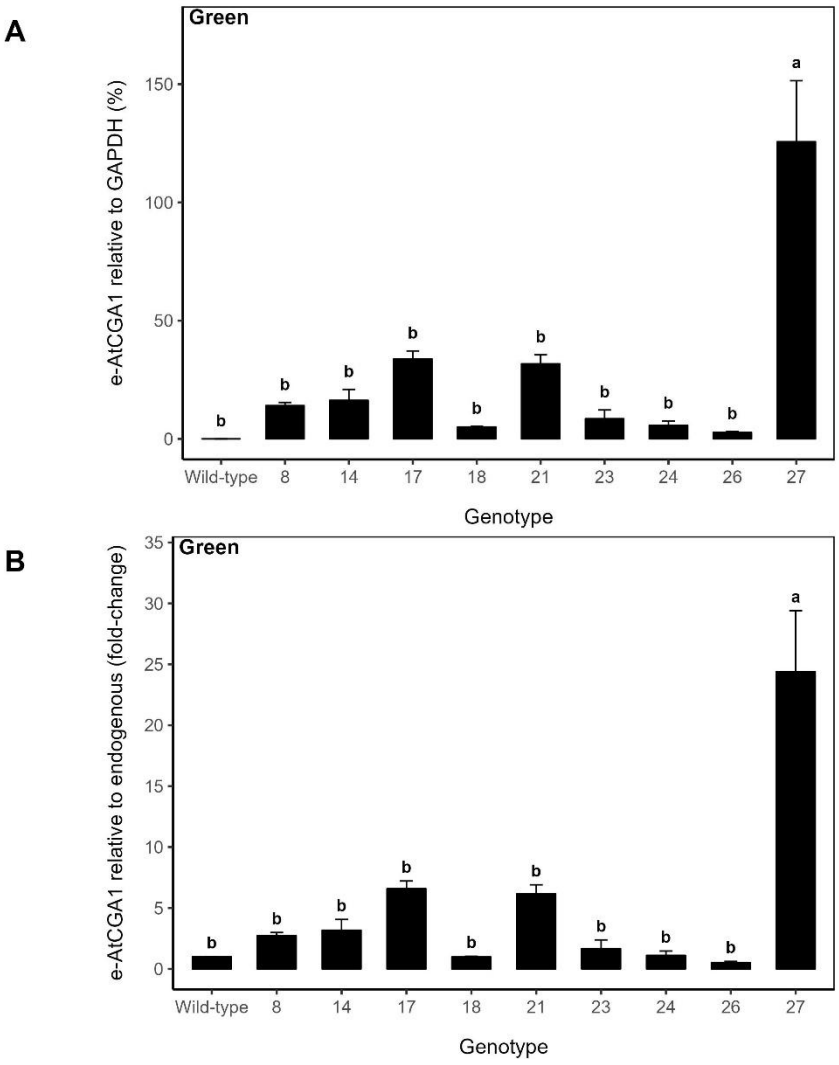

Figure 3.13. Relative *AtCGA1* expression in transgenic Micro-Tom tomato genotypes. Bar charts show relative transcript levels of *AtCGA1* driven by *SlTFM7* early fruit-specific promoter (e-*AtCGA1*) in independent transgenic lines, quantified by qPCR and normalised to the housekeeping gene *GAPDH*. (A) *AtCGA1* expression relative to *GAPDH*. (B) *AtCGA1* expression relative to *SlGATA22* expression in wild-type plants. All values represent means ± SE from three biological replicates per genotype, each analysed in three technical replicates. Statistically significant differences were determined using a 1-way ANOVA followed by Duncan's multiple range test. Different letters indicate statistically significant differences ($P<0.05$).

Among the generated e-*AtGNC* lines, lines 2 (0.62 ± 0.06%) and 5 (0.23 ± 0.02%) showed the lowest relative expression relative to *GAPDH*, while lines 4 (4.11 ± 1.27%) and 6 (6.83 ± 0.24%) displayed slightly higher values (Figure 3.14A). *SlGATA16* (*GNC-like*) was selected as the endogenous reference for *AtGNC*. Expression relative to wild-type *GATA16* was lowest in lines 2 (0.148 ± 0.0145-fold) and 3 (0.588 ± 0.107-fold). Expression in line 4 was comparable to the

endogenous level in wild-type (0.990 ± 0.306-fold) and moderately higher in line 6 (1.64 ± 0.0578-fold). Line 5 showed negligible expression (Figure 3.14B).

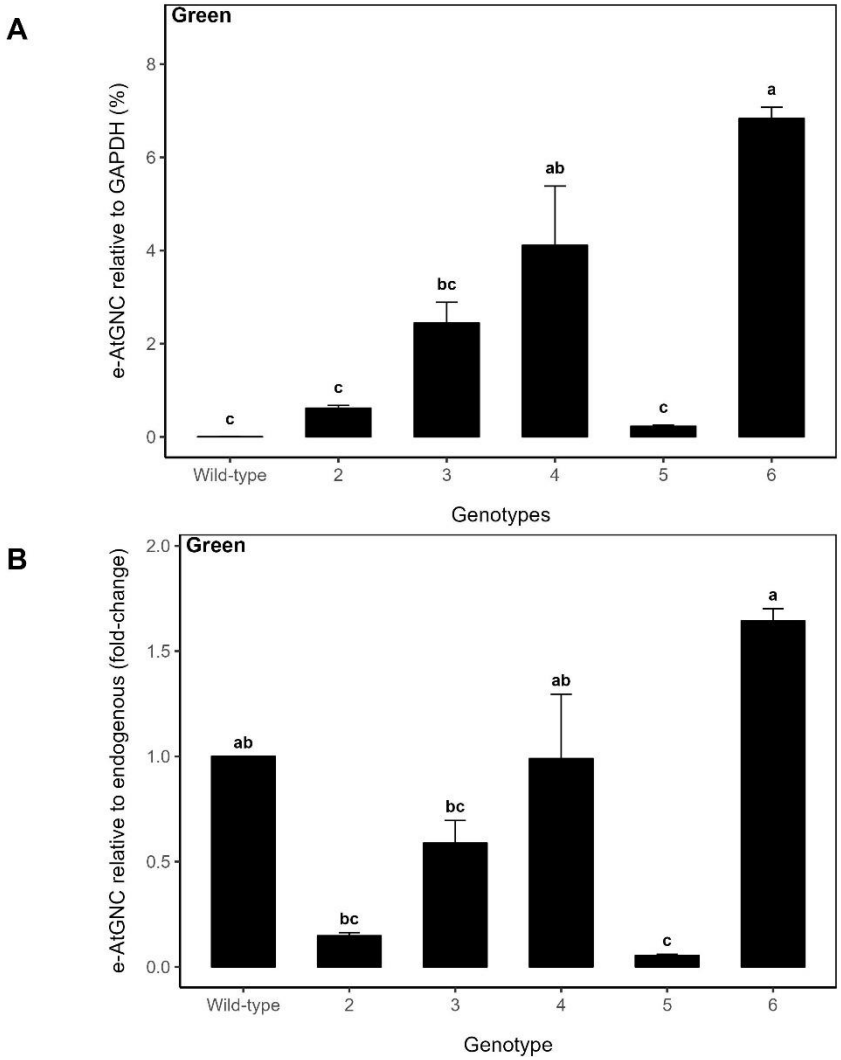

Figure 3.14. Relative expression of *AtGNC* in transgenic Micro-Tom tomato lines. Bar charts show relative transcript levels of *AtGNC* driven by the *SlAFF* early fruit-specific promoter (e-*AtGNC*) in independent transgenic lines, quantified by qPCR and normalised to the housekeeping gene *GAPDH*. (A) *AtGNC* expression relative to *GAPDH*. (B) *AtGNC* expression relative to *SlGATA16* expression in wild-type plants. All values represent means ± SE from three biological replicates per genotype, each analysed in three technical replicates. Statistically significant differences were determined using a 1-way ANOVA

followed by Duncan's multiple range test. Different letters indicate statistically significant differences ($P<0.05$).

Lines were selected to capture a range of expression levels, ranging from very low to moderate or high transcript abundance. Following selection, the transgene copy number of each chosen line was quantified (Tables 3.3 and 3.4).

Table 3.3. Transgene copy number in e-*AtCGA1*. *AtCGA1* genotypes driven by *SlTFM7* early fruit-specific promoter (e-*AtCGA1*).

Genotype	Copy Number
23	1
17	2
21	2
14	4
24	4

Table 3.4. Transgene copy number in e-*AtGNC*. *AtGNC* genotypes driven by *SlAFF* early-specific promoter (e-*AtGNC*).

Genotype	Copy Number
2	1
6	2
3	7
4	8

Transgenic e-*AtCGA1* Lines 14, 17 and 23 were selected for biochemical and physiological analysis of early-specific *AtCGA1* overexpression, while e-*AtGNC* lines 2, 3, and 6 were chosen for e-*AtGNC*, along with wild type and azygous plants (null segregants).

3.2.4.3 *AtPDV1/PDV2*

Transgenic line e-*AtPDV1*/*PDV2* 11 exhibited *AtPDV1* transcript levels of 10,242.87 ± 4,181.68% relative to *GAPDH*. Similarly, line 19 showed elevated *AtPDV1* expression of 7,116.63 ± 235.11% of *GAPDH*. Line 12 also displayed increased *AtPDV1* transcript abundance of 3,976.72 ± 1,084.97% relative to *GAPDH* (Figure 3.15A). *AtPDV1* transcript levels relative to wild-type *SlPDV1* varied from reduced levels in lines 1 and 2 to substantial increases, with lines 11 and 19 showing the highest values (17.8 ± 7.28-fold and 12.4 ± 0.410-fold, respectively). Lines 12 and 8 exhibited increases of 6.93 ± 1.89-fold and 2.32 ± 0.149-fold, respectively (Figure 3.15B).

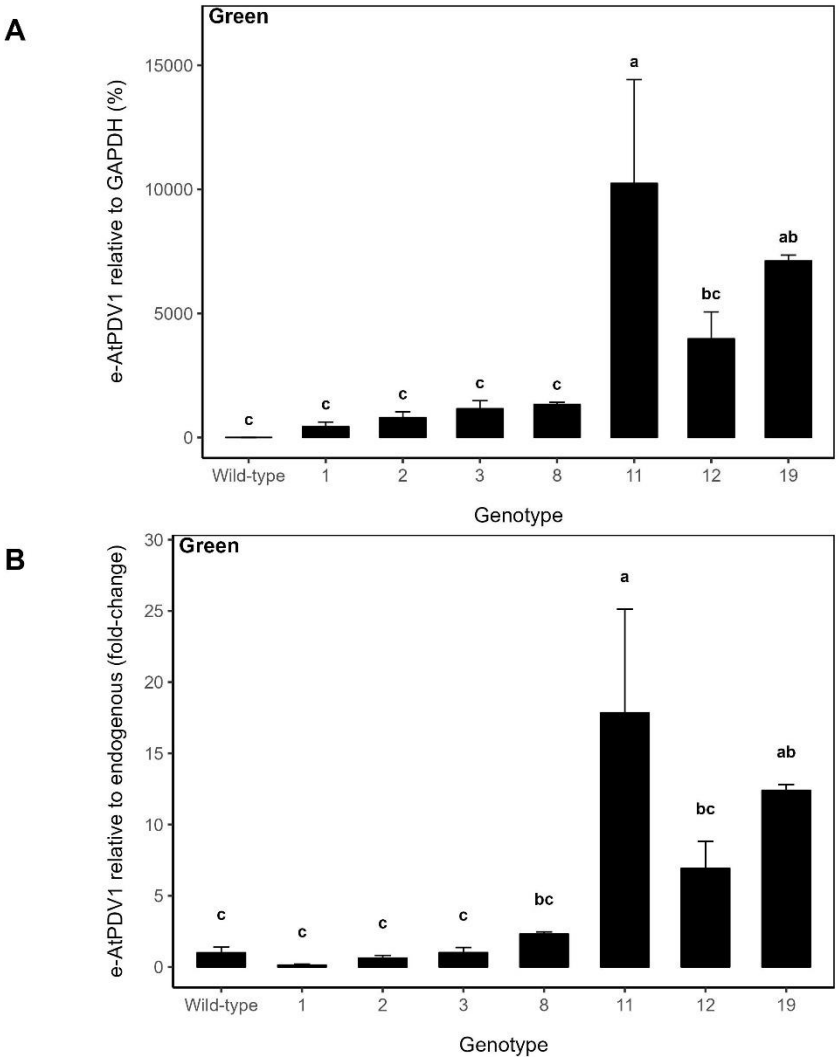

Figure 3.15. Relative *AtPDV1* expression in transgenic Micro-Tom tomato genotypes. Bar charts show relative transcript levels of *AtPDV1* driven by *SlTFM7* early fruit-specific promoter in independent transgenic lines, quantified by qPCR and normalised to the housekeeping gene *GAPDH*. (A) *AtPDV1* expression relative to *GAPDH*. (B) *AtPDV1* expression shown relative to *SlPDV1* expression in wild-type plants. All values represent means ± SE from three biological replicates per genotype, each analysed in

three technical replicates. Statistically significant differences were determined using a 1-way ANOVA followed by Duncan's multiple range test. Different letters indicate statistically significant differences (P<0.05).

Transgenic line e-*AtPDV1*/*PDV2* 11 exhibited *AtPDV2* expression of 155.83 ± 34.87% of *GAPDH*. Line 19 showed *AtPDV2* levels at 72.41 ± 12.15 %. Line 12 also had a high relative *AtPDV2* expression (124.51 ± 56.98% of *GAPDH*). All other lines displayed lower *AtPDV2* expression (Figure 3.16A). For *AtPDV2*, expression relative to wild-type *SlPDV2* was lower in lines 1, 2, 3, and 8, but considerably higher in lines 11 (22.9 ± 5.13-fold), 12 (18.3 ± 8.38-fold), and 19 (10.6 ± 1.79-fold) (Figure 3.16B).

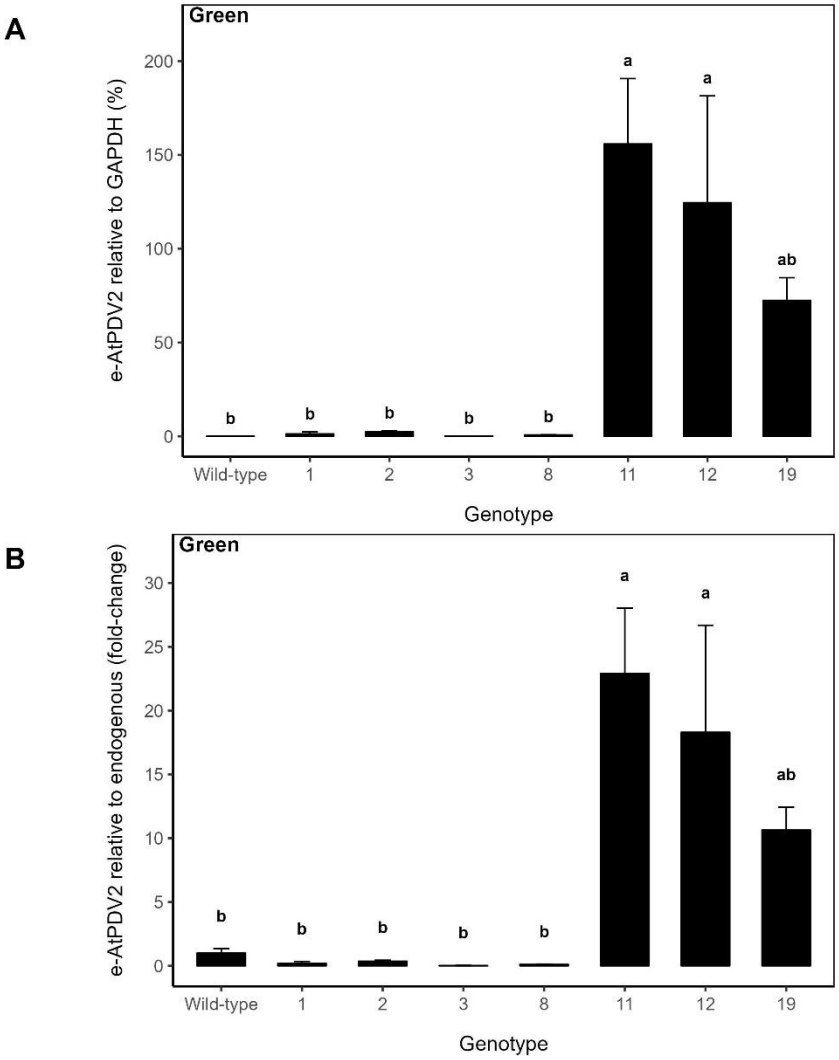

Figure 3.16. Relative expression of *AtPDV2* in transgenic Micro-Tom tomato lines. Bar charts show relative transcript levels of *AtPDV2* driven by *SlAFF* early fruit-specific promoter in independent transgenic

lines, quantified by qPCR and normalised to the housekeeping gene *GAPDH*. (A) *AtPDV2* expression relative to *GAPDH*. (B) *AtPDV2* expression shown relative to *SlPDV2* expression in wild-type plants. All values represent means ± SE from three biological replicates per genotype, each analysed in three technical replicates. Statistically significant differences were determined using a 1-way ANOVA followed by Duncan's multiple range test. Different letters indicate statistically significant differences (P<0.05).

Following qPCR, the transgene copy number of selected lines was quantified (Table 3.5).

Table 3.5. **Transgene copy number in e-*AtPDV1/PDV2*.** *AtPDV1/PDV2* genotypes driven by *SlTFM7* Early-Specific and *SlAFF* Early-Specific promoter, respectively (e-*AtPDV1/PDV2*).

Genotype	Copy Number
12	1
8	2
2	4
19	4
11	9

3.3 Discussion

Golden Gate cloning technology was used to build overexpression constructs for the target genes, and several rounds of *Agrobacterium tumefaciens*-mediated transformation of tomato cotyledons were performed. Production of the constructs was relatively straightforward, as the advent of Golden Gate revolutionised the field of genetic engineering, allowing the generation of multiple transgenic lines with different promoter sets to specifically modify enzyme levels (Engler & Marillonnet, 2014). The principle of Golden Gate cloning is based on the ability of type IIS restriction enzymes to cleave outside of their recognition site, which allows the assembly of sets of unique overhangs in the correct order and orientation. As a result, restriction and ligation can be performed in a one-step reaction, making it a rapid and efficient molecular cloning method (Engler et al., 2009). Firstly, level 1 modules were created by cloning a promoter, coding sequence, and terminator into a destination vector. Following that, each one of these modules was assembled with *nptII* (kanamycin resistance) and the appropriate end-linker in a plant expression vector to create level 2 modules. High levels of efficiency were observed for level 1

constructs, following that described by Weber et al. (2011), decreasing in the level 2 assembly, which presented a higher number of non-transformed colonies displaying the red phenotype produced by the intact canthaxanthin biosynthesis operon (Weber et al., 2011). Nevertheless, level 2 modules were successfully assembled and sequenced for all constructs.

The tissue-specific expression of the genes of interest could allow the delivery of target changes whilst reducing or eliminating the adverse effects of constitutive promoters such as the Cauliflower mosaic virus 35S constitutive promoter (*CaMV 35S*) (Chung et al., 2020; Hudson, 2010). Work by Davuluri et al. (2005) developed transgenic tomato plants with increased carotenoid content without pleiotropic effects, which was attributed to the use of fruit-specific promoters. The authors suggested that, because typically the fruit is a sink organ, localised overexpression or silencing signals are not transmitted to the rest of the plant, leading to the lack of aberrant phenotypes often observed with constitutive promoters (Davuluri et al., 2005). In tomato, the *SlTFM7* promoter acts predominantly during early fruit development, with weak expression in the ripe fruit and very weak/undetectable in leaves (Conner, 1997; Santino et al., 1997). Similarly, *SlAFF* has been reported to be strongly expressed in green fruit with mild expression in the red fruit, weak in the flower and undetectable in other tissues (Hiwasa-Tanase et al., 2012). The *CaFIB* promoter is expressed at high levels in tomato fruit ripening, although activity can be observed at lower levels in other organs, such as the leaf and stem (Kuntz et al., 1998; Smirnova & Kochetov, 2020). Outside the fruit, *CaFIB* activity has been associated with stress conditions such as wounding, water deficit, or photodamage (Chen et al., 1998; Manac'h & Kuntz, 1999).

Whilst fruit-ripening promoters have been extensively used and described in the literature, the use of promoters driving the expression of transgenes in fruit in the early stages of development has traditionally been less usual (Hiwasa-Tanase et al., 2012). In this study, the use of promoters expressed at different stages of fruit development represents a significant advance in the genetic engineering of fruits. It can also provide insight into the role of the plastid compartment in photochemical efficiency and nutritional quality through the direct manipulation of chloroplast development in both green and ripening fruit. Finally, the choice of the *heat shock protein 18.2* (*HSP*) as a terminator was based on its potential to enhance transgene expression. *HSP* has been shown to efficiently increase the levels of accumulated mRNA by 2-fold when compared to other terminators commonly used in foreign gene expression (Nagaya et al., 2010). In addition, the

terminators of *octopine synthase* (*OCS*) and *nopaline synthase* (*NOS*) are also widely used in plant biotechnology as generic terminators in overexpression constructs (Nagaya et al., 2010).

In our first experiments, the selective regeneration medium lacked the presence of auxin. However, all explants failed to regenerate using this method and died shortly after co-culture. We adapted a protocol (Dan et al., 2006; H. J. Sun et al., 2006) that has proved successful, with the development of calluses and successful regeneration of explants. Two weeks after transfer to regeneration media, the explants started forming calluses, and the selective pressure was increased to 100 mg L^{-1}. All control explants started losing their colour at the initial stages and died in the selection medium after 6-8 weeks. The selective regeneration medium was supplemented with 0.1 mg L^{-1} IAA and 2.0 mg L^{-1} Trans-zeatin-riboside in the first two weeks. Then the explants were transferred to a new regeneration medium with a reduced trans-zeatin-riboside concentration (1.0 mg L^{-1}). The combined action of Zeatin riboside with IAA in tomato regeneration contributes to callus formation and the reduction of the Zeatin concentration (2 mg L^{-1}, then 1 mg L^{-1}, and finally 0.5 mg L^{-1} in the shoot elongation medium) has been shown to promote faster shoot development (Dan et al., 2006). Initiation of root formation was observed from 2 to 4 weeks in rooting media, from both the base and lateral of the shoots (adventitious roots).

After successful generation of transgenic plants, selection of independent lines was based on expression levels, copy number (ensuring at least one single-copy line for each genotype), seed availability (as fruits not always fruits produced viable seeds) and overall plant status at the time of selection. Wild-type and azygous plants (null segregants) were selected as controls. The qPCR and copy number analysis revealed that transgene copy number did not show a consistent correlation with transcript abundance in all genotypes, indicating that copy number alone is not a reliable predictor of expression. Previous studies have suggested that high transgene copy numbers could cause silencing, leading to an inverse relationship between copy number and gene expression. This could happen through transcriptional gene silencing (TGS), where DNA methylation suppresses transcription, or post-transcriptional gene silencing (PTGS), where transcribed RNA is degraded, preventing its translation into a functional protein (Rajeevkumar et al., 2015). In addition to gene silencing, the site of integration has also been identified as a key factor affecting transgene expression. This is due to characteristics of the DNA ultrastructure and the influence of adjacent plant genomic DNA, which can affect the transgene stability and make their expression either easier or harder (Donnarumma et al., 2011; Klimaszewska et al., 2003). Moving forward, comprehensive expression profiling at different fruit stages, accompanied by the

quantification of protein concentrations, would be valuable for elucidating the regulatory mechanisms underlying chloroplast development and their impact on photochemical efficiency.

To conclude:

1. Tomato plants overexpressing *BpMADS*, *AtCGA1, AtGNC* and *AtPDV1/AtPDV2* were generated.
2. The low efficiency of tomato transformation was a challenge to overcome.
3. The relatively short regeneration period (12-18 weeks) made it possible to perform several rounds of transformation and obtain several independent transgenic lines.
4. Independent lines of interest were selected for biochemical and physiological characterisation.

Chapter 4 Fruit-Specific *BpMADS* Overexpression Enhances Photochemical Capacity and Pigment Accumulation in Tomato

4.1 Introduction

A significant body of research has shown that fruits are photosynthetically active. The presence of a functional photochemical apparatus and an efficient electron transport chain indicates that they contribute to their own growth and development (Cocaliadis et al., 2014; Garrido et al., 2023). The manipulation of genes involved in chloroplast development and pigment accumulation has emerged as a promising strategy to enhance chlorophyll content, photochemical capacity and nutritional quality (Hudson et al., 2011; Pan et al., 2013; Powell et al., 2012). While these studies have shown the potential of improving components of the photosynthetic machinery, their application in fruits is still in the early stages, with many aspects yet to be explored. One key aspect of interest is evaluating the actual impact of increasing pigment content or changes in chloroplast development on the photochemical capacity of fruits. Another aspect is the link between the chloroplast compartment in the green fruit and the nutrient content in the ripe stage. The constitutive overexpression of the *Betula platyphylla* MADS-box transcription factor *BpMADS* has been previously associated with chloroplast development in transgenic tobacco leaves (Qu et al., 2013). The authors reported that transgenic plants exhibited larger and more numerous chloroplasts, increased chlorophyll levels and enhanced photosynthetic efficiency by two-fold. However, its precise function in this process remains unclear. Given the ability of MADS-box to dimerise and interact with other transcription factors, the overexpression of *BpMADS* could potentially affect aspects of plastid development, including chloroplast biogenesis, division, or chlorophyll biosynthesis (Grimplet et al., 2016; Riechmann & Meyerowitz, 1997; Zhang et al., 2024).

Transgenic tomato (*Solanum lycopersicum* cv. Micro-Tom) lines expressing *BpMADS* under the control of two distinct fruit-specific promoters were generated, one active during early fruit development, and another active during ripening. This dual-promoter approach allows a comparative analysis of the effects of *BpMADS* overexpression on early plastid development as well as its impact on nutrient content during fruit ripening. This chapter outlines the

morphological, biochemical and physiological characterisation of the engineered tomato lines. Confocal and light microscopy were performed to evaluate changes in chloroplast size, number, and cellular coverage. Chlorophyll and carotenoid content across different developmental stages were measured to assess whether the overexpression of *BpMADS* influences pigment accumulation. Following that, the analysis of photochemical activity using chlorophyll fluorescence techniques provided insights into the functionality of the fruit's major photosynthetic structures. In addition, a gas exchange measurement protocol optimised for non-foliar tissue was performed to assess carbon assimilation performance. Understanding how *BpMADS* affects fruit photosynthetic performance and nutritional quality may contribute to broader strategies for improving fruit yield and quality, offering new perspectives on the genetic regulation of fruit development. To the author's knowledge, this is the first study to explore the effects of *BpMADS* overexpression on fruit photosynthesis and pigment composition.

4.2 Results

4.2.1 BpMADS Is Closely Related to AP1-Like MADS-Box Proteins

The cDNA for the *BpMADS* ORF is 750 bp long from the ATG start codon to the TGA stop codon, encoding a predicted polypeptide of 249 amino acids. The sequence was obtained from GenBank (accession number JX565468) and used for phylogenetic analysis. NCBI BLAST analysis showed that the predicted polypeptide has a high similarity (74%) with AP1 (AT1G69120) in *Arabidopsis thaliana* and (97%) with BpMADS3 (GenBank No. X99653) a previously characterised AP1-like MADS-box protein from *Betula pendula* (Elo et al., 2001; Qu et al., 2013). The present analysis does not resolve whether this high level of similarity reflects minor sequence differences or close paralogous relationships within the Betula *AP1-like* MADS-box gene family. In the tomato genome, the BpMADS protein displays 66% identity (85% similarity) with MADS-MC (MACROCALYX) (GenBank No KY471426.1), a MADS-box protein previously described as the tomato orthologue of AP1 and involved in sepal development (Burko et al., 2013; Nakano et al., 2012; Vrebalov et al., 2002). BpMADS also shares 71% identity (85% similarity) with FUL2 (GenBank No. KX590895), a MADS-box protein expressed from the early stages of fruit development through fruit growth and ripening (Bemer et al., 2012).

Two amino acid level phylogenetic analyses were performed to understand the evolutionary relationships of BpMADS further. The first analysis examined a broad range of species, while the

second focused specifically on MADS-box proteins in tomato. Representative proteins were selected as top BLASTP hits per species from the NCBI database. Arabidopsis AP1 was included as a well-characterised AP1/FUL-clade reference sequence and was not used to root the tree. Therefore, evolutionary directionality was not inferred. The phylogenetic trees were constructed using the maximum likelihood method with 1000 bootstrap replicates. The general analysis (Figure 4.1) revealed that BpMADS clustered most closely with MADS3 from *Betula pendula*, suggesting conservation within Betulaceae. BpMADS also grouped with AP1 homologues from *Alnus glutinosa*, *Corylus avellana*, *Quercus lobata*, and *Ricinus communis*. Members of the APETALA1 (AP1) family are well characterised as A-class floral identity genes involved in specifying floral meristems and the development of sepals and petals (Irish, 2017). These phylogenetic relationships suggest that BpMADS shares a common evolutionary origin with AP1 homologues and may retain conserved functional roles.

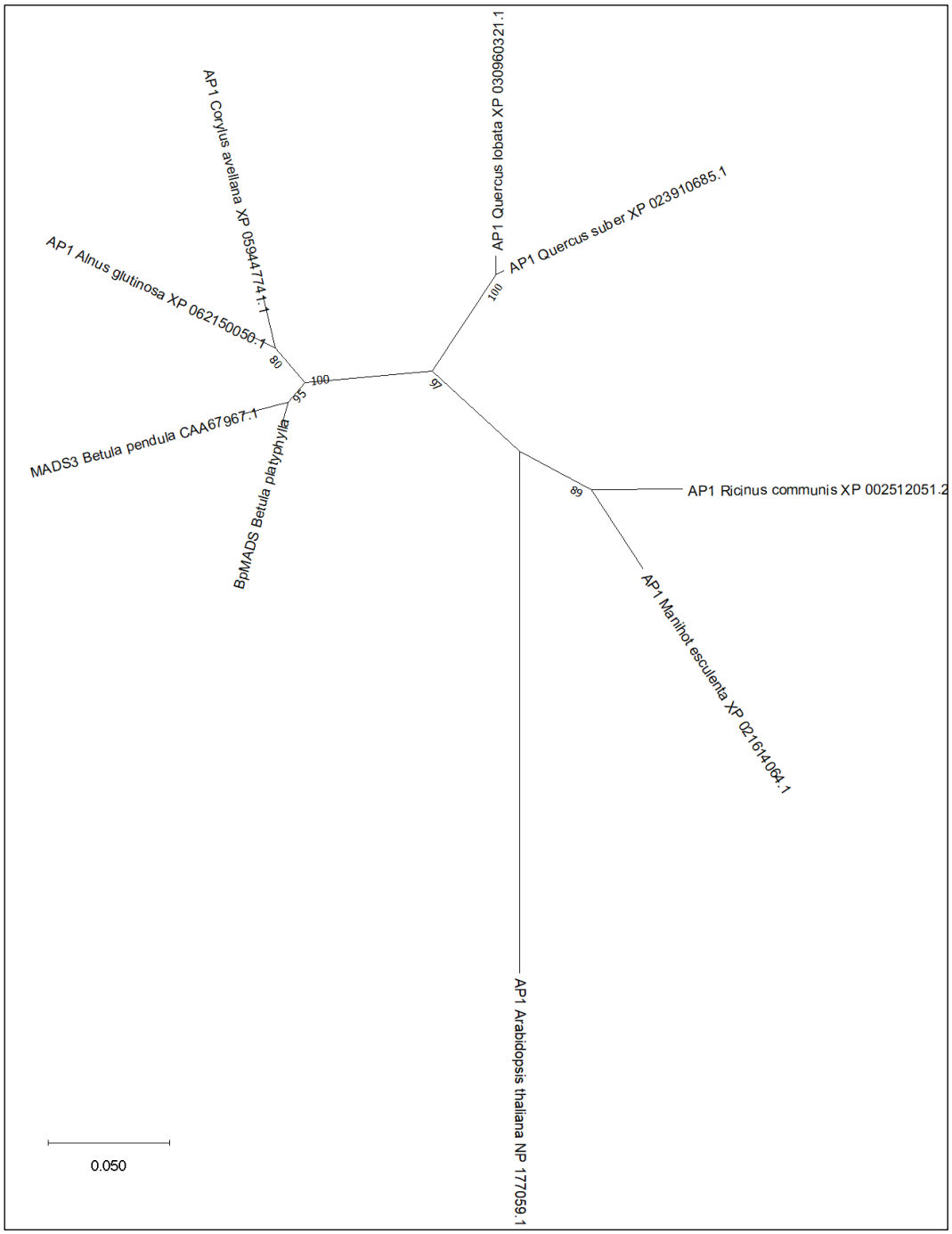

Figure 4.1. Evolutionary Relationships Between BpMADS and Representative MADS-box Proteins. A phylogenetic tree was inferred from amino acid sequences of selected MADS-box proteins using the maximum likelihood method. Bootstrap values are indicated at each node to represent the level of support for the individual clade. Higher values reflect stronger support for the evolutionary groupings. The tree is presented as an unrooted phylogram, with branch lengths proportional to the number of amino acid substitutions per site.

A second analysis explored the relationships between BpMADS and selected tomato MADS-box transcription factors identified based on BLASTP similarity (Figure 4.2). In this analysis, BpMADS

grouped within the AP1/FUL-related clade and showed closest association with MADS-MC and MADS-RIN. Previous research has demonstrated that MADS-MC and Arabidopsis AP1 share conserved functions and tissue expression patterns (Vrebalov et al., 2002). Based on these functional similarities and the molecular relationships observed here, BpMADS and MADS-MC are proposed as putative orthologues. More distant relationships were observed with TAGL2 and FUL1 (also known as TDR4), both MADS-box genes previously described to be expressed during the early stages of tomato fruit development (Busi et al., 2003; Nezhdanova et al., 2021).

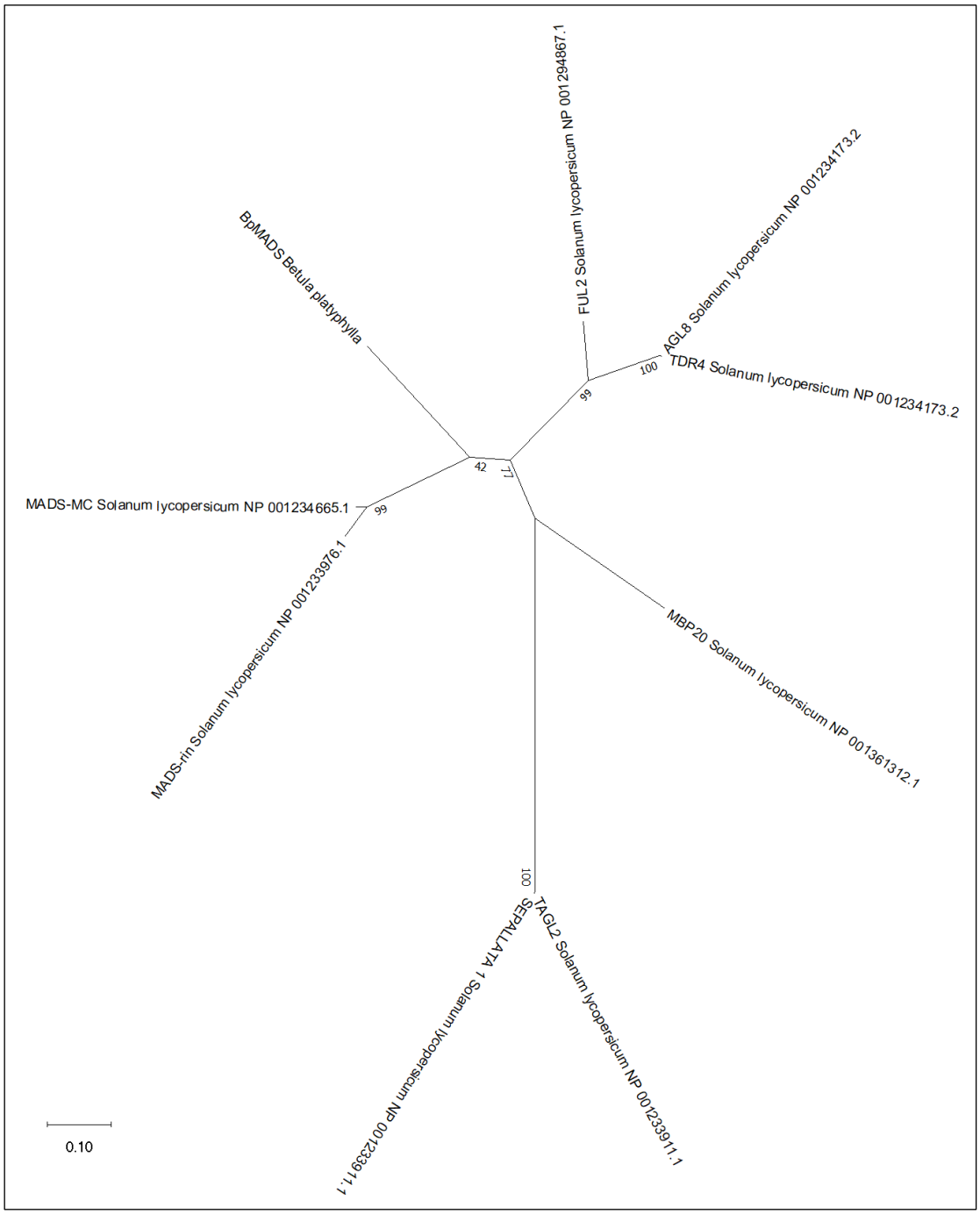

Figure 4.2. Evolutionary Relationships Between BpMADS and Tomato MADS-box Proteins. A phylogenetic tree based on amino acid sequences of MADS-box proteins was inferred using the maximum likelihood method. Bootstrap values are indicated at each node to represent the level of support for the individual clade. Higher values reflect stronger support for the evolutionary groupings. The tree is presented as an unrooted phylogram, with branch lengths proportional to the number of amino acid substitutions per site.

Taken together, these analyses suggest that BpMADS is closely related to members of the AP1 family across different species and may share conserved functions. Moreover, these results are

consistent with previous findings that certain AP1/FUL-related MADS-box genes have diversified to regulate fruit development. The well-characterised ability of MADS-box proteins to form dimers (Shore & Sharrocks, 1995) raises the possibility that BpMADS may interact with other MADS-box proteins expressed in the fruit to regulate aspects of early fruit development and ripening. Further, phylogenetic and expression analyses are needed to fully characterise the evolutionary relationships of BpMADS and its potential role in fruit development.

4.2.2 Microscopy Analysis Reveals a Larger Chloroplast Compartment in Early-Specific *BpMADS* Fruit Pericarp

This section outlines the effects of the early-specific *BpMADS* overexpression on chloroplast morphology in tomato pericarp cells of mature green (MG) fruits. Confocal laser scanning microscopy (Figure 4.3) enabled the visualisation of chloroplasts as fluorescent structures. Transmitted light imaging (Figure 4.4) provided complementary structural detail. Then, changes in chloroplast size, number, and total coverage per cell across e-*BpMADS* transgenic fruits were quantified.

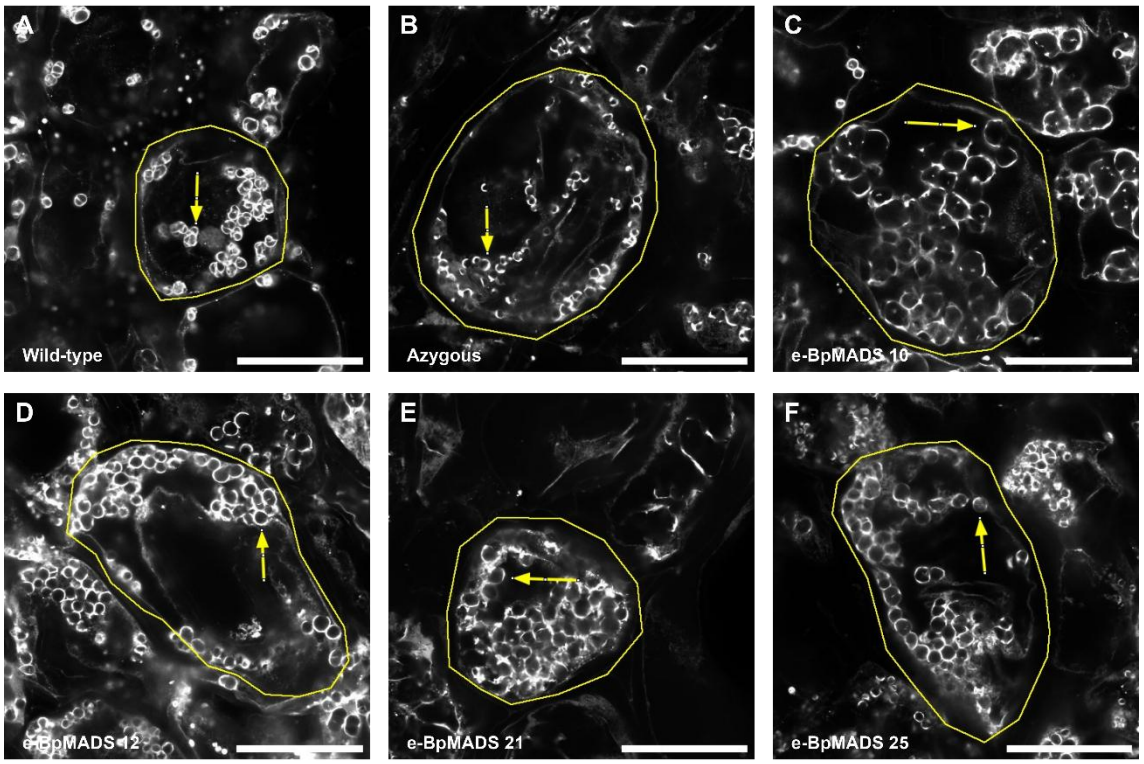

Figure 4.3. Confocal laser scanning microscopy of mature green (MG) fruit from early-specific *BpMADS* tomato lines. Representative micrographs of pericarp cells from fruits expressing *BpMADS*

driven by the *SlTFM7* early fruit-specific promoter (e-*BpMADS*), azygous and wild type controls. Individual cells are outlined in yellow, and representative chloroplasts are indicated by arrows. (A) Wild-type. (B) Azygous. (C) e-*BpMADS* 10. (D) e-*BpMADS* 12. (E) e-*BpMADS* 21. (F) e-*BpMADS* 25. MG = 20–23 days post-anthesis. Scale bars = 100 µm.

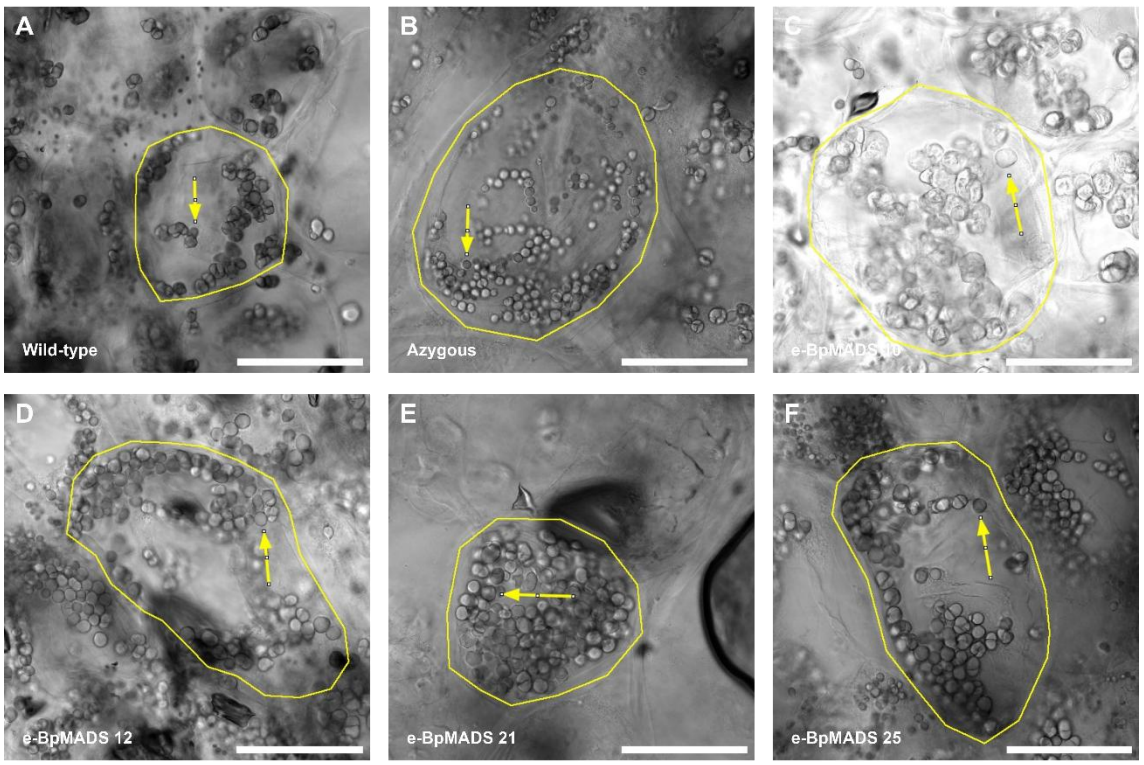

Figure 4.4. Transmitted light microscopy of mature green (MG) fruit from early-specific *BpMADS* tomato lines. Representative micrographs of pericarp cells from fruits expressing *BpMADS* driven by the *SlTFM7* early fruit-specific promoter (e-*BpMADS*), azygous and wild type controls. Individual cells are outlined in yellow, and representative chloroplasts are indicated by arrows. (A) Wild-type. (B) Azygous. (C) e-*BpMADS* 10. (D) e-*BpMADS* 12. (E) e-*BpMADS* 21. (F) e-*BpMADS* 25. MG = 20–23 days post-anthesis. Scale bars = 100 µm.

Significant biological variation was observed both between and within lines, as well as between wild-type and azygous lines. These extreme differences were also reported by Cookson et al. (2003), who reported that the relationship between pericarp cell size, chloroplast area, and chloroplast number was complex in high pigment-1 tomato mutants. All e-*BpMADS* lines showed statistically significant increases in chloroplast plan area compared to wild-type. The largest chloroplast plan area observed was in e-*BpMADS* 10 (86.01 ± 9.56 µm^2) and e-*BpMADS* 12 (70.9 ± 6.71 µm^2), compared to wild-type (38.05 ± 2.81 µm^2) and azygous (43.31 ± 4.5 µm^2). These values correspond to approximately 1.8 to 2-fold increases in chloroplast plan area compared to wild-type and azygous control, respectively (Figure 4.5A). In addition, e-*BpMADS* 21 (53.42 ± 4.47

μm^2) and 25 (62.21 ± 6.66 μm^2), exhibited a 1.5-fold change compared to both wild-type and azygous control. However, these lines shared overlapping significance groups with the azygous control. The number of chloroplasts per cell (Figure 4.5B) observed in this study (88.06 ± 5.25) aligns with previous results from the literature, in which the average number of chloroplasts per cell for both Micro-Tom and *Ailsa Craig* was about 70 (Egea et al., 2011). Although some differences were observed, they were mostly not significant. Transgenic lines e-*BpMADS* 12 (100.65 ± 4.78), e-*BpMADS* 21 (104.36 ± 7.82) and e-*BpMADS* 25 (120.91 ± 9.66) exhibited slightly more chloroplasts per cell than the wild type (88.06 ± 5.25), but fewer when compared to the azygous line (126.10 ± 11.19). Additionally, while e-*BpMADS* 10 exhibited larger chloroplasts, it did not correlate with an increase in number (80.72 ± 6.41). These results suggest that, although chloroplast number and size are important parameters for understanding chloroplast biology, they provide only a partial view of the subject. Assessing the proportion of cellular volume occupied by chloroplasts offers a more powerful approach to understanding the mechanisms driving chloroplast development within the cell.

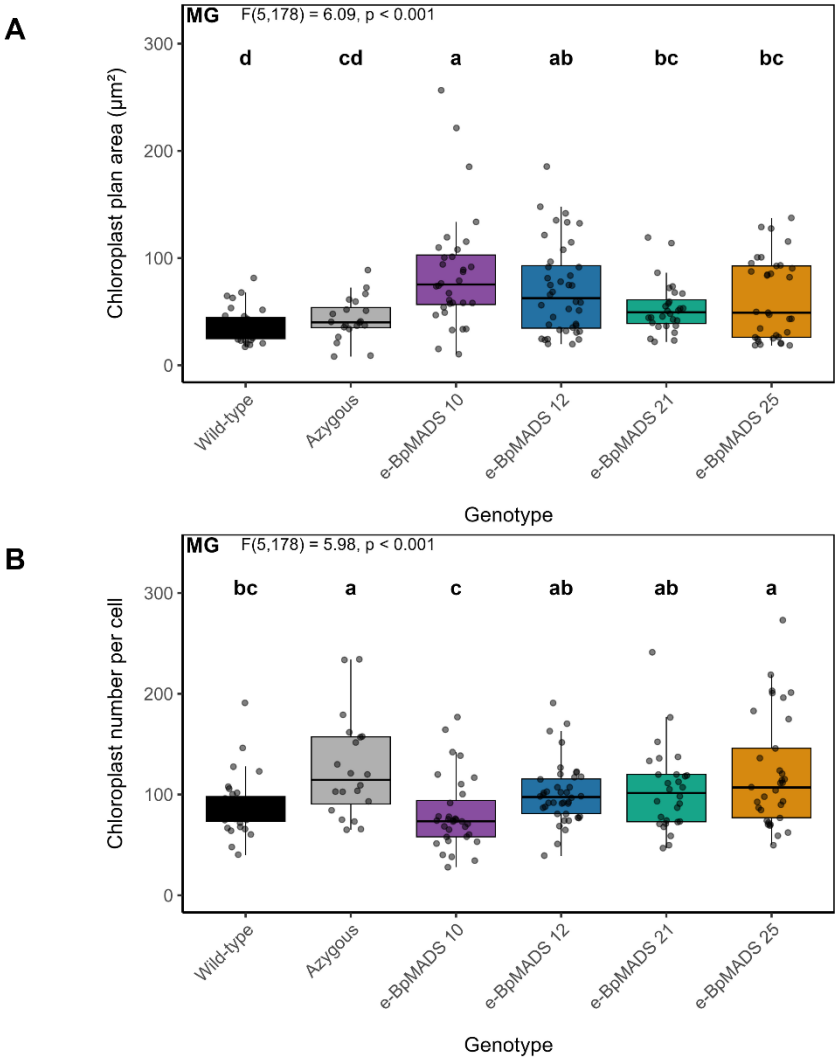

Figure 4.5. Chloroplast morphology in mature green (MG) fruits of early-specific *BpMADS* tomato lines. Boxplots show chloroplast morphology traits in fruits from lines expressing *BpMADS* under the *SlTFM7* early fruit-specific promoter (e-*BpMADS*), compared with azygous and wild-type controls. (A) Chloroplast plan area. (B) Chloroplast number per cell. MG = 20–23 days post-anthesis. The boxes represent the interquartile range (25th to 75th percentile), the horizontal line shows the median, and the whiskers extend to 1.5 times the interquartile range. At least six individual cells of at least three biological replicates were analysed for each genotype. Statistically significant differences were determined using a 1-way ANOVA followed by Duncan's multiple range test. Dots show individual data points. Different letters indicate statistically significant differences (P<0.05).

The estimated chloroplast coverage in a cell is calculated by multiplying the number of chloroplasts by their average plan area and then dividing by the cell's total plan area. This provides an estimate of the space in the cell occupied by chloroplasts, often referred to as chloroplast coverage or the chloroplast index (Hu et al., 2024). Mean chloroplast coverage values were 24.47 ± 2.63% in e-*BpMADS* 10, 24.56 ± 2.15% in e-*BpMADS* 12, 23.22 ± 2.26% in e-*BpMADS* 21, and 24.03 ± 2.56% in e-*BpMADS* 25, compared to 16.35 ± 1.52% in wild-type and 16.75 ±

1.69% in the azygous control. These values represent relative increases of approximately 36-49% compared to the wild-type and 33-46% compared to the azygous control (Figure 4.6A). Wild-type and azygous control cellular coverage of mature green fruits were in accordance with values observed for mature green fruits of *Ailsa Craig*, which have a cellular cell index of around 16.5% (Cookson, 2003). Although all transgenic lines exhibited statistically significant increases relative to the wild type, the differences were less consistent when compared with the azygous control, where the same trend was observed, but not all reached significance, possibly due to the high biological variability.

The analysis of chloroplast density (the number of chloroplasts divided by cell area) revealed that all genotypes maintained a relatively consistent proportion of chloroplasts, with the exception of e-*BpMADS* 10 (Figure 4.6B). Density values were 0.00443 chloroplasts μm^{-2} in wild-type and 0.00424 in azygous fruits. In the transgenic lines, e-*BpMADS* 10 displayed the lowest density, 0.00315 chloroplasts μm^{-2}, representing a reduction of approximately 29% relative to wild-type and 26% relative to azygous plants. In contrast, e-*BpMADS* 12, with 0.00407 chloroplasts μm^{-2}, exhibited only small decreases of about 8% and 5% compared with wild-type and azygous control, respectively. On the other hand, chloroplast densities in e-*BpMADS* 21 (0.00451) and e-*BpMADS 25* (0.00463) were slightly higher than those of the controls. These results suggest that, excluding e-*BpMADS* 10, the number of chloroplasts per unit area was overall conserved across genotypes.

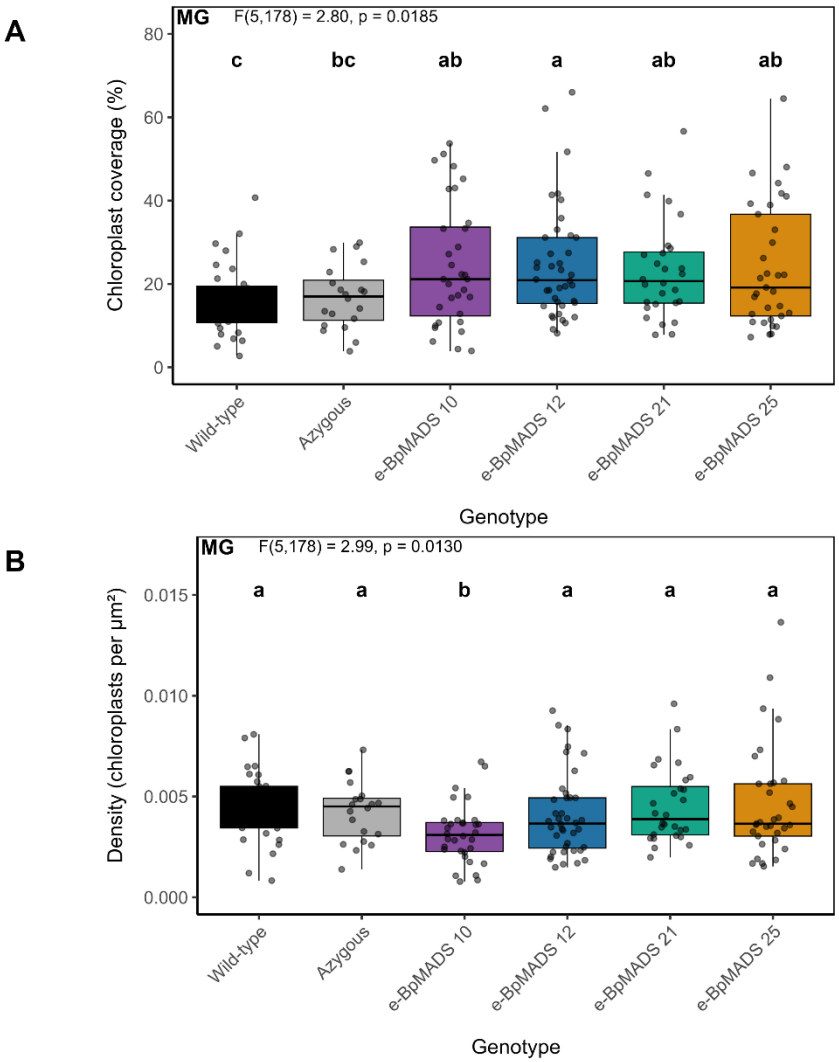

Figure 4.6. Chloroplast morphology in mature green (MG) fruits of early-specific *BpMADS* tomato lines. Boxplots chloroplast morphology traits in fruits from lines expressing *BpMADS* under the *SlTFM7* early fruit-specific promoter (e-*BpMADS*), compared with azygous and wild-type controls. (A) Chloroplast coverage. (B) Chloroplast density. MG = 20–23 days post-anthesis. The boxes represent the interquartile range (25th to 75th percentile), the horizontal line shows the median, and the whiskers extend to 1.5 times the interquartile range. At least six individual cells of at least three biological replicates were analysed for each genotype. Statistically significant differences were determined using a 1-way ANOVA followed by Duncan's multiple range test. Dots show individual data points. Different letters indicate statistically significant differences (P<0.05).

A nested one-way ANOVA was used to test whether chloroplast morphology traits were associated with an overall transgene effect, while accounting for variation among individual genotypes nested within type. The analysis detected no significant effect of type (wild-type/azygous vs e-*BpMADS*) for chloroplast number (p = 0.894). In contrast, chloroplast plan area showed a significant effect of type (p = 0.0296). Similarly, the same analysis showed no significant effect of type (wild-type/azygous vs e-*BpMADS*) on chloroplast density (p = 0.500), as opposed to

chloroplast coverage, which displayed a significant effect ($p < 0.001$). Together, these results suggest that the observed differences are primarily associated with changes in chloroplast plan area and coverage, rather than with chloroplast number or density.

4.2.3 Greater Chlorophyll and Carotenoid Content in Early-Specific *BpMADS* Lines

The impact of *BpMADS* overexpression on fruit development was investigated at the biochemical and physiological levels in four lines for the *BpMADS* early-specific construct (e-*BpMADS*) and three for *BpMADS* ripening-specific (r-*BpMADS*), along with wild-type and azygous (null segregant) lines. Chlorophyll measurements were conducted in both immature green (IG) and mature green fruits (MG) to assess whether *BpMADS* had an impact on the chlorophyll levels of Micro-Tom fruits and the role played by different developmental stages on chlorophyll accumulation in the expressing lines. All e-*BpMADS* lines exhibited visible changes in pigmentation at the mature green (MG) stage, as displayed in Figure 4.7.

Figure 4.7. Phenotypes of mature green (MG) fruits of early-specific *BpMADS* tomato lines. Images display representative MG fruits from transgenic lines expressing *BpMADS* driven by the *SlTFM7* early fruit-specific promoter (e-*BpMADS*), as well as azygous and wild-type controls. (A) Wild-type. (B) Azygous. (C) e-*BpMADS* 10. (D) e-*BpMADS* 12. (E) e-*BpMADS* 21. (F) e-*BpMADS* 25. MG = 20–23 days post-anthesis. Scale bars = 1 cm.

Consistent with the phenotypic changes, the measurement of chlorophyll content revealed significantly higher values at the mature green stage. Among them, e-*BpMADS* 12 showed the most striking phenotype, with an increase of approximately 90% (73.24 ± 7.82 µg/g) compared to the wild-type (38.45 ± 2.92 µg/g), and 78% to azygous fruits (40.18 ± 6.05 µg/g). Lines e-*BpMADS* 10, 21 and 25 also exhibited significant differences, with chlorophyll content greater by 49%, 58% and 57%, respectively, relative to wild-type, and 43%, 51% and 50%, compared to azygous (Figure 4.8). Although e-*BpMADS* immature green fruits showed greater mean chlorophyll content, genotype-level comparisons did not show statistically significant differences among individual lines. Finally, the chlorophyll *a*/*b* ratio provides insight into the relative allocation of pigments between reaction centres and light-harvesting antenna complexes. A higher ratio generally indicates a smaller antenna size per reaction centre, a strategy associated with adaptation to low-light environments (Jin et al., 2016; Simkin et al., 2022). In this study, the chlorophyll *a*/*b* ratio was relatively conserved across transgenic lines, ranging from 2.13 to 2.26, with no significant differences compared to wild-type or azygous controls (Figure 4.8C). This suggests that *BpMADS* overexpression did not significantly affect antenna size.

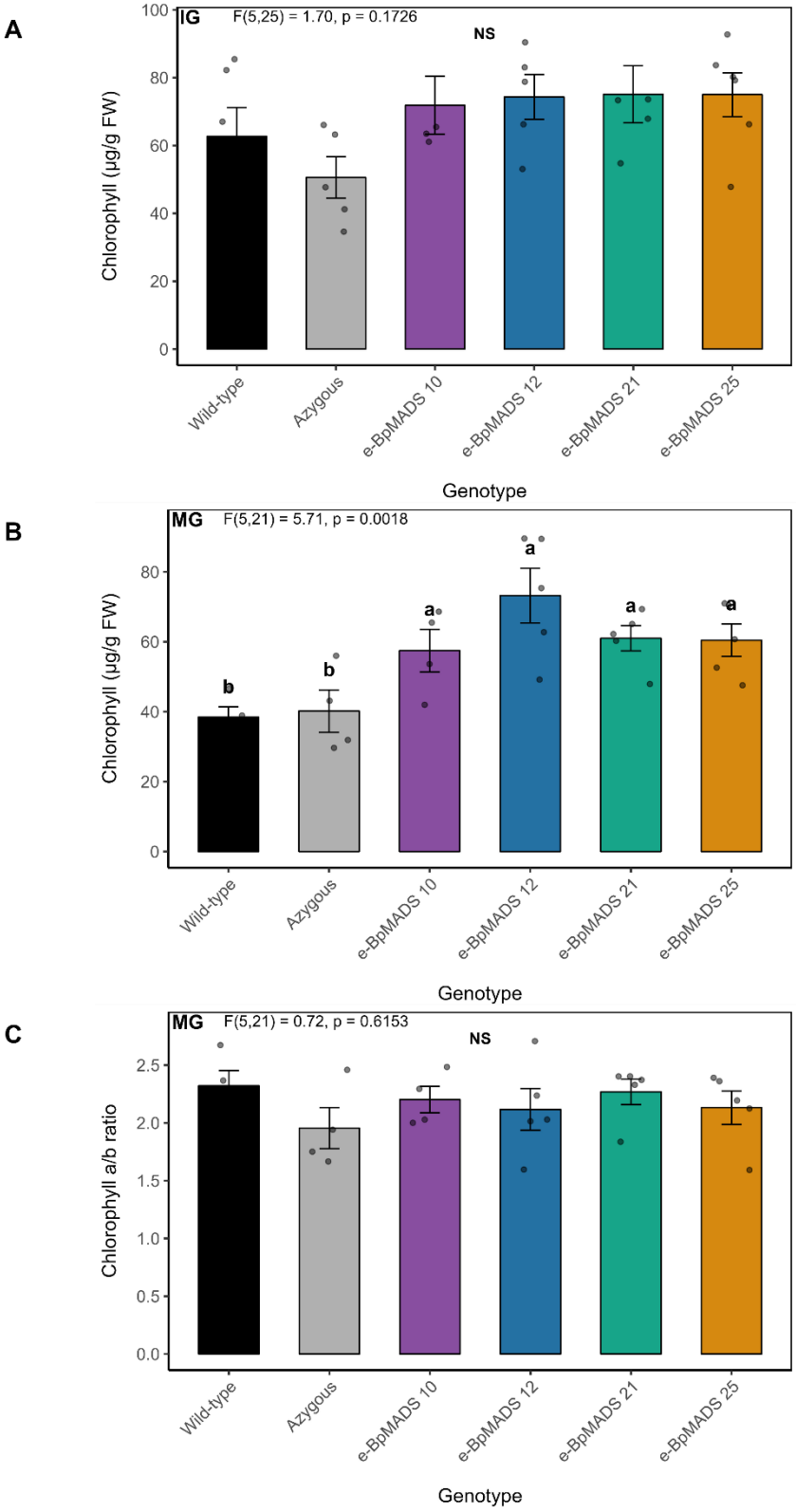

Figure 4.8. Chlorophyll levels in early-specific *BpMADS* tomato lines. Bar charts display the total chlorophyll content in independent lines of *BpMADS* driven by the *SlTFM7* early fruit-specific promoter (e-*BpMADS*), as well as azygous and wild-type controls. (A) Immature green (IG). (B) Mature green (MG). (C) Chlorophyll *a*/*b* ratio. IG = 7–10 days post-anthesis. MG = 20–23 days post-anthesis. All values represent means ± SE from at least four biological replicates per genotype, each analysed in three technical

replicates. Statistically significant differences were determined using a 1-way ANOVA followed by Duncan's multiple range test. Dots show individual data points. Different letters indicate statistically significant differences ($P<0.05$).

In line with the increases in chlorophyll content, the evaluation of total carotenoid levels in mature green e-*BpMADS* lines revealed a similar pattern (Figure 4.9). Line 12 (18.7 ± 2.04 µg/g) once again showed the highest increase, approximately 81% compared to the wild-type (10.3 ± 0.754 µg/g) and 76% compared to the azygous fruits (10.6 ± 1.49 µg/g). Likewise, e-*BpMADS* lines 21 and 25 also showed significant increases of approximately 51% and 46%, respectively, compared to the wild type, and 48% and 43% relative to the azygous control. The increase in carotenoid content in e-*BpMADS* 10, however, was not significant relative to either wild-type or azygous. In addition, similarly to what was observed in the chlorophyll analysis, no statistically significant differences were detected in the immature green fruits. Finally, no significant differences were observed between the wild-type and the azygous plants.

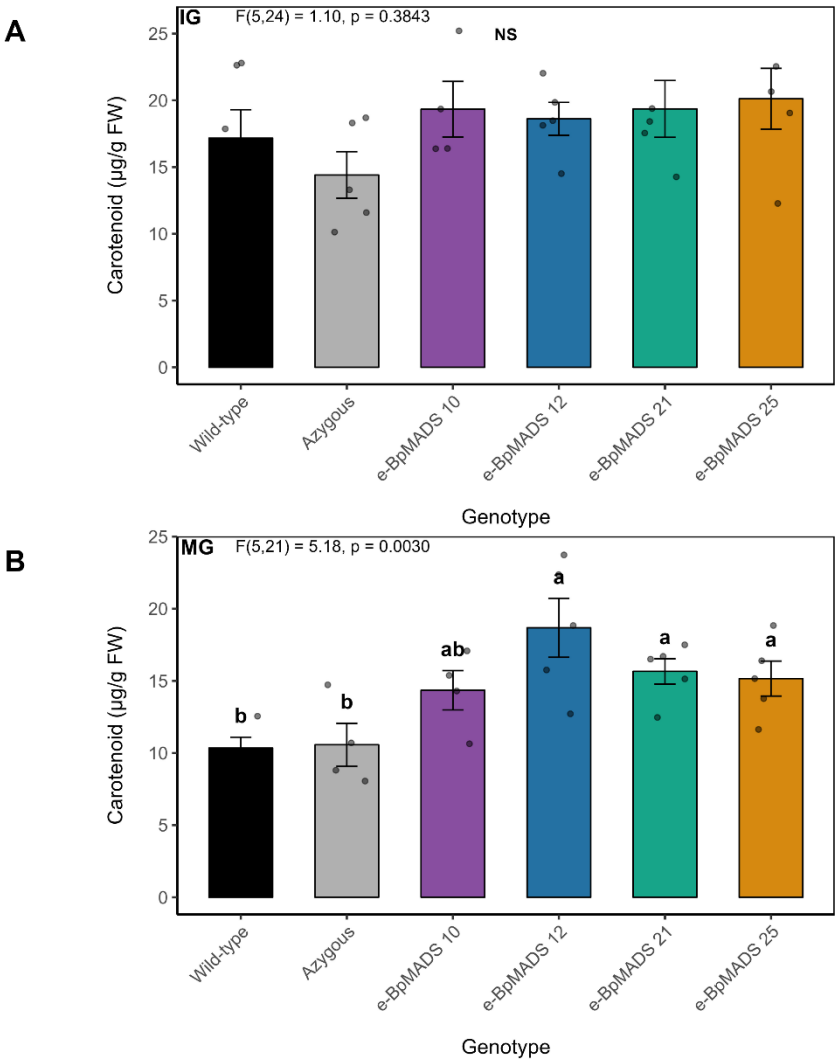

Figure 4.9. Carotenoid levels in early-specific *BpMADS* tomato lines. Bar charts display the total carotenoid content in independent lines of *BpMADS* driven by the *SlTFM7* early fruit-specific promoter (e-*BpMADS*), as well as azygous and wild-type controls. (A) Immature green (IG). (B) Mature green (MG). IG = 7–10 days post-anthesis. MG = 20–23 days post-anthesis. All values represent means ± SE from at least four biological replicates per genotype, each analysed in three technical replicates. Statistically significant differences were determined using a 1-way ANOVA followed by Duncan's multiple range test. Dots show individual data points. Different letters indicate statistically significant differences (P<0.05).

Chlorophyll and carotenoid levels were assessed in e-*BpMADS* transgenic lines across developmental stages. A two-way nested ANOVA with stage (immature green x mature green) and genotype type (wild-type/azygous vs e-*BpMADS*) as main factors, with individual genotypes nested within type, indicated that developmental stage and type each had significant independent effects on chlorophyll and carotenoid content, while accounting for variation among independent transgenic lines (Figure 4.10). These results indicate that e-*BpMADS* expression is associated with a consistent variation in chlorophyll and carotenoid levels across developmental

stages, with e-*BpMADS* lines exhibiting greater values than controls at both immature and mature green. Neither chlorophyll nor carotenoid content showed a significant stage and type interaction, although genotype-level differences were more evident at the mature green stage.

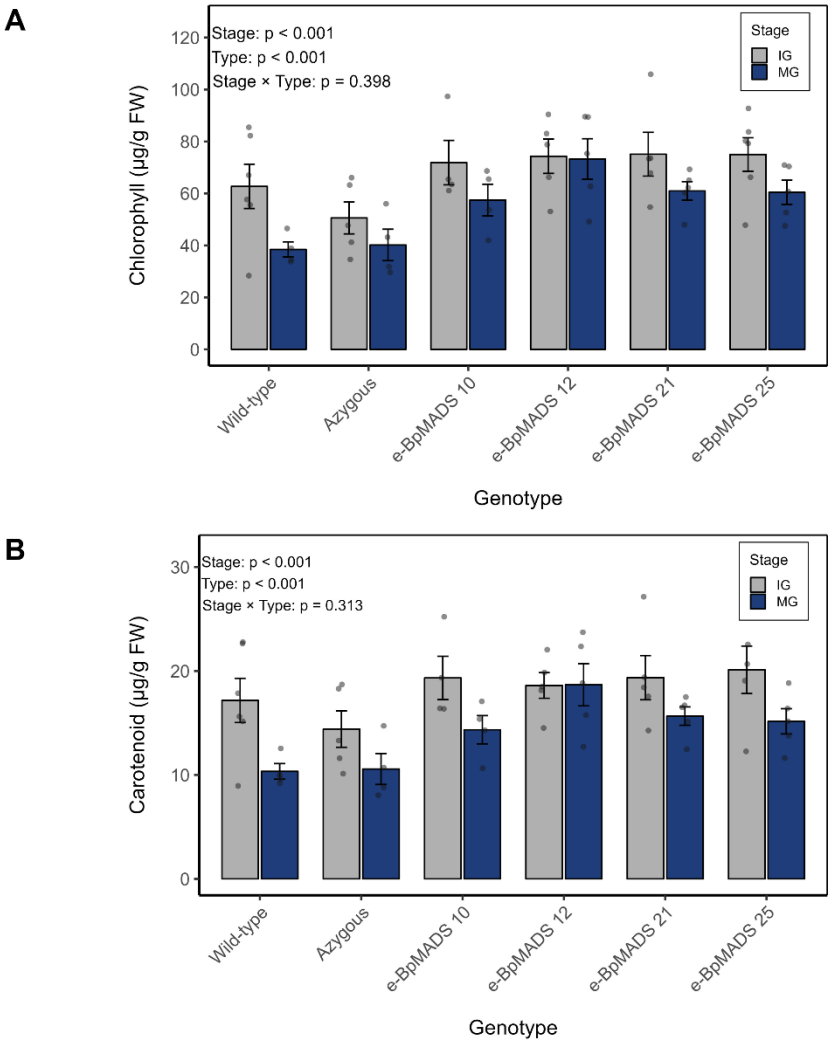

Figure 4.10. Changes in chlorophyll and carotenoid content during fruit development in early-specific *BpMADS* tomato lines. Bar charts show pigment levels in immature green (IG) and mature green (MG) fruits of *BpMADS* driven by the *SlTFM7* early fruit-specific promoter (e-*BpMADS*), as well as azygous and wild-type controls. (A) Chlorophyll levels. (B) Carotenoid levels. IG = 7–10 days post-anthesis. MG = 20–23 days post-anthesis. All values represent means ± SE from at least four biological replicates per genotype, each analysed in three technical replicates. Dots show individual data points. Statistically significant differences were assessed using a 2-way nested ANOVA, with developmental stage (IG vs MG) and genotype type (wild-type/azygous vs e-*BpMADS*) included as fixed factors and genotype (line) nested within type. Main effects and the stage × type interaction were tested, with significance accepted at $P < 0.05$.

Overall, genotypes with greater chloroplast coverage exhibited higher pigment content. An association was observed between chlorophyll content and chloroplast coverage ($R^2 = 0.86$), with

carotenoid content displaying a comparable trend (R^2 = 0.81), indicating that genotypes allocating a greater proportion of cellular space to chloroplasts generally accumulated higher levels of photosynthetic pigments (Figure 4.11). Notably, this relationship was primarily driven by the large differences between wild-type/azygous controls and transgenic genotypes, with no clear trend observed within the e-*BpMADS* independent lines themselves.

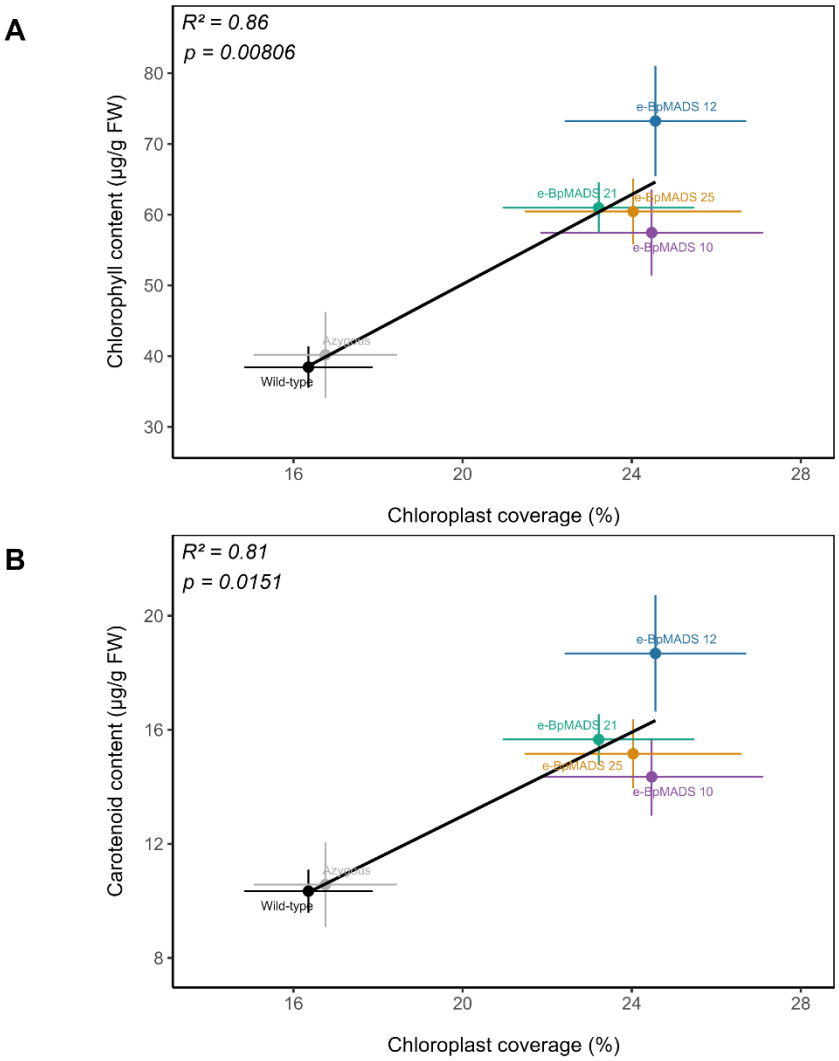

Figure 4.11. Relationship between chloroplast coverage and pigment accumulation in mature green (MG) fruit of early-specific *BpMADS* tomato lines. Scatterplots showing the correlation between chloroplast coverage and pigment content in independent genotypes expressing *BpMADS* under the *SlTFM7* early fruit-specific promoter (e-*BpMADS*), compared to azygous and wild-type controls. (A) Chlorophyll. (B) Carotenoid. MG = 20–23 days post-anthesis. Linear regression lines are shown, with associated coefficients of determination (R^2) and p-values reported in each panel. Each point represents the mean value per genotype. Horizontal error bars indicate ± SE of chloroplast coverage, while vertical error bars indicate ± SE of pigment content.

4.2.4 Lycopene and β-Carotene Show Distinct Responses in Early-Specific *BpMADS* Tomato Lines

Levels of lycopene and β-carotene in ripe fruits were also assessed. The analysis of independent lines revealed that, consistent with the chlorophyll content, e-*BpMADS* 12 also exhibited the most striking fruit colour phenotype (Figure 4.12), which was further confirmed by the quantitative analysis.

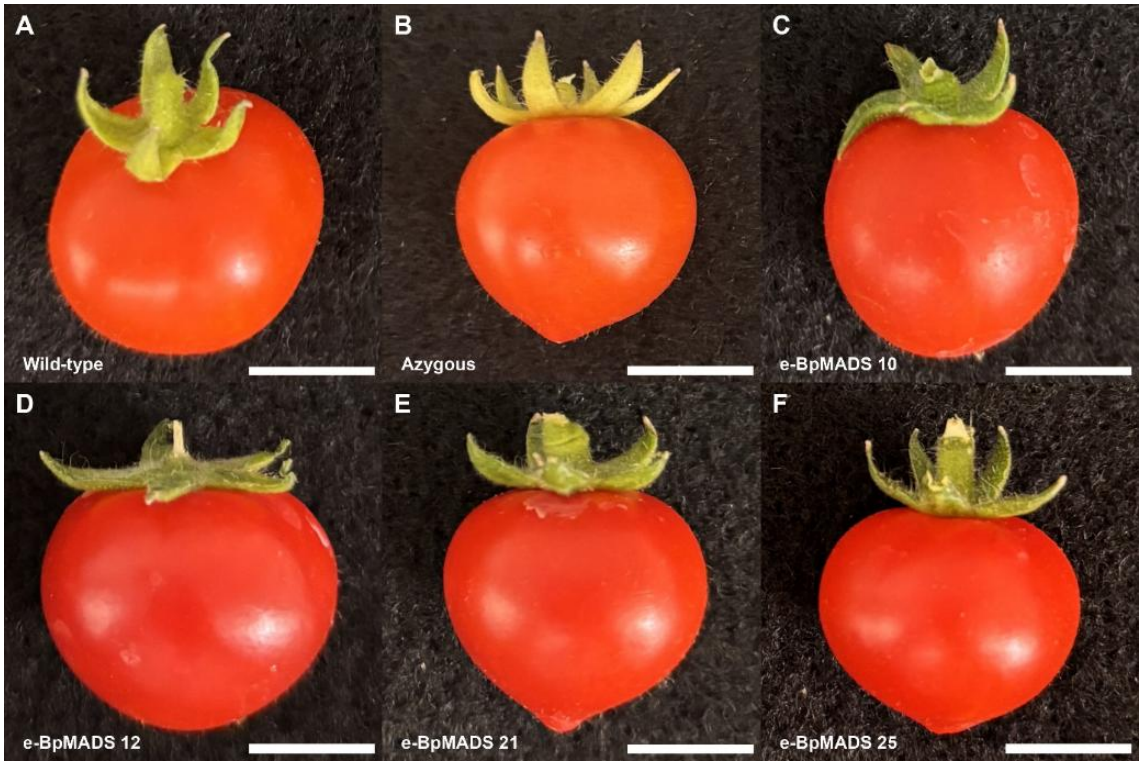

Figure 4.12. Phenotypes of ripe fruits of early-specific *BpMADS* tomato lines. Images display representative ripe fruits from transgenic lines expressing *BpMADS* driven by the *SlTFM7* early fruit-specific promoter (e-*BpMADS*), as well as azygous and wild-type controls. (A) Wild-type. (B) Azygous. (C) e-*BpMADS* 10. (D) e-*BpMADS* 12. (E) e-*BpMADS* 21. (F) e-*BpMADS* 25. Ripe = breaker +7–10 days. Scale bars = 1 cm.

Lycopene levels were greater by approximately 56% in e-*BpMADS* 12 (146.22 ± 18.40 µg/g) compared to wild-type fruits (93.48 ± 9.63 µg/g), and by 54% relative to the azygous control (94.67 ± 14.32 µg/g) (Figure 4.13A). This result is comparable to those observed by the overexpression of *AtGLK2* in tomato fruit, which resulted in a 60% increase in lycopene content (Powell et al., 2012). Moreover, e-*BpMADS* 12 levels of β-carotene were greater by approximately 77% compared to the wild-type and by 39% compared to the azygous control (Figure 4.13B). Similarly, e-*BpMADS*

25 showed increases in both lycopene (147.02 ± 11.11 µg/g) and β-carotene (15.6 ± 1.20 µg/g). These values represent increases of 56% and 22% relative to the wild-type and azygous control, respectively. While e-*BpMADS* 21 exhibited significantly greater levels of β-carotene, about 40% more than the wild-type, lycopene accumulation in this line remained relatively low, with an increase of less than 10% compared to both controls. Similarly, e-*BpMADS* 10 showed only a slight difference in lycopene, while its β-carotene content was greater by 37% compared to the wild-type, with a more subtle increase relative to the azygous control.

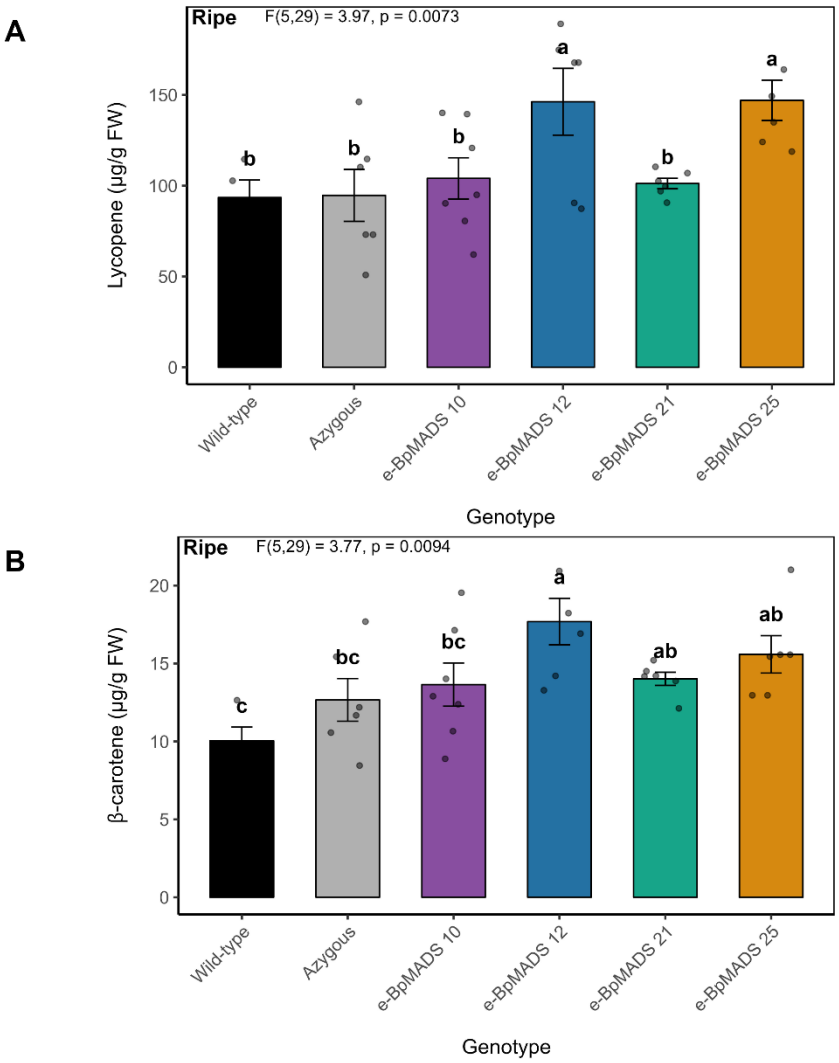

Figure 4.13. Carotenoid levels in early-specific *BpMADS* tomato lines. Bar charts display the carotenoid content in independent lines of *BpMADS* driven by the *SlTFM7* early fruit-specific promoter (e-*BpMADS*), as well as azygous and wild-type controls. (A) Lycopene. (B) β-carotene. Ripe = breaker +7–10 days. All values represent means ± SE from at least four biological replicates per genotype, each analysed in two technical replicates. Statistically significant differences were determined using a 1-way ANOVA followed by a Duncan's multiple range test. Dots show individual data points. Different letters indicate statistically significant differences (P<0.05).

4.2.5 Chlorophyll and Carotenoid Levels Are Unaffected in Ripening-Specific *BpMADS* Tomato Lines

In addition to the early-specific expression, the effects of *BpMADS* overexpression on fruit pigment accumulation were also investigated in lines driven by the ripening *CaFIB* promoter. Representative fruit images illustrate the external phenotypes observed at the mature green stage (Figure 4.14).

Figure 4.14. Phenotypes of mature green (MG) fruits of ripening-specific *BpMADS* tomato lines. Images display representative MG fruits from transgenic lines expressing *BpMADS* driven by the *CaFIB* ripening fruit-specific promoter (r-*BpMADS*), as well as azygous and wild-type controls. (A) Wild-type. (B) Azygous. (C) r-*BpMADS* 8. (D) r-*BpMADS* 16. (E) r-*BpMADS* 25. MG = 20–23 days post-anthesis. Scale bars = 1 cm.

The analysis of transgenic lines individually revealed that the mature green fruits of lines r-*BpMADS* 8 and 25 exhibited a slight increase in chlorophyll compared to both the wild-type and azygous lines (Figure 4.15). Transgenic line r-*BpMADS* 8 exhibited total chlorophyll levels of 46.11 ± 0.76 µg/g at the mature green stage, while r-*BpMADS* 25 displayed 44.06 ± 1.4 µg/g. In comparison, wild-type levels were 38.45 ± 2.92 µg/g, and in the azygous control, levels were 40.18

± 6.05 µg/g. Transgenic line r-*BpMADS* 16 showed comparable values to both controls, at 37.43 ± 5.1 µg/g. These small differences observed, however, were not statistically significant.

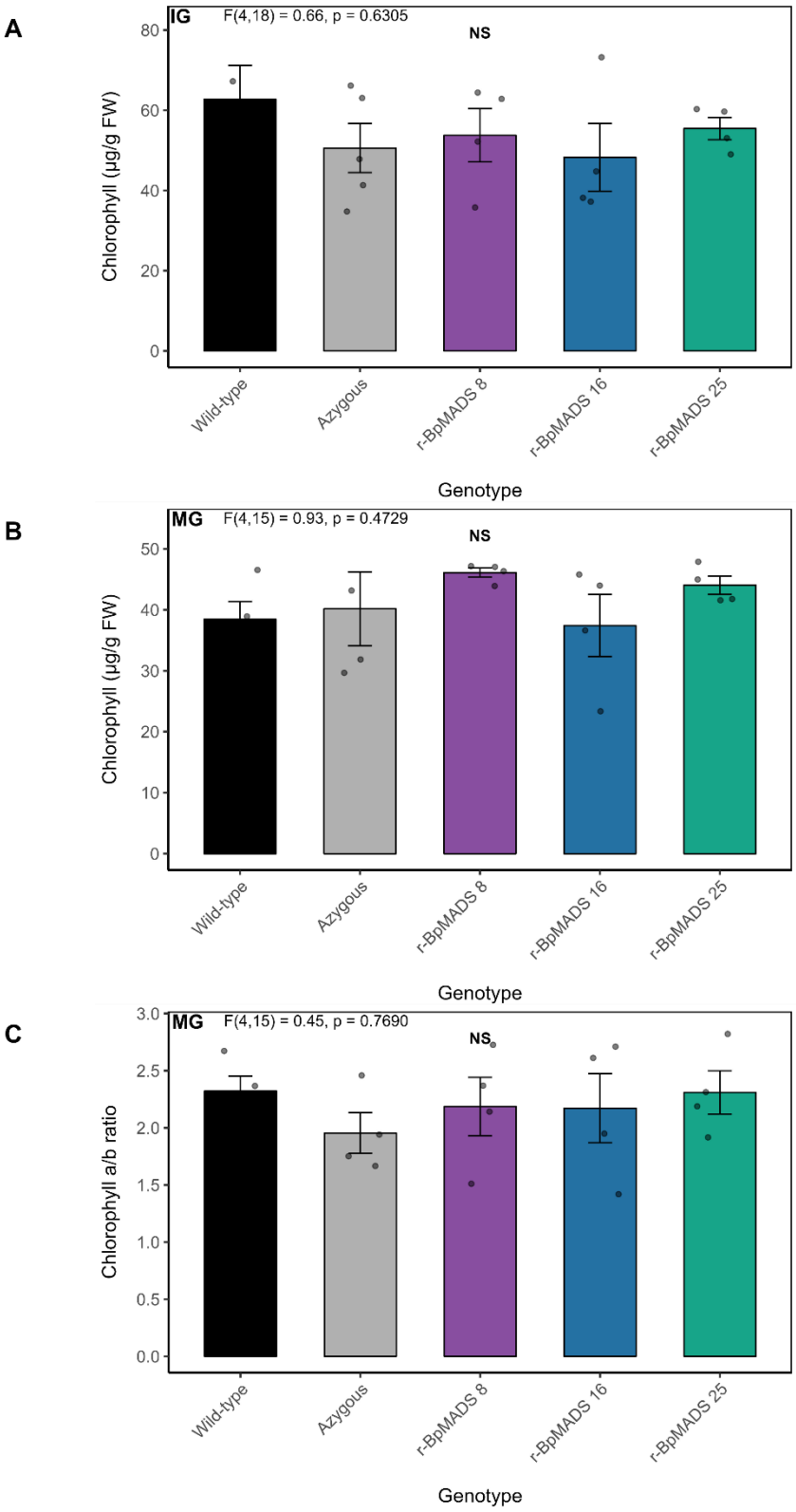

Figure 4.15. Chlorophyll levels in ripening-specific *BpMADS* tomato lines. Bar charts display the total chlorophyll content in independent lines of *BpMADS* driven by the *CaFIB* ripening fruit-specific promoter (r-*BpMADS*), as well as azygous and wild-type controls. (A) Immature green (IG). (B) Mature green (MG). (C) Chlorophyll *a*/*b* ratio. IG = 7–10 days post-anthesis. MG = 20–23 days post-anthesis. All values represent means ± SE from at least four biological replicates per genotype, each analysed in three technical

replicates. Statistically significant differences were determined using a 1-way ANOVA followed by Duncan's multiple range test. Dots show individual data points. Different letters indicate statistically significant differences (P<0.05).

Similarly, both r-*BpMADS* 8 and 25 showed slight increases in carotenoid content, approximately 12% compared to the wild-type and 9% compared to azygous, at the mature green stage, although these differences were not significant. Similar to the chlorophyll analysis, the analysis of carotenoid content at the immature green fruit level yielded no significant differences (Figure 4.16).

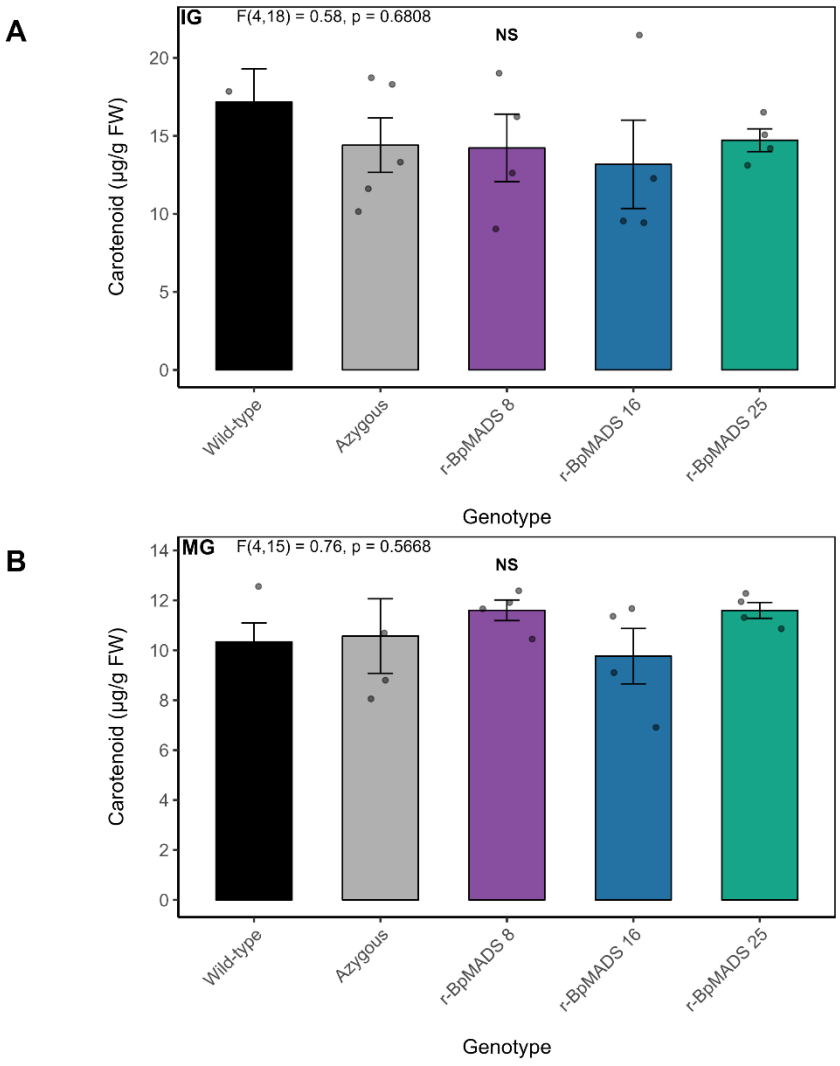

Figure 4.16. Carotenoid levels in ripening-specific *BpMADS* tomato lines. Bar charts display the total carotenoid content in independent lines of *BpMADS* driven by the *CaFIB* ripening fruit-specific promoter (r-*BpMADS*), as well as azygous and wild-type controls. (A) Immature green (IG). (B) Mature green (MG). IG = 7–10 days post-anthesis. MG = 20–23 days post-anthesis. All values represent means ± SE from at least four biological replicates per genotype, each analysed in three technical replicates. Statistically significant

differences were determined using a 1-way ANOVA followed by a Duncan's multiple range test. Dots show individual data points. Different letters indicate statistically significant differences (P<0.05).

4.2.6 Lycopene and β-Carotene Show Distinct Responses in Ripening-Specific *BpMADS* Tomato Lines

To assess the impact of the ripening-specific *BpMADS* overexpression on carotenoid accumulation in ripe fruit, lycopene and β-carotene levels were assessed in transgenic lines. Representative ripe fruits r-*BpMADS* are shown in Figure 4.17.

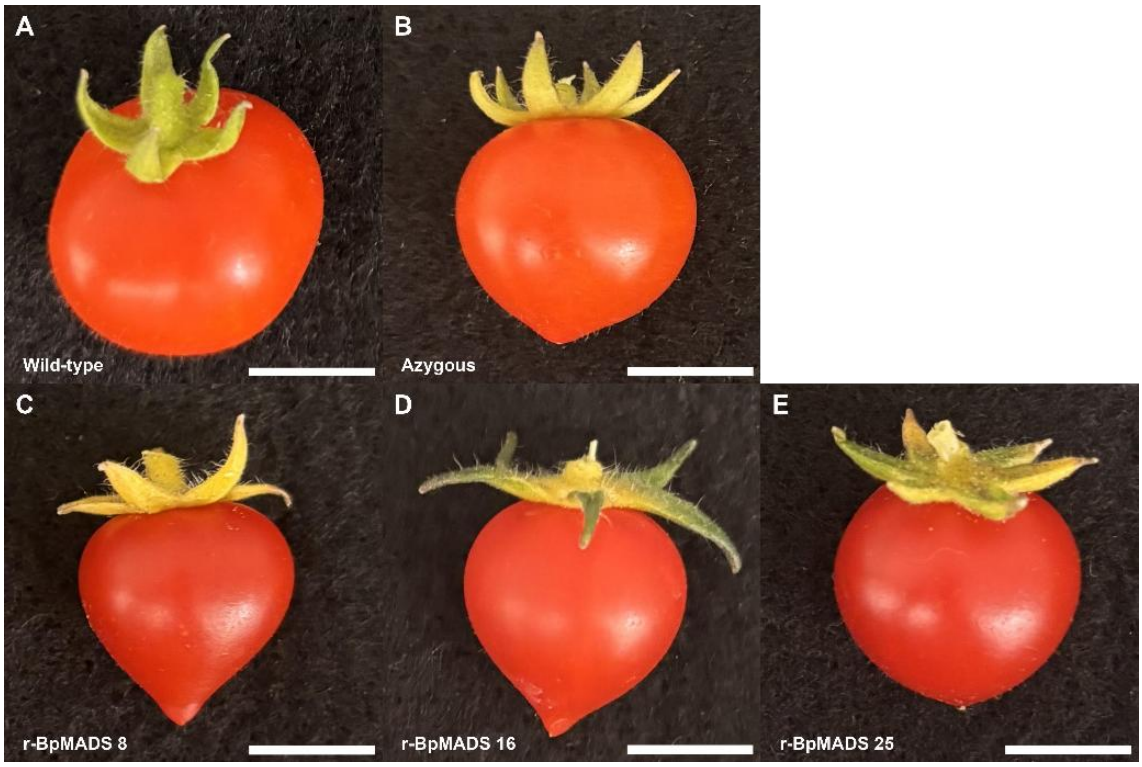

Figure 4.17. Phenotypes of ripe fruits of ripening-specific *BpMADS* tomato lines. Images display representative ripe fruits from transgenic lines expressing *BpMADS* driven by the *CaFIB* ripening fruit-specific promoter (r-*BpMADS*), as well as azygous and wild-type controls. (A) Wild-type. (B) Azygous. (C) r-*BpMADS* 8. (D) r-*BpMADS* 16. (E) r-*BpMADS* 16. Ripe = breaker +7–10 days. Scale bars = 1 cm.

The analysis of transgenic lines showed that lycopene levels were greater by approximately 59% and 49% in r-*BpMADS* 8 and r-*BpMADS* 25, respectively, compared to the wild-type, and by 56% and 45% relative to the azygous line (Figure 4.18A). Furthermore, levels of β-carotene in those lines were 59% and 54% greater than in wild-type fruit, and 24% and 20% higher relative to the azygous line (Figure 4.18B). Line r-*BpMADS* 16 displayed no significant lycopene increase but

exhibited greater β-carotene accumulation relative to wild-type, by approximately 67%, supporting the previously mentioned hypothesis that in some lines, enzymatic reactions involved in β-carotene biosynthesis could be favoured, leading to enhancement of this carotenoid at the detriment of lycopene.

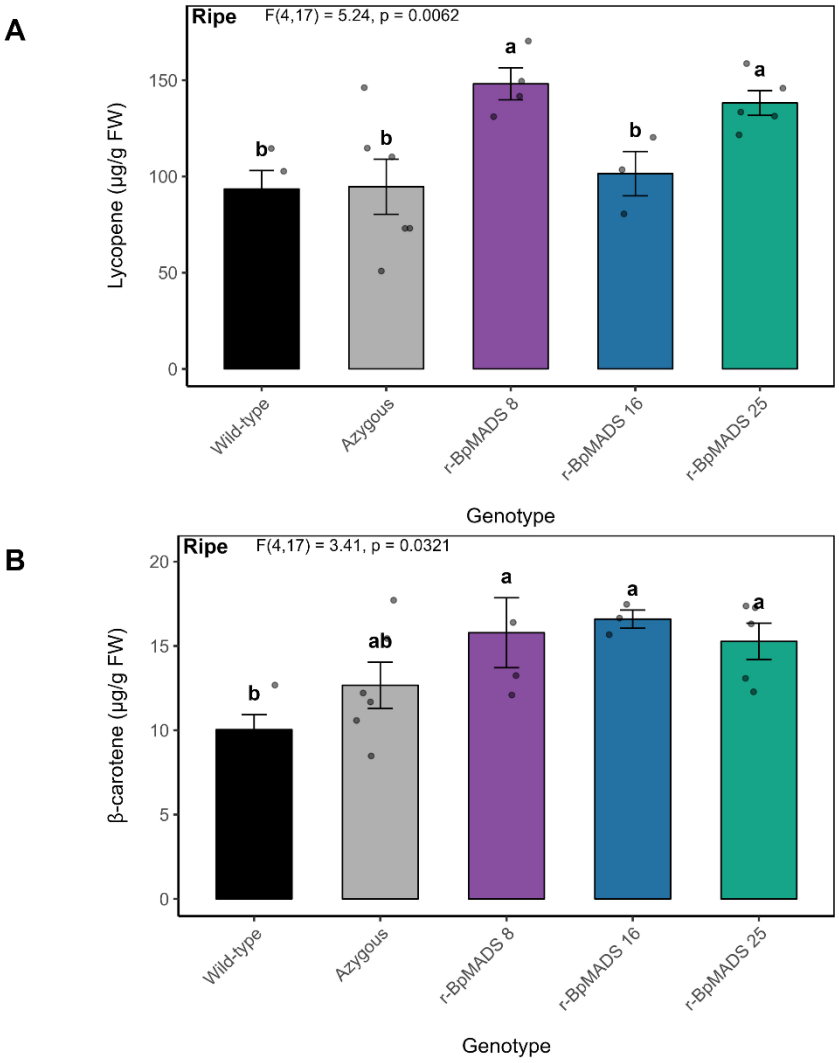

Figure 4.18. Carotenoid levels in ripening-specific *BpMADS* tomato lines. Bar charts display the carotenoid content in independent lines of *BpMADS* driven by the *CaFIB* ripening fruit-specific promoter (r-*BpMADS*), as well as azygous and wild-type controls. (A) Lycopene. (B) β-carotene. Ripe = breaker +7–10 days. All values represent means ± SE from at least four biological replicates per genotype, each analysed in two technical replicates. Statistically significant differences were determined using a 1-way ANOVA followed by a Duncan's multiple range test. Dots show individual data points. Different letters indicate statistically significant differences (P<0.05).

4.2.7 Early-Specific *BpMADS* Overexpression Increases Maximum PSII Quantum Yield (F_v/F_m)

The maximum quantum yield of PSII (F_v/F_m) reflects the maximum ability of antenna pigments to absorb and transfer light energy to PSII when non-photochemical pathways are minimal. Across all genotypes and developmental stages, F_v/F_m values were close to 0.8, consistent with an intact and functional photosynthetic apparatus with little evidence of photoinhibition or stress-induced damage. These results are consistent with previous findings in the literature. First, in leaf tissues, F_v/F_m is generally a conserved parameter, being around 0.8 to 0.85 in most tomato cultivars (Liang et al., 2020). Moreover, in tomato fruit, recorded values typically ranged from 0.78 to 0.83 (Carrara et al., 2001; Hetherington et al., 1998).

The analysis of e-*BpMADS* transgenic lines revealed no statistically significant differences in F_v/F_m between immature green fruits of transgenic lines and the wild-type control (0.811 ± 0.003) or azygous (0.821 ± 0.004), except for e-*BpMADS* 12 (0.830 ± 0.003), which exhibited a significantly higher value than wild-type. All the remaining lines ranged from 0.815 to 0.824 (Figure 4.19A). This finding aligns with the variability in pigment content observed at this developmental stage in the previous section. On the other hand, mature green fruits from three transgenic lines, e-*BpMADS* 10 (0.812 ± 0.013), e-*BpMADS* 21 (0.817 ± 0.009), and e-*BpMADS* 25 (0.818 ± 0.008), exhibited significantly higher F_v/F_m values compared to wild-type (0.788 ± 0.024), although the increase relative to azygous (0.793 ± 0.025) was not statistically significant (Figure 4.19B).

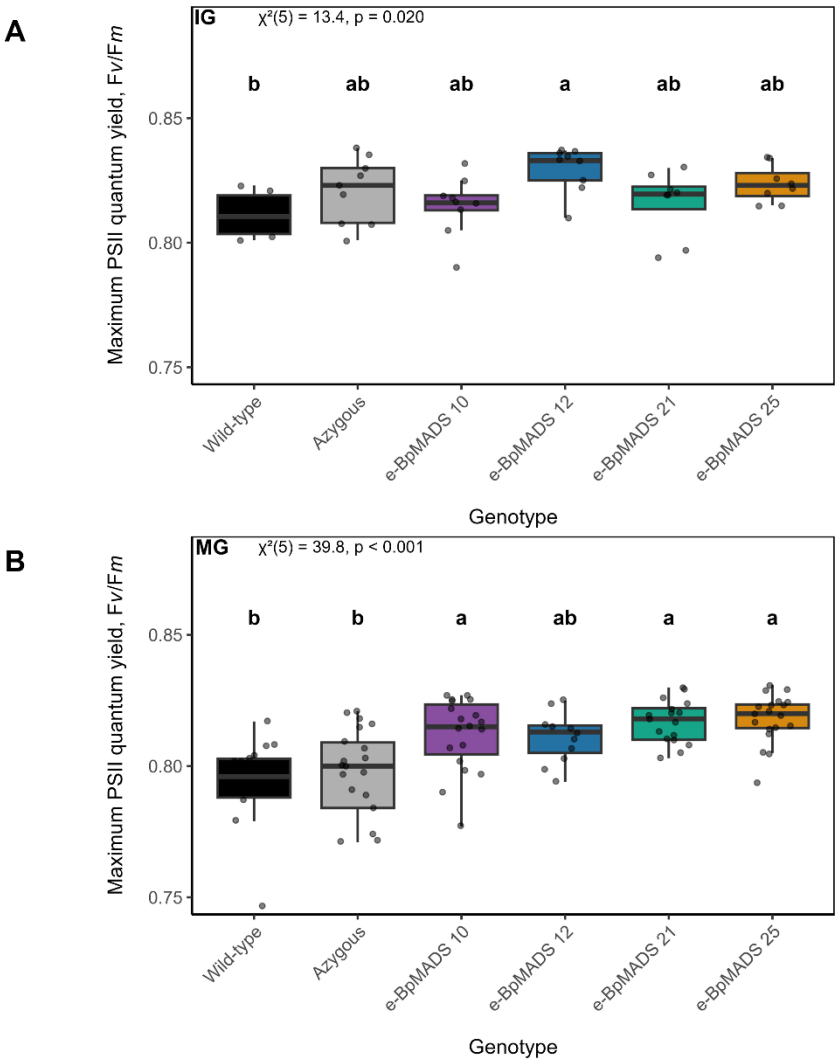

Figure 4.19. Maximum PSII quantum yield (F_v/F_m) in early-specific *BpMADS* tomato lines. Boxplots display F_v/F_m in fruits from independent lines of *BpMADS* driven by the *SlTFM7* early fruit-specific promoter (e-*BpMADS*), compared with azygous and wild-type controls. (A) Immature green (IG). (B) Mature green (MG). IG = 7–10 days post-anthesis. MG = 20–23 days post-anthesis. The boxes represent the interquartile range (25th to 75th percentile), the horizontal line shows the median, and the whiskers extend to 1.5 times the interquartile range. Statistically significant differences were determined using a Kruskal-Wallis test followed by Dunn's multiple range test. Dots show individual data points. Different letters indicate statistically significant differences (P < 0.05).

4.2.8 Early-Specific *BpMADS* Overexpression Increases Effective PSII Quantum Yield (ΦPSII)

The analysis of chlorophyll fluorescence light response curves provides a physiologically relevant analysis of PSII performance and energy partitioning under increasing photochemical demand and allows us to select specific data points for deeper analysis. The results showed that all transgenic lines exhibited greater values than the wild-type across all light intensities at both

developmental stages, although the effects were clearer in mature green fruits (Figure 4.20). Notably, immature green fruits, which exhibited modest increases in pigment content relative to wild-type (15-20%), also exhibited enhanced effective PSII quantum yield (ΦPSII). Nevertheless, the increase in ΦPSII relative to azygous was less pronounced. These results reinforce the biological variability observed at the immature green stage.

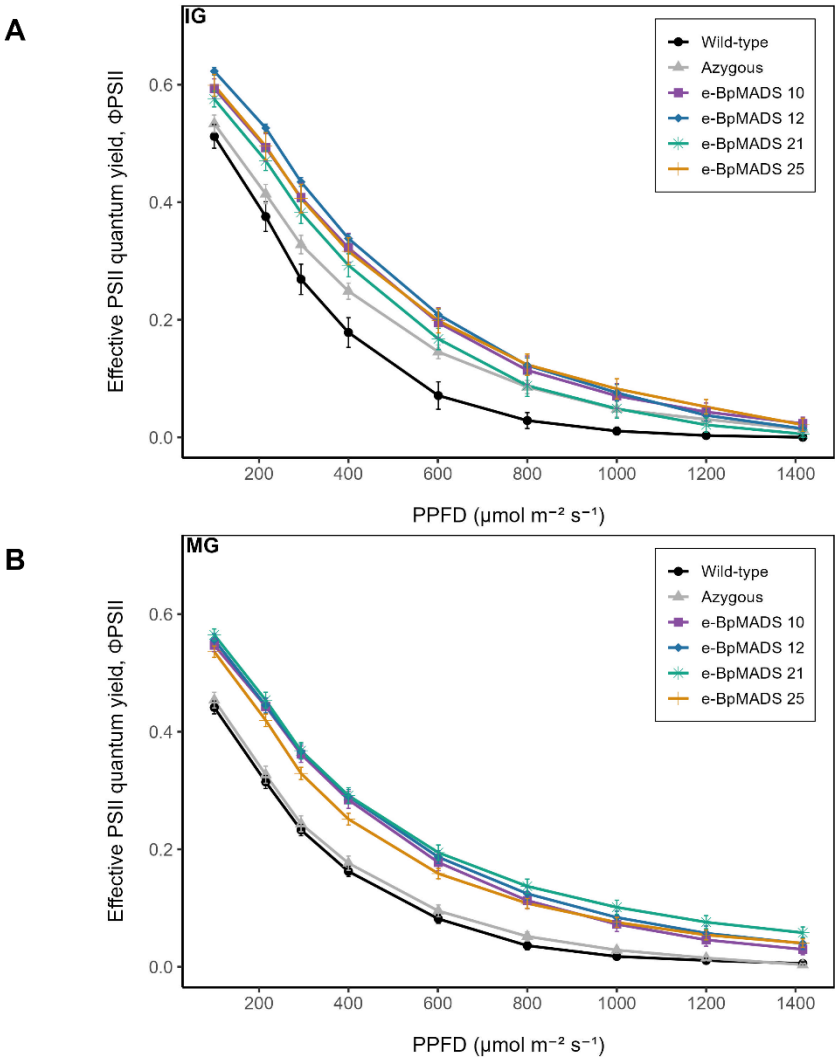

Figure 4.20. Light responses of effective PSII quantum yield (ΦPSII) in early-specific *BpMADS* tomato lines. Light curves display ΦPSII in fruits from independent lines of *BpMADS* driven by the *SlTFM7* early fruit-specific promoter (e-*BpMADS*), compared with azygous and wild-type controls. (A) Immature green (IG). (B) Mature green (MG). IG = 7–10 days post-anthesis. MG = 20–23 days post-anthesis. All values represent means ± SE from at least four biological replicates per genotype, with two fruits sampled per plant.

For more detailed comparisons, light intensities of 294 and 601 µmol m^{-2} s^{-1} were selected to represent moderate and high PAR levels, respectively, within the developmental context and the

physiological range experienced by tomato fruit tissue. Intensities above 601 µmol m^{-2} s^{-1} were avoided to minimise the effects of photoinhibition. At 294 µmol m^{-2} s^{-1}, ΦPSII was significantly greater in immature green fruits of e-*BpMADS* 12 (0.434 ± 0.007) compared to wild-type (0.269 ± 0.025) and azygous control (0.328 ± 0.015). Lines e-*BpMADS* 10 (0.408 ± 0.024), e-*BpMADS* 21 (0.382 ± 0.018), and e-*BpMADS* 25 (0.406 ± 0.024) also exhibited greater values, however, these differences were not statistically significant (Figure 4.21A). The analysis of mature green fruits revealed that all four transgenic lines displayed significantly greater ΦPSII values than both wild-type and azygous controls, values ranging from 0.329 to 0.368, outperforming those of wild-type (0.233 ± 0.009) and azygous (0.243 ± 0.013) fruits (Figure 4.21B). These results correspond to increases of approximately 41 to 58% relative to wild-type and 35 to 51% relative to azygous controls, confirming that the effect of early-specific *BpMADS* overexpression was consistently stronger at the mature green stage.

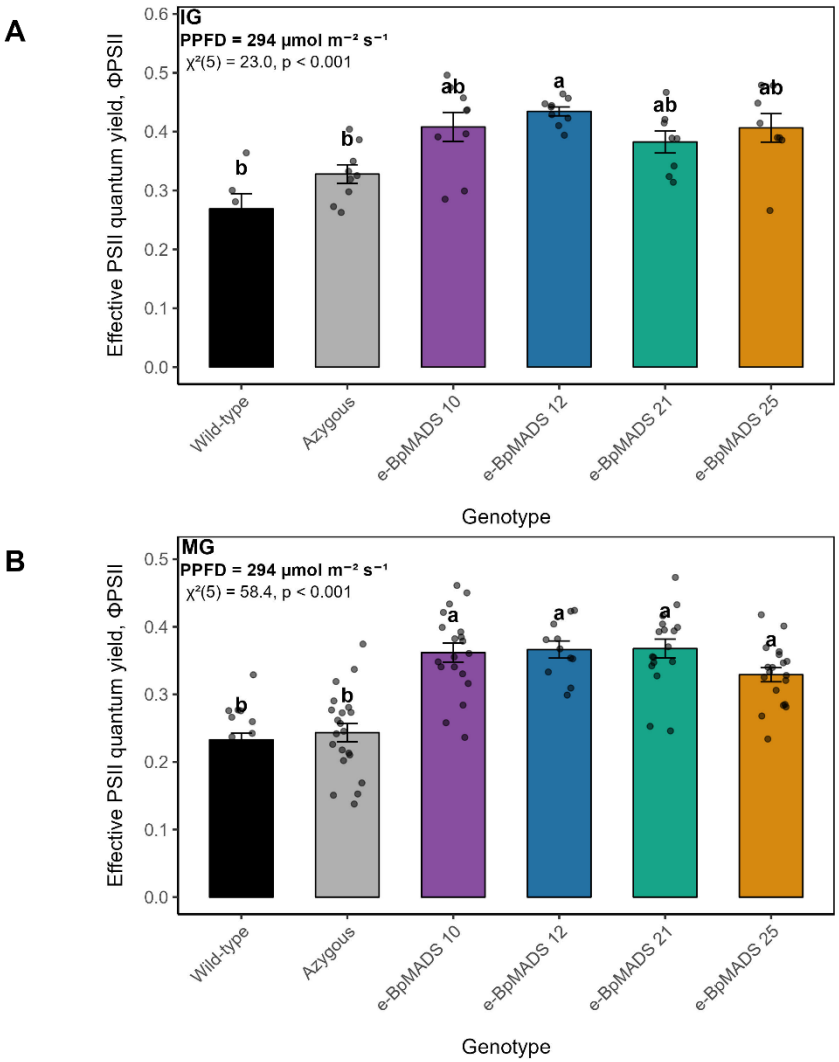

Figure 4.21. Effective PSII quantum yield (ΦPSII) in early-specific *BpMADS* tomato lines. Bar charts display ΦPSII in fruits from independent lines of *BpMADS* driven by the *SlTFM7* early-specific promoter (e-*BpMADS*), compared with azygous and wild-type controls at 294 µmol m^{-2} s^{-1}. (A) Immature green (IG). (B) Mature green (MG). IG = 7–10 days post-anthesis. MG = 20–23 days post-anthesis. All values represent means ± SE from at least four biological replicates per genotype, with two fruits sampled per plant. Statistically significant differences were determined using a Kruskal-Wallis test followed by Dunn's multiple range test. Dots show individual data points. Different letters indicate statistically significant differences (P < 0.05).

At a PAR of 601 µmol m^{-2} s^{-1} (Figure 4.22), immature green fruits of e-*BpMADS* 10, 12 and 25 exhibited significantly greater ΦPSII compared to wild-type, but not to the azygous control. The trend was, once again, more consistent in mature green fruits, where all transgenic lines showed a clear and significant increase in ΦPSII (0.178-0.184) relative to both wild-type (0.081 ± 0.007) and azygous (0.095 ± 0.010) at the same light intensity. These values represent increases of approximately 120-127% relative to the wild type and 87-94% to the azygous control.

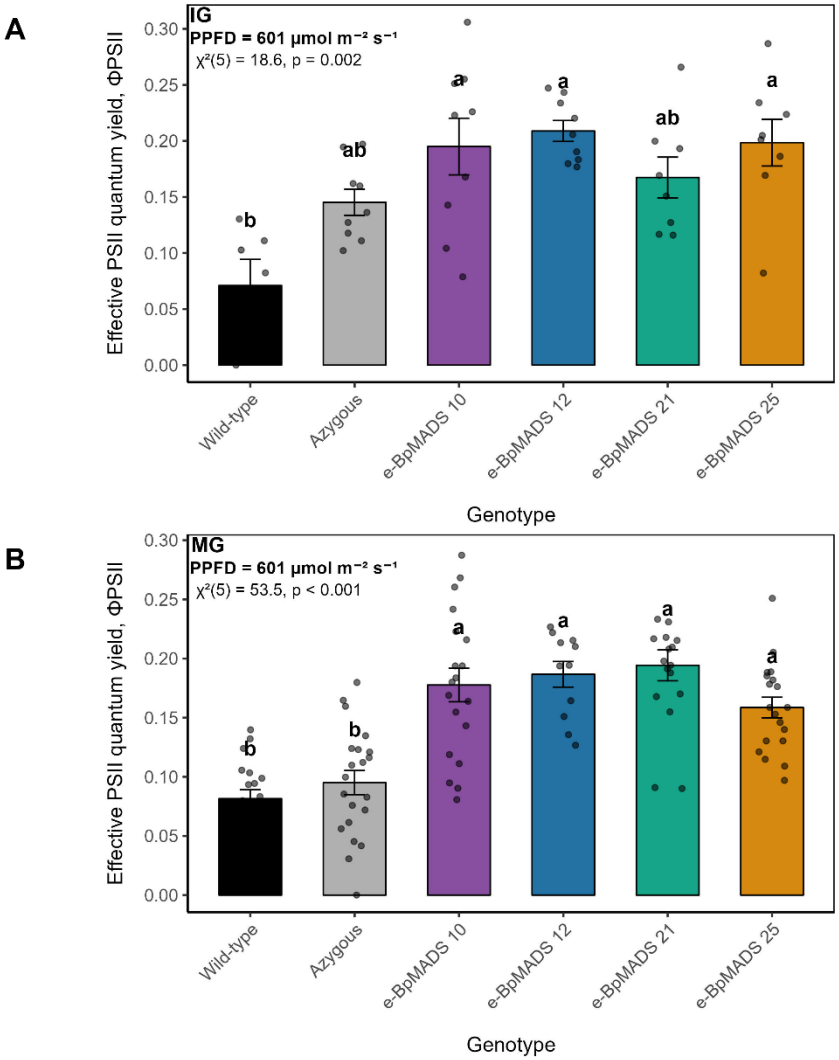

Figure 4.22. Effective PSII quantum yield (ΦPSII) in early-specific *BpMADS* tomato lines. Bar charts display ΦPSII in fruits from independent lines of *BpMADS* driven by the *SlTFM7* early fruit-specific promoter (e-*BpMADS*), compared with azygous and wild-type controls at 601 µmol m^{-2} s^{-1}. (A) Immature green (IG). (B) Mature green (MG). IG = 7–10 days post-anthesis. MG = 20–23 days post-anthesis. All values represent means ± SE from at least four biological replicates per genotype, with two fruits sampled per plant. Statistically significant differences were determined using a Kruskal-Wallis test followed by Dunn's multiple range test. Dots show individual data points. Different letters indicate statistically significant differences ($P < 0.05$).

4.2.9 Effective PSII Quantum Yield (ΦPSII) at Different Developmental Stages in Early-Specific *BpMADS* Tomato Lines

A two-way ANOVA revealed a significant effect of developmental stage (IG vs MG), with ΦPSII declining as fruit progressed from the immature to the mature green stage. Genotype type (wild-type/azygous vs e-*BpMADS*) also had a significant effect at both light intensities tested (294 and

601 µmol m^{-2} s^{-1}), indicating higher ΦPSII in e-*BpMADS* lines relative to controls (Figure 4.23). No significant stage × type interaction was detected, suggesting that the relative effect of e-*BpMADS* expression was comparable at both developmental stages. Nevertheless, ΦPSII values in mature green fruit were generally less variable across genotypes, whereas immature green fruit showed higher variation. These observations indicate that, although e-*BpMADS* enhances photochemical efficiency at both stages, the mature green stage provides a more consistent stage for assessing transgene activity on photochemical capacity.

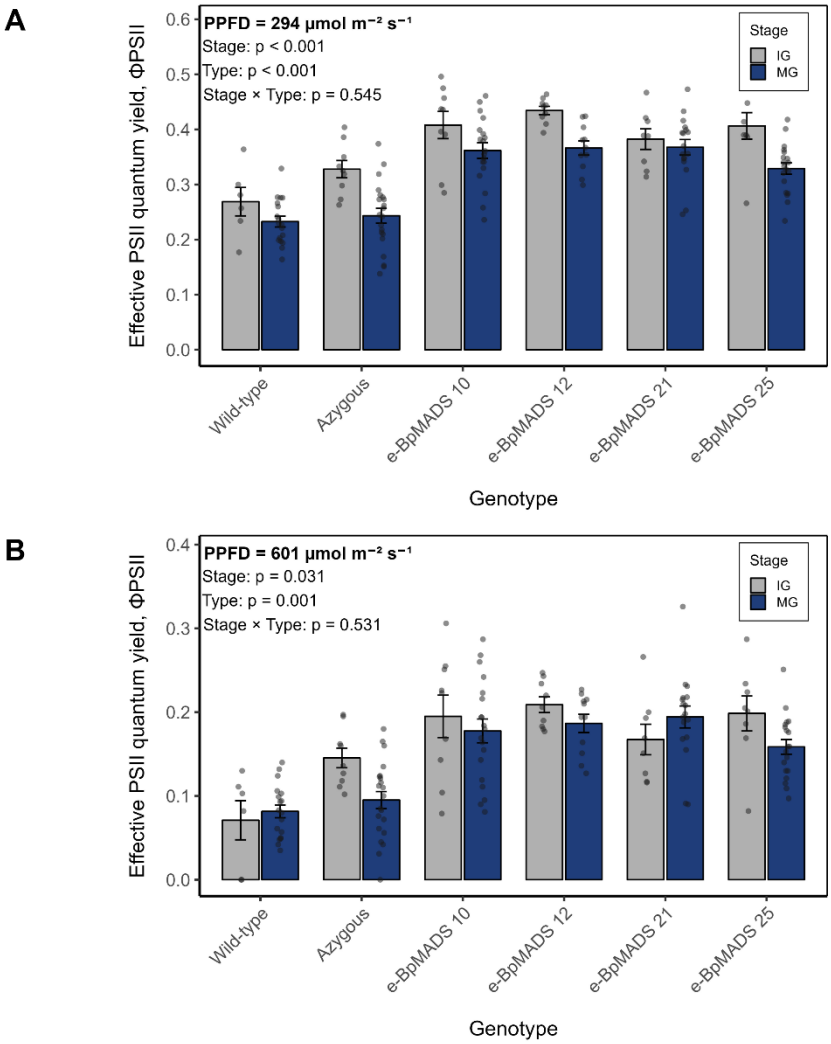

Figure 4.23. Changes in light responses of effective PSII quantum yield (ΦPSII) during fruit development in early-specific *BpMADS* tomato lines. The bar charts display ΦPSII in fruits of *BpMADS* driven by the *SlTFM7* early fruit-specific promoter, as well as azygous and wild-type controls. (A) ΦPSII at 294 µmol m^{-2} s^{-1}. (B) ΦPSII at 601 µmol m^{-2} s^{-1}. IG = 7–10 days post-anthesis. MG = 20–23 days post-anthesis. All values represent means ± SE from at least four biological replicates per genotype, with two fruits sampled per plant. Dots show individual data points. Statistically significant were assessed using a

2-way nested ANOVA, with developmental stage (IG vs MG) and genotype type (wild-type/azygous vs e-*BpMADS*) included as fixed factors and genotype (line) nested within type. Main effects and the stage × type interaction were tested, with significance accepted at $P < 0.05$.

4.2.10 Chlorophyll Fluorescence Images of Effective PSII Quantum Yield (ΦPSII) in Early-Specific *BpMADS* Tomato Lines

Chlorophyll fluorescence imaging of whole fruits further supported the quantitative measurements. Images of ΦPSII showed that in e-*BpMADS* fruits, photochemical efficiency was uniform across the fruit surface, while wild-type and azygous fruits exhibited localised signs of photodamage under high light intensity (Figure 4.24). Exposure to 601 µmol m^{-2} s^{-1} actinic light caused wild-type fruits to develop regions in which the chlorophyll fluorescence signal was too low to determine a ΦPSII value (black regions), indicative of severe photodamage. In contrast, most e-*BpMADS* fruits maintained PSII efficiency. Together, these results demonstrate that e-*BpMADS* transgenic tomato fruits exhibit enhanced and sustained photochemistry, which correlates with the quantitative data, especially under elevated light conditions.

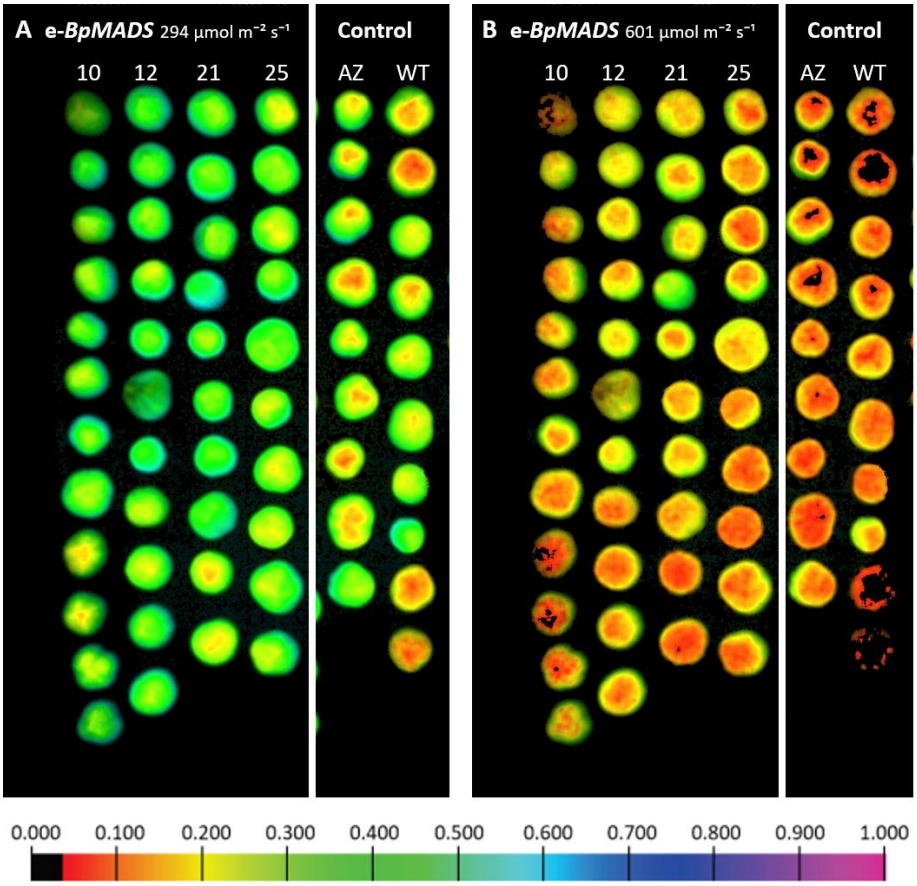

Figure 4.24. Chlorophyll fluorescence imaging of Effective PSII quantum yield (ΦPSII) in early-specific *BpMADS* tomato lines. Fluorescence imaging displays ΦPSII under two light intensities in mature green fruits (MG) of *BpMADS* lines driven by the *SlTFM7* early fruit-specific promoter (e-*BpMADS*), azygous and wild-type controls. (A) ΦPSII images of fruits at 294 µmol m^{-2} s^{-1}. (B) ΦPSII images of fruits at 601 µmol m^{-2} s^{-1}. Transgenic e-*BpMADS* lines 10, 12, 21 and 25 are compared against azygous (AZ) and wild-type (WT) controls. MG = 20–23 days post-anthesis. Colour scales range from 0 (black) to 1 (purple) and represent ΦPSII values. Green to blue regions indicate high photochemical efficiency, whereas yellow to red areas indicate reduced PSII activity, suggesting photoinhibition or increased excitation pressure under higher PPFD.

4.2.11 Early-Specific *BpMADS* Overexpression Enhances Electron Transport Rate (ETR) in Mature Green Tomato Fruits

Given that the differences observed in immature green fruits were generally more variable, the following analyses focus primarily on mature green fruits, as this stage appears to provide a more consistent and reliable indicator of transgene-induced changes in photochemical capacity.

The light response curve for electron transport rate (ETR) shows that ETR increases with increasing light intensity (PPFD) for all genotypes up to a point, then reaches saturation and eventually declines (Figure 4.25A). The low ETR values at the beginning indicate that at low PPFD, photosynthesis is limited by light. As light increases, electron transport is limited by downstream sinks. It is also evident that wild-type and azygous lines saturate earlier, around 300–400 µmol m^{-2} s^{-1}. In contrast, e-*BpMADS* genotypes exhibit higher ETR and saturate at a higher light intensity, around 400–600 µmol m^{-2} s^{-1}, with e-*BpMADS* 12 and 21 being the highest performers.

A deeper analysis of ETR at 294 and 601 µmol m^{-2} s^{-1} reveals that all four e-*BpMADS* transgenic lines showed greater ETRs compared to wild-type and azygous controls at both light intensities. At 294 µmol m^{-2} s^{-1}, the ETR values for wild-type and azygous fruits were 28.7 ± 1.21 and 30.0 ± 1.66 µmol electrons m^{-2} s^{-1}, respectively, whereas the e-*BpMADS* lines exhibited higher rates, between 40.6 ± 1.29 and 45.4 ± 1.73 µmol electrons m^{-2} s^{-1} (Figure 25B). Similarly, at 601 µmol m^{-2} s^{-1}, the ETR for wild-type and azygous fruits was relatively low at 20.6 ± 1.91 and 24.0 ± 2.56 µmol electrons m^{-2} s^{-1}, contrasting with the significantly higher values found in e-*BpMADS* lines (40.0 - 49.0 µmol electrons m^{-2} s^{-1}) (Figure 4.25C).

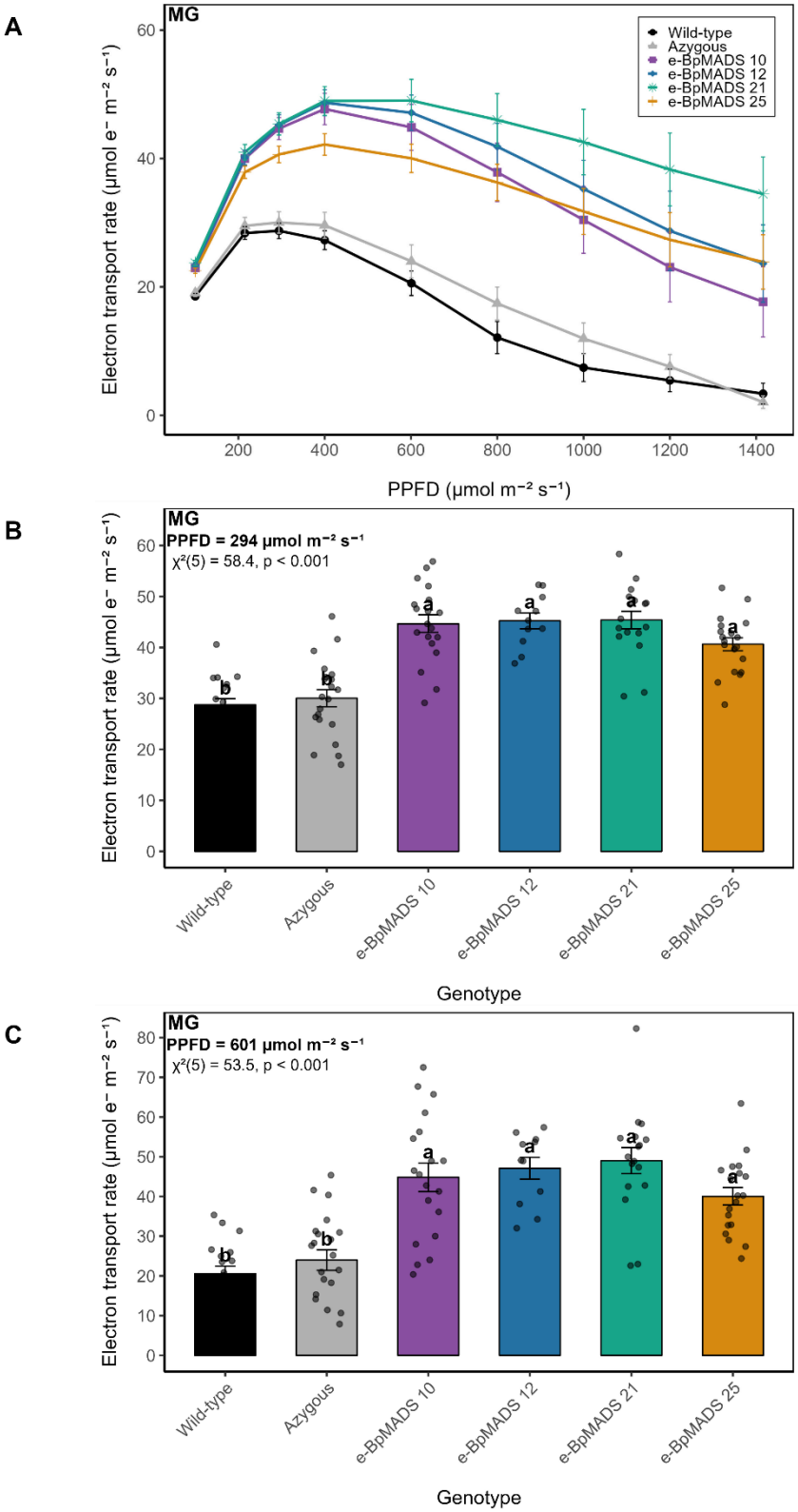

Figure 4.25. Electron transport rate (ETR) in early-specific *BpMADS* lines. Bar charts display ETR in mature green fruits (MG) of independent lines of *BpMADS* driven by the *SlTFM7* early fruit-specific promoter (e-*BpMADS*), compared with azygous and wild-type controls. (A) Light response of ETR across all light

intensities (100–1400 µmol m^{-2} s^{-1}). (B) ETR at 294 µmol m^{-2} s^{-1}. (C) ETR at 601 µmol m^{-2} s^{-1}. MG = 20–23 days post-anthesis. All values represent means ± SE from at least four biological replicates per genotype, with two fruits sampled per plant. Statistically significant differences were determined using a Kruskal-Wallis test followed by Dunn's multiple range test. Dots show individual data points. Different letters indicate statistically significant differences ($P < 0.05$).

4.2.12 Photochemical Quenching (qL) and Non-Photochemical Quenching (qN) Coefficients in Mature Green Early-Specific *BpMADS* Tomato Lines

The light energy absorbed by photosystems is processed in several ways, such as to drive photochemistry, re-emission as light, or heat (non-photochemical quenching) (Murchie & Lawson, 2013). To further investigate the impact of *BpMADS* overexpression on photoprotection and light energy distribution, the coefficient of photochemical quenching (qL) and coefficient of non-photochemical quenching (qN) were analysed in e-*BpMADS* mature green fruits under increasing light intensities. Initially, qL is higher, indicating a higher potential for photochemical activity. With increased PPFD, an increasing proportion of reaction centres becomes reduced, reflected in the decrease in qL values (Hetherington et al., 1998; Smillie et al., 1999). Transgenic fruits showed higher photochemical quenching (qL) values relative to wild-type and azygous at both 294 µmol m^{-2} s^{-1} and 601 µmol m^{-2} s^{-1}, indicating a larger fraction of open PSII reaction centres during illumination (Figure 4.26).

At 294 µmol m^{-2} s^{-1}, e-*BpMADS* lines already maintained a higher proportion of open PSII reaction centres compared to wild-type and azygous line, a difference that became even more pronounced under stronger illumination (Figure 4.26A). At 601 µmol m^{-2} s^{-1} PPFD, the photosystem II acceptor was 7.42 ± 1.51 % oxidised in wild-type fruits, and 9.71 ± 1.37 % in azygous, while e-*BpMADS* lines exhibited higher values, 17.9 ± 1.59 % in e-*BpMADS* 10, 20 ± 1.40 % in e-*BpMADS* 12, 20.2 ± 1.42 % in e-*BpMADS* 21 and 16.7 ± 0.78% in e-*BpMADS* 25 (Figure 4.26B).

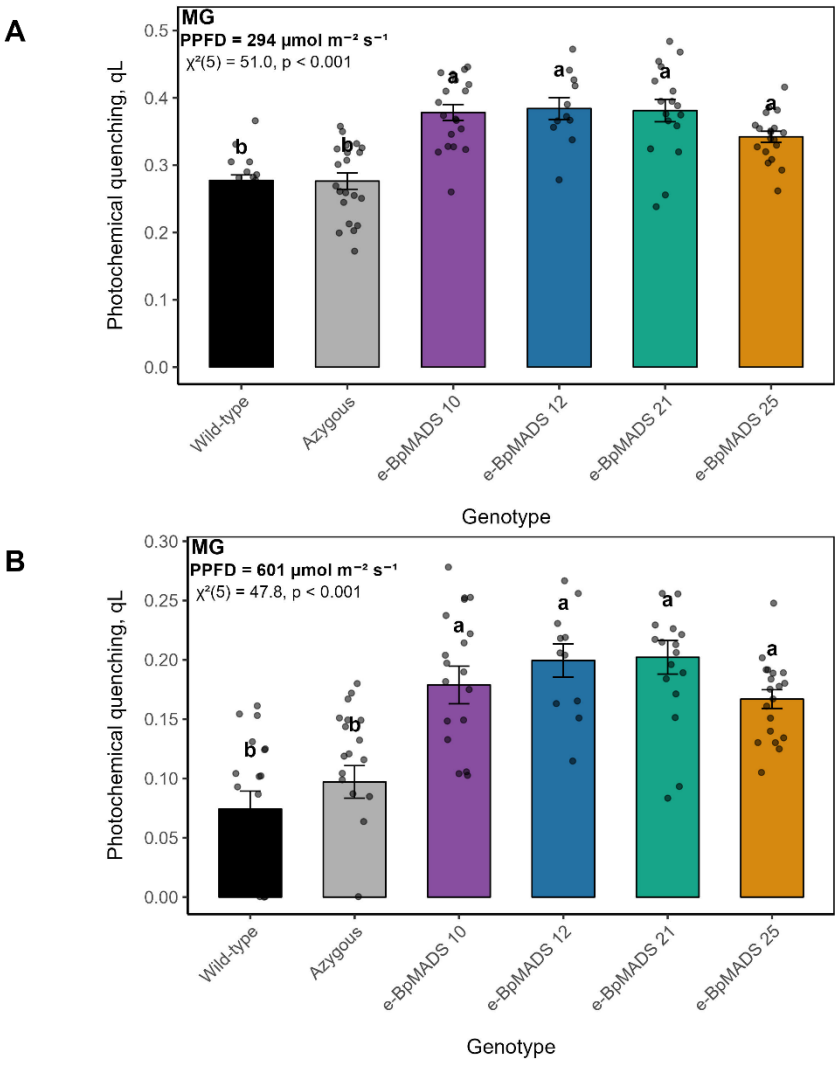

Figure 4.26. Coefficient of photochemical quenching (qL) in early-specific *BpMADS* lines. Bar charts display qL of mature green fruits (MG) of independent lines of *BpMADS* driven by the *SlTFM7* early fruit-specific promoter (e-*BpMADS*), compared with azygous and wild-type controls. (A) qL at 294 µmol m^{-2} s^{-1} (B) qL at 601 µmol m^{-2} s^{-1}. MG = 20–23 days post-anthesis. All values represent means ± SE from at least four biological replicates per genotype, with two fruits sampled per plant. Statistically significant differences were determined using a Kruskal-Wallis test followed by Dunn's multiple range test. Dots show individual data points. Different letters indicate statistically significant differences ($P < 0.05$).

Increasing PPFD from 294 to 601 µmol m^{-2} s^{-1} led to a greater allocation of photon energy to non-photochemical pathways, as reflected by rising qN values across all genotypes (Figure 4.27). The need for non-photochemical quenching (qN), which reflects heat dissipation of excess excitation energy, was reduced in e-*BpMADS* fruits. At 294 µmol m^{-2} s^{-1}, wild-type and azygous fruits exhibited the highest qN values (0.823 ± 0.005 and 0.813 ± 0.005, respectively), whereas all e-*BpMADS* lines showed significantly lower values (ranging from 0.752 to 0.783), with e-*BpMADS* 12

and 21 having the lowest. At 601 µmol m^2s^1, a similar trend is observed, with the wild-type once again displaying the highest qN (0.871 ± 0.003), followed by azygous (0.862 ± 0.002), while e-*BpMADS* 10, 12, and 21 maintained significantly lower values (0.832-0.837).

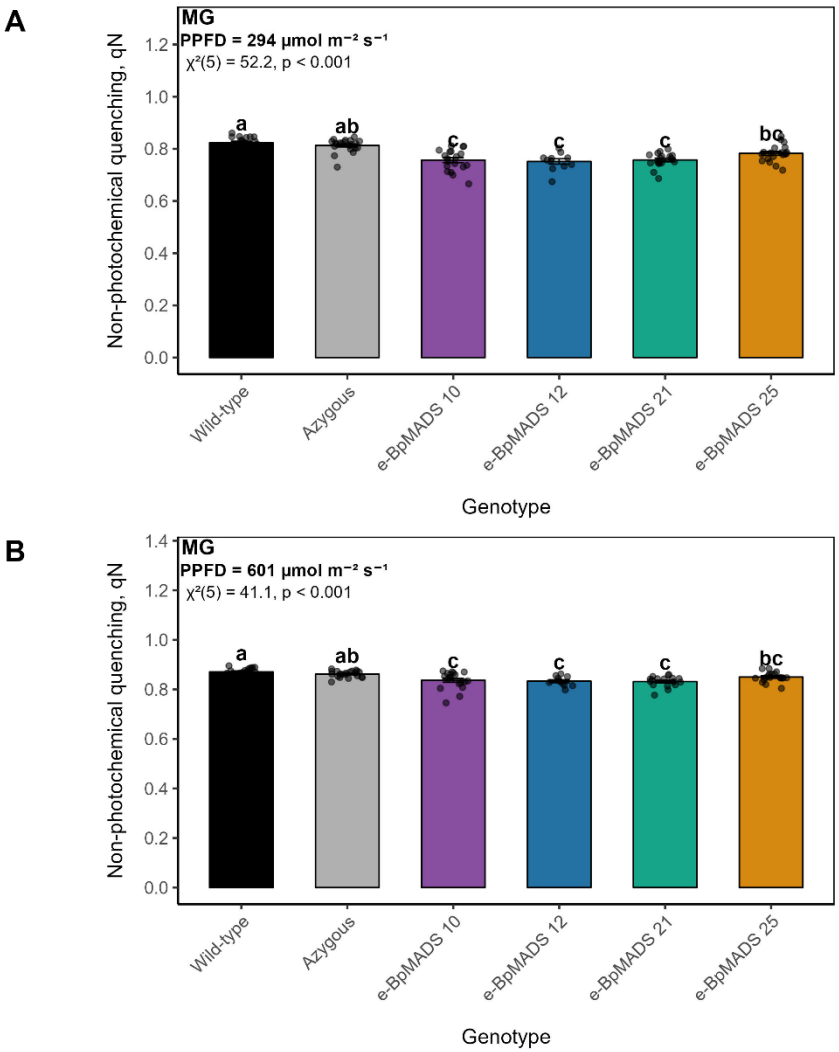

Figure 4.27. Coefficient of non-photochemical quenching (qN) in early-specific *BpMADS* lines. Bar charts display qN of mature green fruits (MG) of independent lines of *BpMADS* driven by the *SlTFM7* early fruit-specific promoter (e-*BpMADS*), compared with azygous and wild-type controls. (A) qN at 294 µmol m^{-2} s^{-1} (B) qN at 601 µmol m^{-2} s^{-1}. MG = 20–23 days post-anthesis. All values represent means ± SE from at least four biological replicates per genotype, with two fruits sampled per plant. Statistically significant differences were determined using a Kruskal-Wallis test followed by Dunn's multiple range test. Dots show individual data points. Different letters indicate statistically significant differences ($P < 0.05$).

4.2.13 Photochemical Performance of Early-Specific *BpMADS* Tomato T2 Lines

To assess the stability and heritability of the transgene effect, a second generation of transgenic plants was cultivated and evaluated for photochemical efficiency. The selected genotypes, e-

BpMADS 12, e-*BpMADS* 21, and e-*BpMADS* 25, were analysed alongside azygous and wild-type controls. Light response analyses revealed that ΦPSII values were consistently higher in e-*BpMADS* 12 and e-*BpMADS* 21 across all light intensities (Figure 4.28A). Similarly, electron transport rates (ETR) were increased in these two lines (Figure 4.28B). Notably, e-*BpMADS* 12 exhibited a peak at 600 µmol m^{-2} s^{-1} (PPFD), reaching nearly 50 µmol electrons m^{-2} s^{-1}, while e-*BpMADS* 21 peaked at 400 µmol m^{-2} s^{-1} with approximately 45 µmol electrons m^{-2} s^{-1}. Although e-*BpMADS* 25 also outperformed the wild-type under low and moderate light conditions, the differences were less pronounced at higher light intensities.

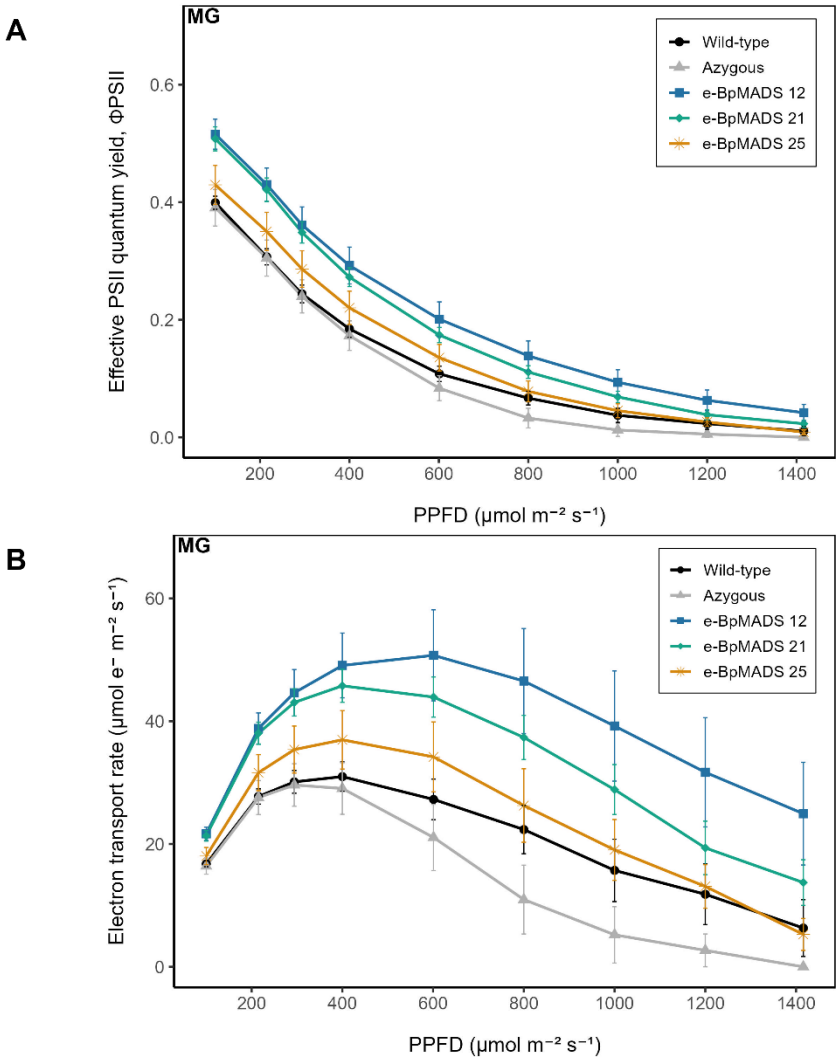

Figure 4.28. Effective quantum yield (ΦPSII) and electron transport rate (ETR) in early-specific *BpMADS* T2 tomato lines. Photosynthetic responses were measured in T2 mature green (MG) independent lines of *BpMADS* driven by the *SlTFM7* early fruit-specific promoter (e-*BpMADS*), compared with azygous and wild-type controls. (A) Light responses of effective PSII quantum yield (ΦPSII). (B) Electron

transport rate (ETR). MG = 20–23 days post-anthesis. All values represent means ± SE from at least four biological replicates per genotype, with two fruits sampled per plant.

The measurements taken at different light intensities, 294 µmol m^{-2} s^{-1} and 601 µmol m^{-2} s^{-1}, further reinforced e-*BpMADS* 12 and e-*BpMADS* 21 as the lines with the most efficient photochemical apparatus. At 294 µmol m^{-2} s^{-1}, ΦPSII was higher in both transgenic lines. Kruskal–Wallis test detected a significant overall genotype effect on ΦPSII ($p = 0.006$). While post-hoc Dunn tests did not identify any statistically significant pairwise differences between individual genotypes ($p > 0.05$), the low p-values relative to both wild-type (e-*BpMADS* 12 $p = 0.072$, e-*BpMADS* 21 $p = 0.068$) and azygous (e-*BpMADS* 12 $p = 0.067$, e-*BpMADS* 21 $p = 0.062$), indicate a consistent trend toward enhanced photochemical performance of both lines (Figure 4.29A).

At PAR 601 µmol m^{-2} s^{-1}, e-*BpMADS* 12 and 21 exhibited significantly greater results compared to the azygous control. This effect was, however, less evident for both genotypes when compared to wild-type (Figure 4.29B). While e-*BpMADS* 25 exhibited small increases under both conditions, these differences were not statistically significant compared to either azygous control or wild-type. Although these findings highlight the robustness of the transgene effect over successive generations in e-*BpMADS* 12 and e-*BpMADS* 21, the lack of significant results in e-*BpMADS* 25 could suggest a lack of transgene stability in this line. As previously mentioned, several mechanisms can affect the expression of a foreign gene in a plant organism, including the site of integration, which can be close to regions of the DNA that can either enhance or reduce expression, and therefore, downstream effects (Donnarumma et al., 2011; Klimaszewska et al., 2003).

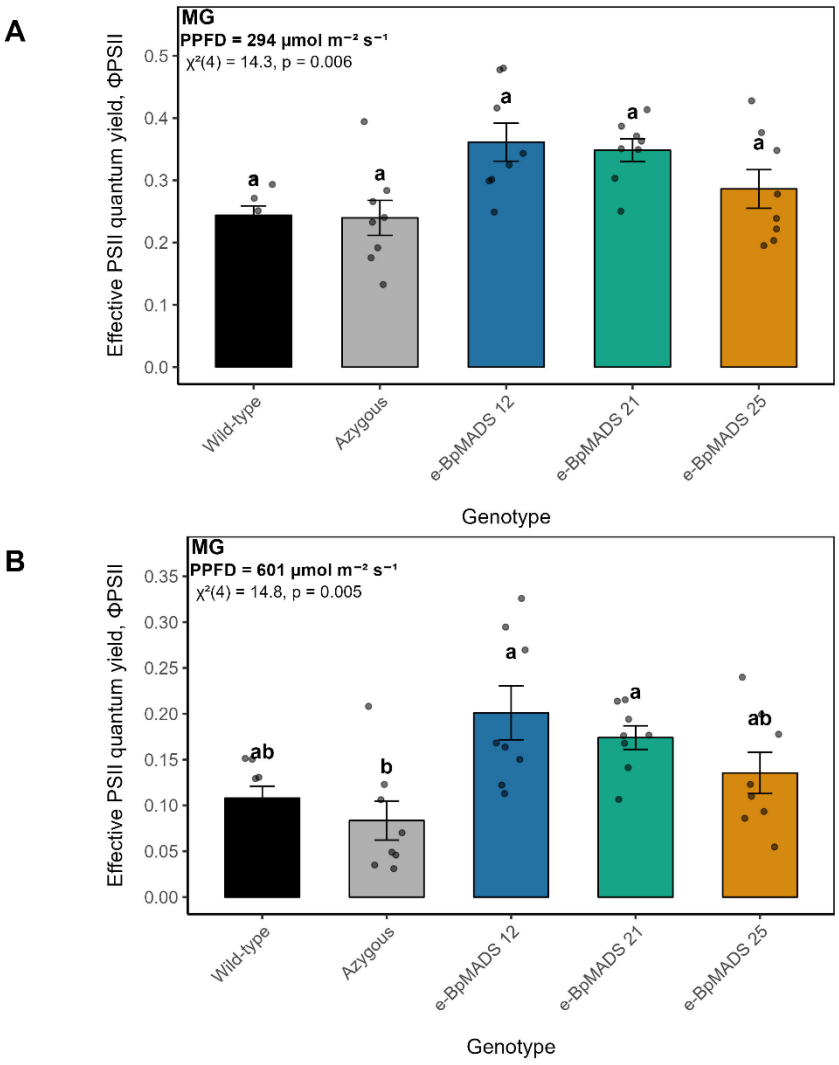

Figure 4.29. Effective quantum yield (ΦPSII) in early-specific *BpMADS* tomato T2 lines. Bar charts display ΦPSII in fruits from independent lines of *BpMADS* driven by the *SlTFM7* early fruit-specific promoter (e-*BpMADS*), compared with azygous and wild-type controls. (A) ΦPSII at 294 µmol m^{-2} s^{-1}. (B) ΦPSII at 601 µmol m^{-2} s^{-1}. MG = 20–23 days post-anthesis. All values represent means ± SE from at least four biological replicates per genotype, with two fruits sampled per plant. Statistically significant differences were determined using a Kruskal-Wallis test followed by Dunn's multiple range test. Dots show individual data points. Different letters indicate statistically significant differences (P < 0.05).

4.2.14 Gas Exchange Measurements of Early-Specific *BpMADS* Tomato T2 Lines

To better understand how fruit chloroplasts contribute to photosynthesis under varying environmental conditions, gas exchange measurements was conducted on T2 lines at the mature green stage. The analysis was performed over two independent experiments. The first analysis round focused on the transgenic line e-*BpMADS 12,* which had consistently exhibited enhanced chlorophyll fluorescence parameters in mature green fruit versus the wild-type. The second

round extended the analysis to include e-*BpMADS* 12, 21, and 25, allowing for a comparative assessment of photosynthetic performance across multiple transgenic lines. Fruits were subjected to a range of light intensities (light response) and ambient CO_2 concentrations (CO_2 response). The light responses were performed at photon flux densities of 200, 500, and 800 µmol m^{-2} s^{-1}. In parallel, CO_2 responses were measured using stepwise increases in ambient CO_2 concentration (200, 400, 1500 µmol mol^{-1}).

Results from the first light response experiment could indicate a decrease in respired CO_2 being released with increasing PPFD (Figure 4.30A). However, fruits still failed to reach the CO_2 compensation point, which represents the point at which assimilation and respiration are the same, which contrasts with the strong positive responses typically observed in leaf tissues. Notably, while net CO_2 uptake remained negative in both e-*BpMADS* 12 and wild-type, the former exhibited a reduced CO_2 efflux under different light conditions compared to wild-type fruit across all light intensities, indicating a more efficient internal refixation of respiratory CO_2.

To ensure consistency and expand the analysis to additional genotypes, a second round of light response measurements was conducted. Interestingly, the analysis provided contrasting results to the first one (Figure 4.30B). While e-*BpMADS* 12 outperformed wild-type in the first analysis, the same result did not happen in the second one. In the second experiment, e-*BpMADS* 12 and 25 exhibited higher CO_2 efflux than both wild-type and azygous controls, which could reflect elevated respiratory activity and/or reduced CO_2 fixation. Nevertheless, e-*BpMADS* 21 outperformed the wild-type. It is important to note that despite all fruits being at the same stage (mature green), the plants analysed in the first round were younger (14-week-old plants) than the ones in the second round (18-week-old plants). This difference reflects logistical and time constraints associated with experimental access during this period, as experiments required travel to the University of Essex. Furthermore, while these results in the second experiment revealed important trends, they were not statistically significant. Hence, it is possible that more replicates are required to increase the power of the analysis.

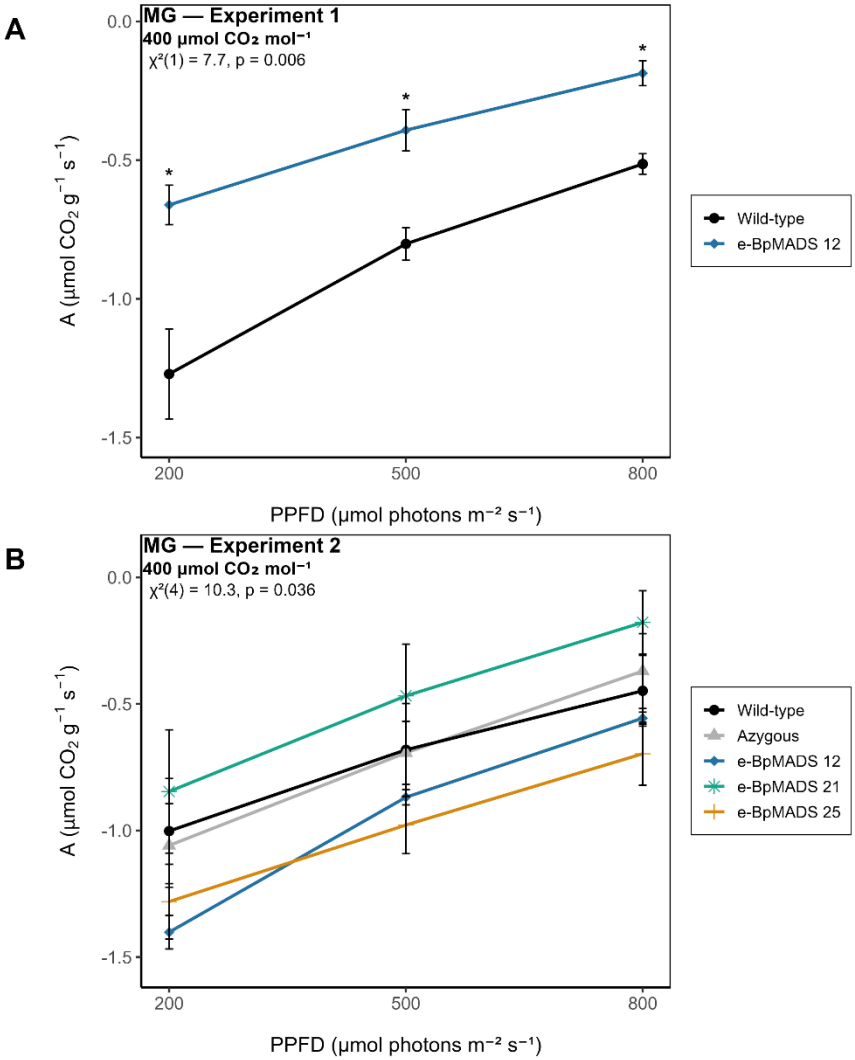

Figure 4.30. Gas exchange light response curves of early-specific *BpMADS* T2 lines. The photosynthetic responses display net CO_2 assimilation as a function of incident photosynthetic photon flux density (PPFD) in mature green fruits (MG) of independent lines of *BpMADS* driven by the *SlTFM7* early fruit-specific promoter (e-*BpMADS*), compared with azygous and wild-type controls. (A) Net CO_2 assimilation as a function of incident photosynthetic photon flux density (PPFD) of e-*BpMADS* 12 and wild-type. (B) CO_2 assimilation as a function of incident photosynthetic photon flux density (PPFD) of e-*BpMADS* 12, e-*BpMADS* 21, e-*BpMADS* 25, azygous and wild-type control. MG = 20–23 days post-anthesis. All values represent means ± SE from four biological replicates per genotype, each analysed in triplicate. Statistically significant differences were determined using a Kruskal-Wallis test followed by Dunn's multiple range test. Different letters indicate statistically significant differences ($P < 0.05$).

The CO_2 response curve provided additional insights into the role of atmospheric carbon in fruit photosynthesis and the dynamics of e-*BpMADS* overexpression in modulating this process. Interestingly, as external CO_2 concentrations increased, all genotypes showed a reduction in CO_2 efflux (Figure 4.31A). In the first analysis, both wild-type and e-*BpMADS* 12 fruits showed a

decrease in CO_2 release, indicating stimulation of the photosynthetic apparatus. However, wild-type fruits never reached the compensation point. In contrast, in really high CO_2 levels, the respiratory CO_2 efflux of e-*BpMADS* 12 was completely compensated, and even a slight net carbon fixation was observed, consistently outperforming wild-type across all data points analysed. Similar results were reported in maple fruits by Aschan & Pfanz (2003), who demonstrated that respiratory CO_2 efflux could be fully compensated under high light and CO_2 conditions, resulting in a slight net carbon gain. Nevertheless, the second experiment with additional genotypes included exhibited again contrasting results, with only e-*BpMADS* 21 outperforming wild-type and azygous, while e-*BpMADS* 12 and 25 exhibited a higher efflux (Figure 4.31B). This could suggest that either the internal CO_2 pool or the activity of carbon assimilation enzymes might have been affected by the plant stage at the time of measurement, and hence, the slower response in the second experiment with older plants.

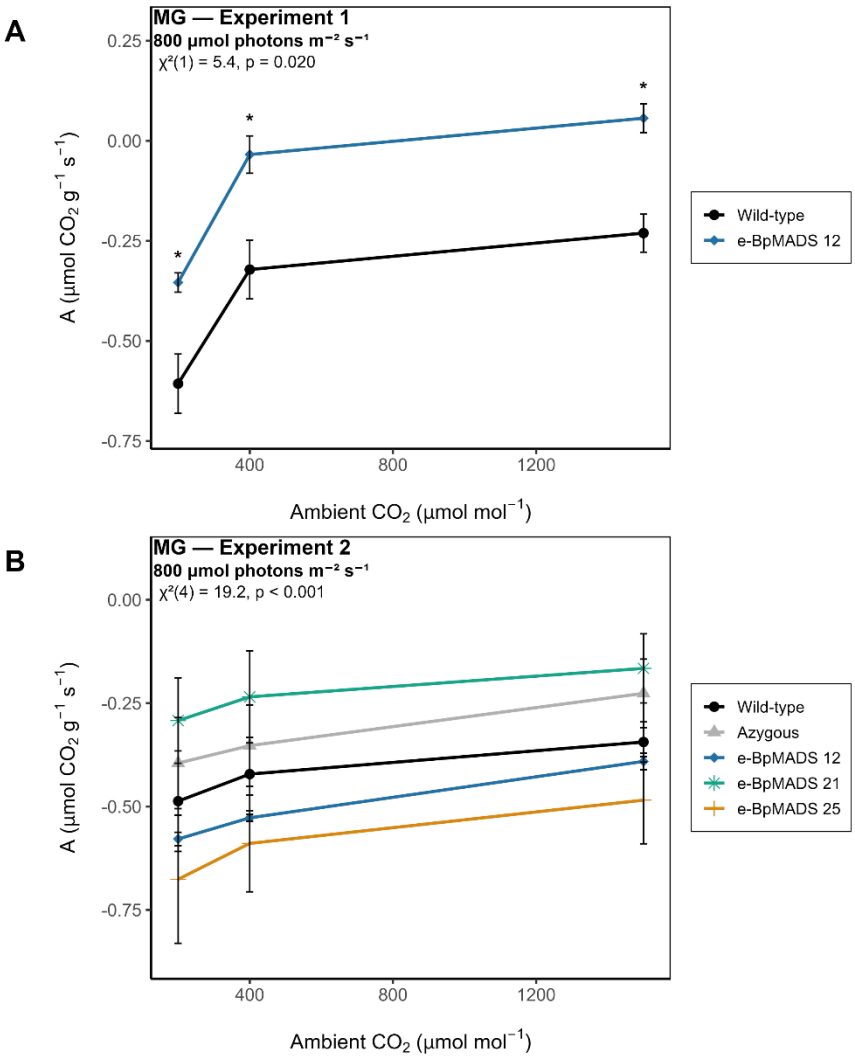

Figure 4.31. Gas exchange light response curves of early-specific *BpMADS* T2 lines. The photosynthetic responses display net CO_2 assimilation as a function of ambient CO_2 concentration in mature green fruits (MG) of independent lines of *BpMADS* driven by the *SlTFM7* early fruit-specific promoter (e-*BpMADS*), compared with azygous and wild-type controls. (A) Net CO_2 assimilation as a function of ambient CO_2 concentration of e-*BpMADS* 12 and wild-type. (B) Net CO_2 assimilation as a function of ambient CO_2 concentration of -*BpMADS* 12, e-*BpMADS* 21, e-*BpMADS* 25, azygous and wild-type control. MG = 20–23 days post-anthesis. All values represent means ± SE from four biological replicates per genotype, each analysed in triplicate. Statistically significant differences were determined using a Kruskal-Wallis test followed by Dunn's multiple range test. Different letters indicate statistically significant differences ($P < 0.05$).

4.2.15 Effective PSII Quantum Yield (ΦPSII) in Independent Ripening-Specific *BpMADS* Tomato Lines

Photosynthetic responses were assessed in mature green fruits from the ripening-specific r-*BpMADS* lines 8 and 25 under dark-adapted conditions and at the two light intensities, 294 µmol m^{-2} s^{-1} and 601 µmol m^{-2} s^{-1}. Line r-*BpMADS* 16 was excluded from this analysis due to an insufficient number of replicates at the time of analysis.

Line r-*BpMADS* 8 exhibited a higher F_v/F_m compared to the wild-type and azygous controls, and no differences were observed in r-*BpMADS* 25 (Figure 4.32A). At 294 µmol m^{-2} s^{-1}, no significant increases were observed for either genotype relative to the wild-type and azygous controls (Figure 4.32B). Nevertheless, at 601 µmol m^{-2} s^{-1}, r-*BpMADS* 8 exhibited a significantly greater F_v/F_m compared to the wild-type (Figure 4.32C).

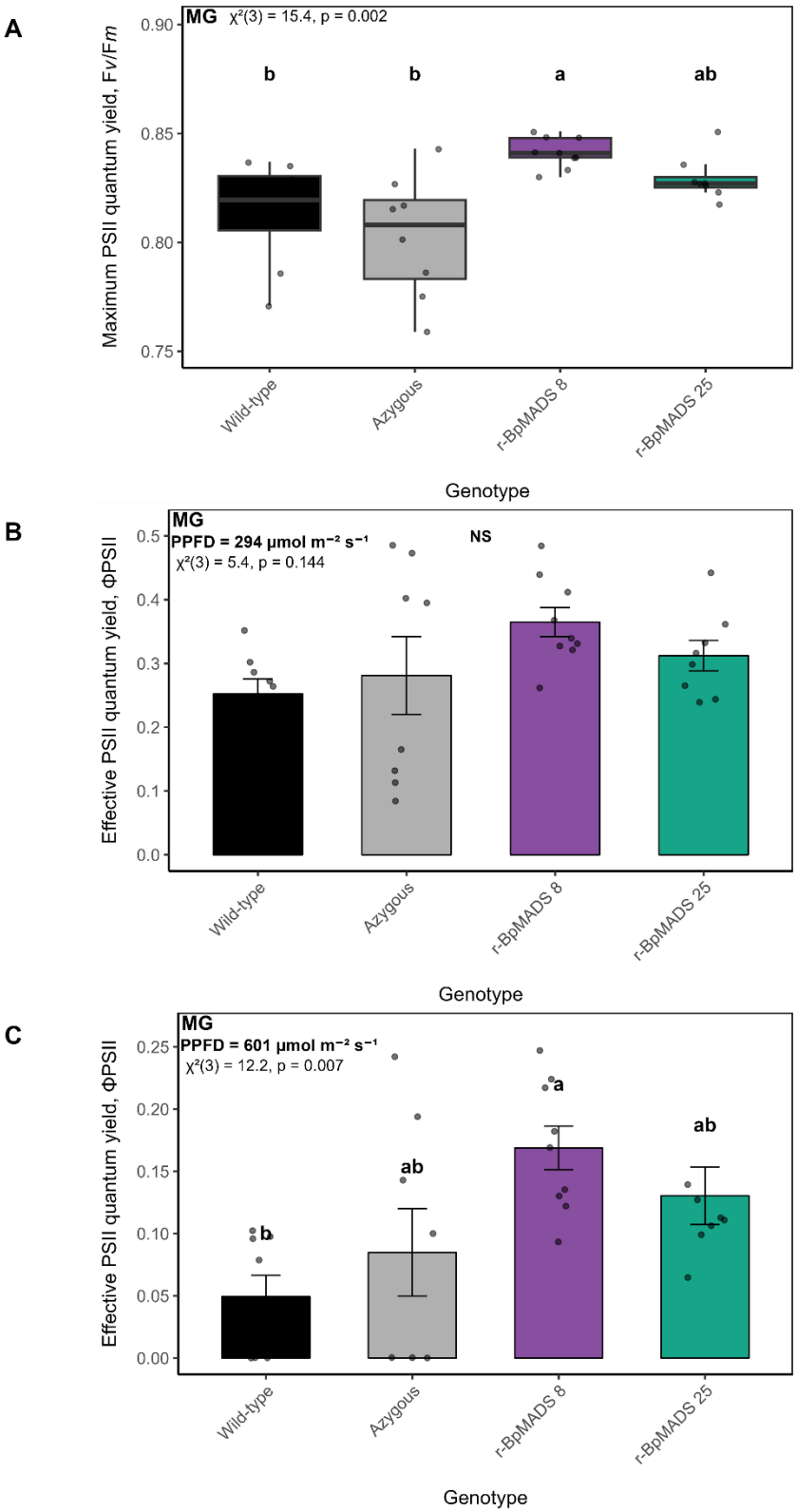

Figure 4.32. Maximum PSII quantum yield (F_v/F_m) and effective PSII quantum yield (ΦPSII) in ripening-specific *BpMADS* lines. The boxplot and bar charts display photosynthetic responses of mature green (MG) fruits of independent lines of *BpMADS* driven by the *CaFIB* ripening fruit-specific promoter (r-

BpMADS), compared with azygous and wild-type controls. (A) F_v/F_m. (B) ΦPSII at 294 µmol m^{-2} s^{-1}. (C) ΦPSII at 601 µmol $m^{-2}s^{-1}$. MG = 20–23 days post-anthesis. All values represent means ± SE from at least four biological replicates per genotype, with two fruits sampled per plant. Statistically significant differences were determined using a Kruskal-Wallis test followed by Dunn's multiple range test. Dots show individual data points. Different letters indicate statistically significant differences ($P < 0.05$).

4.3 Discussion

4.3.1 *BpMADS* Effect on Chloroplast Compartment

In mesophyll cells, the amount of cellular space dedicated to chloroplasts is remarkably constant, independent of cell size (Pyke, 1999). Although both chloroplast number and size were altered in the *e-BpMADS* lines, the more pronounced changes in chloroplast plan area suggest that e-*BpMADS* expression may have primarily affected pathways regulating chloroplast size. This is further supported by the fact that total chloroplast coverage increased more markedly than density, reflecting that increased chloroplast size, rather than the number of chloroplasts per unit area, was the main effect of the transgene expression. A possible resource allocation strategy is observed in transgenic line e-*BpMADS* 10, which had the largest chloroplast size but the lowest number and density. Therefore, the increase in size likely caused a slight reduction in numbers. A similar, but more severe, phenotype has been described in the *arc* mutants, in which larger chloroplasts are associated with a reduction in chloroplast number (Pyke et al., 1994; Pyke & Leech, 1992).

The extent of the chloroplast size increase has been suggested to be a key factor affecting photosynthetic efficiency. For instance, extremely large chloroplasts have lower mesophyll conductance in Arabidopsis leaf tissue (Weise et al., 2015). More recently, a 3-fold increase in chloroplast size in transgenic tobacco was associated with a decrease in mesophyll conductance and a reduction in chloroplast movement. The same study showed that while a slight reduction in chloroplast size did not affect productivity in transgenic plants compared to wild-type, severe reductions in chloroplast size led to a decline in productivity (Głowacka et al., 2023). Interestingly, although e-*BpMADS* 25 showed the highest relative transcript level among the selected transgenic lines, this did not translate into the largest chloroplast size (62.21 ± 6.66 μm^2). This result suggests that a higher transcript level does not necessarily translate into a stronger phenotype. This may be caused by feedback mechanisms that reduce the expression of chloroplast-associated genes to avoid the excessive accumulation of metabolic intermediates (Mielecki et al., 2020).

The results with e-*BpMADS* lines contribute to the existing literature, demonstrating that the manipulation of chloroplast compartment can be achieved through the overexpression or downregulation of specific transcription factors. Although *BpMADS* has not been directly implicated with the chloroplast division apparatus, the data suggest that e-*BpMADS* overexpression primarily affected chloroplast size in the transgenic lines. By increasing plastid area, tomato fruits may accumulate more chlorophyll and carotenoids, which play important roles in light harvesting, photoprotection, and nutrition. These changes could have practical implications for yield and sustainability.

4.3.2 The Differential Effects of Early-Specific *BpMADS* Overexpression on Pigment Biosynthesis at Different Stages

The stage of fruit development was an important factor for the evaluation of the effects of *BpMADS* on pigment accumulation. Although no significant stage and type interaction was detected, indicating that the magnitude of the overall transgene effect was comparable at both developmental stages, the absence of statistically significant differences in immature fruits may indicate a high biological variability observed at this stage. The increases observed in chlorophyll content at this stage could indicate that the downstream effects on chlorophyll accumulation had already started but were not consistent across all replicates. These results align with previous research in which both the overexpression and downregulation of *DEAR1*, identified as a positive regulator of chlorophyll metabolism, did not produce significant differences in chlorophyll content compared to wild-type plants at the early stages of fruit development (Pei et al., 2025). It is possible that as the fruit undergoes cell division and cell enlargement, the effects of e-*BpMADS* overexpression become more visible, possibly following the transcriptional activation of *BpMADS* by the *SlTFM7* early-specific promoter, which has been reported to be primarily active at a stage of development requiring cell wall synthesis (Santino et al., 1997). Following initial activation, *SlTFM7* drives *BpMADS* expression and initiates downstream effects on chlorophyll accumulation that were more consistent in the later stages of green fruit. In the *CaFIB* lines, the subtle phenotype changes observed at the mature green stage might also indicate the beginning of promoter activation. The *CaFIB* promoter has been reported to be activated at the late stages of the mature green stage, just before ripening (Smirnova & Kochetov, 2020). A significant upregulation of *CaFIB* occurs as early as the initial mature green stage, with expression levels continuing to rise toward the late mature green stage (Kuntz et al., 1998).

An association between chloroplast coverage and pigment content was observed (R^2 =0.86 for chlorophyll; R^2 = 0.81 for carotenoid), although this relationship was primarily driven by the large differences between wild-type/azygous controls and transgenic genotypes. The increased allocation of the cellular compartment to plastids in mature green e-*BpMADS* lines was associated with a greater accumulation of both chlorophyll and carotenoids. Moreover, the data shows a clear association between chlorophyll and carotenoid levels in e-*BpMADS* green fruits, reflecting the role of photosynthetic membranes in accumulating both pigments within the thylakoid membranes (Jarvis & López-Juez, 2013; Simkin et al., 2022). Pigment accumulation is known to be determined by the balance between biosynthetic rate and storage capacity (Li & Yuan, 2013). Therefore, improving pigment biosynthetic rates or the total area of the plastid compartment are tightly linked processes that are used as a strategy in biofortification (Morelli et al., 2023).

By contrast, the correlation between pigments in green and ripe fruits was more complex. While some lines exhibited an increase in chlorophyll content at the mature green stage and subsequent lycopene accumulation in ripe fruits, this trend wasn't consistent across all genotypes. For instance, e-*BpMADS* 12 and 25 showed increases in both lycopene and β-carotene, which aligns with previous studies demonstrating that enhanced chlorophyll levels may be associated with increased carotenoid accumulation in ripe fruits (Galpaz et al., 2008; Pan et al., 2013; Powell et al., 2012). However, e-*BpMADS* 10 and 21 only showed increases in β-carotene levels. This could indicate that in these lines, the β-carotene branch of the carotenoid biosynthesis pathway might be upregulated, whereas the one for lycopene remains unaffected. Previous studies have suggested that while a connection exists between chlorophyll levels during the green stage and carotenoid levels at the ripe stage, the role of chlorophyll degradation in carotenoid accumulation remains poorly understood (Barry et al., 2008). Furthermore, previous research has shown that tomatoes engineered to have increased chlorophyll at the green stage exhibited lower lycopene levels when ripe, despite a rise in β-carotene, reinforcing the idea that chlorophyll degradation and carotenoid biosynthesis are not necessarily interdependent processes (Wang et al., 2024; Wu et al., 2020). It is important to note that although lutein levels are greatly reduced during ripening, red tomato fruit still contains trace amounts of this pigment (Dharmapuri et al., 2002). Therefore, the spectrophotometric method used for the quantification of β-carotene in this study may overestimate its concentration due to spectral overlap with lutein.

4.3.3 Improved Photosynthetic Performance and Energy Distribution in Early-Specific *BpMADS* Tomato Lines

The higher ΦPSII observed in e-*BpMADS* transgenic fruits compared to either wild-type or azygous indicates that a greater proportion of light energy is being directed into photochemistry rather than being dissipated as heat. Physiologically, this suggests that *BpMADS* overexpression results in fruit chloroplasts with an improved capacity for utilising absorbed light. One likely explanation is the increase in chloroplast coverage, which enhances the capacity of pigment storage. Next, the increased chlorophyll content would allow more light absorption. Previous studies on *BpMADS* in tobacco support this idea. The constitutive overexpression of *BpMADS* in tobacco led to the generation of transgenic plants with elevated leaf chlorophyll levels and doubled photosynthetic rates (Qu et al., 2013).

To further explore how e-*BpMADS* overexpression affects energy distribution, ETR, qL and qN were assessed in mature green fruit. The analysis revealed that at higher light intensities, electron transport becomes limiting, revealing a physiological point in the context of fruit photosynthesis, beyond which further increases in PPFD do not enhance ETR. This limitation was observed earlier in wild-type and azygous fruits, whereas e-*BpMADS* lines saturated at higher light intensities. In all transgenic lines, qL was higher than in wild-type and azygous at both light intensities, which correlates with the greater ΦPSII observed in the same lines. The higher fraction of open PSII reaction centres across both light intensities was associated with reduced allocation of absorbed light to non-photochemical quenching pathways. It is worth noting that non-photochemical and photochemical pathways are competing processes, and therefore, it is expected that an increase in light being driven to photochemistry will lead to a decrease in light being lost as heat. Moreover, e-*BpMADS* transgenic lines also exhibited higher carotenoid levels in green fruit, which function in light harvesting and photoprotection. In addition, these pigments provide structural stability for lipid membranes and contribute to the direct quenching of triplet Chl or ROS after they are formed (Nisar et al., 2015; Simkin, 2021). This antioxidant role and structural support may reduce or delay the need to activate non-photochemical quenching, as the photosynthetic apparatus becomes more robust and excess energy is more effectively managed.

Overall, the potential for greater photochemistry in e-*BpMADS* fruits could be related to their increased light absorption and electron transport capacity, coupled with increased photoprotection, which allows a rapid electron flow through PSII and maintains reaction centres

open, helping to prevent a build-up of electrons that could react with oxygen, forming reactive oxygen species (ROS).

4.3.4 Assessing Photosynthesis in Tomato Fruits: Limitations and Genetic Insights into Carbon Fixation

Photosynthetic measurements in fruits have been traditionally performed using chlorophyll fluorescence techniques. The near absence of stomata and the still not fully understood mechanism by which cuticles control the exchange of CO_2 with the atmosphere have made the application of gas exchange techniques limited to date (Garrido et al., 2023). Traditional net CO_2 assimilation assays can underestimate photosynthetic rates as carbon can be sourced from two different pathways. First, atmospheric CO_2 and second, internally recycled carbon from mitochondrial respiration, which is reinforced by the presence of PEPC (Blanke, 1989; Willmer & Johnston, 1976). Several factors can influence fruit gas exchange, such as incident light, chlorophyll content and CO_2 availability (Garrido et al., 2023).

The decrease in respired CO_2 observed in both light and CO_2 response experiments, where the values become "less negative", is an indicator that carbon may be fixed in the fruit. The results presented in this thesis align closely with findings from Carrara et al. (2001), who reported that green tomato fruits exhibited limited net CO_2 fixation despite being photosynthetically active. In addition, O_2 has a lower diffusion rate compared to CO_2, and because of that, its concentration inside the fruit is relatively low compared to CO_2. As a result, under increasing PPFD and at ambient CO_2, it is possible that the production of new available respiratory CO_2 may become limited by the insufficient supply of O_2 for respiration (Ho et al., 2008). Nonetheless, the almost linear curves in the light response experiment, without a clear saturation point or plateau, suggest that internal CO_2 production remained sufficient. On the other hand, the early plateau in the CO_2 response curve suggests that carbon fixation capacity was limited by the capacity to access atmospheric CO_2.

Taken together, both CO_2 and light response results shed light on the unique limitations of photosynthesis performed by fruits, such as CO_2 uptake by the bulky pericarp tissue with near-absent stomata, cuticle gas diffusion and internal CO_2 availability. The responses observed in e-*BpMADS* 12 in the first analysis highlight the potential for manipulation of carbon fixation in fruits. Compared to wild-type, the e-*BpMADS* 12 genotype maintained a reduced CO_2 efflux, which may be associated with internal CO_2 re-fixation. The results of the second analysis, however, highlight

the complexity of the manipulation of photosynthesis, especially in fruit tissue. The contrasting results between photochemical performance and net carbon fixation in some lines suggest that enhanced light harvesting and electron transport may not necessarily translate into increased carbon assimilation. This could reflect downstream limitations imposed by RuBisCO, which is the main limiting factor in C_3 photosynthesis (De Souza et al., 2020; Long et al., 2004; Orr et al., 2016; Parry et al., 2013). The activity of the C_4 enzyme PEPC in fruit tissues, along with the coordinated action of proteins involved in CO_2 recapture and transport from the cytosol to the chloroplast, may further (Aschan & Pfanz, 2003; Garrido et al., 2023).

4.3.5 Summary

Overall, the work presented here has demonstrated that the photochemical capacity and lycopene/β-Carotene levels of tomato fruit can be improved through the overexpression of *BpMADS*. These results align closely with previous research on other transcription factors such as *APRR2-Like* and *GLKs* in which the manipulation of genes involved in chloroplast development increased pigment accumulation in fruit tissue (Nguyen et al., 2014; Powell et al., 2012). The phenotypes observed strongly suggest that e-*BpMADS* fruits have more robust photosynthetic machinery.

Although changes in the transcriptome were not directly analysed, it is possible that the overexpression of *BpMADS* could be associated with the up-regulation of photosynthetic nuclear-associated genes and electron transport proteins. This hypothesis aligns with previous studies where tomato fruits engineered to have enhanced chlorophyll accumulation via silencing of *SlBEL11*, a negative regulator of fruit chloroplast development, showed increased expression of many light-harvesting chlorophyll-binding (CAB) proteins and photosynthetic apparatus genes (Meng et al., 2018). In contrast to our overexpression lines, which showed enhanced chlorophyll levels and improved photochemical performance, the RNAi-*SlBEL11* phenotypes demonstrates the opposite outcome, thereby reinforcing the central role of chlorophyll content and plastid compartment in determining fruit photosynthetic efficiency.

The initial stages of tomato fruit development, fruit set and early growth are tightly linked to active cell division and the initiation of chloroplast biogenesis. Our amino-acid phylogenetic analysis revealed that BpMADS shares evolutionary proximity with TAGL2, FUL1/TDR4 and FUL2, MADS-box transcription factors expressed in those stages. It is possible that the early expression of BpMADS could participate in developmental networks associated with early fruit development,

acting alongside or downstream of TAGL2 and FUL2 to fine-tune these processes. These pathways remain to be characterised, and the role of FUL1/TDR4 in this process remains not fully elucidated (Busi et al., 2003; Nezhdanova et al., 2021). The ripening effects of BpMADS expression may be due to a possible interaction between BpMADS and other MADS-box transcription factors, such as RIN, TDR4/FUL1 and FUL2, which are part of a regulatory network that modulates processes such as ethylene biosynthesis, pigment accumulation and cell wall metabolism (Bemer et al., 2012; Jiang et al., 2022). These findings support the hypothesis that BpMADS could possibly function as part of a MADS-box regulatory transcriptional network that is active throughout tomato fruit development to fruit ripening, potentially acting upstream of, in parallel with some of these known regulators.

It is important to note that some gas exchange and fluorescence parameters were derived from values established in leaf tissue. However, as these constants were applied uniformly across all fruit samples, they do not affect relative comparisons between genotypes or treatments. Moving forward, a more complete expression profile of *BpMADS* (both early and ripening promoters) and target genes involved in chlorophyll and carotenoid biosynthesis across developmental stages would help understand the downstream effects and targets of *BpMADS* at different stages of fruit development. Regardless of exactly how these processes happen, even small increases in chlorophyll could improve light capture and photosynthetic activity. In addition, increased carotenoid levels in green fruits could potentially contribute to improved photoprotection and thylakoid membrane stability.

Chapter 5 Fruit-Specific *AtCGA1* Overexpression Enhances Photochemical Capacity and Pigment Accumulation in Tomato

5.1 Introduction

The homologues *CGA1* and *GNC* belong to the GATA transcription factor family, with orthologs identified across a wide range of plant species. Due to their conserved nature and well-established roles in regulating photosynthesis-related processes, acting downstream of light and cytokinin, these genes have emerged as promising candidates for photosynthetic genetic engineering efforts (Chiang et al., 2012). Additionally, the role of *CGA1* and *GNC* in modulating nitrogen assimilation could have a direct impact on fruit photosynthetic capacity, as chloroplasts are major nitrogen sinks due to the large amounts required to produce RuBisCO (Hudson, 2010). Since a significant proportion of nitrogen is allocated to photosynthetic proteins, there is strong evidence of a positive correlation between tissue nitrogen content and CO_2 fixation rates in green tissues (Xiong et al., 2017). Furthermore, photosynthetic nitrogen use efficiency (PNUE), defined as the rate of CO_2 assimilation per unit of tissue nitrogen, has been identified as a key indicator of photosynthetic performance and the overall carbon status of plants (Zhong et al., 2019). Therefore, a more efficient carbon assimilation relative to nitrogen uptake in the plant could enhance overall carbon partitioning. Moreover, *CGA1* and *GNC* also play a role in starch metabolism, which could have an impact on overall fruit quality. The content of soluble sugar at the mature stage has been previously associated with starch levels at the green stage (Cocaliadis et al., 2014; Davies & Cocking, 1965; Hudson et al., 2011). In plants, GATA transcription factors, as well as binding to the DNA sequence GATA, have been described to interact with other proteins. These interactions enable these transcription factors to form homo or heterodimers, expanding their transcription network and ability to function as transcriptional activators or repressors (Behringer & Schwechheimer, 2015). A significant body of research has focused on manipulating GATA transcription factors in model species such as Arabidopsis (Hudson, 2010; Hudson et al., 2011) as well as in cereals like rice (Hudson, 2010), and non-crop plants such as poplar (An et al., 2020). However, the role of GATA transcription factors in fruit development remains largely unexplored.

Fruit genetic engineering research has traditionally given more attention to the *GOLDEN2-LIKE* (*GLK*) family of transcription factors, which also regulate aspects of chloroplast development, acting in concert, with both overlapping and unique functions to *CGA1* and *GNC* (Chiang et al., 2012). The following sections outline the biochemical and physiological characterisation of tomato plants expressing *AtCGA1* driven by *SlTFM7* Early Fruit Specific Promoter (e-*AtCGA1*) and *AtGNC* driven by *SlAFF* Early Fruit Specific Promoter (e-*AtGNC*). The use of different promoters allows the evaluation of how promoter choice influences phenotype strength. This chapter presents the first attempt, to our knowledge, to investigate the effect of the overexpression of the Arabidopsis thaliana *AtCGA1* and *AtGNC* on tomato fruit development

5.2 Results

5.2.1 Phylogenetic Relationships Between AtCGA1, AtGNC and Tomato GATA Transcription Factors

The cDNA of the *AtCGA1* ORF is 1,059 bp in length, spanning from the ATG start codon to the TGA stop codon, and encodes a predicted polypeptide of 352 amino acids. The cDNA for the *AtGNC* ORF is 1197 bp long from the ATG start codon to the TGA stop codon, encoding a predicted polypeptide of 398 amino acids. A BLASTP search against the tomato genome identified SlGATA16 and SlGATA22 as the closest orthologues. AtCGA1 exhibited 48.4% identity to SlGATA16, with an alignment covering 45% of the AtCGA1 sequence. A second alignment was found with SlGATA22, with 44.2% identity. AtGNC showed similar levels of homology: 48% identity with SlGATA22 and 47% identity with SlGATA16, both spanning 44% of the query length.

Amino acid–based phylogenetic analysis indicates that AtCGA1 and AtGNC cluster together in a distinct branch separate from the majority of SlGATA transcription factors. Among the tomato sequences, SlGATA16 and SlGATA22 grouped most closely with the Arabidopsis CGA1/GNC clade, suggesting that they represent the closest tomato homologs within this lineage.

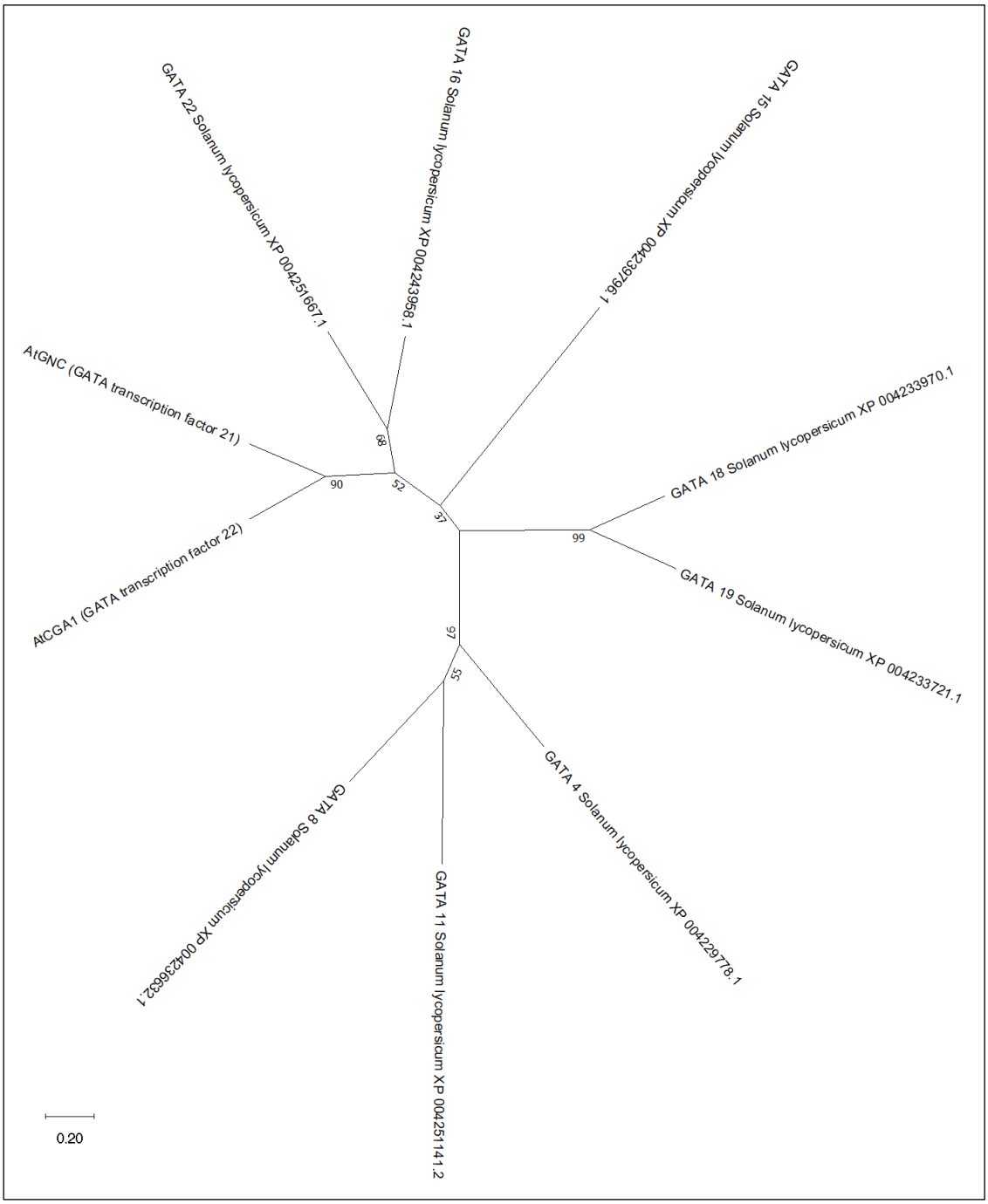

Figure 5.1. Phylogenetic Relationship Between AtCGA1, AtGNC and Tomato GATA Proteins. A phylogenetic tree based on amino acid sequences of GATA proteins was inferred using the maximum likelihood method. Bootstrap values are indicated at each node to represent the level of support for the individual clade. Higher values reflect stronger support for the evolutionary groupings. The tree is presented as an unrooted phylogram, with branch lengths proportional to the number of amino acid substitutions per site.

Together, these findings indicate that CGA1 and GNC have conserved roles in plant species such as rice and Arabidopsis. While GATA transcription factors in tomato remain largely

uncharacterised, the phylogenetic analysis of the tomato GATA family identified SlGATA22 and SlGATA16 as putative orthologues. These results suggest that they could share overlapping functions, although this remains to be experimentally validated.

5.2.2 Microscopy Reveals Increased Chloroplast Size in *AtCGA1* Fruit Pericarp

This chapter section outlines the effects of the early-specific *AtCGA1* overexpression on chloroplast morphology in tomato pericarp cells of mature green (MG) fruits. Confocal laser scanning microscopy (Figure 5.2) enabled the visualisation of chloroplasts as fluorescent structures. Transmitted light imaging (Figure 5.3) provided complementary structural detail.

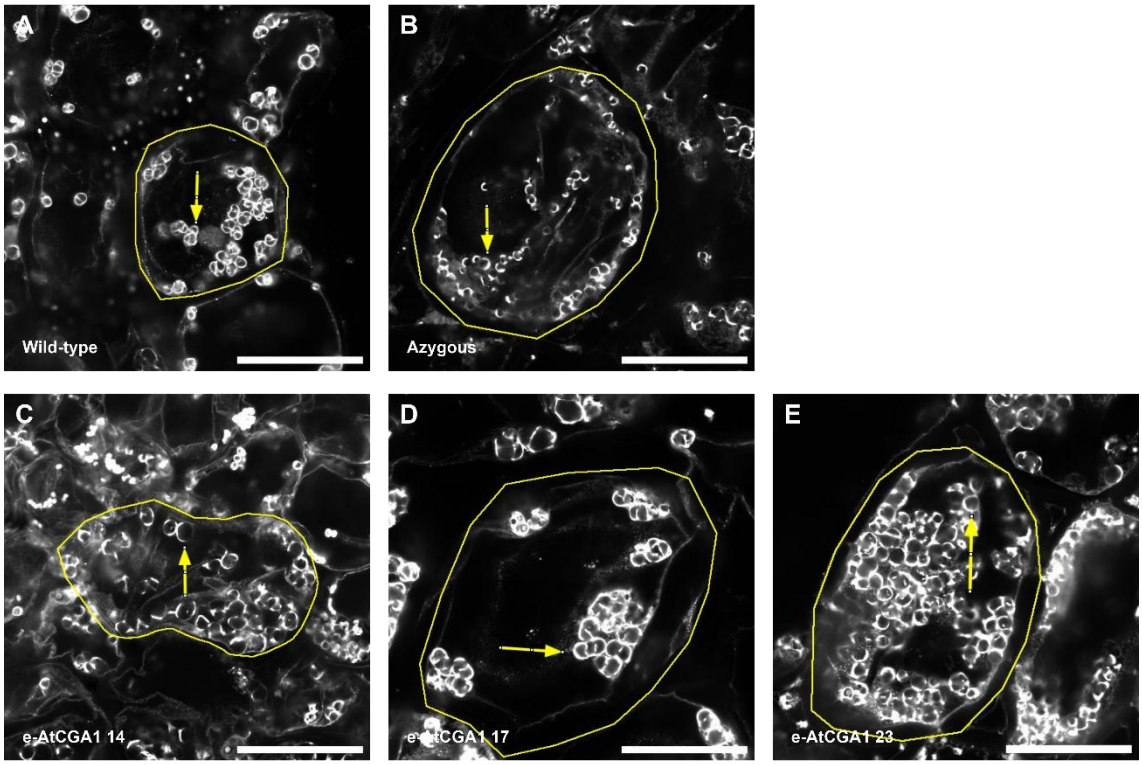

Figure 5.2. Confocal laser scanning microscopy of mature green fruit from early-specific *AtCGA1* tomato lines. Representative micrographs of pericarp cells from fruits expressing *AtCGA1* driven by the *SlTFM7* early-specific promoter (e-*AtCGA1*), azygous and wild-type controls. Individual cells are outlined in yellow, and representative chloroplasts are indicated by arrows. (A) Wild-type (B) Azygous (C) e-*AtCGA1* 14 (D) e-*AtCGA1* 17 (E) e-*AtCGA1* 23. Scale bars = 100 µm. MG = 20–23 days post-anthesis. Scale bars = 100 µm.

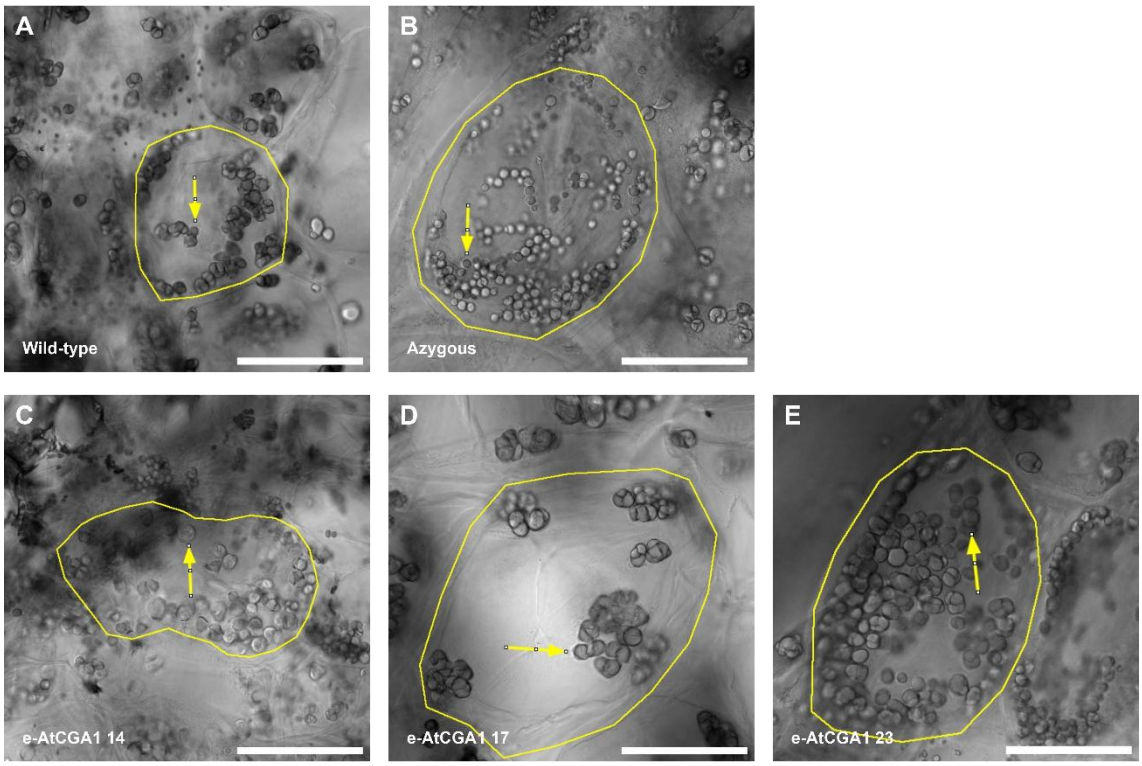

Figure 5.3. Transmitted light microscopy of mature green fruit from early-specific *AtCGA1* tomato lines. Representative micrographs of pericarp cells from fruits expressing *AtCGA1* genotypes driven by the *SlTFM7* early-specific promoter (e-*AtCGA1*), azygous and wild-type controls. Individual cells are outlined in yellow, and representative chloroplasts are indicated by arrows. (A) Wild-type (B) Azygous (C) e-*AtCGA1* 14 (D) e-*AtCGA1* 17 (E) e-*AtCGA1* 23. MG = 20–23 days post-anthesis. Scale bars = 100 µm.

Among independent transgenic lines, e-*AtCGA1* 14 exhibited the largest chloroplast size (89.09 ± 14.66 µm^2) compared to wild-type (38.05 ± 2.81 µm^2) and azygous control (43.31 ± 4.5 µm^2). This corresponds to an approximately 2 to 2.2-fold increase in chloroplast size compared to both wild-type and azygous plants (Figure 5.4A). Chloroplast size in e-*AtCGA1* 17 (was 71.82 ± 5.66 µm^2) was significantly higher than in both the wild-type and azygous plants. Line e-*AtCGA1* 23 exhibited the lowest mean chloroplast size (56.84 ± 8.4 µm^2) among transgenic lines. Chloroplast numbers were greater in e-*AtCGA1 23* (144.37 ± 14.17) compared to the wild-type (88.06 ± 5.25), but not to the azygous (126.1 ± 11.19). Transgenic line e-*AtCGA1* 14, which exhibited the largest chloroplast size, showed a reduction in chloroplast number (80.47 ± 6.59), possibly a resource allocation response to maintain optimum chloroplast allocation space for photosynthesis. Line e-*AtCGA1* 17 exhibited an intermediate phenotype with 102.59 ± 7.68 chloroplasts per cell, comparable to both wild-type and azygous (Figure 5.4B).

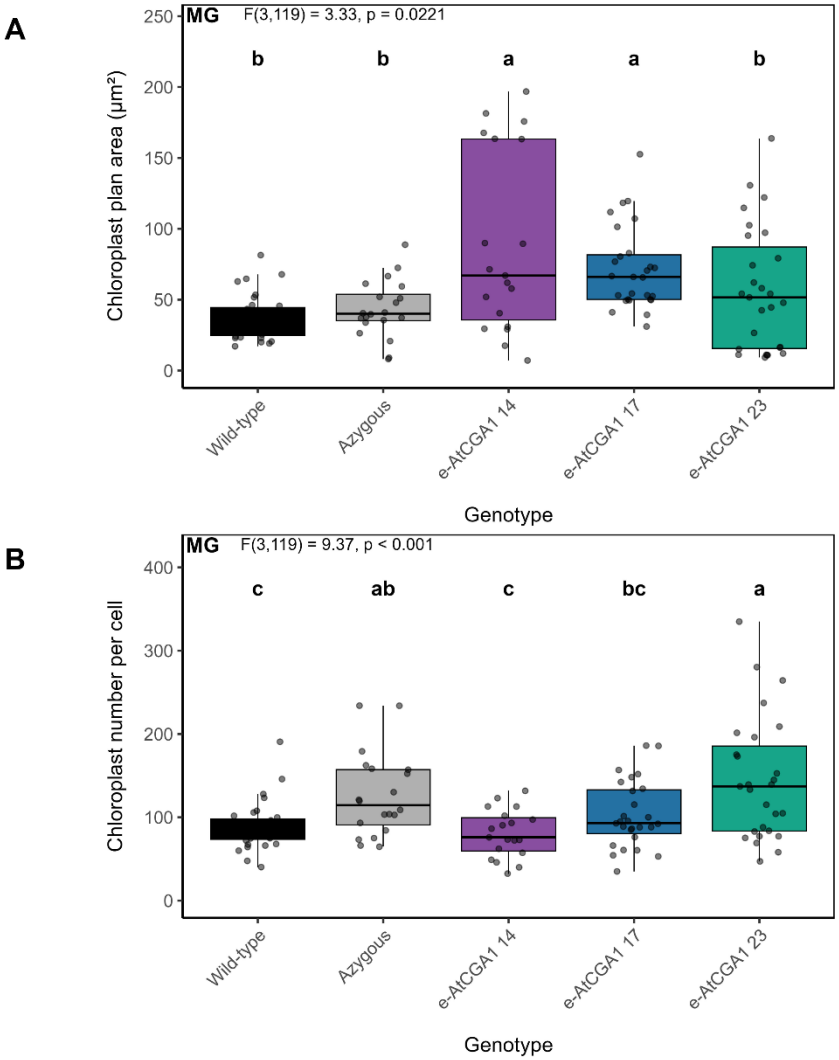

Figure 5.4. Chloroplast morphology in mature green (MG) fruits of early-specific *AtCGA1* tomato lines. Boxplots show chloroplast morphology traits in fruits from lines expressing *AtCGA1* under the *SlTFM7* early fruit-specific promoter (e-*AtCGA1*), compared with azygous and wild-type controls. (A) Chloroplast plan area. (B) Chloroplast number per cell. MG = 20–23 days post-anthesis. The boxes represent the interquartile range (25th to 75th percentile), the horizontal line shows the median, and the whiskers extend to 1.5 times the interquartile range. At least six individual cells of at least three biological replicates were analysed for each genotype. Statistically significant differences were determined using a 1-way ANOVA followed by Duncan's multiple range test. Dots show individual data points. Different letters indicate statistically significant differences (P<0.05).

In terms of chloroplast coverage, line e-*AtCGA1* 17 exhibited the highest mean value (30.38 ± 8.95%), which exceeded the values observed in both the wild-type (16.35 ± 1.52%) and azygous fruits (16.75 ± 0.39%), representing an increase of approximately 80% relative to both controls. Meanwhile, coverage in e-*AtCGA1* 14 (22.67% ± 8.94%) and e-*AtCGA1* 23 (20.08% ± 7.29%) exhibited increases of approximately 35% and 20% relative to wild-type and azygous controls (Figure 5.5A).

The hypothesis of resource allocation in some lines is further reinforced by the analysis of chloroplast density (Figure 5.5B). The line with the largest chloroplast size was also accompanied by the lowest chloroplast density (e-*AtCGA1* 14), which could indicate a plant response to ensure a more efficient resource use during chloroplast biogenesis and division. However, the ANOVA test found no significant differences in density among genotypes (ANOVA, p = 0.492). Therefore, density values were overall conserved among different lines. For instance, e-*AtCGA1* 17 showed an increase in density of only 12% compared to wild-type and 18% compared to wild-type, while its chloroplast coverage was higher by 92% and 85%, respectively. Similarly, e-*AtCGA1* 23 showed higher increases in coverage (28% and 32%) compared to density (13% and 18%).

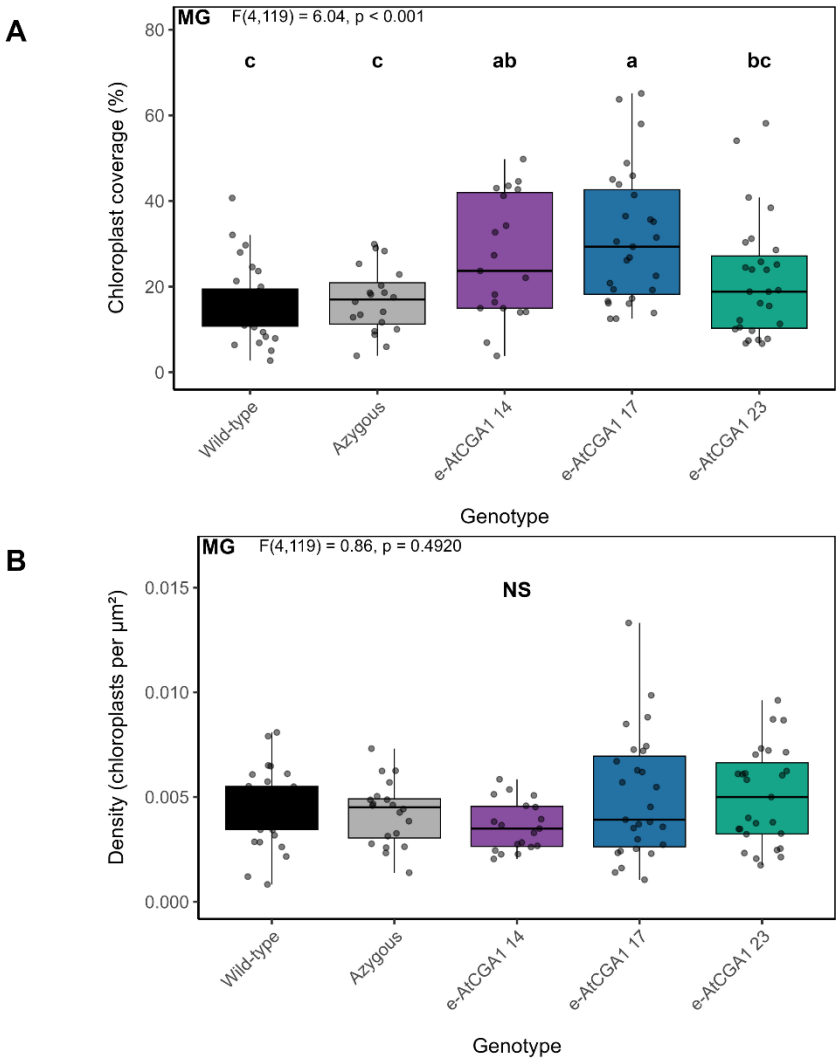

Figure 5.5. Chloroplast morphology in mature green (MG) fruits of early-specific *AtCGA1* tomato lines. Boxplots show chloroplast morphology traits in fruits from lines expressing *AtCGA1* under the *SlTFM7* early fruit-specific promoter (e-*AtCGA1*), compared with azygous and wild-type controls. (A) Chloroplast coverage. (B) Chloroplast density. MG = 20–23 days post-anthesis. The boxes represent the interquartile

range (25th to 75th percentile), the horizontal line shows the median, and the whiskers extend to 1.5 times the interquartile range. At least six individual cells of at least three biological replicates were analysed for each genotype. Statistically significant differences were determined using a 1-way ANOVA followed by Duncan's multiple range test. Dots show individual data points. Different letters indicate statistically significant differences ($P<0.05$).

To determine whether the observed differences reflected a general effect of e-*AtCGA1* expression, a nested one-way ANOVA was performed with genotype nested within type (wild-type/azygous vs e-*AtCGA1*). This analysis revealed no significant effect of type on chloroplast number ($p = 0.871$), chloroplast plan area ($p = 0.160$), or chloroplast density ($p = 0.854$). Nevertheless, chloroplast coverage showed a trend towards a type-level effect ($p = 0.0905$), although this did not reach statistical significance at the 0.05 threshold. Overall, these results indicate that the observed changes were not uniform across all transgenic lines but instead reflect line-specific responses among independent transgenic lines.

5.2.3 Greater Chlorophyll and Carotenoid Content in *AtCGA1* Tomato Lines

The impact of *AtCGA1* overexpression on fruit development was investigated at the biochemical and physiological levels in three lines for the *AtCGA1* early-specific construct (e-*AtCGA1*) alongside wild-type and azygous control. Both immature green (IG) and mature green (MG) stages were analysed to assess developmental stage-dependent effects on chlorophyll and carotenoid levels. Representative fruits of mature green (MG) e-*AtCGA1* lines displaying visible pigmentation changes at the mature green stage are shown in Figure 5.6.

Figure 5.6. **Phenotypes of mature green (MG) fruits of early-specific *AtCGA1* tomato lines**. Images display representative MG fruits from transgenic lines expressing *AtCGA1* driven by the *SlTFM7* early fruit-specific promoter (e-*AtCGA1*), as well as azygous and wild-type controls. (A) Wild-type. (B) Azygous. (C) e-*AtCGA1* 14. (D) e-*AtCGA1* 17. (E) e-*AtCGA1* 23. MG = 20–23 days post-anthesis. Scale bars = 1 cm.

At the immature green stage, e-*AtCGA1* 14 and e-*AtCGA1* 17 exhibited mean chlorophyll contents of (79.89 ± 15.31 µg/g) and (81.07 ± 6.63 µg/g), respectively, representing increases of approximately 30% relative to the wild-type (62.72 ± 8.51 µg/g) and 60% relative to the azygous control (50.58 ± 6.13 µg/g). Similarly, e-*AtCGA1* 23, with a mean chlorophyll content of (65.88 ± 7.16 µg/g), also showed increases (Figure 5.7A). Nevertheless, it is possible that the high biological variability at the immature green stage limited the statistical significance of the analysis. Consistent with the phenotypic changes, chlorophyll content measurements showed significantly higher levels at the mature green stage (Figure 5.7B). Transgenic line e-*AtCGA1* 17 (68.34 ± 5.86 µg/g) exhibited the highest increase, with an increase of approximately 77% compared to the wild-type (38.45 ± 2.92 µg/g) and 70% compared to the azygous (40.18 ± 6.05 µg/g). Meanwhile, lines e-*AtCGA1 23* (57.93 ± 2.99 µg/g) and e-*AtCGA1 14* (56.80 ± 5.76 µg/g) showed chlorophyll content increases of approximately 50% and 47%, respectively, compared to the wild-type, and 44% and 41% compared to the azygous control. The chlorophyll *a*/*b* ratio (Figure 5.7C) reflects the balance of pigments between reaction centres and light-harvesting antenna complexes, where a higher ratio indicates proportionally smaller antenna per reaction

centre (Jin et al., 2016; Simkin et al., 2022). Here, chlorophyll *a*/*b* ratios varied significantly across genotypes. The azygous line (1.95 ± 0.17) and e-*AtCGA1* 14 (2.13 ± 0.10) displayed significantly lower ratios than wild-type e-*AtCGA1* 17 (2.69 ± 0.14). Wild-type and e-*AtCGA1* 23 showed intermediate phenotypes with a ratio of 2.32 ± 0.13 and 2.39 ± 0.13. These results suggest that e-*AtCGA1* 17 has a smaller antenna cross-section per reaction centre compared to both azygous and e-*AtCGA1* 14.

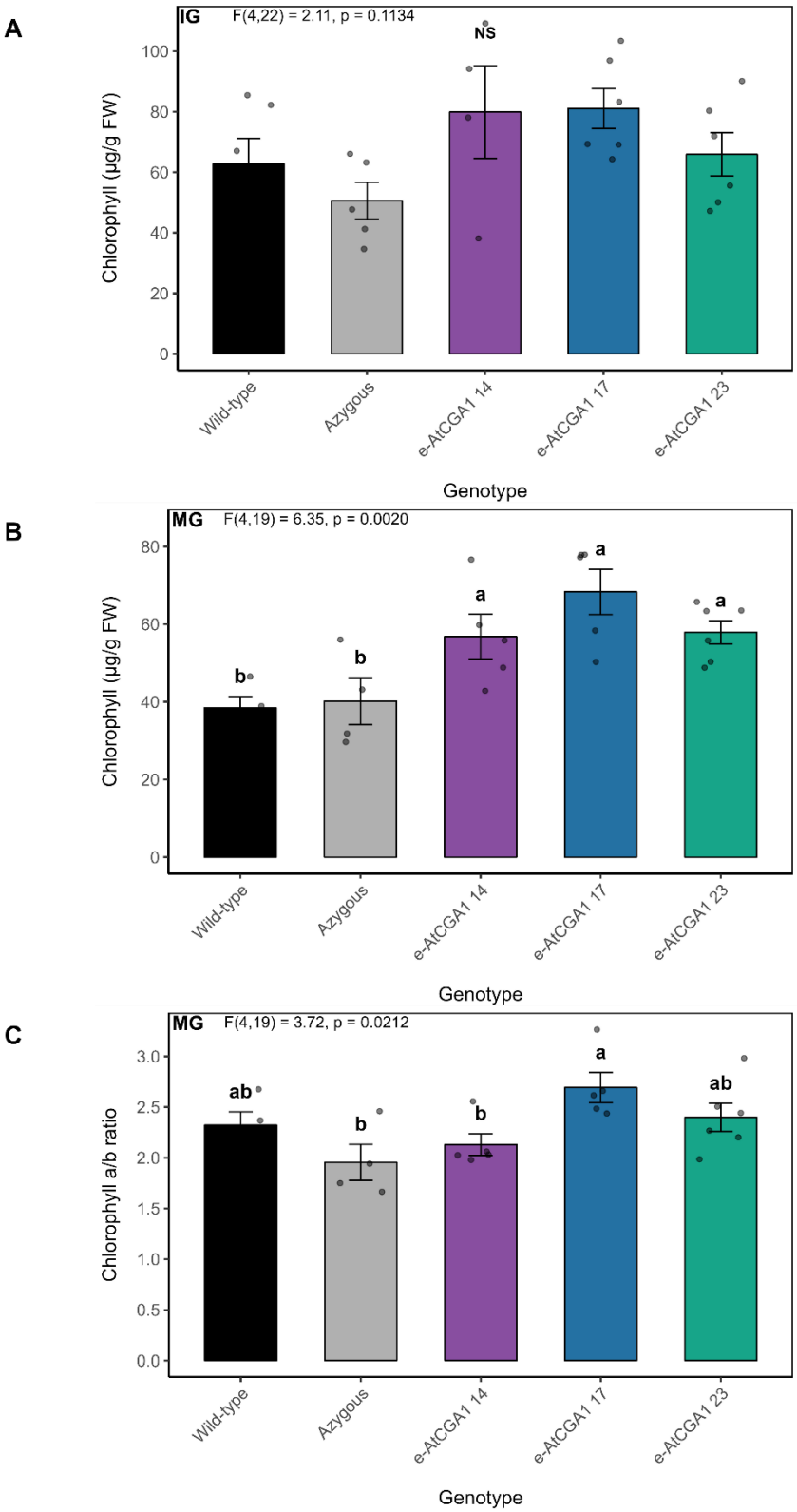

Figure 5.7. Chlorophyll levels in early-specific *AtCGA1* tomato lines. Bar charts display the total chlorophyll content in independent lines of *AtCGA1* driven by the *SlTFM7* early fruit-specific promoter (e-*AtCGA1*), as well as azygous and wild-type controls. (A) Immature green (IG). (B) Mature green (MG). (C) Chlorophyll *a*/*b* ratio. IG = 7–10 days post-anthesis. MG = 20–23 days post-anthesis. All values represent means ± SE from at least four biological replicates per genotype, each analysed in three technical

replicates. Statistically significant differences were determined using a 1-way ANOVA followed by Duncan's multiple range test. Dots show individual data points. Different letters indicate statistically significant differences (P<0.05).

The total carotenoid content analysis showed similar trends at both stages, reinforcing the pattern of carotenoid accumulation in thylakoid membranes of green fruits. Carotenoid levels in mature green fruits were approximately 30%, 75%, and 40% higher in e-*AtCGA1* lines 14, 17, and 23, respectively, compared to both the wild-type and azygous lines (Figure 5.8).

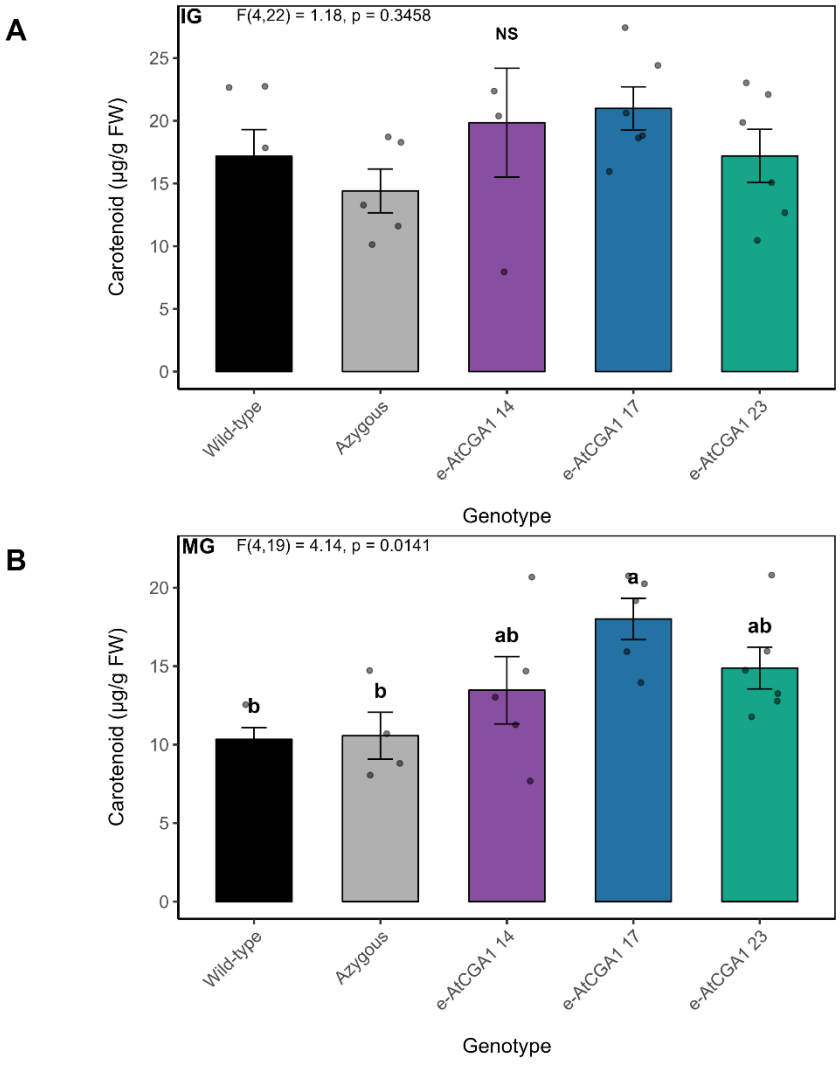

Figure 5.8. Carotenoid levels in early-specific *AtCGA1* tomato lines. Bar charts display the total carotenoid content in independent lines of *AtCGA1* driven by the *SlTFM7* early fruit-specific promoter (e-*AtCGA1*), as well as azygous and wild-type controls. (A) Immature green (IG). (B) Mature green (MG). IG = 7–10 days post-anthesis. MG = 20–23 days post-anthesis. All values represent means ± SE from at least four biological replicates per genotype, each analysed in three technical replicates. Statistically significant differences were determined using a 1-way ANOVA followed by Duncan's multiple range test. Dots show individual data points. Different letters indicate statistically significant differences (P<0.05).

Chlorophyll and carotenoid levels were assessed in e-*AtCGA1* transgenic lines across developmental stages using a two-way nested ANOVA. This method was used to test for the effects of developmental stage (IG vs MG) and genotype type (wild-type/azygous vs e-*AtCGA1*), while accounting for variation among individual lines nested within genotype type. The pigment content analysis of e-*AtCGA1* revealed a stage-dependent effect on chlorophyll content, with immature green fruits exhibiting greater relative chlorophyll content (expressed in µg/g) than mature green in both wild-type and e-*AtCGA1* fruits. At the genotype-type level, e-*AtCGA1* fruits exhibited higher chlorophyll content than wild-type azygous controls at both developmental stages (Figure 5.9A). Carotenoid content also displayed a significant effect of developmental stage. However, genotype type did not reach statistical significance ($p = 0.067$), despite a consistent trend towards increased carotenoid content in e-*AtCGA1* lines (Figure 5.9B). No stage and type interaction was observed for either pigment, indicating that overall differences between e-*AtCGA1* lines and controls were comparable at both developmental stages.

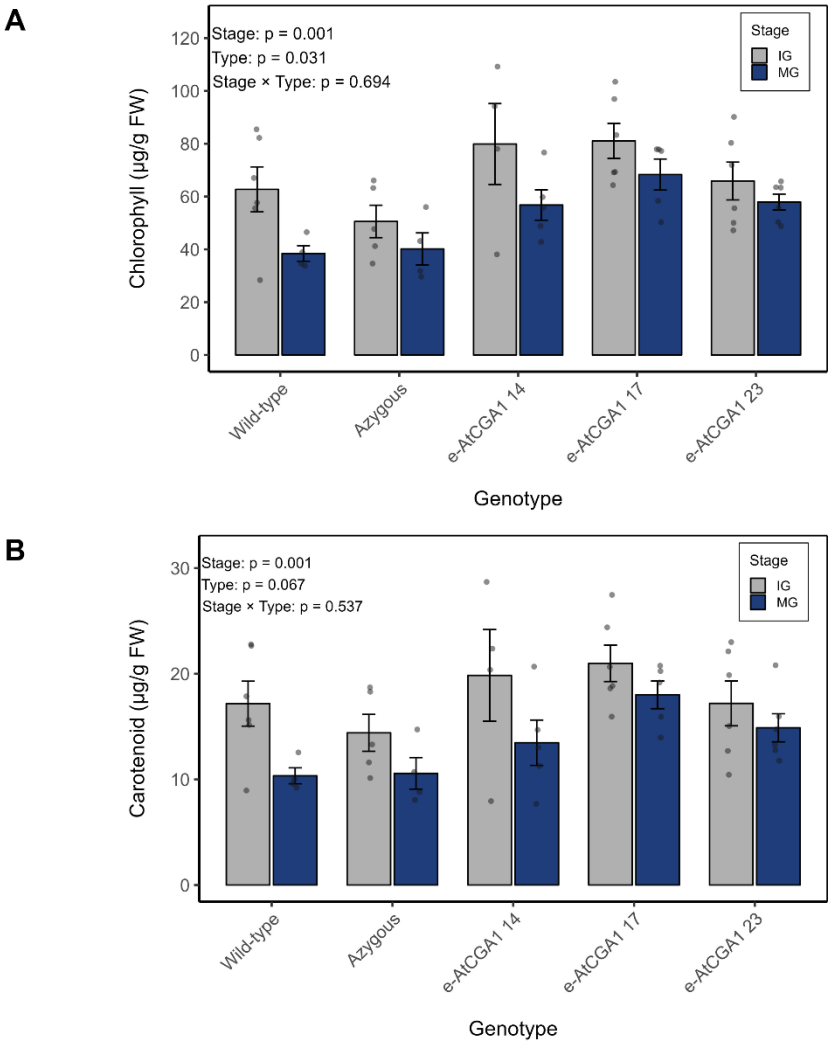

Figure 5.9. Changes in chlorophyll and carotenoid content during fruit development in early-specific *AtCGA1* tomato lines. Bar charts show pigment levels in immature green (IG) and mature green (MG) fruits of *AtCGA1* driven by the *SlTFM7* early fruit-specific promoter (e-*AtCGA1*), as well as azygous and wild-type controls. (A) Chlorophyll levels. (B) Carotenoid levels. IG = 7–10 days post-anthesis. MG = 20–23 days post-anthesis. All values represent means ± SE from at least four biological replicates per genotype, each analysed in three technical replicates. Dots show individual data points. Statistically significant differences were assessed using a two-way nested ANOVA, with developmental stage (IG vs MG) and genotype type (wild-type/azygous vs e-*AtCGA1*) included as fixed factors and genotype (line) nested within type. Main effects and the stage × type interaction were tested, with significance accepted at $P < 0.05$.

Overall, the relationship between chlorophyll and carotenoid content in e-*AtCGA1* lines showed a moderate to high correlation with chloroplast coverage (Figure 5.10). Increased chloroplast coverage was associated with higher pigment content. Chlorophyll content exhibited a correlation of $R^2 = 0.89$, whereas carotenoids exhibited $R^2 = 0.82$, indicating that a greater allocation of cellular space led to more pigment biosynthesis.

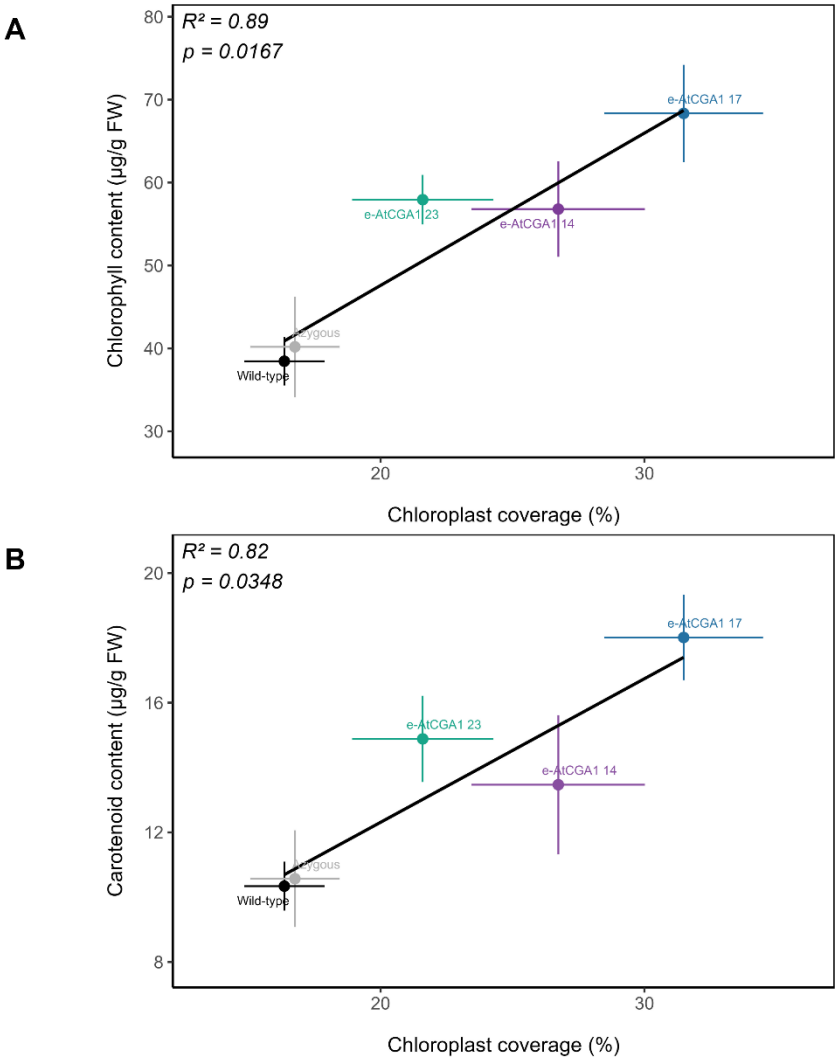

Figure 5.10. Relationship between chloroplast coverage and pigment accumulation in early-specific *AtCGA1* tomato lines. Scatterplots showing the correlation between chloroplast coverage and pigment content in independent genotypes expressing *AtCGA1* under the *SlTFM7* early fruit-specific promoter (e-*AtCGA1*), compared to azygous and wild-type controls. (A) Chlorophyll. (B) Carotenoid. MG = 20–23 days post-anthesis. MG = 20–23 days post-anthesis. Linear regression lines are shown, with associated coefficients of determination (R^2) and p-values reported in each panel. Each point represents the mean value per genotype. Horizontal error bars indicate ± SE of chloroplast coverage, while vertical error bars indicate ± SE of pigment content.

5.2.4 Different Accumulation of Lycopene and β-Carotene in *AtCGA1* Tomato Lines

Levels of lycopene and β-carotene were assessed in ripe fruit from e-*AtCGA1* lines to determine whether transgene expression influenced carotenoid accumulation at the ripening stage. Representative ripe fruits from each genotype are shown in Figure 5.11. Among the transgenic

lines, e-*AtCGA1* 23 displayed the most striking phenotype, characterised by an intense bright-red colour.

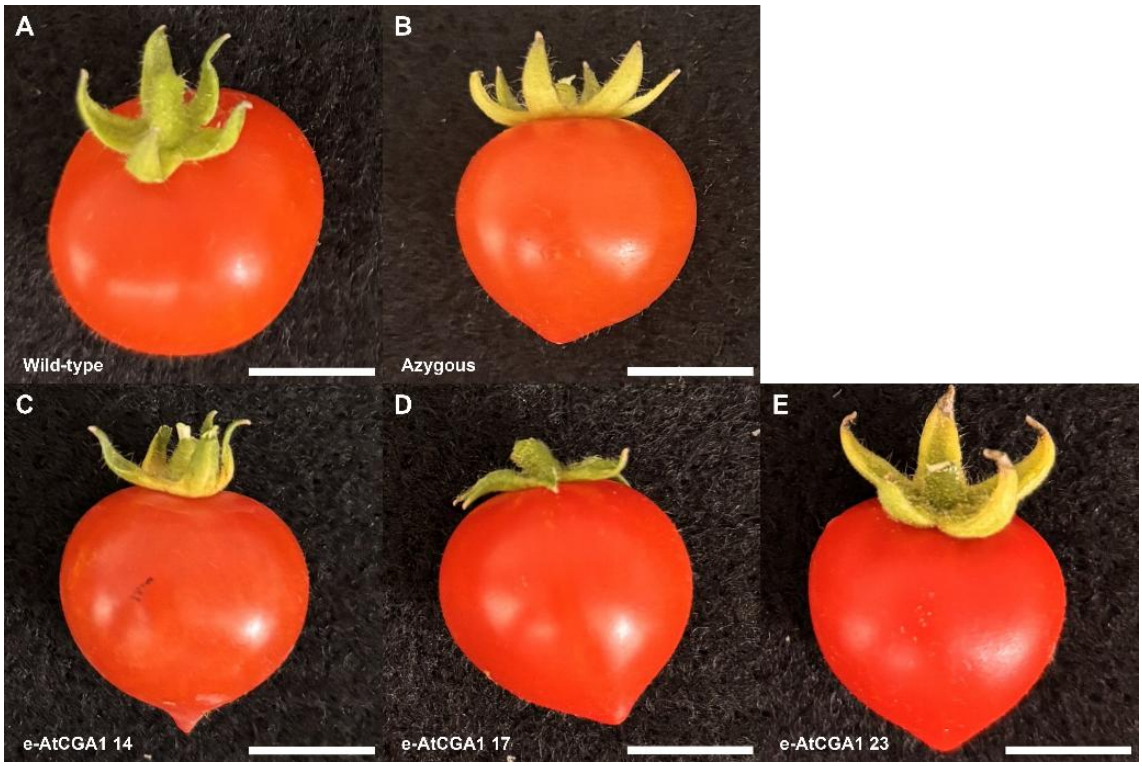

Figure 5.11. Phenotypes of ripe fruits of early-specific *AtCGA1* tomato lines. Images display representative ripe fruits from transgenic lines expressing *AtCGA1* driven by the *SlTFM7* early fruit-specific promoter (e-*AtCGA1*), as well as azygous and wild-type controls. (A) Wild-type. (B) Azygous. (C) e-*AtCGA1* 14. (D) e-*AtCGA1* 17. (E) e-*AtCGA1* 23. Ripe = breaker +7–10 days. Scale bars = 1 cm.

Two of the transgenic lines displayed a clear trend toward increased lycopene levels, although the overall ANOVA did not reach statistical significance ($p = 0.106$). Lycopene levels were greater by approximately 30% in *e-AtCGA1* 23 (124 ± 7.31 µg/g) compared to both wild-type (93.48 ± 9.63 µg/g) and azygous control (94.67 ± 14.32 µg/g), making it the line with the largest increase. On the other hand, e-*AtCGA1* 17 (108 ± 8.32 µg/g) showed a more modest increase of around 15% compared to both controls, whereas e-*AtCGA1* 14 actually exhibited a reduction of approximately 7-8% (87 ± 7.55 µg/g). Interestingly, e-*AtCGA1* 17, which was the line with the most significant chlorophyll increase, only showed a modest change in lycopene content (Figure 5.12A). Furthermore, β-carotene levels also showed a trend of increase in the transgenic lines (ANOVA, $p = 0.097$). In both e-*AtCGA1* 17 and 23, the increases in β-carotene were of the order of 41% relative to wild-type and 11%, relative azygous. In contrast, although e-*AtCGA1* 14 was greater by

approximately 25% compared to wild-type, the difference to azygous was negligible (Figure 5.12B).

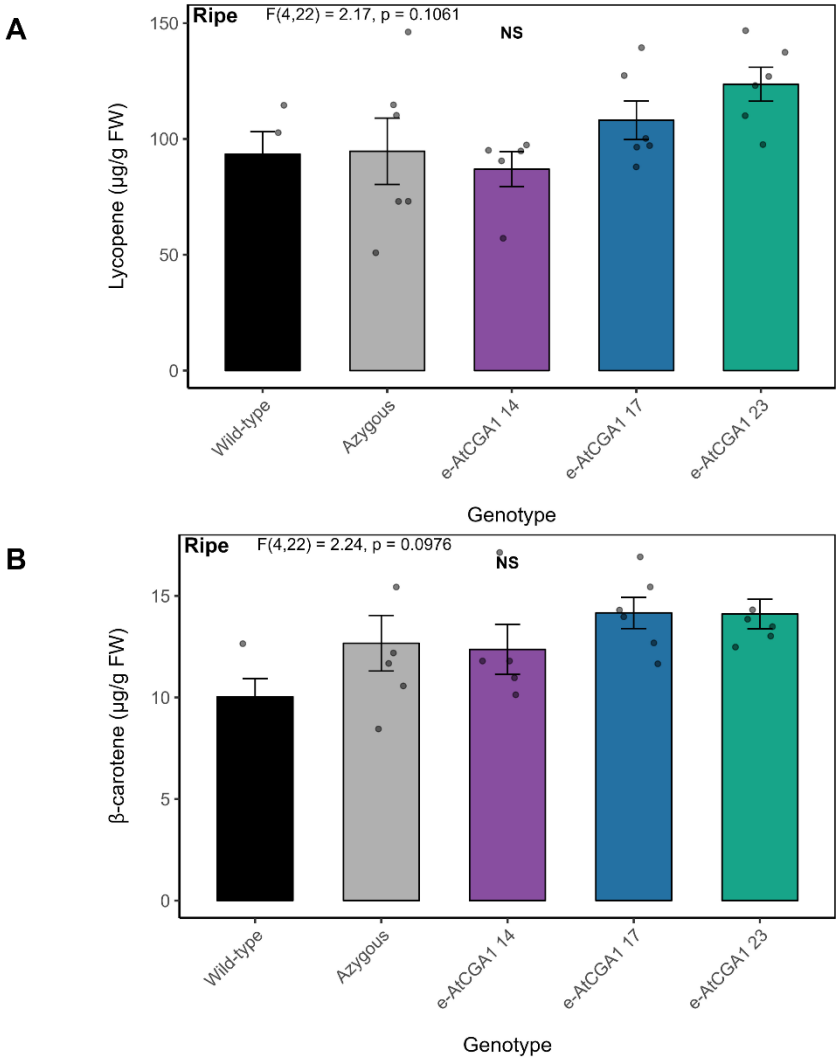

Figure 5.12. Carotenoid levels in early-specific *AtCGA1* tomato lines. Bar charts display the carotenoid content in independent lines of *AtCGA1* driven by the *SlTFM7* early fruit-specific promoter (e-*AtCGA1*), as well as azygous and wild-type controls. (A) Lycopene. (B) β-carotene. Ripe = breaker +7–10 days. All values represent means ± SE from at least four biological replicates per genotype, each analysed in two technical replicates. Statistically significant differences were determined using a 1-way ANOVA followed by a Duncan's multiple range test. Dots show individual data points. Different letters indicate statistically significant differences (P<0.05).

5.2.5 Chlorophyll and Carotenoid Levels in *AtGNC* Tomato Lines

Chlorophyll measurements were conducted in both immature green (IG) and mature green fruits (MG) to assess whether *AtGNC* had an impact on the chlorophyll levels of Micro-Tom fruits and

the role played by different developmental stages on chlorophyll accumulation in the overexpressing lines. Representative images of mature green (MG) fruits from early-specific *AtGNC* transgenic lines, along with wild-type and azygous controls, are shown in Figure 5.13.

Figure 5.13. Phenotypes of mature green (MG) fruits of early-specific *AtGNC* tomato lines. Images display representative MG fruits from transgenic lines expressing *AtGNC* driven by the *SlAFF* early fruit-specific promoter (e-*AtGNC*), as well as azygous and wild-type controls. (A) Wild-type. (B) Azygous. (C) e-*AtGNC* 2. (D) e-*AtGNC* 3. (E) e-*AtGNC* 6. MG = 20–23 days post-anthesis. Scale bars = 1 cm.

The analysis of chlorophyll content in e-*AtGNC* lines revealed that at the immature green stage, no significant differences were observed between genotypes (Figure 5.14A). In mature green fruits, however, e-*AtGNC* 2 (64.4 ± 6.74 µg/g) showed the highest increases in both chlorophyll and carotenoid, around 67% and 60% relative to wild-type (38.4 ± 2.92 µg/g) and azygous control (40.2 ± 6.05 µg/g), respectively. On the other hand, line e-*AtGNC* 6 (42.7± 2.99 µg/g) presented the lowest chlorophyll increases (around 5% relative to azygous and 10% to wild-type). Meanwhile, e-*AtGNC* 3 (49.1 ± 5.57 µg/g) displayed an intermediate phenotype in both experiments (Figure 5.14B).

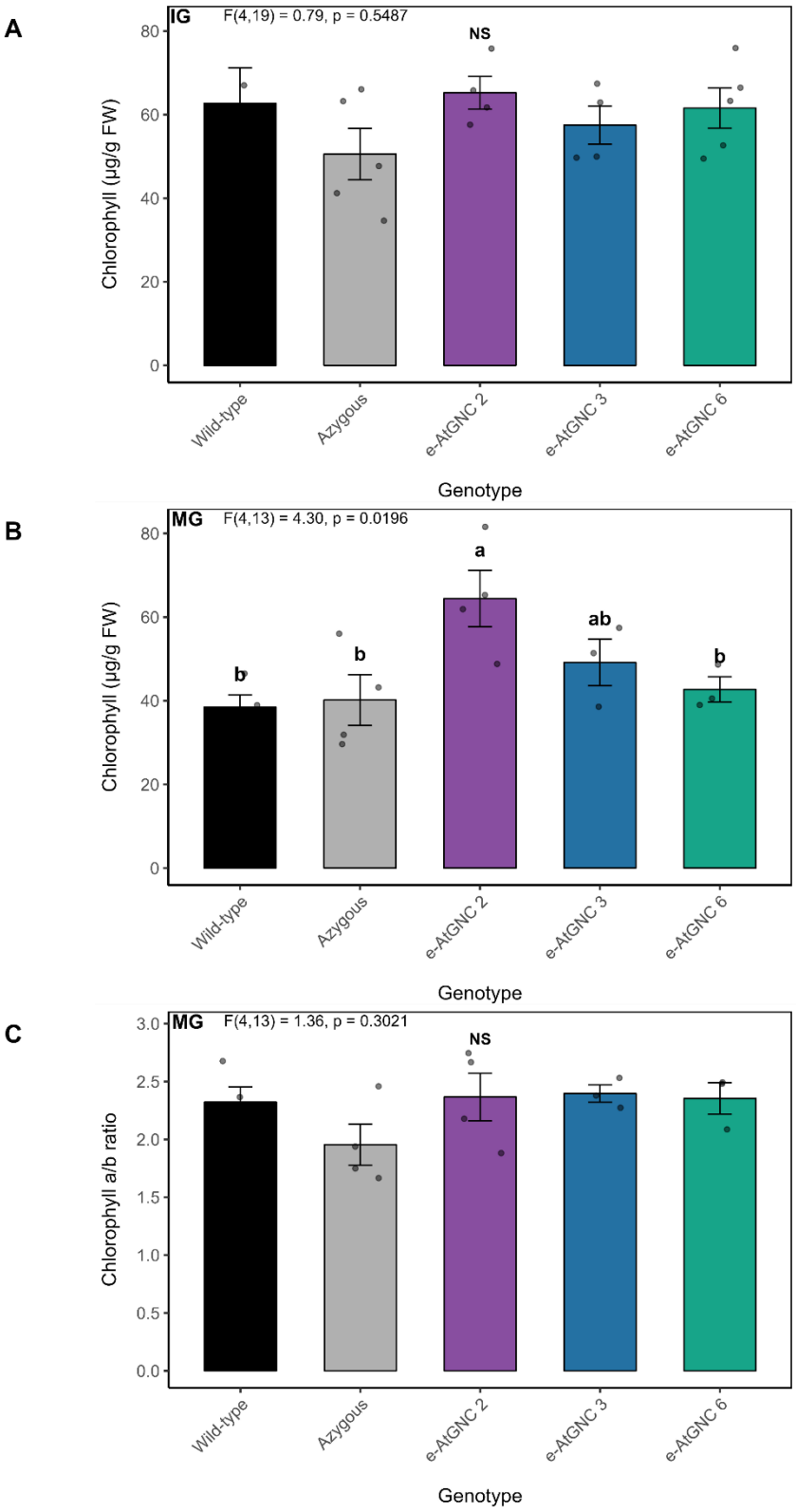

Figure 5.14. Chlorophyll levels in early-specific *AtGNC* tomato lines. Bar charts display the total chlorophyll content in independent lines of *AtGNC* driven by the *SlAFF* early fruit-specific promoter (e-

AtGNC), as well as azygous and wild-type controls. (A) Immature green (IG). (B) Mature green (MG). (C) Chlorophyll *a*/*b* ratio. IG = 7–10 days post-anthesis. MG = 20–23 days post-anthesis. All values represent means ± SE from at least three biological replicates per genotype, each analysed in three technical replicates. Statistically significant differences were determined using a 1-way ANOVA followed by Duncan's multiple range test. Dots show individual data points. Different letters indicate statistically significant differences (P<0.05).

In line with the results from the chlorophyll analysis, at the mature green stage, transgenic line e-*AtGNC* 2 exhibited significantly higher carotenoid content (16.7 ± 2.07 µg/g) compared to both wild-type (10.3 ± 0.75 µg/g) and azygous (10.6 ± 1.49 µg/g). Line e-*AtGNC* 6 exhibited the lowest increase in carotenoid (11.7 ± 0.596 µg/g), and e-*AtGNC* 3 exhibited an intermediate phenotype (13.7 ± 1.50 µg/g) (Figure 5.15).

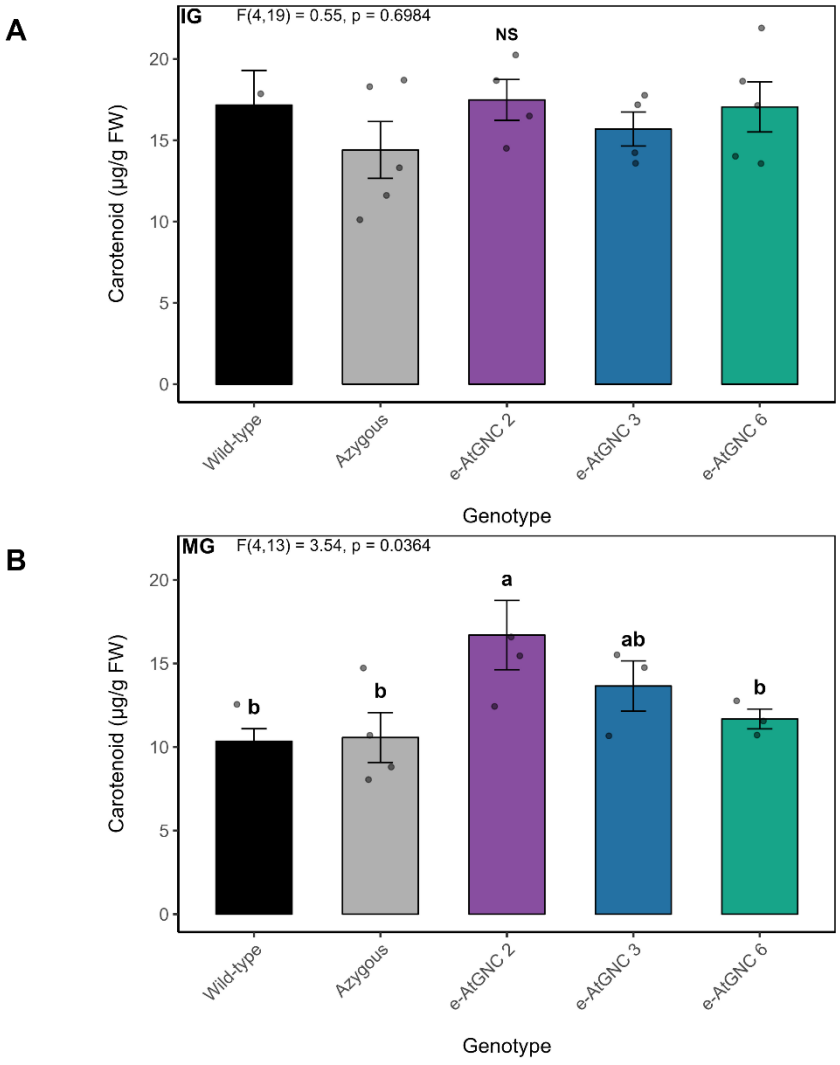

Figure 5.15. Carotenoid levels in early-specific *AtGNC* tomato lines. Bar charts display the total carotenoid content in independent lines of *AtGNC* driven by the *SlAFF* early fruit-specific promoter (e-

AtGNC), as well as azygous and wild-type controls. (A) Immature green (IG). (B) Mature green (MG). IG = 7–10 days post-anthesis. MG = 20–23 days post-anthesis. All values represent means ± SE from at least three biological replicates per genotype, each analysed in three technical replicates. Statistically significant differences were determined using a 1-way ANOVA followed by Duncan's multiple range test. Dots show individual data points. Different letters indicate statistically significant differences (P<0.05).

5.2.6 Lycopene and β-Carotene Levels in *AtGNC* Tomato Lines

Ripe fruits (breaker +7–10 days) from e-*AtGNC* lines, wild-type, and azygous fruits are shown in Figure 5.16. No striking phenotypic differences were observed between transgenic lines and wild-type and azygous controls.

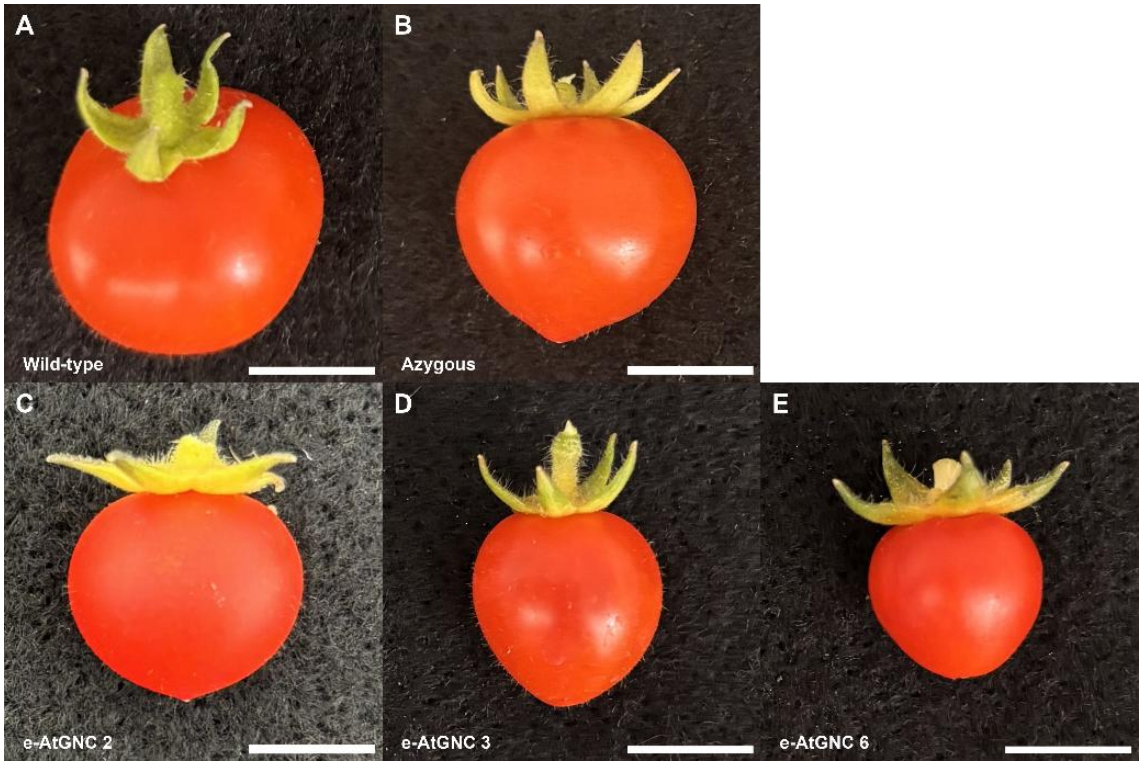

Figure 5.16. Phenotypes of ripe fruits of early-specific *AtGNC* tomato lines. Images display representative ripe fruits from transgenic lines expressing *AtGNC* driven by the *SlAFF* early fruit-specific promoter (e-*AtGNC*), as well as azygous and wild-type controls. (A) Wild-type. (B) Azygous. (C) e-*AtGNC* 2 10. (D) e-*AtGNC* 3. (E) e-*AtGNC* 6. Ripe = breaker +7–10 days. Scale bars = 1 cm.

Consistent with the absence of visible phenotypic differences in ripe fruits, the analysis of independent e-*AtGNC* lines showed that none of the transgenic lines exhibited an increase in lycopene content (Figure 5.17). Nevertheless, while e-*AtGNC* 2 exhibited lycopene levels (99.8 ± 10.6 µg/g) comparable to those of wild-type (93.5 ± 9.63 µg/g) and azygous fruits (94.7 ± 14.3

µg/g), it showed a significant increase in β-carotene accumulation, reaching approximately 108% higher than wild-type and 64% higher than the azygous control. In contrast, lines e-*AtGNC* 3 and e-*AtGNC* 6 showed β-carotene levels similar to both controls and a modest reduction in lycopene, although these differences were not statistically significant.

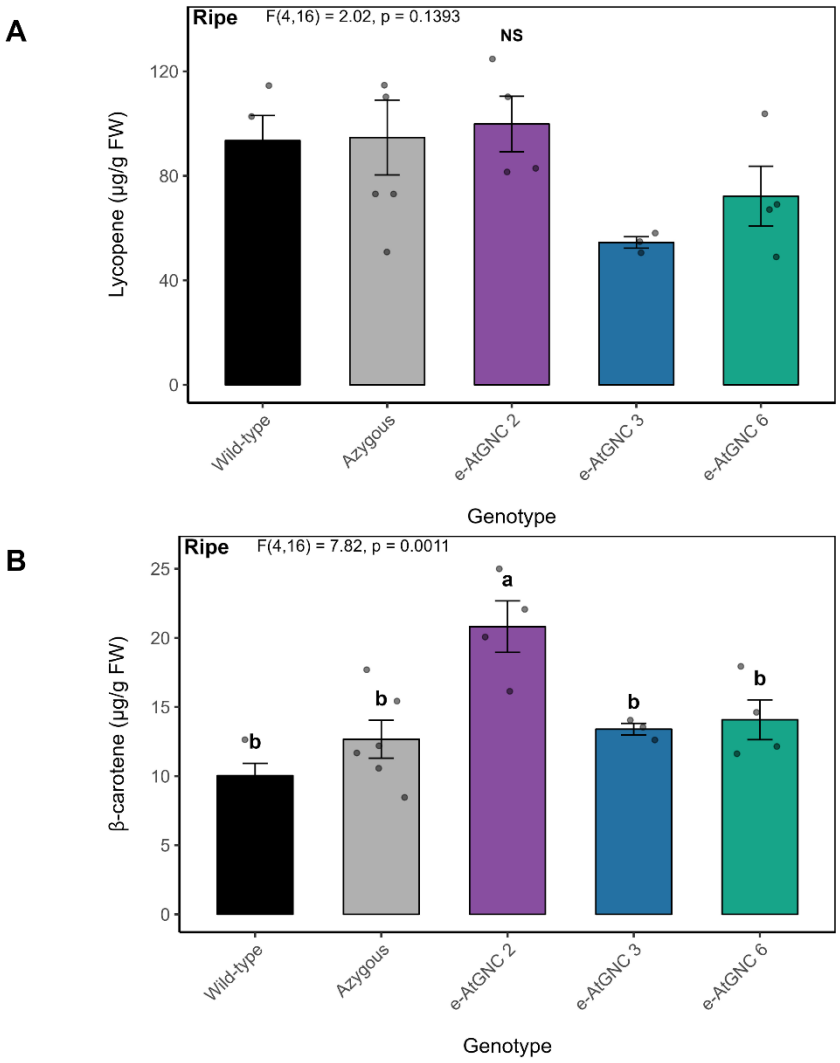

Figure 5.17. Carotenoid levels in early-specific *AtGNC* tomato lines. Bar charts display the carotenoid content in independent lines of *AtGNC* driven by the *SlAFF* early fruit-specific promoter (e-*AtGNC*), as well as azygous and wild-type controls. (A) Lycopene. (B) β-carotene. All values represent means ± SE from at least three biological replicates per genotype, each analysed in two technical replicates (except e-*AtGNC* 3, which consisted of 3 biological replicates). Ripe = breaker +7–10 days. Statistically significant differences were determined using a 1-way ANOVA followed by a Duncan's multiple range test. Dots show individual data points. Different letters indicate statistically significant differences (P<0.05).

5.2.7 Maximum PSII Quantum Yield (F_v/F_m) of *AtCGA1* Lines

The analysis of independent transgenic lines revealed no statistically significant differences in F_v/F_m between immature green of the transgenic lines relative to the wild-type and azygous fruits (Figure 5.18A). At the immature green stage, transgenic lines ranged from 0.775 to 0.827, whereas the wild-type control showed F_v/F_m of 0.811 ± 0.009 and azygous 0.821 ± 0.013. Mature green e-*AtCGA1* 17 (0.815 ± 0.002) and e-*AtCGA1* 23 (0.811 ± 0.003) fruits exhibited significantly higher F_v/F_m values compared to wild-type (0.788 ± 0.005) and azygous (0.793 ± 0.025). Mature green e-*AtCGA1* 14 (0.786 ± 0.006) showed a comparable F_v/F_m to both controls (Figure 5.18B).

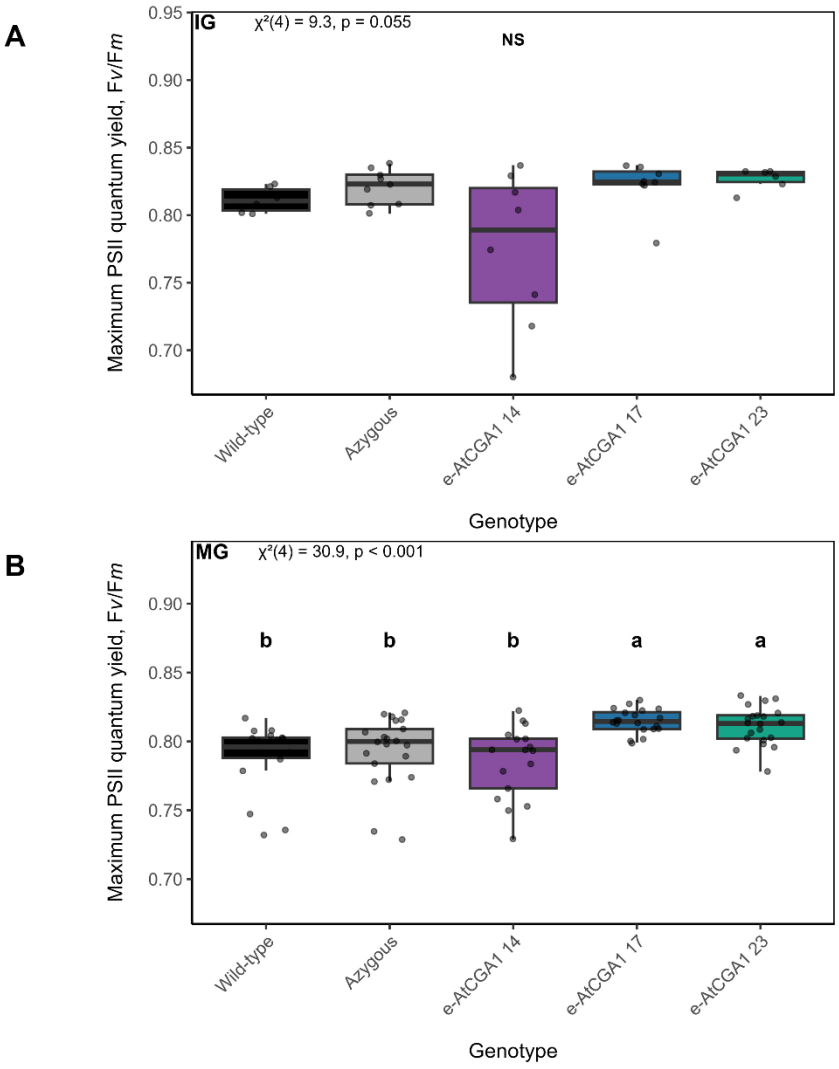

Figure 5.18. Maximum PSII quantum yield (F_v/F_m) in early-specific *AtCGA1* tomato lines. Boxplots display F_v/F_m in fruits from independent lines of *AtCGA1* driven by the *SlTFM7* early fruit-specific promoter (e-*AtCGA1*), compared with azygous and wild-type controls. (A) Immature green (IG). (B) Mature green (MG). IG = 7–10 days post-anthesis. MG = 20–23 days post-anthesis. The boxes represent the interquartile range (25th to 75th percentile), the horizontal line shows the median, and the whiskers extend to 1.5 times the

interquartile range. Statistically significant differences were determined using a Kruskal-Wallis test followed by Dunn's multiple range test. Dots show individual data points. Different letters indicate statistically significant differences ($P < 0.05$).

5.2.8 *AtCGA1* Overexpression Increases Effective PSII Quantum Yield (ΦPSII)

Chlorophyll fluorescence light response curves were performed across a range of light intensities (Figure 5.19). The analysis revealed that, at the immature green stage, only e-*AtCGA1*-23 consistently outperformed both the wild-type and azygous lines across all light intensities. In contrast, e-*AtCGA1* 14 exhibited responses comparable to the wild-type, while e-*AtCGA1* 17 aligned closely with the azygous control. Moreover, wild-type and azygous exhibited different responses. At the mature green stage, both e-*AtCGA1* 17 and 23 outperformed wild-type and azygous lines across all light intensities, reinforcing the more evident transgene effect at this developmental stage. On the other hand, e-*AtCGA1* 14 showed no improvement, with performance similar to that of both wild-type and azygous. It is important to note that at light intensities of 800 µmol m^{-2} s^{-1} and above, severe photodamage was observed in all lines.

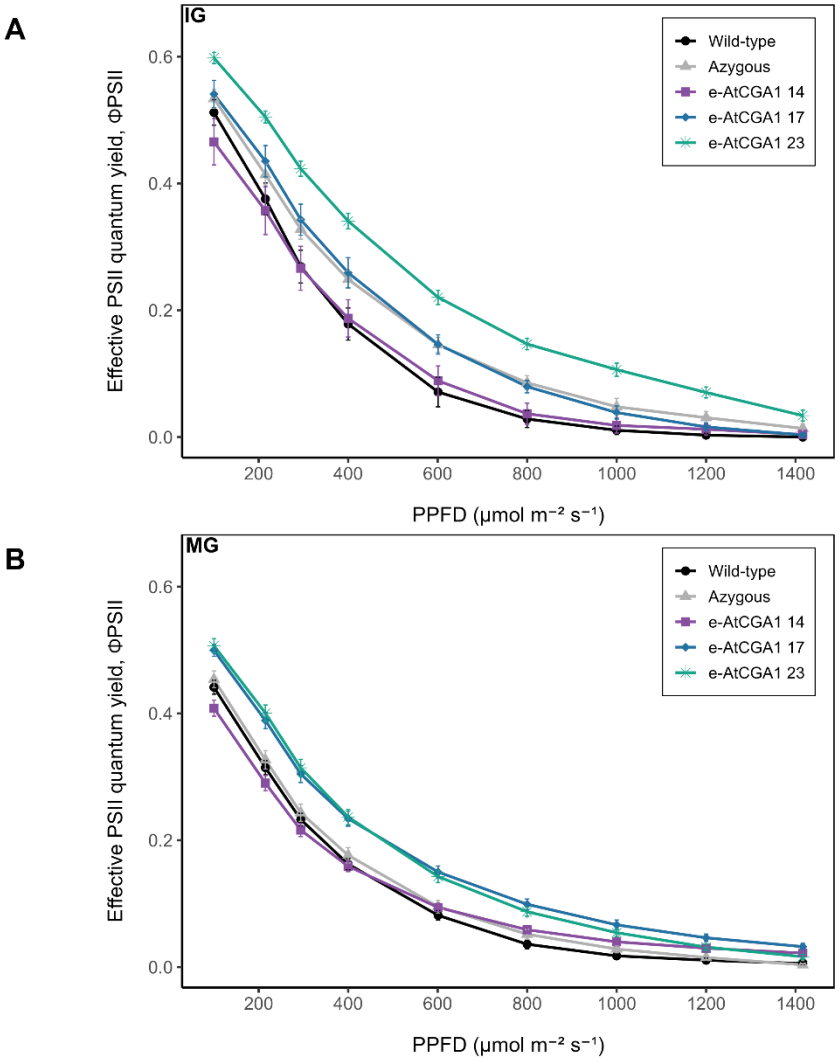

Figure 5.19. Light responses of effective PSII quantum yield (ΦPSII) in early-specific *AtCGA1* tomato lines. Light curves display ΦPSII in fruits from independent lines of *AtCGA1* driven by the *SlTFM7* early fruit-specific promoter (e-*AtCGA1*), compared with azygous and wild-type controls. (A) Immature green (IG). (B) Mature green (MG). IG = 7–10 days post-anthesis. MG = 20–23 days post-anthesis. All values represent means ± SE from at least four biological replicates per genotype, with two fruits sampled per plant.

The analysis of PSII quantum yield (ΦPSII) of independent immature green lines at 294 µmol m^{-2} s^{-1} showed that no statistically significant differences were observed between the wild-type (0.269 ± 0.025), azygous (0.328 ± 0.015), and the transgenic lines e-*AtCGA1* 14 (0.266 ± 0.034) and e-*AtCGA1* 17 (0.343 ± 0.024). Transgenic line e-*AtCGA1* 23 displayed a significant increase (0.423 ± 0.011) relative to wild-type (0.269 ± 0.025), although the increase relative to azygous (0.328 ± 0.015) was less substantial (Figure 5.20A). At the mature green stage, both e-*AtCGA1* 17 (0.304 ± 0.013) and 23 (0.314 ± 0.013) exhibited significant increases relative to both wild-type

(0.233 ± 0.009) and azygous control (0.243 ± 0.013) (Figure 5.20B). In contrast, transgenic line e-*AtCGA1* 14 did not differ significantly from either control at either developmental stage.

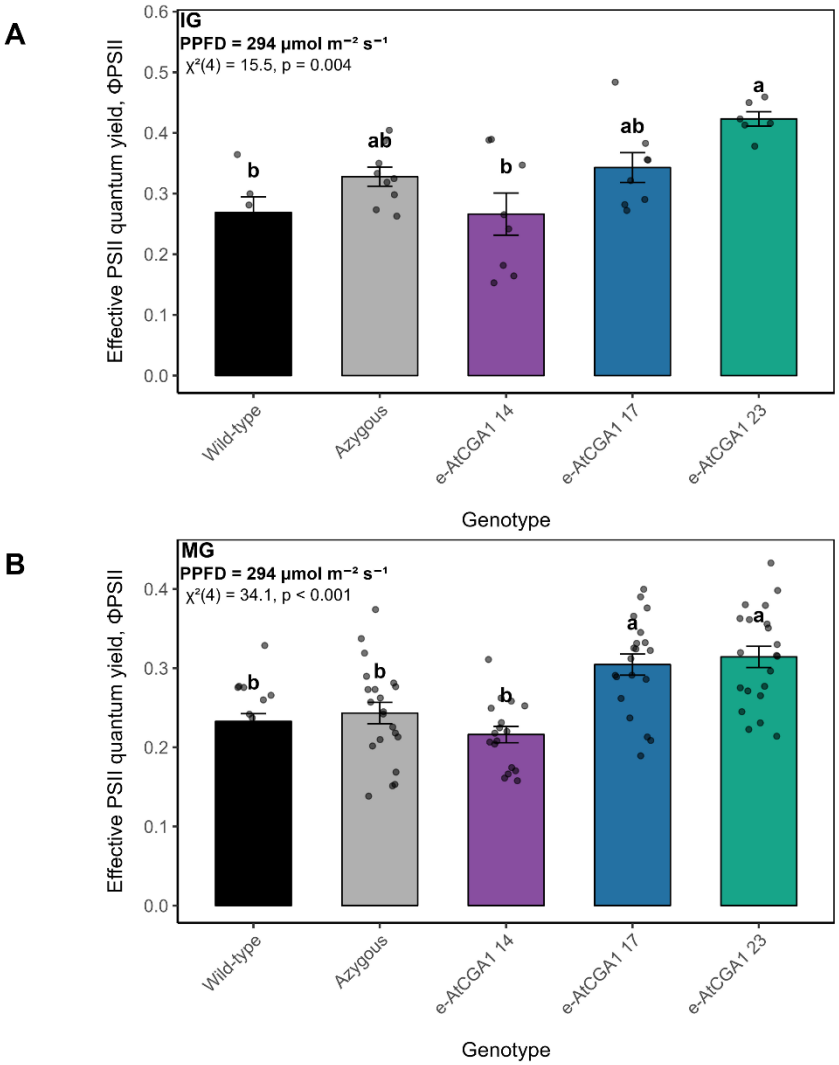

Figure 5.20. Effective PSII quantum yield (ΦPSII) in early-specific *AtCGA1* tomato lines. Bar charts display ΦPSII in fruits from independent lines of *AtCGA1* driven by the *SlTFM7* early fruit-specific promoter (e-*AtCGA1*), compared with azygous and wild-type controls at 294 µmol m^{-2} s^{-1}. (A) Immature green (IG). (B) Mature green (MG). All values represent means ± SE from at least four biological replicates per genotype, with two fruits sampled per plant. IG = 7–10 days post-anthesis. MG = 20–23 days post-anthesis. Statistically significant differences were determined using a Kruskal-Wallis test followed by Dunn's multiple range test. Dots show individual data points. Different letters indicate statistically significant differences ($P < 0.05$).

At 601 µmol m^{-2} s^{-1}, the most consistent improvement in ΦPSII was observed in e-*AtCGA1* 23, which outperformed both wild-type and azygous lines at the immature green and mature green stages (Figure 5.21). In contrast, e-*AtCGA1* 17 showed a significant improvement only at the

mature green stage, while e-*AtCGA1* 14 did not differ significantly from either control at any stage. At the mature green stage, ΦPSII values were (0.150 ± 0.009) in e-*AtCGA1* 17 and (0.143 ± 0.009) in e-*AtCGA1* 23, significantly higher than in wild-type (0.081 ± 0.007) and azygous (0.095 ± 0.010) fruits. These correspond to increases of approximately 85% and 76% over wild-type, and 57% and 50% over the azygous controls, respectively.

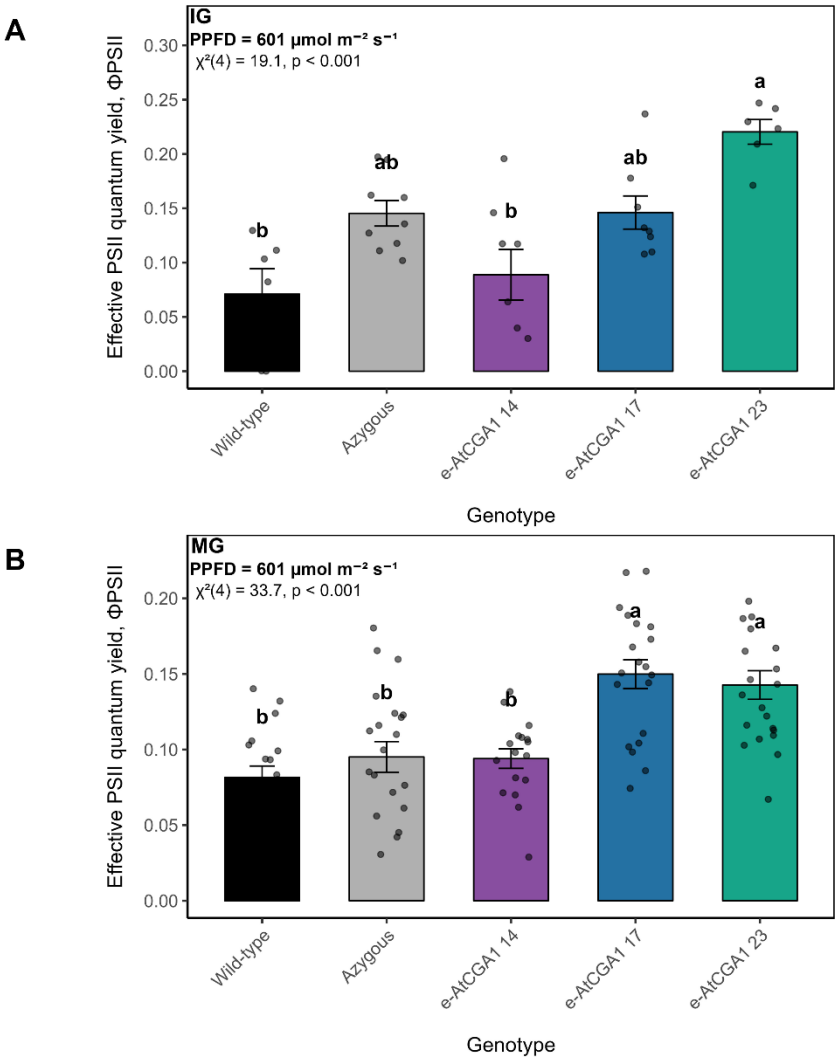

Figure 5.21. Effective PSII quantum yield (ΦPSII) in early-specific *AtCGA1* tomato lines. Bar charts display ΦPSII in fruits from independent lines of *AtCGA1* driven by the *SlTFM7* early fruit-specific promoter (e-*AtCGA1*), compared with azygous and wild-type controls at 601 µmol m^{-2} s^{-1}. (A) Immature green (IG). (B) Mature green (MG). IG = 7–10 days post-anthesis. MG = 20–23 days post-anthesis. All values represent means ± SE from at least four biological replicates per genotype, with two fruits sampled per plant. Statistically significant differences were determined using a Kruskal-Wallis test followed by Dunn's multiple range test. Dots show individual data points. Different letters indicate statistically significant differences ($P < 0.05$).

5.2.9 Effective PSII Quantum Yield (ΦPSII) at Different Developmental Stages in *AtCGA1* Tomato Lines

The effective PSII quantum yield (ΦPSII) was assessed in fruits of early-specific *AtCGA1* transgenic lines across developmental stages (Figure 5.22). At both light intensities (294 and 601 µmol m^{-2} s^{-1}), developmental stage (immature green vs mature green) had a significant effect, consistent with the overall decline in ΦPSII from immature to mature green fruit. In contrast, genotype type (wild-type/azygous vs e-*AtCGA1*) did not show a significant effect, indicating that the impact of *AtCGA1* expression on ΦPSII was not uniform across transgenic lines. This is consistent with the one-way genotype analysis, in which only e-*AtCGA1* lines 17 and 23 exhibited significantly greater ΦPSII values, while e-*AtCGA1* 14 did not differ from controls.

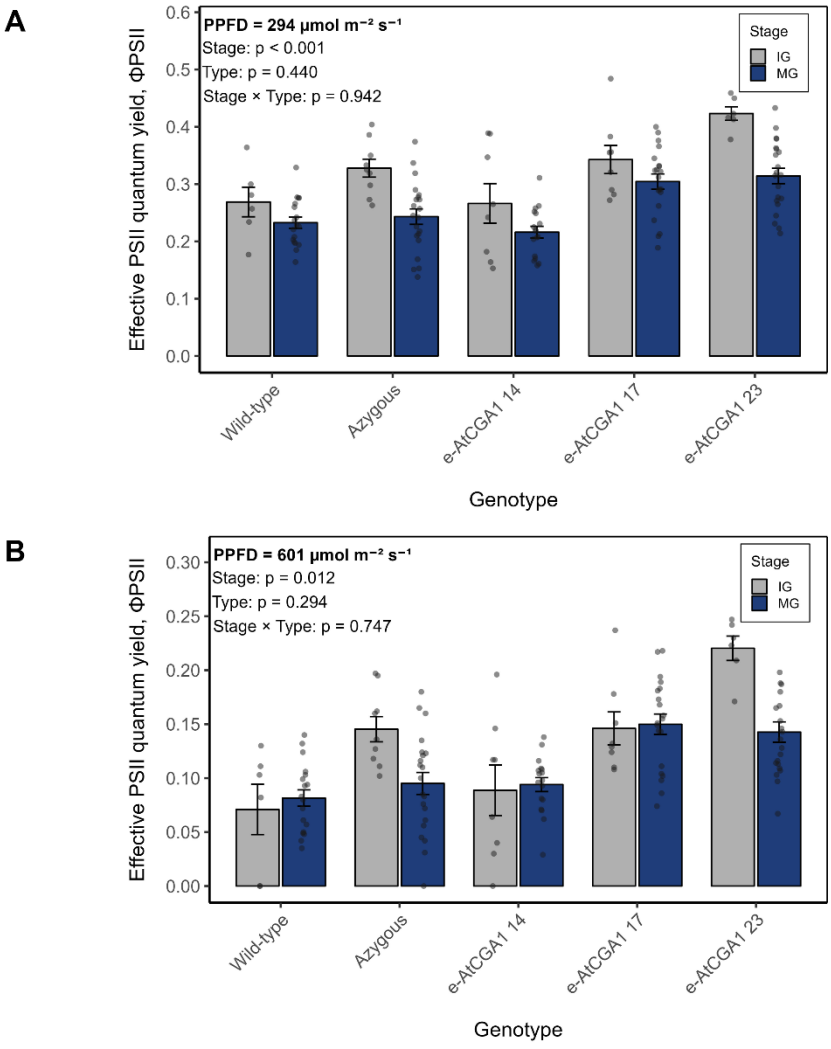

Figure 5.22. Changes in light responses of effective PSII quantum yield (ΦPSII) during fruit development in early-specific *AtCGA1* tomato lines. The bar charts display ΦPSII in fruits of *AtCGA1* driven by the *SlTFM7* early-specific promoter. (A) ΦPSII at 294 µmol m^{-2} s^{-1}. (B) ΦPSII at 601 µmol m^{-2} s^{-1}.

IG = 7–10 days post-anthesis. MG = 20–23 days post-anthesis. All values represent means ± SE from at least four biological replicates per genotype, with two fruits sampled per plant. Dots show individual data points. Statistically significant differences were assessed using a 2-way nested ANOVA, with developmental stage (IG vs MG) and genotype type (wild-type/azygous vs e-*AtCGA1*) included as fixed factors and genotype (line) nested within type. Main effects and the stage × type interaction were tested, with significance accepted at $P < 0.05$.

5.2.10 Chlorophyll Fluorescence Images of Effective PSII Quantum Yield (ΦPSII) in *AtCGA1* Tomato Lines

Chlorophyll fluorescence imaging of whole fruits further supported the quantitative measurements (Figure 5.23). This analysis of ΦPSII imaging revealed that e-*AtCGA1* 17 and 23 exhibited a more consistent photochemical apparatus at both light intensities. At 294 µmol m^{-2} s^{-1}, it exhibits predominantly green colours, indicative of higher photochemistry capacity. At 601 µmol m^{-2} s^{-1}, both lines still maintained a yellow profile. In contrast, while e-*AtCGA1* 14, wild-type and azygous control exhibited some photochemistry at the lower light intensity, the orange over the surface of the fruit at 601 µmol m^{-2} s^{-1} indicates severe photodamage, and black regions indicate no photochemistry being driven.

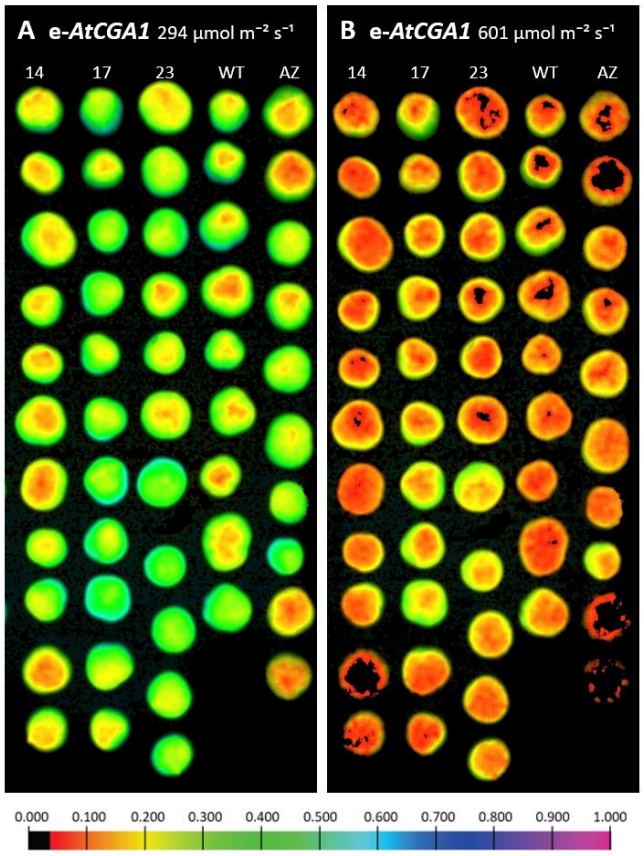

Figure 5.23. Chlorophyll fluorescence imaging of Effective PSII quantum yield (ΦPSII) in early-specific *AtCGA1* tomato lines. Fluorescence imaging displays ΦPSII under two light intensities in mature green fruits (MG) of *AtCGA1* lines driven by the *SlTFM7* early fruit-specific promoter (e-*AtCGA1*), azygous and wild-type controls. (A) ΦPSII images of fruits at 294 µmol m^{-2} s^{-1}. (B) ΦPSII images of fruits at 601 µmol m^{-2} s^{-1}. Transgenic e-*AtCGA1* lines 14, 17 and 23 are compared against azygous (AZ) and wild-type (WT) controls. MG = 20–23 days post-anthesis. Colour scales range from 0 (black) to 1 (purple) and represent ΦPSII values. Green to blue regions indicate high photochemical efficiency, whereas yellow to red areas indicate reduced PSII activity, suggesting photoinhibition or increased excitation pressure under higher PPFD.

5.2.11 *AtCGA1* Overexpression Enhances Electron Transport Rate (ETR) in Tomato Fruits

The electron transport rate (ETR) further reinforced the enhanced photosynthetic performance of mature green e-*AtCGA1* 17 and 23 compared to wild-type, azygous controls. Both transgenic lines reached peak ETR values close to 40 µmol electrons m^{-2} s^{-1}, while the maximum values for wild-type and azygous lines remained below 30 µmol electrons m^{-2} s^{-1}. e-*AtCGA1 14* showed ETR responses comparable to both control genotypes, except at higher light intensities, which could indicate a light-dependent transgene effect. In addition, e-*AtCGA1* 17 and 23 saturate at around 400 µmol m^{-2} s^{-1}, whereas wild-type and azygous plants saturate at approximately 300 µmol µmol m^{-2} s^{-1} (Figure 5.24A). These saturation points suggest that light harvesting may not be a

limiting factor in these transgenic lines, and that the main limitations may come from electron transport capacity and/or downstream processes.

A deeper analysis at 294 µmol m^{-2} s^{-1} shows that ETR values for wild-type and azygous fruits were 28.7 ± 1.21 and 30.0 ± 1.66 µmol electrons m^{-2} s^{-1}, respectively, whereas e-*AtCGA1* lines 17 and 23 showed higher rates of 37.6 ± 1.65 and 38.8 ± 1.65 µmol electrons m^{-2} s^{-1}, respectively (Figure 5.24B). A similar pattern was observed at 601 µmol m^{-2} s^{-1}, where ETR values in wild-type and azygous fruits declined to 20.6 ± 1.91 and 24 ± 2.56 µmol electrons $m^{-2}s^{-1}$, while e-*AtCGA1* lines 17 and 23 maintained significantly higher rates, 37.8 ± 2.39 and 36.0 ± 2.39 µmol electrons m^{-2} s^{-1}, respectively (Figure 5.24C). In contrast, e-*AtCGA1* 14 exhibited ETR values comparable to wild-type and azygous controls. Importantly, e-*AtCGA1* 14 displayed significantly lower chlorophyll *a*/*b* ratio compared to e-*AtCGA1* 17, and a comparable ratio to those of the wild-type and azygous. These results suggest that the larger antenna size per reaction centre in line 14 impacts the efficiency of electron transport flow.

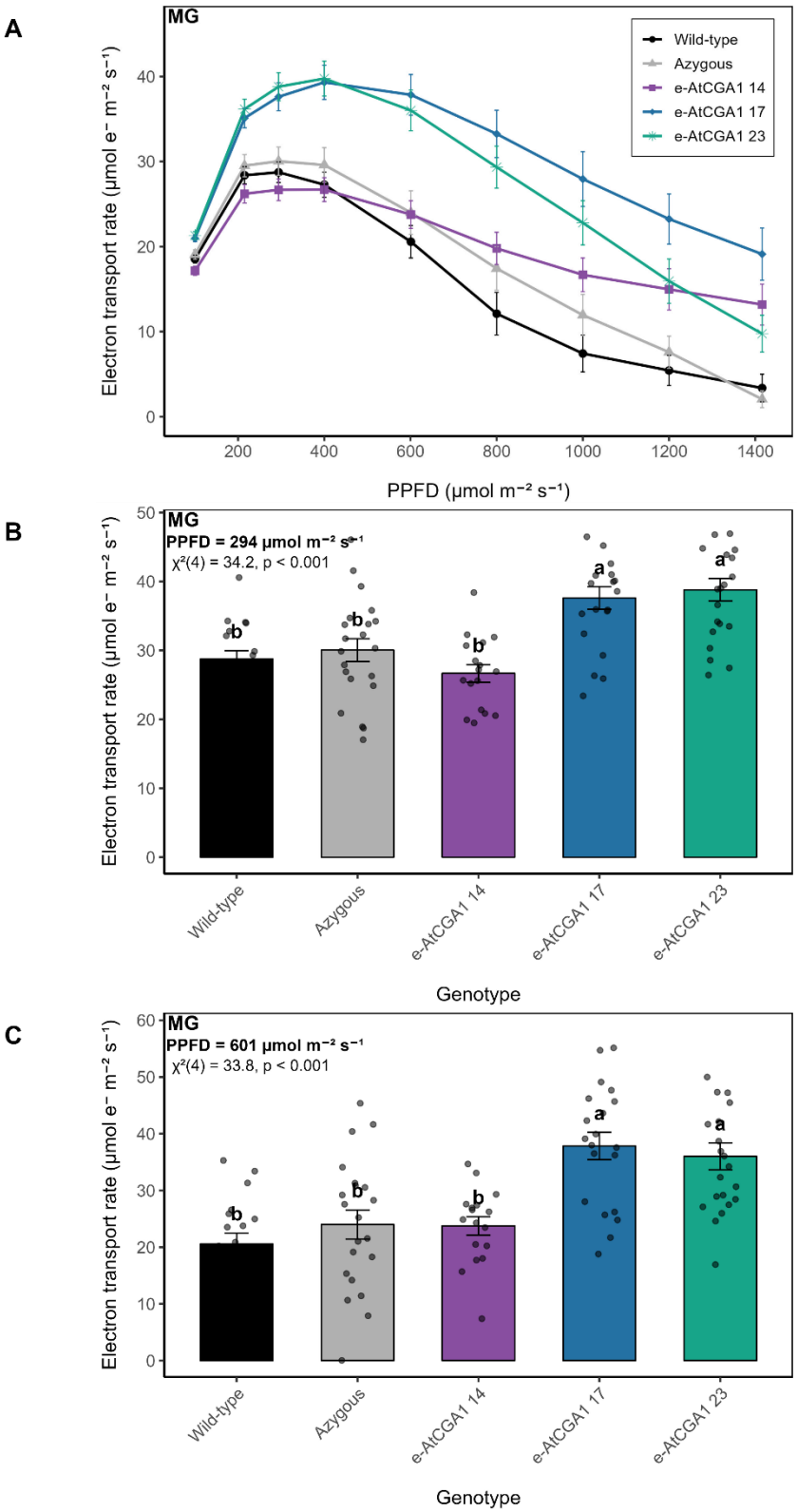

Figure 5.24. Electron transport rate (ETR) in early-specific *AtCGA1* lines. Bar charts display ETR in mature green fruits (MG) of independent lines of *AtCGA1* driven by the *SlTFM7* early fruit-specific promoter (e-*AtCGA1*), compared with azygous and wild-type controls. (A) Light response of ETR across all light intensities (100–1400 µmol m^{-2} s^{-1}). (B) ETR at 294 µmol m^{-2} s^{-1}. (C) ETR at 601 µmol m^{-2} s^{-1}. MG = 20–23 days post-anthesis. All values represent means ± SE from at least four biological replicates per genotype,

with two fruits sampled per plant. Statistically significant differences were determined using a Kruskal-Wallis test followed by Dunn's multiple range test. Dots show individual data points. Different letters indicate statistically significant differences ($P < 0.05$).

5.2.12 Photochemical Quenching (qL) and Non-Photochemical Quenching (qN) coefficients in *AtCGA1*

The differences in photochemical quenching (qL) were not evident for any genotype at 294 µmol m^{-2} s^{-1}, with only non-significant increases observed between e-*AtCGA1* 17 and 23 and the controls (Figure 5.25A). The results contrast with the previous observations from e-*BpMADS* in Chapter 4, where e-*BpMADS* lines already maintained a higher proportion of open PSII reaction centres compared to wild-type and azygous at lower light intensities. In contrast, at 601 µmol m^{-2} s^{-1}, lines e-*AtCGA1* 17 and 23 exhibited a higher proportion of reaction centres open, 0.151 ± 0.007 and 0.148 ± 0.008, respectively, compared to 0.074 ± 0.015 in wild-type and 0.097 ± 0.013 in azygous. The increases in e-*AtCGA1* 17 were approximately 104% relative to the wild-type and 55% relative to the azygous. In e-*AtCGA1* 23, these increases represented 100% and 52% compared to wild-type and azygous, respectively. Line e-*AtCGA1* 14 exhibited comparable results to wild-type and azygous control at both light intensities (Figure 5.25B).

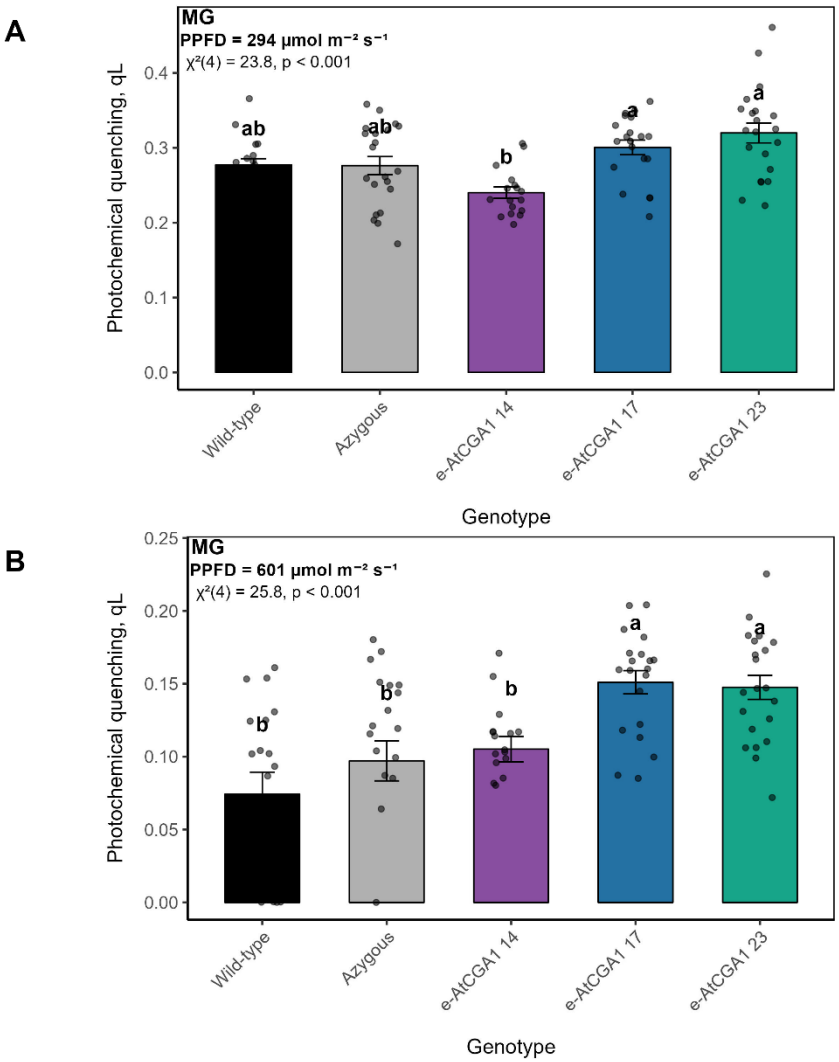

Figure 5.25. Coefficient of photochemical quenching (qL) in early-specific *AtCGA1* lines. Bar charts display qL of mature green fruits (MG) of independent lines of *AtCGA1* driven by the *SlTFM7* early fruit-specific promoter (e-*AtCGA1*), compared with azygous and wild-type controls. (A) qL at 294 µmol m^{-2} s^{-1} (B) qL at 601 µmol m^{-2} s^{-1}. MG = 20–23 days post-anthesis. All values represent means ± SE from at least four biological replicates per genotype, with two fruits sampled per plant. Statistically significant differences were determined using a Kruskal-Wallis test followed by Dunn's multiple range test. Dots show individual data points. Different letters indicate statistically significant differences ($P < 0.05$).

Increasing PPFD from 294 to 601 µmol m^{-2} s^{-1} led to a greater allocation of photon energy to non-photochemical pathways, as reflected by rising qN values across all genotypes (Figure 5.26). The need for non-photochemical quenching (qN), which reflects heat dissipation of excess excitation energy, was reduced in e-*AtCGA1* fruits. Whit increased light intensity, wild-type and azygous fruits showed an increase in qN from 0.823 ± 0.005 and 0.813 ± 0.005, respectively to 0.871 ± 0.003 and 0.862 ± 0.002. Among the transgenic lines, e-*AtCGA1* 23 consistently exhibited lower qN values, with a mean of 0.771 ± 0.010 at 294 µmol m^{-2} s^{-1} and 0.843 ± 0.004 at 601 µmol m^{-2}

s^{-1}. Similarly, e-*AtCGA1* 17 followed a similar trend, showing reduced qN compared to both controls (0.771 ± 0.010 at 294 µmol m^{-2} s^{-1} and 0.837 ± 0.006 at 601 µmol m^{-2} s^{-1}). By contrast, e-*AtCGA1* 14 exhibited intermediate values at both light intensities, with a mean qN of 0.808 ± 0.005 at 294 µmol m^{-2} s^{-1} and 0.851 ± 0.004 at 601 µmol m^{-2} s^{-1}.

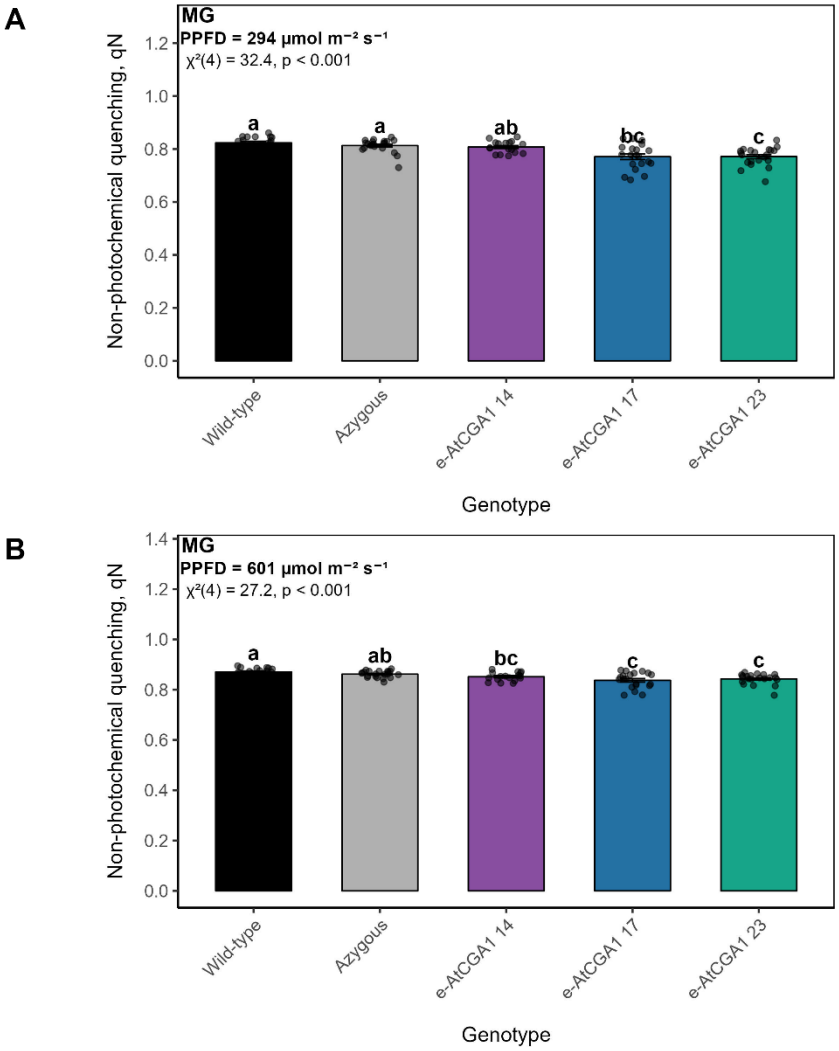

Figure 5.26. Coefficient of non-photochemical quenching (qN) in early-specific *AtCGA1* lines. Bar charts display qN of mature green fruits (MG) of independent lines of *AtCGA1* driven by the *SlTFM7* early fruit-specific promoter (e-*AtCGA1*), compared with azygous and wild-type controls. (A) qN at 294 µmol m^{-2} s^{-1} (B) qN at 601 µmol m^{-2} s^{-1}. MG = 20–23 days post-anthesis. All values represent means ± SE from at least four biological replicates per genotype, with two fruits sampled per plant. Statistically significant differences were determined using a Kruskal-Wallis test followed by Dunn's multiple range test. Dots show individual data points. Different letters indicate statistically significant differences ($P < 0.05$).

5.2.13 Gas Exchange Measurements of *AtCGA1* T2 Tomato Lines

The analysis of light responses revealed that increasing PPFD led to a reduction in CO_2 efflux in T2 fruits of e-*AtCGA1* 23, azygous and wild type. This indicates that a lower proportion of respired carbon is being released, presumably being internally refixed (Figure 5.27A). The CO_2 response rose sharply at the beginning of the experiment. This may be because more CO_2 becomes available in pericarp cells, enhancing CO_2 fixation. After the initial rise, the increase slows down, indicating limited access to CO_2 (Figure 5.27B). In both light and CO_2 responses, e-*AtCGA1* 23 outperformed wild-type. These results were more evident at 400 and 1500 µmol mol^{-1} in the CO_2 response analysis (Dunn post-hoc, p = 0.09 for both) and 800 µmol m^{-2} s^{-1}in the light response (Dunn post-hoc, p = 0.12).

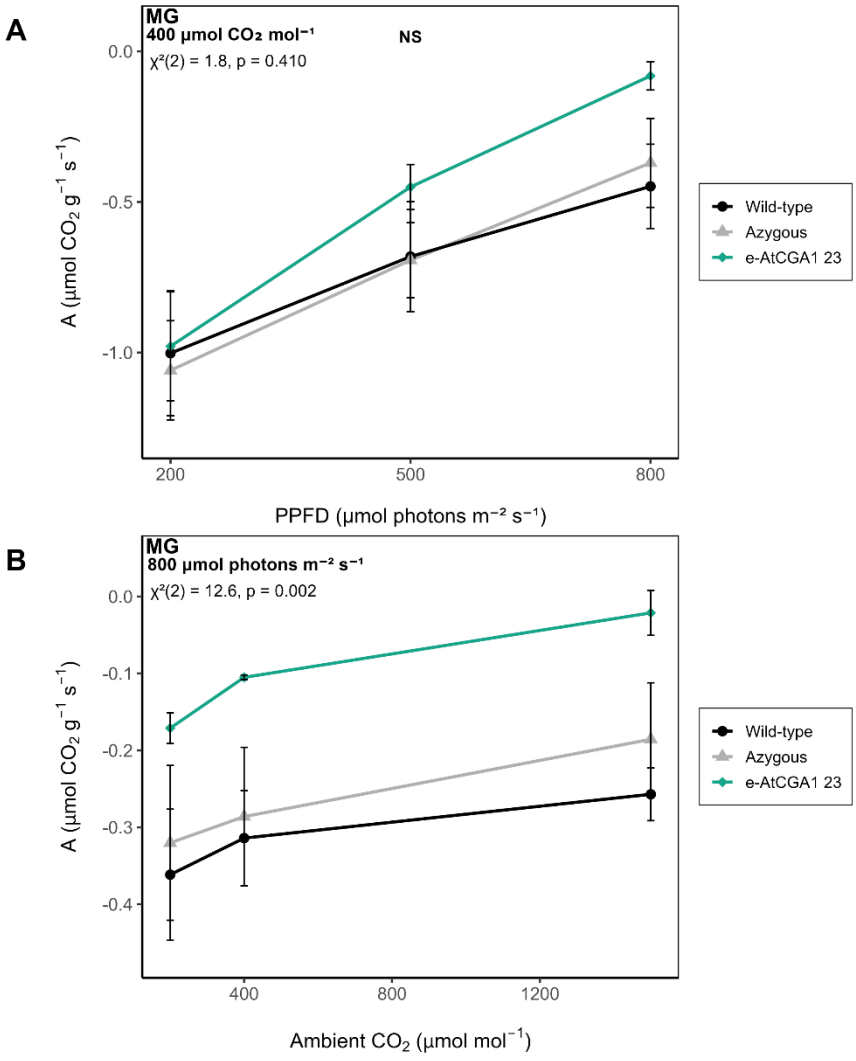

Figure 5.27. Gas exchange light response curves of early-specific *AtCGA1* lines. The photosynthetic responses display net CO_2 assimilation as a function of ambient CO_2 concentration in mature green fruits

(MG) of independent lines of *AtCGA1* driven by the *SlTFM7* early fruit-specific promoter (e-*AtCGA1*), compared with azygous and wild-type controls. (A) Net CO_2 assimilation as a function of incident photosynthetic photon flux density (PPFD) (B). Net CO_2 assimilation as a function of ambient CO_2 concentration. MG = 20–23 days post-anthesis. All values represent means ± SE from four biological replicates per genotype, each analysed in triplicate. Statistically significant differences were determined using a Kruskal-Wallis test followed by Dunn's multiple range test. Different letters indicate statistically significant differences ($P < 0.05$).

5.2.14 Effective PSII Quantum Yield (ΦPSII) and Electron Transport Rate (ETR) in *AtGNC* Tomato Lines

Light response values for ΦPSII and ETR were also assessed for mature green (MG) e-*AtGNC* fruits (Figure 5.28). Line e-*AtGNC* 2 considerably outperformed (ΦPSII) not only wild-type and azygous control but also the other two transgenic lines across all light intensities. Moreover, e-*AtGNC* 2 ETR saturates at around 400 µmol m^{-2} s^{-1}, while all other genotypes saturate earlier at around 300 µmol m^{-2} s^{-1}, besides achieving higher rates, of approximately 55 µmol electrons m^{-2} s^{-1}. On the other hand, e-*AtGNC* 3 and e-*AtGNC* 6 exhibited comparable results with both controls, with the former underperforming under higher light intensities.

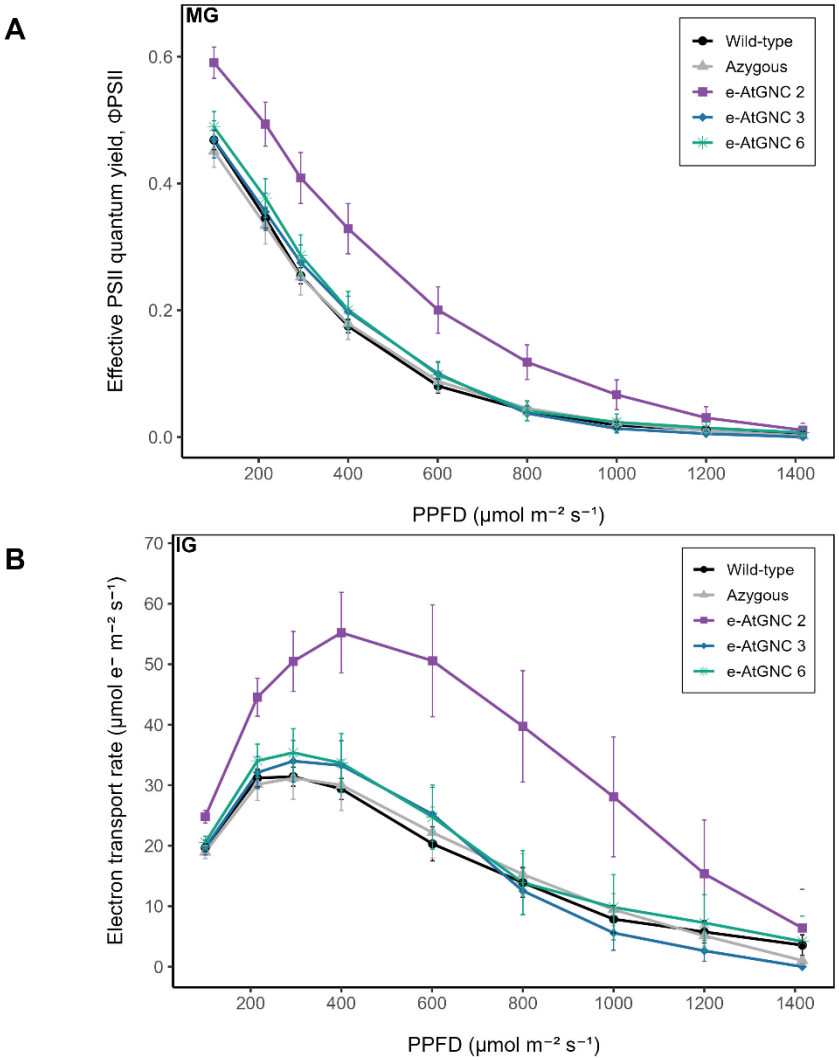

Figure 5.28. Light responses of effective PSII quantum yield (ΦPSII) and electron transport rate (ETR) in early-specific *AtGNC* tomato lines. Light curves display photosynthetic responses in mature green (MG) fruits from independent lines of *AtGNC* driven by the *SlAFF* early fruit-specific promoter (e-*AtGNC*), compared with azygous and wild-type controls. (A) ΦPSII. (B) ETR. MG = 20–23 days post-anthesis. All values represent means ± SE from at least three biological replicates per genotype, with two fruits sampled per plant.

The analysis of ΦPSII at 294 µmol m^{-2} s^{-1} and 601 µmol m^{-2} s^{-1} showed that at both light intensities, e-*AtGNC* 2 exhibited significantly higher values (Figure 5.29). No significant differences were detected between the remaining genotypes and controls.

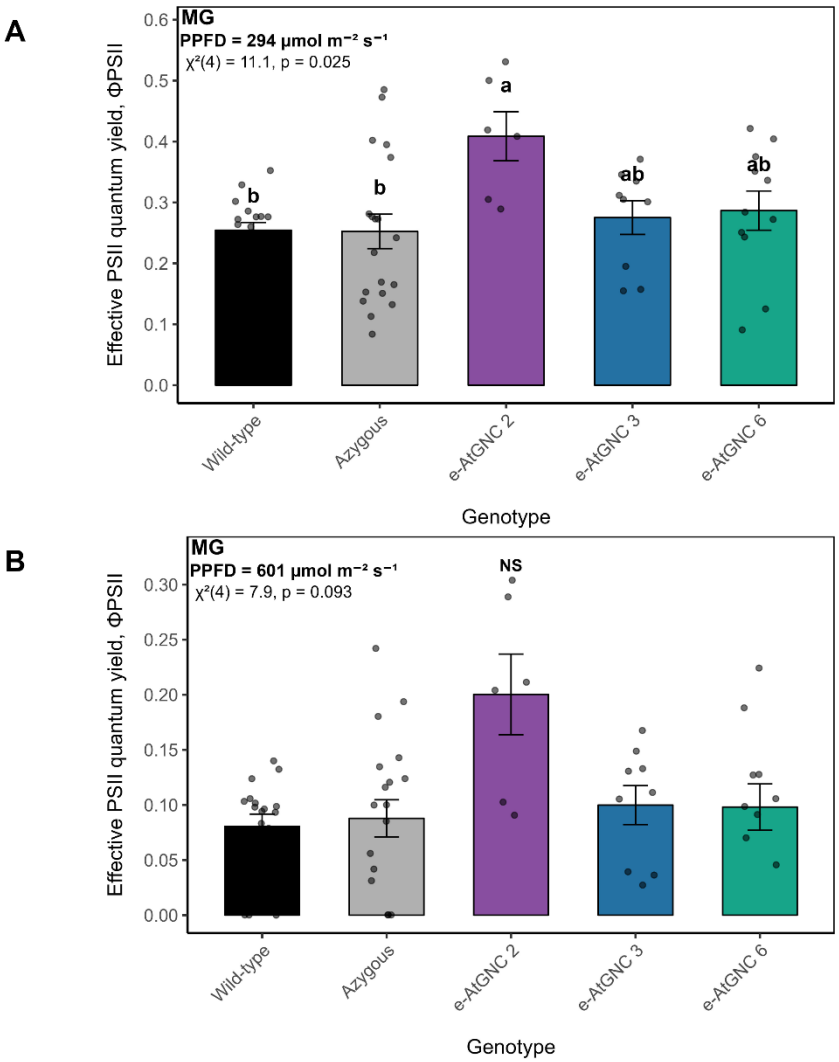

Figure 5.29. Effective PSII quantum yield (ΦPSII) in early-specific *AtGNC* tomato lines. Bar charts display ΦPSII in mature green (MG) fruits from independent lines of *AtGNC* driven by the *SlAFF* early fruit-specific promoter (e-*AtGNC*), compared with azygous and wild-type controls. (A) ΦPSII at 294 µmol m^{-2} s^{-1}. (B) ΦPSII at 601 µmol m^{-2} s^{-1}. MG = 20–23 days post-anthesis. All values represent means ± SE from at least three biological replicates per genotype, with two fruits sampled per plant. Statistically significant differences were determined using a Kruskal-Wallis test followed by Dunn's multiple range test. Dots show individual data points. Different letters indicate statistically significant differences ($P < 0.05$).

5.3 Discussion

5.3.1 *AtCGA1* Effect on Chloroplast Compartment

Expanding the chloroplast compartment, either by increasing chloroplast area or coverage, represents an avenue to improve photochemical capacity and fruit quality. The GATA transcription factor *AtCGA1* promotes plastid biogenesis and activates chlorophyll-biosynthetic genes (Chiang et al., 2012; Hudson et al., 2011). Previous research has shown that *cga1 gnc*

double mutants form hypocotyl chloroplasts about 27% smaller than wild type, with little change in chloroplast number (Cackett et al., 2022; Chiang et al., 2012). The results presented here align with this pattern. In the e-*AtCGA1* overexpression lines, chloroplast coverage was higher than in the controls, while chloroplast density was mostly conserved. Interestingly, e-*AtCGA1* 23, which exhibited the lowest relative transcript levels among lines, also exhibited the lowest mean chloroplast size (56.84 ± 8.4 μm^2) among transgenic lines. The larger chloroplast sizes in transgenic lines e-*AtCGA1* 14 (89.09 ± 14.66 μm^2) and 17 (71.82 ± 5.66 μm^2) also correlated with higher relative transcript levels. Taken together, these data suggest that e-*AtCGA1* overexpression primarily modulates chloroplast size, rather than increasing the number of chloroplasts per area, providing a practical route to expand the chloroplast compartment and pigment accumulation.

5.3.2 *AtCGA1* and *AtGNC* Exhibit Distinct Effects on Pigment Biosynthesis in Tomato Fruit

At the core of chlorophyll biosynthesis lie the well-characterised GATA transcription factors *CGA1* and *GNC* (Hudson et al., 2011). To date, there have been no reports on the overexpression of *CGA1* and *GNC* in tomato fruit. Previous research has shown that the overexpression of both *GLK1* and *GLK2* using the 35S promoter led to transgenic tomato fruit with an increased chlorophyll content (Nguyen et al., 2014; Powell et al., 2012).

Overall results indicate that the chlorophyll and carotenoid content of green tomato fruit can be increased by overexpressing *AtCGA1* and *AtGNC*. It is essential to note that the changes were not consistent between the two constructs, with all e-*AtCGA1* lines, driven by the *SlTFM7* promoter, exhibiting increases in chlorophyll at the mature green stage, whereas only one e-*AtGNC*, under the control of *SlAFF*, showed a similar increase. While both *AtCGA1* and *AtGNC* are closely related GATA transcription factors with partially redundant roles, they may still differ in their regulatory roles or expression patterns. For instance, it has been reported that *SlGKL2* is expressed differently in different parts of the fruit. Also, independent overexpression of both *SlGLK* genes in tomato fruit, *GLK1* and *GLK2*, resulted in increased chlorophyll accumulation and expression of target genes, with results being higher in *SlGLK2* overexpressing plants (Nguyen et al., 2014). A similar mechanism could be present in the fruit-specific expression of the Arabidopsis GATA factors in this study. In addition, it is possible that the results in this study could be related to a promoter-dependent expression strength. Therefore, *AtCGA1* and *AtGNC*

may affect downstream pathways differently, which could be further accentuated by the use of different promoters. Further research is needed to confirm these hypotheses.

Neither lycopene nor β-carotene differed significantly among e-*AtCGA1* lines. However, a trend of increase was observed in two lines. These increases were in the order of 10-30%, which could suggest that more biological replicates may be needed to increase the statistical power of the analysis. Moreover, the decrease in lycopene in some e-*AtGNC* lines aligns with previous studies in which tomatoes engineered to have a higher chlorophyll content at the green stage displayed lower lycopene content at the ripe stage (Shi et al., 2021; Wu et al., 2020). Furthermore, Nguyen et al. (2014) highlighted that changes in β-carotene can be more challenging to interpret as they reflect a much smaller proportion of the total carotenoid pool. The same authors reported that in *u/u uniform* mutants overexpressing *GLK2*, the increase in β-carotene was much more pronounced than that of lycopene, with β-carotene levels increasing by approximately 160%, whereas lycopene increased by only about 20% relative to *u/u* controls (Nguyen et al., 2014).

5.3.3 Improved Photosynthetic Performance and Energy Distribution in *AtCGA1* Transgenic Tomato Fruit

Overall, the evidence supports the hypothesis that early *AtCGA1* overexpression has the potential to enhance the photochemical capacity of tomato fruits by increasing total plastid coverage and pigment content, allowing more light to be absorbed and efficiently used. Our results showed that e-*AtCGA1* lines exhibited higher ΦPSII, ETR, and qL observed across multiple transgenic lines. Notably, e-*AtCGA1* 17 and e-*AtCGA1* 23 outperformed wild-type across all light intensities.

One possible explanation is the role played by *AtCGA1* in modulating the expression of key genes involved in nitrogen assimilation and chlorophyll biosynthesis, such as *GLU1*, *GUN4* and *HEMA1* (Hudson et al., 2011). Although the expression of target genes was not quantified in this study, they are known to be co-expressed with *CGA1* (Chiang et al., 2012; Hudson et al., 2011). Therefore, an enhanced nitrogen pool and chlorophyll biosynthesis could lead to increased chlorophyll levels, and consequently, an enhanced light-harvesting capacity. Another possible explanation is the greater allocation of cellular space to chloroplasts, as transgenic lines exhibited higher plastid coverage. A higher chloroplast plan area/coverage likely reflects a higher density of thylakoid membranes and PSII reaction centres, increasing surface area and enabling the additional absorbed light to be processed more efficiently. Previous research by Nguyen et al. (2014) shows that the increase in chlorophyll content observed by the independent

overexpression of both *GLK1* and *GLK2* in transgenic tomato was associated with increased thylakoid grana stacks in green fruit. The authors highlight the links between grana stacks and chlorophyll levels, in which chlorophyll increases scaled proportionally with thylakoid density (Nguyen et al., 2014).

Among the genotypes studied, e-*AtCGA1* 14, which exhibited the largest increase in chloroplast size, followed by a reduction in number, consistently underperformed. Early studies with chloroplast division mutants in Arabidopsis revealed that plants maintain a fine-tuned balance between chloroplast number and size, and that further increases in chloroplast size can lead to impaired chloroplast division, photosynthetic performance and increased photodamage (Austin II and Webber, 2005; Dutta et al., 2017). Therefore, the increase in chloroplast size in e-*AtCGA1* 14 may have affected the chloroplast surface-to-volume ratio, potentially restricting the rates of intracellular metabolite exchange and leading to metabolic imbalances (Dutta et al., 2017). These findings suggest that a balance between chloroplast size, number, and overall coverage is critical for enhancing fruit photosynthetic potential. Finally, e-*AtGNC*, driven by the *SlAFF* promoter, also exhibited an increase in chlorophyll content and improved photosynthetic parameters; however, this effect was observed only in one line. Notably, e-*AtGNC* 2, despite having the lowest transcript abundance, exhibited the highest pigment content and PSII performance, reinforcing the hypothesis that high transgene expression levels do not necessarily correlate with functional improvements (Rajeevkumar et al., 2015).

The analysis of gas exchange revealed that e-*AtCGA1* 23 showed a reduced carbon efflux in the light and CO_2 gas exchange response, interpreted here as a proxy for carbon assimilation. Although the results were not significant, they highlight the potential of *AtCGA1* in enhancing carbon assimilation and provide a basis for future research. Taken together, our data are consistent with a model in which enhanced chlorophyll biosynthesis provides signals that promote chloroplast development and, ultimately, enhance pigment storage capacity.

5.3.4 Summary

The results presented in this chapter provide an extensive characterisation of *AtCGA1* and *AtGNC* overexpression in tomato. These transcription factors have been extensively studied in different plant species (An et al., 2020; Chiang et al., 2012; Hudson, 2010; Hudson et al., 2011). However, their function in tomato, and particularly in fruit tissues, remains to be fully elucidated. Fruit genetic engineering research has traditionally focused more on the *GOLDEN2-LIKE* (*GLK*) family

of transcription factors, which also regulate aspects of chloroplast development (Chiang et al., 2012). These factors, which play partially overlapping roles with *CGA1* and *GNC* in leaf tissue, have been implicated as key regulators of plastid biogenesis and chlorophyll accumulation in tomato, with *GLK2* being expressed at high levels in fruit tissue (Chiang et al., 2012; Lupi et al., 2019; Nguyen et al., 2014; Powell et al., 2012). Moreover, light and cytokinin have been shown to regulate *GLK1* and *GLK2* expression (Lupi et al., 2019). Therefore, since in leaf tissue, *CGA1* and *GNC* act in concert with *GLK1* and *GLK2*, it is not unreasonable to think that these GATA factors would have a similar mechanism of action in fruits (Chiang et al., 2012).

Here, the use of Arabidopsis *CGA1* and *GNC* driven by fruit-specific promoters represents the first attempt, to our knowledge, to investigate the effect of overexpression of these transcription factors on tomato fruit photochemical capacity, nutritional content, and gas exchange. Overall, this chapter demonstrates that targeting well-characterised regulators of chloroplast biogenesis in Arabidopsis, such as *AtCGA1* and *AtGNC,* can be an effective strategy for enhancing photosynthesis in fruit tissues. The results also reaffirm that the choice of promoter, the expression level of the transgene, and the developmental stage of analysis are key variables that determine the strength and specificity of observed phenotypes. These results could have a direct impact on plant productivity, given the role of these transcription factors in enhancing nitrogen assimilation. Although fruits are strong sink organs and rely on imported nitrogen from leaves, they are capable of reassimilating ammonium internally (Scarpeci et al., 2007). Therefore, improving photosynthetic nitrogen use efficiency (PNUE) could help optimise local nitrogen use and recycling within the fruit, contributing to a better balance of source–sink relations and resource allocation. Moving forward, the investigation of these effects under agronomically relevant field conditions could help translate these tools into real-world applications.

Chapter 6 Simultaneous Overexpression of *AtPDV1* and *AtPDV2* Has Limited Effect on Photochemical Efficiency in Tomato Fruit

6.1 Introduction

The plastid division PDV1/PDV2 proteins form part of the cytosolic compartment involved in plastid division, situated on the outer envelope membrane. They function by interacting with ARC5 to create ring-like structures on the outer membrane, which ultimately causes chloroplast fission (Miyagishima et al., 2006). Interest in these genes has emerged as they have been proposed to be the rate-limiting step of plastid division. While the levels of the other components of plastid division remain constant or increase with cellular maturation, the levels of *PDV1/PDV2* decrease over time (Okazaki et al., 2009). Research with *A. thaliana* chloroplast division mutants has revealed that alterations in chloroplast division can affect both the number and size of chloroplasts (Pyke et al., 1994; Pyke & Leech, 1992). Mutations in several genes involved in chloroplast division lead to abnormally large chloroplasts and have been shown to impair their photosynthetic capacity. This is caused by a reduced ability to adjust to changing light intensities and to export or import metabolites across the membrane, which can affect photoprotection and lead to metabolic imbalances (Austin II and Webber, 2005; Dutta et al., 2017). Overexpression of *PDV1* and *PDV2* in Arabidopsis plants results in smaller and more numerous chloroplasts. Furthermore, simultaneous overexpression of both genes causes a further increase in plastid number and a decrease in size compared to plants with single gene overexpression (Okazaki et al., 2009). A larger population of smaller chloroplasts has been previously suggested to improve CO_2 diffusion, photoprotection and photosynthetic nitrogen use efficiency (PNUE) in Arabidopsis leaf tissues (Xiong et al., 2017). Nevertheless, a recent study with transgenic tobacco overexpressing *PDV1*/*PDV2* showed no benefits in photoprotection or carbon assimilation (Głowacka et al., 2023). The authors suggested that there is a limit for chloroplast size, below which plants grow less efficiently (Głowacka et al., 2023). Here, we aimed to investigate whether the simultaneous overexpression of *PDV1*/*PDV2* in tomato fruits can be used as an alternative to improve pigment content and photochemical performance. The Golden Gate overexpression constructs were assembled using the full-length coding sequence of *AtPDV1* under the control of *SlTFM7* Early Fruit Specific Promoter and *AtPDV2* driven by *SlAFF* Early Fruit Specific Promoter (e-

AtPDV1/PDV2. The use of different promoters allows both genes to be transcribed independently, accounting for variations in promoter strength and ensuring balanced expression of both genes.

6.2 Results

6.2.1 Chloroplast Morphology in Early-Specific *AtPDV1/PDV2* Tomato Lines

To test whether chloroplast development was affected in the double *PDV1/PDV2* lines, we imaged glutaraldehyde-fixed fruit pericarp cells from e-*AtPDV1/PDV2* lines, azygous and wild-type controls using both confocal laser scanning microscopy (CLSM) and transmitted light microscopy (Figures 6.1 and 6.2).

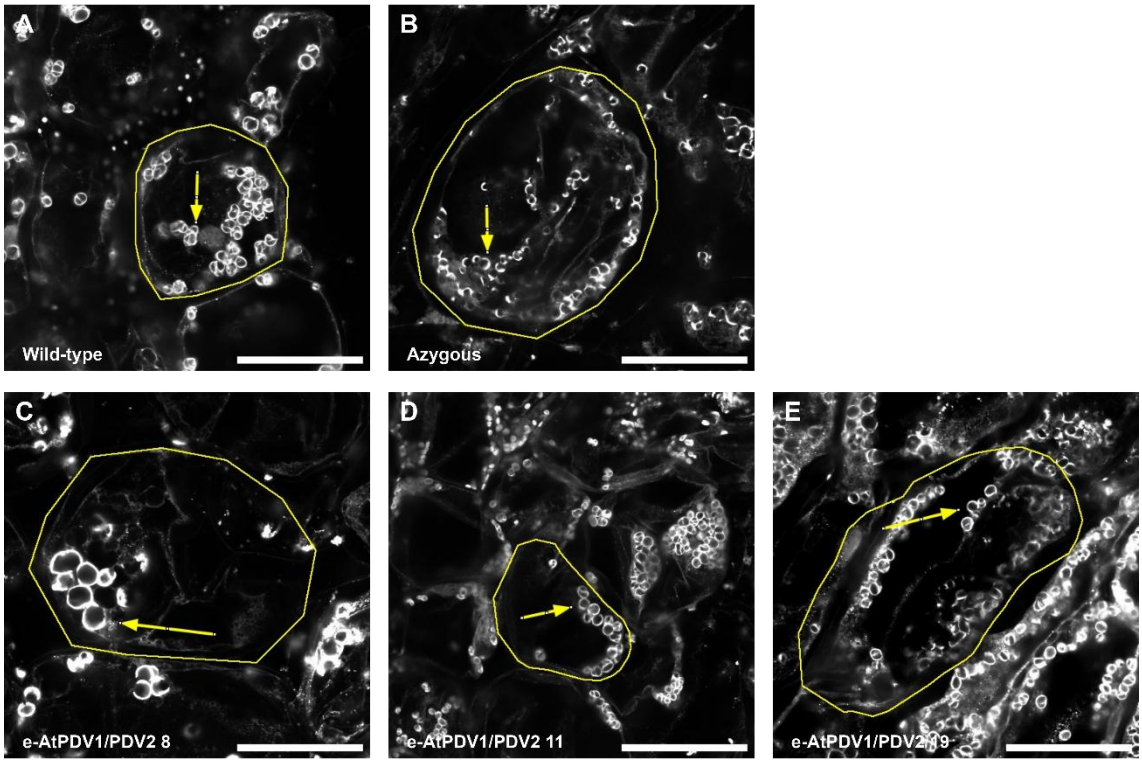

Figure 6.1. Confocal laser scanning microscopy of mature green fruit from early-specific *AtPDV1/PDV2* tomato lines. Representative micrographs of pericarp cells from fruits expressing the double construct *AtPDV1/PDV2*, azygous and wild type controls. *AtPDV1* driven by the *SlTFM7* early-specific promoter and *AtPDV2* driven by the *SlAFF* early-specific promoter. Individual cells are outlined in yellow, and representative chloroplasts are indicated by arrows. (A) Wild-type. (B) Azygous. (C) e-*AtPDV1/PDV2* 8. (D) e-*AtPDV1/PDV2* 11. (E) e-*AtPDV1/PDV2* 19. MG = 20–23 days post-anthesis. Scale bars = 100 µm.

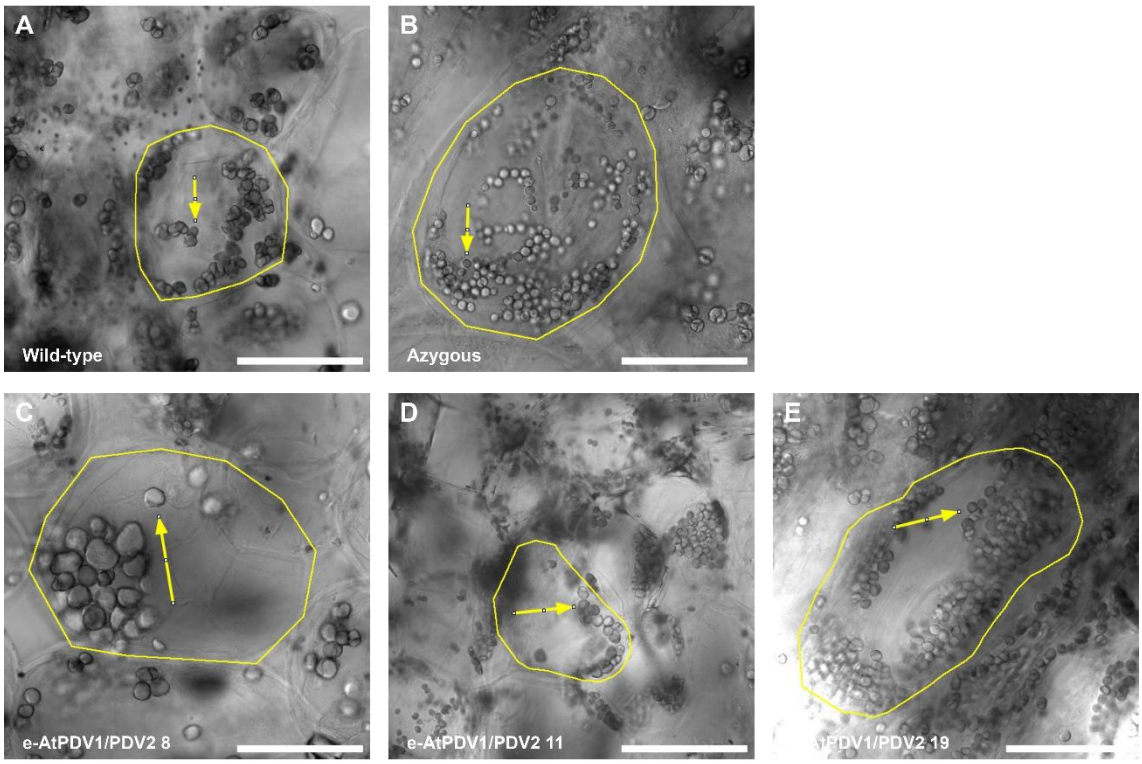

Figure 6.2. Transmitted light microscopy of mature green fruit from early-specific *AtPDV1/PDV2* tomato lines. Representative micrographs of pericarp cells from fruits expressing the double construct *AtPDV1/PDV2*, azygous and wild type controls. *AtPDV1* driven by the *SlTFM7* early fruit-specific promoter and *AtPDV2* driven by the *SlAFF* early fruit-specific promoter. Individual cells are outlined in yellow, and representative chloroplasts are indicated by arrows. (A) Wild-type. (B) Azygous. (C) e-*AtPDV1/PDV2* 8. (D) e-*AtPDV1/PDV2* 11. (E) e-*AtPDV1/PDV2* 19. MG = 20–23 days post-anthesis. Scale bars = 100 µm.

No significant differences were detected in chloroplast plan area between e-*AtPDV1/PDV2* 11 (42.14 ± 3.91 µm^2) and e-*AtPDV1/PDV2* 19 (50.09 ± 5.02 µm^2) compared to wild-type (38.05 ± 2.81 µm^2) and azygous (43.31 ± 4.5 µm^2) (Figure 6.3A). Nevertheless, e-*AtPDV1/PDV2* 8 exhibited significantly larger chloroplasts (91.27 ± 10.02 µm^2).

Similarly, e-*AtPDV1/PDV2* 11 and 19 did not show significant differences in chloroplast number relative to the wild type. Line 11 exhibited 80.81 ± 5.72 chloroplasts per cell, while 19 exhibited 87 ± 4.96, compared to 88.06 ± 5.25 in the wild-type and 126.1 ± 11.19 in the azygous (Figure 6.3B). In addition, chloroplast numbers were significantly reduced in e-*AtPDV1/PDV2* 8 (55.65 ± 4.91).

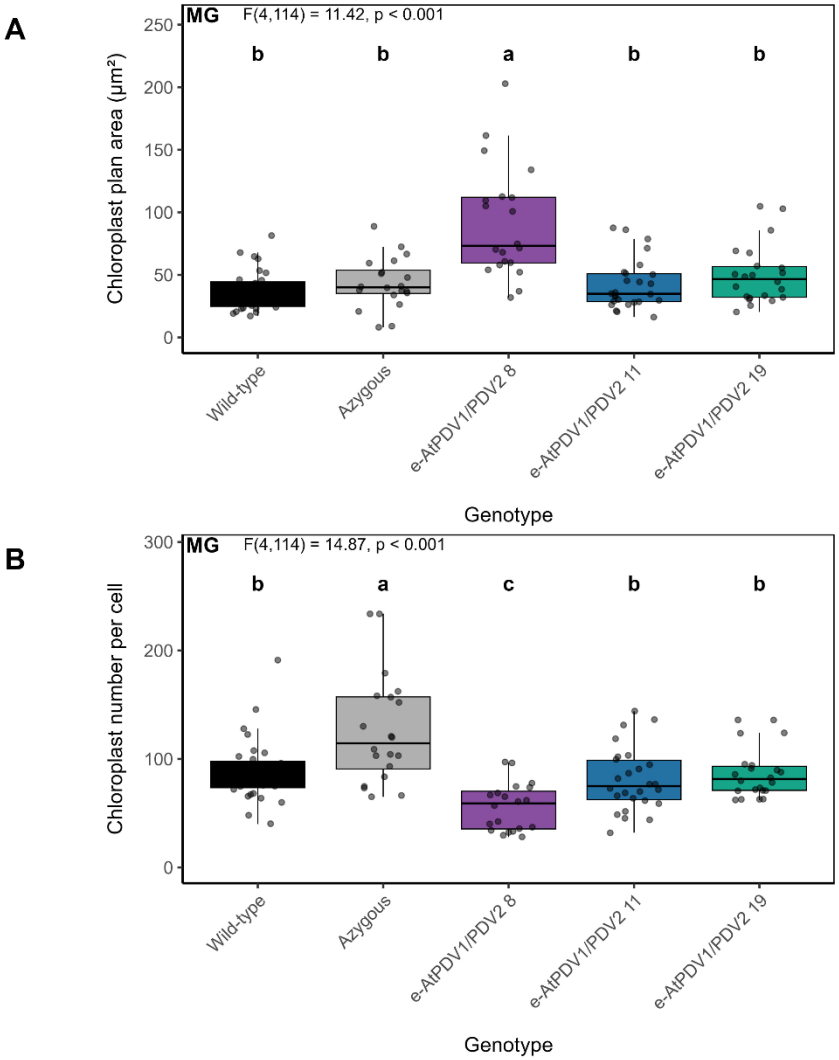

Figure 6.3. Chloroplast morphology in mature green (MG) fruits of early-specific *AtPDV1/PDV2* tomato lines. Boxplots show changes in chloroplast morphology in fruits from lines expressing the *AtPDV1* under the control of *SlTFM7* early fruit-specific promoter and *AtPDV2* under the control of *SlAFF* early fruit-specific Promoter (e-*AtPDV1/PDV2*), azygous and wild-type controls. Both genes were co-expressed as part of the double overexpression construct e-*AtPDV1/PDV2*. (A) Chloroplast plan area. (B) Chloroplast number per cell. MG = 20–23 days post-anthesis. The boxes represent the interquartile range (25th to 75th percentile), the horizontal line shows the median, and the whiskers extend to 1.5 times the interquartile range. At least six individual cells of at least three biological replicates were analysed for each genotype. Statistically significant differences were determined using a 1-way ANOVA followed by Duncan's multiple range test. Dots show individual data points. Different letters indicate statistically significant differences (P<0.05).

No significant differences in chloroplast coverage were detected in the transgenic lines. Mean coverage ranged from 16.35 ± 1.52% in wild type and 16.75 ± 1.69% in azygous to 20.16 ± 1.83% in e-*AtPDV1/PDV2* 8, 16.99 ± 1.67% in e-*AtPDV1/PDV2* 11 and 18.57 ± 1.49% in e-*AtPDV1/PDV2* 19, respectively (Figure 6.4A). Moreover, while e-*AtPDV1/PDV2* 8 showed a reduction in density

(35% relative to wild-type and 32% to azygous), the other genotypes exhibited virtually the same values (Figure 6.4B). These results indicate that density was largely conserved across genotypes.

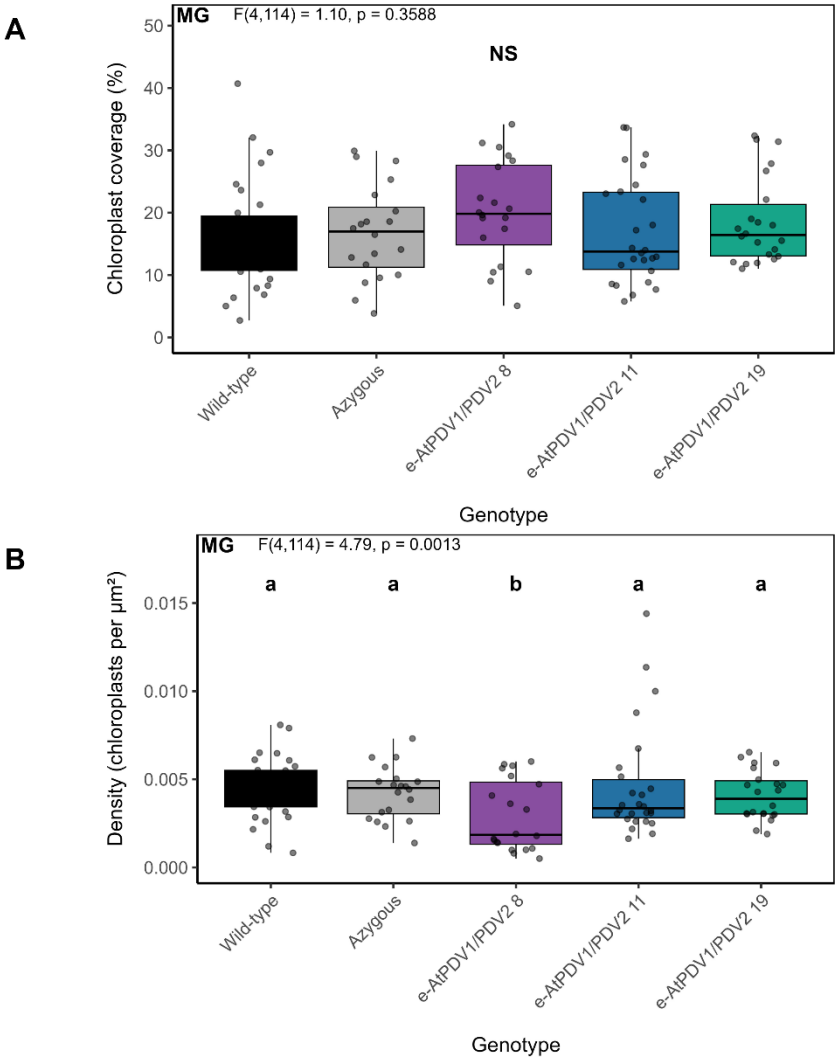

Figure 6.4. Chloroplast morphology in mature green (MG) fruits of early-specific *AtPDV1/PDV2* tomato lines. Boxplots show changes in chloroplast morphology in fruits from lines expressing the *AtPDV1* under the control of *SlTFM7* early fruit-specific promoter and *AtPDV2* under the control of *SlAFF* early fruit-specific promoter (e-*AtPDV1/PDV2*), azygous and wild-type controls. Both genes were co-expressed as part of the double overexpression construct e-*AtPDV1/PDV2*. (A) Chloroplast coverage. (B) Chloroplast density. MG = 20–23 days post-anthesis. The boxes represent the interquartile range (25th to 75th percentile), the horizontal line shows the median, and the whiskers extend to 1.5 times the interquartile range. At least six individual cells of at least three biological replicates were analysed for each genotype. Statistically significant differences were determined using a 1-way ANOVA followed by Duncan's multiple range test. Dots show individual data points. Different letters indicate statistically significant differences ($P<0.05$).

A nested one-way ANOVA was used to evaluate transgene-type effects (wild-type/azygous vs e-*AtPDV1/PDV2*), while considering line-specific variation. This analysis revealed no significant effect of type on chloroplast number ($p = 0.247$), chloroplast density ($p = 0.453$), cell plan area ($p = 0.470$), or chloroplast coverage ($p = 0.159$). Taken together, these results indicate that the overall effect of e-*AtPDV1/PDV2* overexpression on chloroplast morphology traits was limited.

6.2.2 Characterisation of Chlorophyll and Carotenoid Content in *AtPDV1/PDV2* Tomato Lines

The impact of *AtPDV1/PDV2* overexpression on fruit development was investigated at the biochemical level and physiological levels. Representative fruits of mature green (MG) e-*AtPDV1/PDV2* lines are shown in Figure 6.5.

Figure 6.5. **Phenotypes of mature green (MG) fruits of early-specific *AtPDV1/PDV2* tomato lines**. Images display representative MG fruits from transgenic lines expressing the *AtPDV1* under the control of *SlTFM7* early fruit-specific promoter and *AtPDV2* under the control of *SlAFF* early fruit-specific promoter (e-*AtPDV1/PDV2*), as well as azygous and wild-type controls. (A) Wild-type. (B) Azygous. (C) e-*AtPDV1/PDV2* 8. (D) e-*AtPDV1/PDV2* 11. (E) e-*AtPDV1/PDV2* 19. MG = 20–23 days post-anthesis. Scale bars = 1 cm.

At the immature green stage, the chlorophyll content analysis revealed no significant differences among the independent genotypes. (Figure 6.6A). At the mature green stage, transgenic lines 11 (49.7 ± 3.29 µg/g) and 19 (49.0 ± 2.32 µg/g) showed small increases of approximately 27-29% relative to the wild-type (38.4 ± 2.92 µg/g) and 21-23% compared to the azygous control (40.2 ± 6.05µg/g). The transgenic line e-*AtPDV1*/*PDV2* 8 (36.3 ± 5.31 µg/g) exhibited comparable results to both the wild-type and azygous lines (Figure 6.6B). However, these differences were not statistically significant. The chlorophyll *a*/*b* ratio (Figure 6.6C) reflects the balance of pigments between reaction centres and light-harvesting antenna complexes, where a higher ratio indicates proportionally smaller antenna per reaction centre (Jin et al., 2016; Simkin et al., 2022). Here, chlorophyll *a*/*b* ratios did not vary across genotypes.

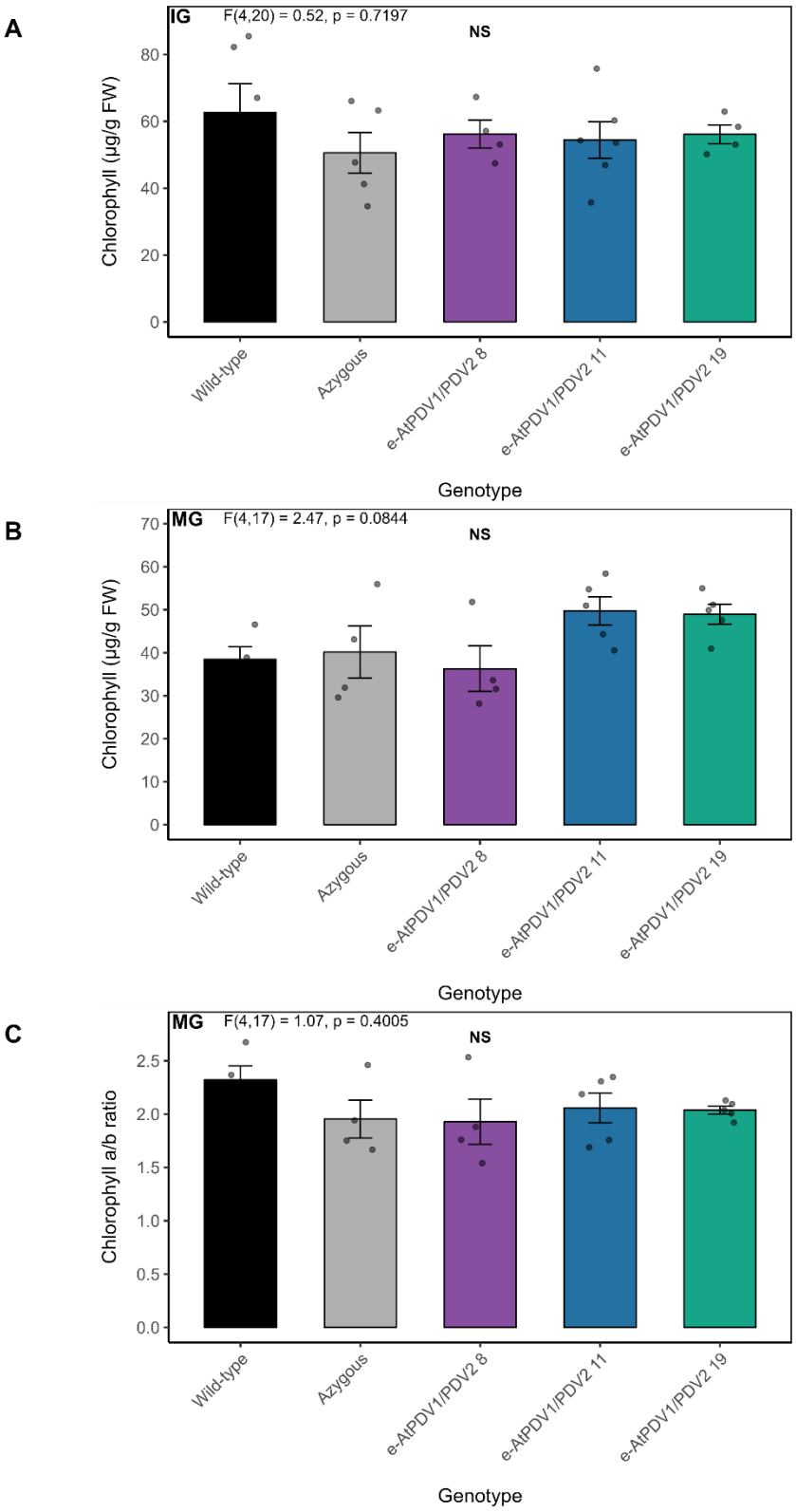

Figure 6.6. Chlorophyll levels in early-specific *AtPDV1/PDV2* tomato lines. Bar charts display the chlorophyll content of independent lines expressing the *AtPDV1* under the control of *SlTFM7* early fruit-specific promoter and *AtPDV2* under the control of *SlAFF* early fruit-specific promoter (e-*AtPDV1/PDV2*), as well as azygous and wild-type controls. (A) Immature green (IG). (B) Mature green (MG). (C) Chlorophyll

a/*b* ratio. IG = 7–10 days post-anthesis. MG = 20–23 days post-anthesis. All values represent means ± SE from at least four biological replicates per genotype, each analysed in three technical replicates. Statistically significant differences were determined using a 1-way ANOVA followed by Duncan's multiple range test. Dots show individual data points. Different letters indicate statistically significant differences (P<0.05).

The carotenoid analysis showed a similar trend to the chlorophyll content, where carotenoid levels did not differ significantly among genotypes at the immature stage (Figure 6.7). At the mature green stage, lines 11 and 19 showed a trend of carotenoid accumulation. However, despite the trend, these results were not significant.

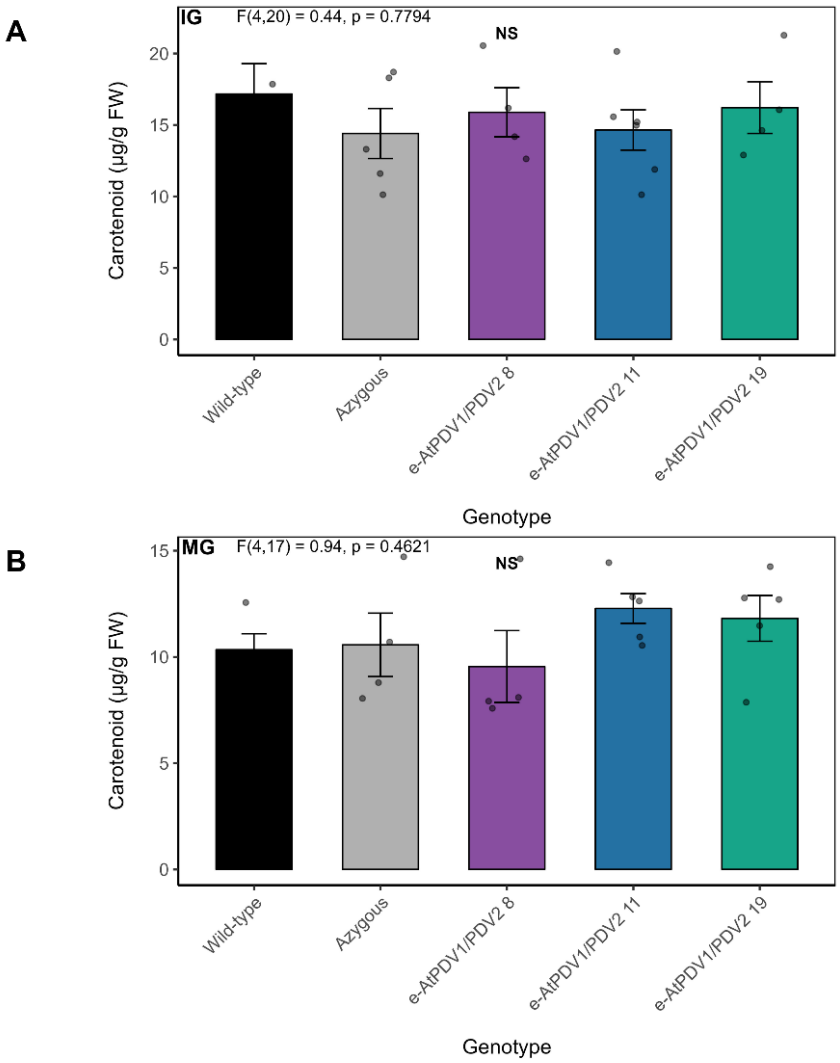

Figure 6.7. Carotenoid levels in early-specific *AtPDV1/PDV2* tomato lines. Bar charts display the chlorophyll content of independent lines expressing the *AtPDV1* under the control of *SlTFM7* early fruit-specific promoter and *AtPDV2* under the control of *SlAFF* early fruit-specific promoter (e-*AtPDV1/PDV2*), as well as azygous and wild-type controls. (A) Immature green (IG). (B) Mature green (MG). IG = 7–10 days

post-anthesis. MG = 20–23 days post-anthesis. All values represent means ± SE from at least four biological replicates per genotype, each analysed in three technical replicates. Statistically significant differences were determined using a 1-way ANOVA followed by Duncan's multiple range test. Dots show individual data points. Different letters indicate statistically significant differences (P<0.05).

Chlorophyll and carotenoid levels were assessed in e-*AtPDV1/PDV2* transgenic lines across developmental stages (Figure 6.8). A two-way nested ANOVA revealed a significant effect of stage (IG vs MG) but not of type (wild-type/azygous vs e-*AtPDV1/PDV2*). Furthermore, no significant stage and type interaction was detected. Taken together, these results suggest that the overall effect of e-*AtPDV1/PDV2* overexpression on green fruit pigment accumulation was limited, despite variation among individual genotypes.

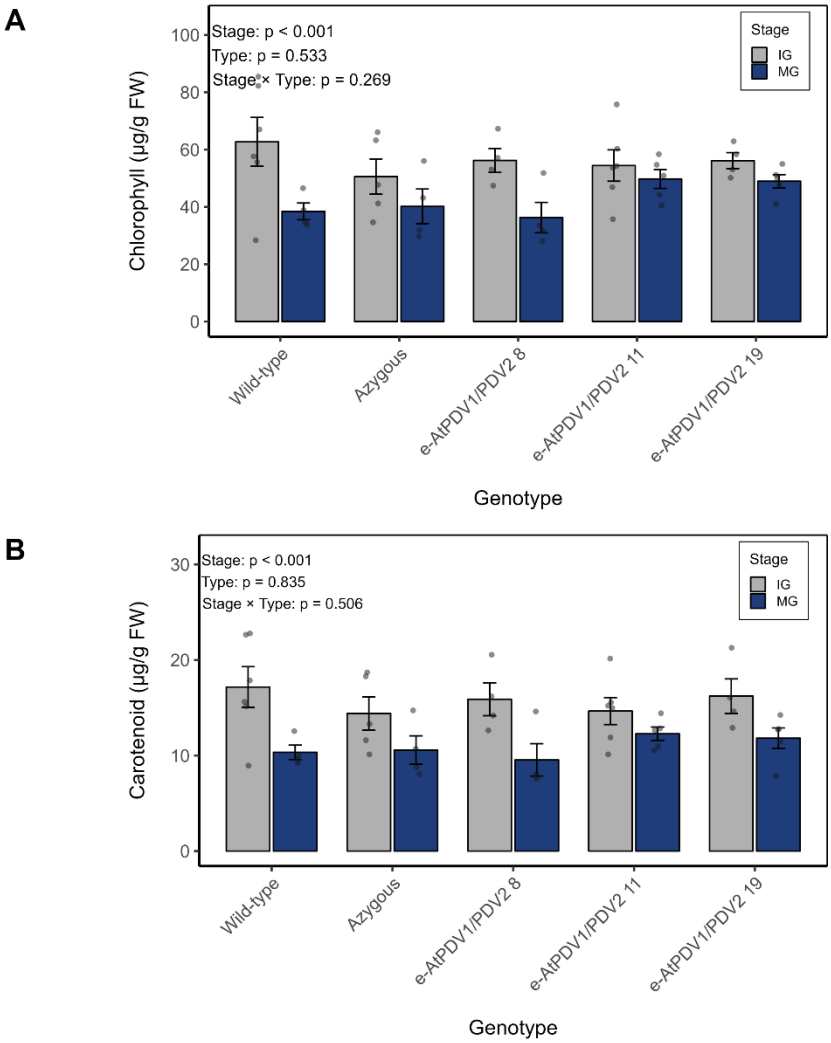

Figure 6.8. Changes in chlorophyll and carotenoid content during fruit development in early-specific *AtPDV1/PDV2* tomato lines. Bar charts show pigment levels in immature green (IG) and mature green (MG) fruits of the *AtPDV1* under the control of *SlTFM7* early fruit- specific promoter and *AtPDV2* under the control of *SlAFF* early fruit-specific promoter (e-*AtPDV1/PDV2*), as well as azygous and wild-type controls.

(A) Chlorophyll levels. (B) Carotenoid levels. IG = 7–10 days post-anthesis. MG = 20–23 days post-anthesis. All values represent means ± SE from at least four biological replicates per genotype, each analysed in three technical replicates. Dots show individual data points. Statistically significant differences were assessed using a two-way nested ANOVA, with developmental stage (IG vs MG) and genotype type (wild-type/azygous vs e-*AtPVD1/PDV2*) included as fixed factors and genotype (line) nested within type. Main effects and the stage × type interaction were tested, with significance accepted at $P < 0.05$.

6.2.3 Characterisation of Lycopene and β-carotene Content in *AtPDV1/PDV2* Tomato Fruit

To explore whether independent transgenic lines differed in carotenoid accumulation, lycopene and β-carotene content were assessed in ripe fruit. Representative ripe fruits (ripe = breaker +7–10 days) from each genotype are shown in Figure 6.9.

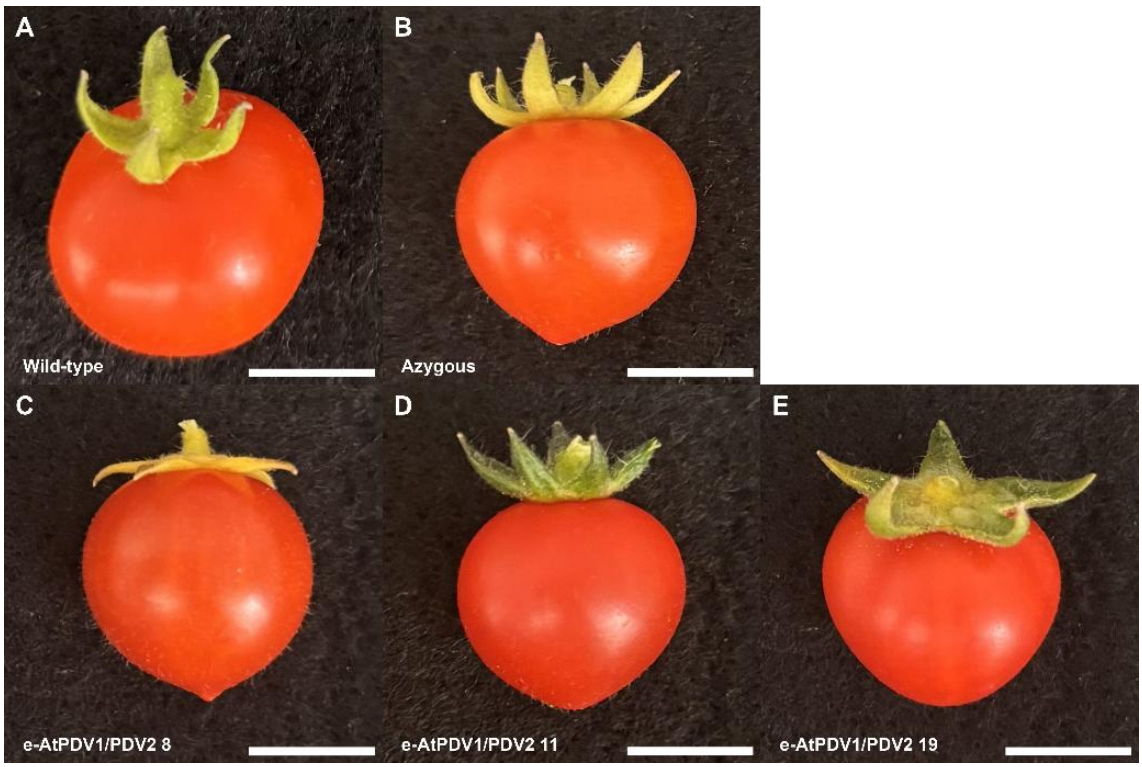

Figure 6.9. Phenotypes of ripe fruits of early-specific *AtPDV1/PDV2* tomato lines. Images display representative ripe fruits from transgenic lines expressing the *AtPDV1* under the control of *SlTFM7* early fruit-specific promoter and *AtPDV2* under the control of *SlAFF* early fruit-specific promoter (e-*AtPDV1/PDV2*), as well as azygous and wild-type controls. (A) Wild-type. (B) Azygous. (C) e-*AtPDV1/PDV2* 8. (D) e-*AtPDV1/PDV2* 11. (E) e-*AtPDV1PDV2* 19. Ripe = breaker +7–10 days. Scale bars = 1 cm.

The carotenoid analysis of independent lines showed that for lycopene content in ripe fruit (Figure 6.10A), e-*AtPDV1/PDV2* 8 (87.6 ± 5.83 µg/g) exhibited comparable results to both wild-type (93.5

± 9.63) and azygous (94.7 ± 14.3 µg/g). In contrast, lines 11 (113 ± 7.39 µg/g) and 19 (125 ± 16.5 µg/g) showed small increases compared to both wild-type and azygous lines. However, despite these differences, the overall variation among genotypes was not statistically significant (ANOVA, p = 0.299).

Transgenic lines e-*AtPDV1/PDV2* 11 (14.3 ± 1.46 µg/g) and 19 (13.5 ± 1.62 µg/g) displayed greater levels of β-carotene compared to 10.0 ± 0.886 µg/g in the wild-type and 12.7 ± 1.37 µg/g in the azygous (Figure 6.10B). Interestingly, while e-*AtPDV1/PDV2* 8 showed a slight, non-significant, reduction in lycopene, it also exhibited greater β-carotene levels (14.6 ± 0.747 µg/g). These results are reported as trends as they are not statistically significant (ANOVA, p = 0.251).

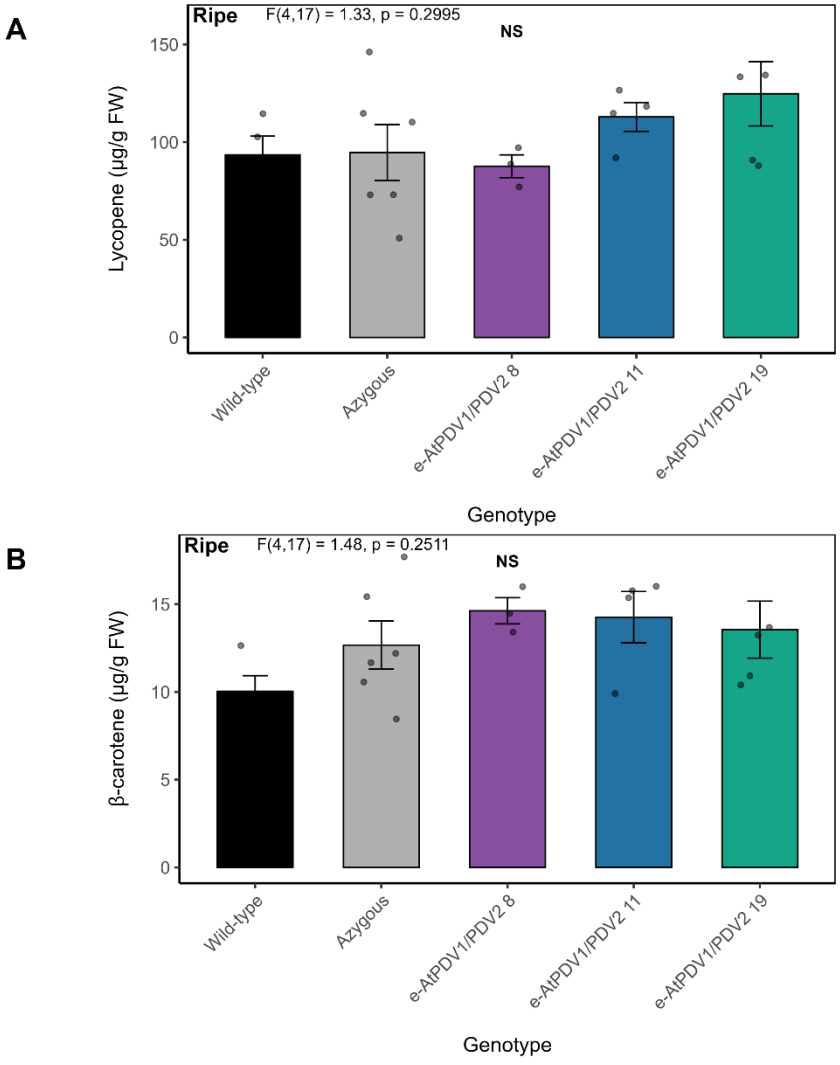

Figure 6.10. Carotenoid levels in early-specific *AtPDV1/PDV2* tomato lines. Bar charts display the carotenoid content of independent lines expressing the *AtPDV1* under the control of *SlTFM7* early fruit-specific promoter and *AtPDV2* under the control of *SlAFF* early fruit-specific promoter (e-*AtPDV1/PDV2*), as well as azygous and wild-type controls. (A) Lycopene. (B) β-carotene. Ripe = breaker +7–10 days. All

values represent means ± SE from at least three biological replicates per genotype, each analysed in two technical replicates. Statistically significant differences were determined using a 1-way ANOVA followed by a Duncan's multiple range test. Dots show individual data points. Different letters indicate statistically significant differences (P<0.05).

6.2.4 Maximum PSII Quantum Yield (F_v/F_m) of *AtPDV1/PDV2* Tomato Lines

Across all genotypes and developmental stages, F_v/F_m values were close to 0.8, indicating an intact and functioning photosynthetic apparatus with little evidence of photoinhibition or stress-induced damage. No statistically significant differences in F_v/F_m were observed between immature green fruits (Figure 6.11A). Similarly, mature green fruits did not show any significant differences in F_v/F_m between the transgenics and wild-type and azygous controls, except for e-*AtPDV1/PDV2* 11, who exhibited a higher F_v/F_m compared to the azygous control (Figure 6.11B).

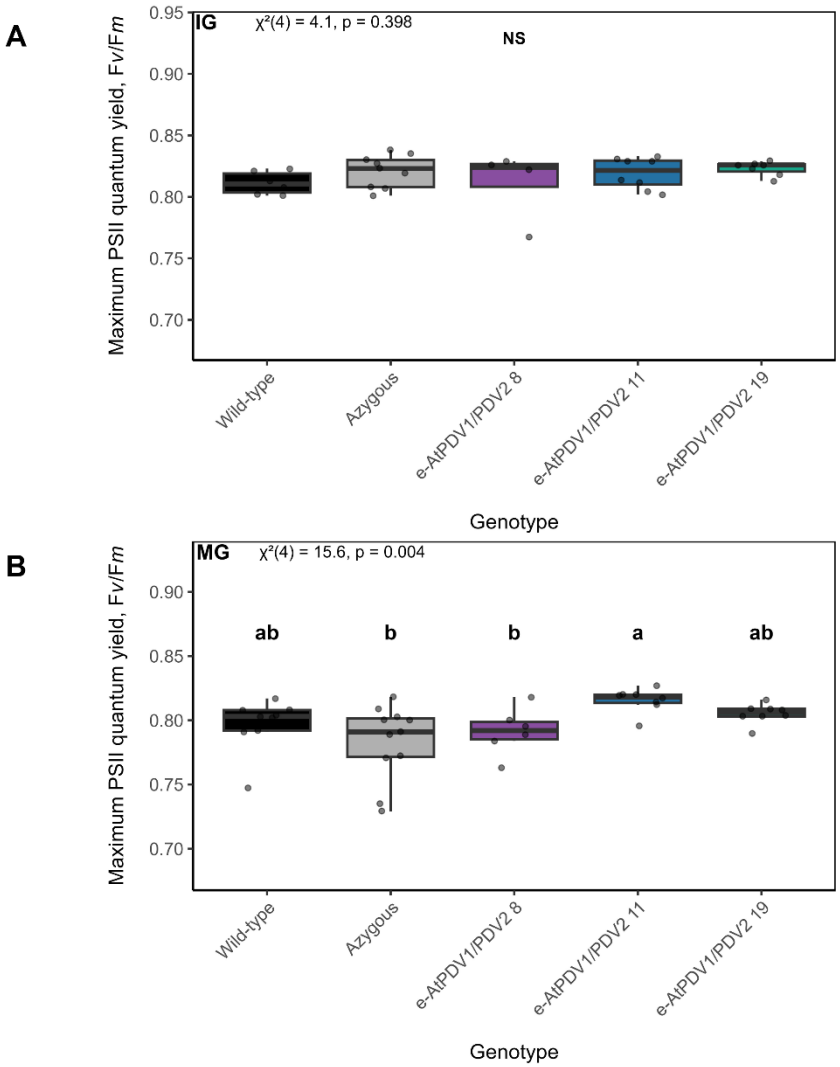

Figure 6.11. Maximum PSII quantum yield (F_v/F_m) in early-specific *AtPDV1/PDV2* tomato lines. Boxplots display F_v/F_m in fruits of independent lines expressing the *AtPDV1* under the control of *SlTFM7* early fruit-specific promoter and *AtPDV2* under the control of *SlAFF* early fruit-specific promoter (e-*AtPDV1/PDV2*), as well as azygous and wild-type controls. (A) Immature green (IG). (B) Mature green (MG). IG = 7–10 days post-anthesis. MG = 20–23 days post-anthesis. The boxes represent the interquartile range (25th to 75th percentile), the horizontal line shows the median, and the whiskers extend to 1.5 times the interquartile range. Statistically significant differences were determined using a Kruskal-Wallis test followed by Dunn's multiple range test. Dots show individual data points. Different letters indicate statistically significant differences ($P < 0.05$).

6.2.5 Effective PSII Quantum Yield (ΦPSII) *AtPDV1/PDV2* Tomato Fruits

The light response curve of immature green fruits showed variable results (Figure 6.12A). First, the azygous and wild-type exhibited different responses, probably due to the azygous line having multiple genetic backgrounds, which may affect azygous photosynthetic responses. Moreover, *e-AtPDV1/PDV2* 8 consistently underperformed across all light intensities. In contrast, *e-*

AtPDV1/PDV2 11 and 19 outperformed wild-type across all light intensities, although they did not outperform the azygous control. In mature green fruits (Figure 6.12B), e-*AtPDV1/PDV2* 8 again underperformed at all light intensities. On the other hand, *e-AtPDV1/PDV2* 11 outperformed both wild-type and azygous at most light intensities. Interestingly, e-*AtPDV1/PDV2* 19 showed a strong response at low and moderate light intensities but did not outperform controls under high light conditions.

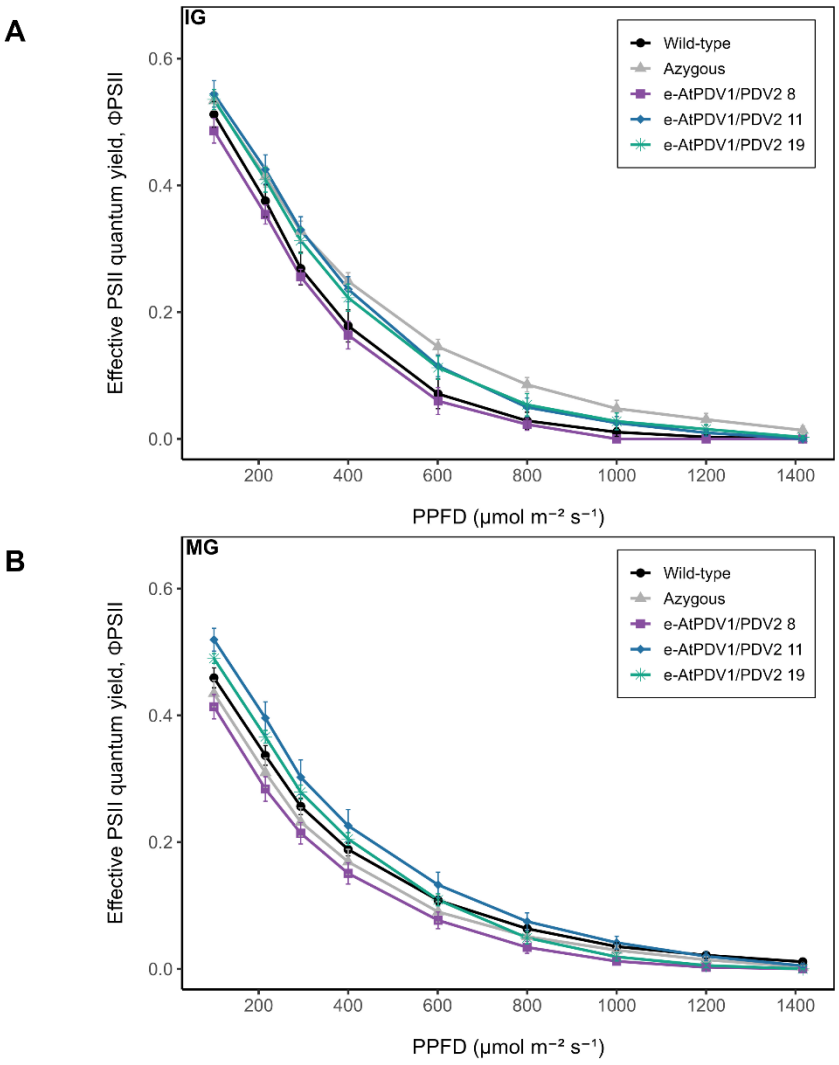

Figure 6.12. Light responses of effective PSII quantum yield (ΦPSII) in early-specific *AtPDV1/PDV2* tomato lines. Light curves display ΦPSII of independent lines expressing the *AtPDV1* under the control of *SlTFM7* early fruit-specific promoter and *AtPDV2* under the control of *SlAFF* early fruit-specific promoter (e-*AtPDV1/PDV2*), as well as azygous and wild-type controls. (A) Immature green (IG). (B) Mature green (MG). IG = 7–10 days post-anthesis. MG = 20–23 days post-anthesis. All values represent means ± SE from at least four biological replicates per genotype, with two fruits sampled per plant.

A deeper analysis of ΦPSII at 294 µmol m^{-2} s^{-1} revealed that, despite the observations from the light curve, no significant differences were observed between the transgenics and controls at both the immature green and mature green stages (Figure 6.13).

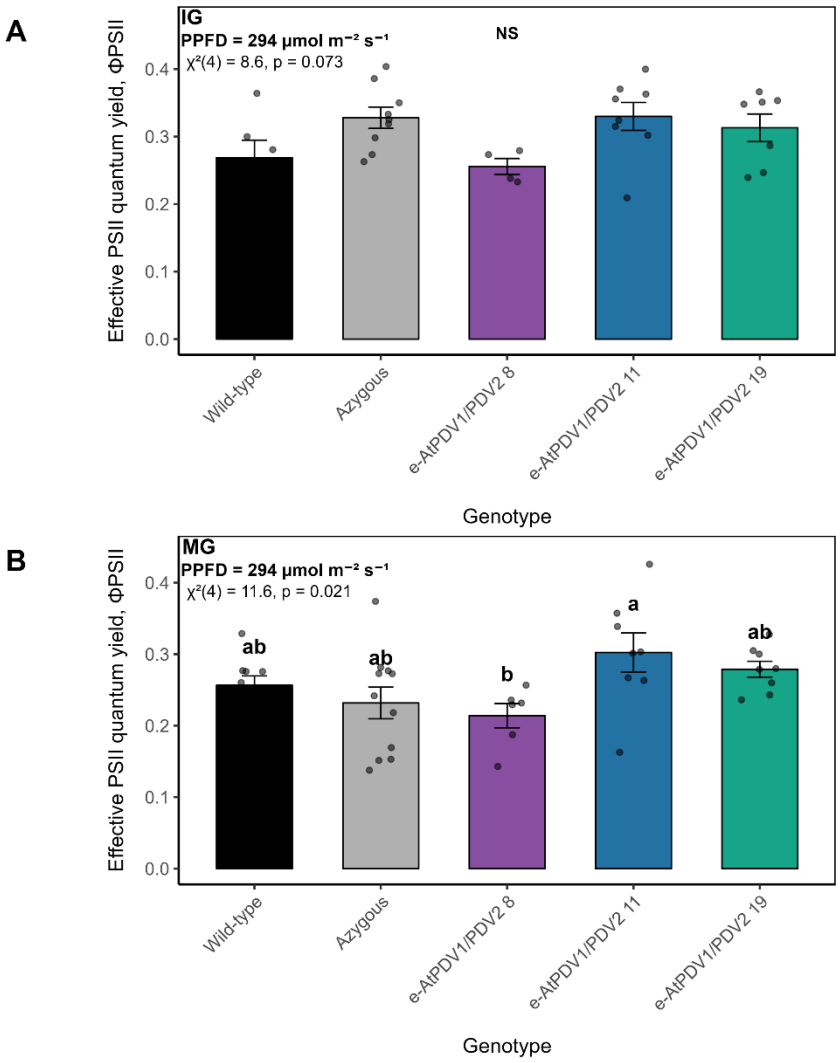

Figure 6.13. Effective PSII quantum yield (ΦPSII) in early-specific *AtPDV1/PDV2* tomato lines. Bar charts display ΦPSII of independent lines expressing the *AtPDV1* under the control of *SlTFM7* early fruit-specific promoter and *AtPDV2* under the control of *SlAFF* early fruit-specific Promoter (e-*AtPDV1/PDV2*), as well as azygous and wild-type controls at 294 µmol m^{-2} s^{-1}. (A) Immature green (IG). (B) Mature green (MG). IG = 7–10 days post-anthesis. MG = 20–23 days post-anthesis. All values represent means ± SE from at least four biological replicates per genotype, with two fruits sampled per plant. Statistically significant differences were determined using a Kruskal-Wallis test followed by Dunn's multiple range test. Dots show individual data points. Different letters indicate statistically significant differences ($P < 0.05$).

At 601 µmol m^{-2} s^{-1}, immature green e-*AtPDV1/PDV2* 11 and 19 showed a slight trend of greater ΦPSII relative to the wild-type but not to the azygous control, whereas e-*AtPDV1/PDV2* 8 was the

lowest-performing line (Figure 6.14). At the mature green stage, line 11 exhibited the highest ΦPSII (0.133 ± 0.020), representing a 23% greater value compared to the wild-type (0.108 ± 0.006) and 47% greater compared to the azygous control (0.090 ± 0.016). In contrast, line 19 performed similarly to the wild-type (0.109 ± 0.009) but showed a 21% increase relative to the azygous. Once again, line 8 underperformed (0.077 ± 0.013), with values approximately 29% lower than the wild-type and 15% lower than those of the azygous control. However, none of these differences were statistically significant.

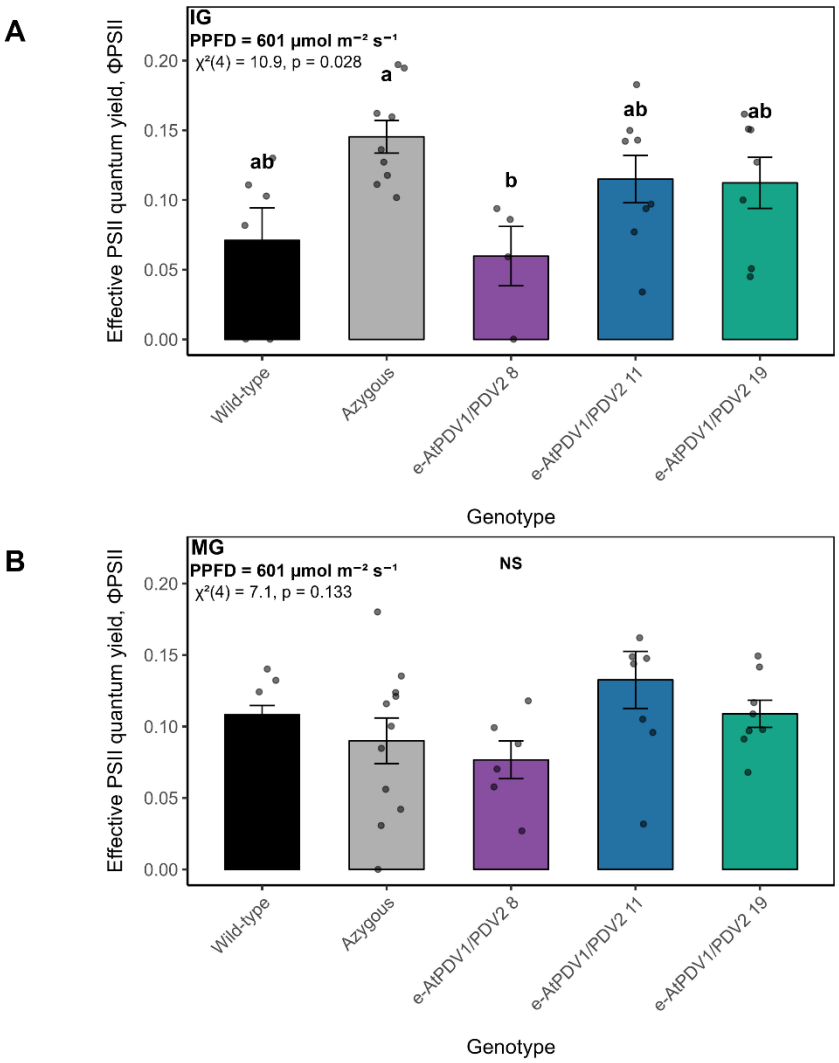

Figure 6.14. Effective PSII quantum yield (ΦPSII) in early-specific *AtPDV1/PDV2* tomato lines. Bar charts display ΦPSII of independent lines expressing the *AtPDV1* under the control of *SlTFM7* early fruit-specific promoter and *AtPDV2* under the control of *SlAFF* early fruit-specific Promoter (e-*AtPDV1/PDV2*), as well as azygous and wild-type controls at 601 µmol m^{-2} s^{-1}. (A) Immature green (IG). (B) Mature green (MG). IG = 7–10 days post-anthesis. MG = 20–23 days post-anthesis. All values represent means ± SE from at least four biological replicates per genotype, with two fruits sampled per plant. Statistically significant

differences were determined using a Kruskal-Wallis test followed by Dunn's multiple range test. Dots show individual data points. Different letters indicate statistically significant differences ($P < 0.05$).

6.2.6 Effective PSII Quantum Yield (ΦPSII) at Different Developmental Stages in Early-Specific *AtPDV1/PDV2* Tomato Lines

Across both 294 and 601 µmol m^{-2} s^{-1}, ΦPSII showed no significant differences of genotype type (wild-type/azygous vs e-*AtPDV1*/*PDV2*). At 294 µmol m^{-2} s^{-1} there is a significant effect of stage but that was not observed at 601 µmol m^{-2} s^{-1}. This is consistent with a decrease in ΦPSII and and light saturation at both stages. Taken together, these results indicate that e-*AtPDV1*/*PDV2* overexpression had little effect on ΦPSII and that differences between IG and MG fruit were reduced under higher light intensity (Figure 6.15).

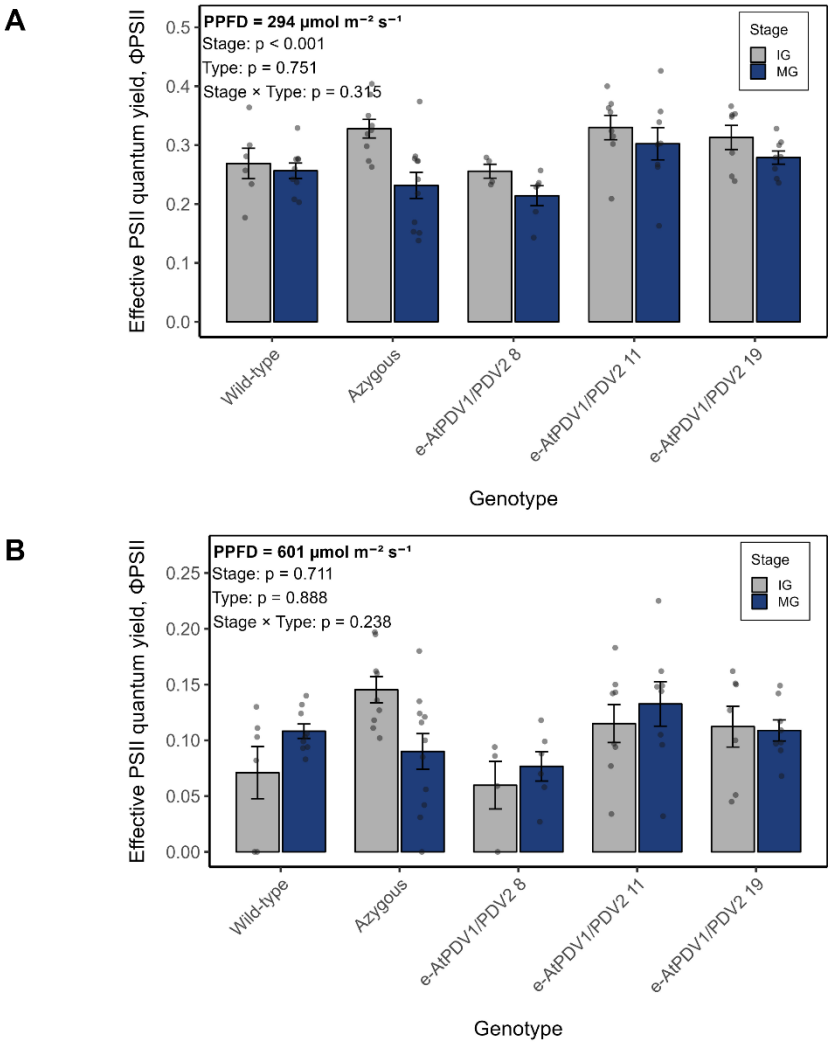

Figure 6.15. Changes in light responses of effective PSII quantum yield (ΦPSII) during fruit development in early-specific *AtPDV1/PDV2* tomato lines. The bar charts display ΦPSII of independent lines expressing the *AtPDV1* under the control of *SlTFM7* early fruit-specific promoter and *AtPDV2* under the control of *SlAFF* early fruit-specific promoter (e-*AtPDV1/PDV2*), as well as azygous and wild-type controls. (A) ΦPSII at 294 µmol m^{-2} s^{-1}. (B) ΦPSII at 601 µmol m^{-2} s^{-1}. IG = 7–10 days post-anthesis. MG = 20–23 days post-anthesis. All values represent means ± SE from at least four biological replicates per genotype, with two fruits sampled per plant. Dots show individual data points. Statistically significant differences were assessed using a 2-way nested ANOVA, with developmental stage (IG vs MG) and genotype type (wild-type/azygous vs e-*AtPDV1/PDV2*) included as fixed factors and genotype (line) nested within type. Main effects and the stage × type interaction were tested, with significance accepted at $P < 0.05$.

6.2.7 Differential Electron Transport Rate (ETR) Patterns in *AtPDV1/PDV2 Lines*

The ETR light response curves of *e-AtPDV1/PDV2* transgenic lines revealed different responses in photosynthetic performance and saturation points compared to the wild-type and azygous controls. First, it showed that ETR rose with increasing light intensity (PPFD) across all genotypes

until it saturated and eventually declined (Figure 6.16A). Moreover, transgenic line *e-AtPDV1/PDV2* 8 consistently underperformed across all light intensities, reaching saturation at approximately 300 µmol m^{-2} s^{-1}, similar to both controls. On the other hand, *e-AtPDV1/PDV2* 11 outperformed wild-type and azygous across all light intensities, with the exception of 1400 µmol m^{-2} s^{-1}, where photodamage possibly limited its performance. It is important to note that all genotypes exhibit extreme signs of photodamage at light intensities exceeding 1000 µmol m^{-2} s^{-1}. Interestingly, e-*AtPDV1/PDV2* 19 displayed enhanced performance at low and moderate light intensities, but underperformed at higher light levels, suggesting a limited capacity to manage excess energy at higher light intensities.

At 294 µmol m^{-2} s^{-1} (Figure 6.16B), line e-*AtPDV1/PDV2* 11 displayed the highest ETR (37.34 ± 3.37 µmol electrons m^{-2} s^{-1}), which represents an increase of approximately 18% relative to wild-type (31.68 ± 1.61 µmol e^- m^{-2} s^{-1}) and about 30% relative to the azygous (28.62 ± 2.73 µmol electrons m^{-2} s^{-1}). Line 19 also outperformed the controls (34.43 ± 1.38 µmol electrons m^{-2} s^{-1}), showing approximately 9% higher ETR than the wild-type and 20% higher than the azygous. In contrast, line 8 underperformed (26.43 ± 2.11 µmol electrons m^{-2} s^{-1}), a decrease of 17% compared to wild-type and 8% to azygous. At 601 µmol m^{-2} s^{-1} (Figure 6.16C), line 11 again was the highest performer, displaying an increase of approximately 23% relative to the wild-type and 47% relative to the azygous. In contrast, Line 19 exhibited values comparable to the wild-type, although approximately 21% higher than those of the azygous. Finally, line 8 remained the lowest performer, approximately 29% below wild-type and 15% below azygous.

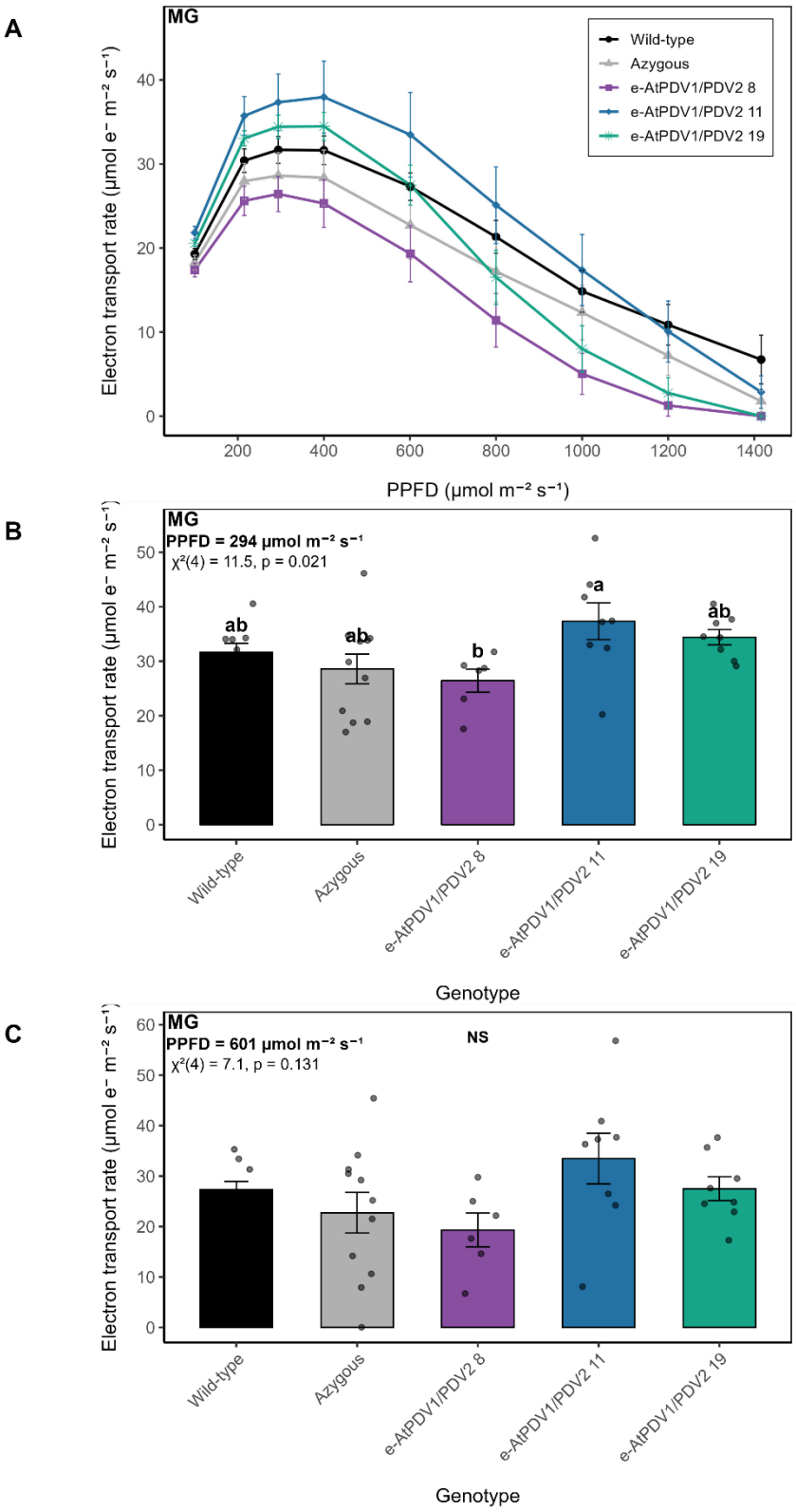

Figure 6.16. Electron transport rate (ETR) in early-specific *AtPDV1/PDV2* lines. Bar charts display ETR in mature green fruits (MG) of independent lines expressing the *AtPDV1* under the control of *SlTFM7* early fruit-specific promoter and *AtPDV2* under the control of *SlAFF* early fruit-specific promoter (e-*AtPDV1/PDV2*), as well as azygous and wild-type controls. (A) Light response of ETR across all light intensities (100–1400 µmol $m^2 s^{-1}$). (B) ETR at 294 µmol m^{-2} s^{-1}. (C) ETR at 601 µmol m^{-2} s^{-1}. MG = 20–23

days post-anthesis. All values represent means ± SE from at least four biological replicates per genotype, with two fruits sampled per plant. Statistically significant differences were determined using a Kruskal-Wallis test followed by Dunn's multiple range test. Dots show individual data points. Different letters indicate statistically significant differences ($P < 0.05$).

6.3 Discussion

This work has demonstrated that the simultaneous overexpression of the Arabidopsis plastid division components *PDV1*/*PDV2* had a limited effect on the photosynthetic characteristics of tomato fruits. Previous research, which overexpressed both genes in Arabidopsis and tobacco, produced transgenic plants with a larger population of smaller leaf chloroplasts. This is because both genes have been described to accelerate the rates of chloroplast division (Głowacka et al., 2023; Miyagishima et al., 2006; Okazaki et al., 2009). However, the extent of these phenotypes varied. While a study with young emerging Arabidopsis leaves (Okazaki et al., 2009), showed more striking phenotypes, results with fully expanded tobacco leaves (Głowacka et al., 2023), showed more moderate effects. For instance, for young Arabidopsis leaves, the chloroplast number was more than doubled in the double overexpression line relative to the wild type. In contrast, in fully expanded tobacco leaves, the increase in chloroplast number was moderate, from 88.5 in wild-type to 93.3 in the *PDV1*/*PDV2* lines, a non-significant difference of approximately 5% (Głowacka et al., 2023).

The results presented here showed that the simultaneous overexpression of *AtPDV1* and *AtPDV2* in tomato fruit did not lead to significant differences in mature green fruit chloroplast plan area and coverage compared with wild-type or azygous plants in two transgenic lines. In addition, the analysis of photochemical capacity revealed that ΦPSII and ETR were not significantly affected in transgenic lines. These results are consistent with Dutta et al. (2017), who reported no significant differences in chloroplast movement or photosynthetic efficiency between *35S-PDV1/PDV2* overexpression lines and wild-type (Col-0). The authors raised a fundamental question of why overexpression of *PDV1* and *PDV2* did not lead to improved photosynthesis.

Although qPCR confirmed that the *AtPDV1/PDV2* transgenes were expressed, their expression at the transcript level may not have translated into effective protein accumulation or functional integration into the plastid division machinery. The effects of *PDV1/PDV2* are dependent on balanced interaction with upstream factors such as *ARC6* and *FtsZ* ring formation and downstream *ARC5* (B. Sun et al., 2020), so it is possible that other components were not proportionally co-regulated, suggesting that the manipulation of *AtPDV1/PDV2* alone was not

sufficient to impact chloroplast morphology. Moreover, because *PDV2* is considered the rate-limiting determinant for *ARC5* recruitment and final division in the outer envelope membrane, an imbalance with excess *PDV1* relative to *PDV2* could potentially disrupt the balance of the division complex. Furthermore, the developmental context of fruit tissues may restrict the ability of plastid division components to modulate plastid division once chloroplasts are established. Fruit chloroplasts are restricted to a developmental window in which the downregulation of photosynthetic genes begins at the mature green stage, coinciding with the onset of ripening (Kahlau & Bock, 2008). In fact, a tissue-specific effect was also evident in a study comparing guard cells and mesophyll cells' chloroplasts. In guard cells, the characterisation of *35S-PDV1*/*PDV2* revealed plastid volumes that were similar to wild-type, while the number of plastids showed a slight, non-significant decrease (Knoblauch et al., 2024). The same study shows that in mesophyll cells, the *35S-PDV1/PDV2* line displayed a slight trend towards smaller and more numerous chloroplasts compared to wild-type. However, these differences were modest and not statistically significant in any of the imaging approaches used (Knoblauch et al., 2024).

In this study, one of the lines was characterised by enlarged chloroplasts and a reduced number. It is possible that this phenotype is associated with a resource allocation trade-off in which an increase in chloroplast size occurs at the expense of plastid number. Another hypothesis is an imbalance between plastid coverage and the photosynthetic pigment complex, as this line exhibited large plastids that covered more of the cell, but did not display a proportional increase in chlorophyll content. This is supported by the slower electron transport rates, possibly due to how photosynthetic proteins are distributed in the thylakoid membrane. The organisation of the thylakoid membrane and how photosynthetic and photoprotective pigments are distributed represent a key factor affecting the efficiency of light use. An altered thylakoid structure has been shown to affect conductance and electron transport rates (Austin II and Webber, 2005; Weise et al., 2015). Moreover, the 2.4-fold increase in chloroplast size in line 8 relative to the controls could influence the chloroplast surface-to-volume ratio, possibly limiting the rates of intracellular exchange of metabolites and leading to metabolic imbalances (Dutta et al., 2017). Previous research has shown that overexpression of *FtsZ1* in tobacco led to an increase in chloroplast area, followed by a decrease in number. The authors reported that a threefold increase in size was enough to impact the chloroplasts' biochemical capacities (Głowacka et al., 2023). Here, it is possible that the 2.4-fold increase in size was nearing the biological limit of chloroplast efficiency in the context of fruit photosynthesis.

Taken together, these findings suggest that although *PDV1/PDV2* overexpression affects chloroplast division, its impact varies depending on tissue type and developmental stage. Here, the simultaneous overexpression of *AtPDV1* and *AtPDV2* in tomato fruit had only a limited effect on chloroplast development and photosynthetic performance. Overall, these findings suggest that increasing plastid division alone is unlikely to improve fruit photosynthesis and that effective strategies will likely require coordinated enhancement of both plastid division and the assembly of photosynthetic machinery. Moving forward, the analysis of chloroplast ultrastructure via electron microscopy, combined with transcriptomic profiling, can provide deeper insight into the degree of thylakoid stacking and how associated changes in gene expression may affect photochemical efficiency.

Chapter 7 General Discussion

7.1 Manipulating Fruit Photosynthesis and Pigment Content in Tomato

This research highlighted the importance of fruit chloroplasts as active contributors to plant metabolism rather than passive organelles that rely on leaf photosynthesis. By showing that fruit specific manipulation of chloroplast development can enhance photochemical efficiency and pigment accumulation in tomato fruits, this work adds to the current understanding of non-foliar photosynthesis, and it demonstrates its relevance to crop improvement. Beyond its mechanistic insights, integrating fruit photosynthesis into strategies aimed at improving yield and nutritional quality can offer a practical avenue for future breeding and biotechnological approaches in horticultural and non-horticultural crops alike. This General Discussion brings together the findings from across the experimental chapters to evaluate what the manipulation of chloroplast development in tomato fruits reveals about the role of non-foliar photosynthesis and what are its potentials and limitations for crop improvement.

The tomato (*Solanum lycopersicum*) is extensively consumed worldwide. It is one of the world's major fresh and processed fruits, with an estimated 192 million tons produced on 5 million hectares every year (FAO, 2023). The tomato is also an economically attractive crop due to its short growth cycle and high yield. The global production of tomatoes has enormously increased in the last decades, and that trend looks set to continue (Costa & Heuvelink, 2018). Moreover, processed forms of tomato also represent an important economic contribution, with a global average of 5 kg of processed tomato per person each year. This number is estimated at 23 kg/year/person in Western Europe (Branthôme, 2020).

The ability to manipulate chloroplast development can lead to significant increases in the productivity and quality of crop plants. The genetic manipulation of pigment content and chloroplast development has been previously explored in both commercial crops, such as tomato (Lupi et al., 2019; Powell et al., 2012), and rice (Hudson, 2010), and model crops (Larkin et al., 2016; Qu et al., 2013), demonstrating the potential of chloroplasts as a target to improve photosynthetic efficiency. The manipulation of photosynthesis in fruits is of particular interest, as fruits contribute to their own growth and the differentiation of chloroplasts into chromoplasts during ripening results in the accumulation of large amounts of carotenoids, predominantly

lycopene and β-Carotene (Lytovchenko et al., 2011; Simkin et al., 2020). Therefore, the genetic manipulation of fruit chloroplasts offers a novel strategy to simultaneously enhance photosynthetic efficiency during early fruit development and improve key quality traits, such as nutritional value, colour and flavour in these organs.

The ability to develop high-quality tomato fruits could have a significant impact on commercialising new tomato varieties and serve as an important tool to ensure that increases in crop productivity keep pace with growing demand for both food and nutritional security (Simkin, 2019). The biofortification of commercial crops has gained traction with biotechnology programmes addressing the manipulation of carotenoid biosynthesis and storage as potential routes to generate commercial crops with increased nutrient content (Lopez et al., 2008; Park et al., 2016; Simkin, 2019; Yazdani et al., 2019). Recently, the global market for genetically modified crops has reached record values, with over 191.7 million hectares cultivated in 2018, benefiting over 1.95 billion people around the world (Verma, 2022). This trend looks set to continue, making genetic engineering an alternative to delivering tomato varieties that benefit both the consumer and the industry. Therefore, investments in research programmes focused on enhancing tomato productivity could lead to a significant economic impact.

The main aim of this project was to produce transgenic tomato plants with fruits overexpressing genes identified as targets for the manipulation of chloroplast development and to explore the effect of such manipulation on the fruits' photochemical capacity and nutritional content. A variety of transgenic tomato plants (*Solanum lycopersicum*) overexpressing the target genes were generated. The overexpression of the MADS-Box gene *BpMADS* from Birch in tobacco was previously associated with chloroplast development and increased photosynthetic rates (Qu et al., 2013). Furthermore, Arabidopsis transcription factors, such as *CGA1* and *GNC*, have been shown to increase leaf chlorophyll content in Arabidopsis (Chiang et al., 2012; Hudson et al., 2011). Finally, the components of the plastid division apparatus *PDV1* and *PDV2* have been identified as targets to improve chloroplast photoprotection (Okazaki et al., 2009). Given the range of phenotypes presented in this study, Table 7.1 provides a brief summary of the main structural, pigment-related and photochemical effects observed for the transgenic constructs.

Table 7.1. Quantitative summary of transgene overexpression phenotypes.

Gene	Promoter	Chloroplast coverage (MG)	Chlorophyll content (MG)	Lycopene and /or β-carotene (Ripe)	ΦPSII (MG)
BpMADS	*SlTFM7*	1.3–1.5× greater than wild-type/azygous control	+40–90% vs wild-type/azygous control	Variable (some lines β-carotene only; others β-carotene + lycopene)	Greater across light intensities
BpMADS	*CaFIB*	Not measured	No significant change	Variable (some lines β-carotene only; others β-carotene + lycopene)	No consistent improvement
AtCGA1	*SlTFM7*	1.3–1.8× greater than wild-type/azygous control	+45–78% vs wild-type/azygous control	Variable (some lines β-carotene only; others β-carotene + lycopene)	Greater across most light intensities; (line-dependent)
AtGNC	*SlAFF*	Not measured	Variable (increase observed in one line; no significant change in others)	Variable (lycopene unchanged; β-carotene increased in some lines)	No consistent improvement
AtPDV1/PDV2	*SlTFM7–SlAFF*	No significant change	No significant change	No significant change	No improvement or reduction

7.2 Chloroplast Compartment Dynamics in Transgenic Tomato Fruit Pericarp

Mature green fruits were assessed via confocal scanning laser and transmitted light microscopy for morphological changes in the chloroplast compartment. It was observed that *BpMADS* and *AtCGA1* overexpression lines allocated more cellular space to plastids in the fruit pericarp cells,

with chloroplast coverage values up to 80% greater than controls. This result aligns with previous research manipulating chloroplast development in tomato. For instance, the chloroplast area in fruits was increased by approximately 80% in *APRR2-like Ailsa craig* overexpressing lines (Pan et al., 2013). Furthermore, the downregulation of *SlZHD17* in tomato, a negative regulator of chlorophyll biosynthesis, led to an increase in chloroplast area of approximately 2-fold in Micro-Tom pericarp chloroplasts (Shi et al., 2021). These results suggest an overall maximum for chloroplast size, beyond which metabolic activity may be negatively affected.

Previous studies have shed light on the extent of chloroplast size increase as a factor to consider in the engineering of plastid development. For instance, a threefold increase in chloroplast diameter in transgenic tobacco led to a reduction in electron transport and carboxylation capacity of RuBisCO (Głowacka et al., 2023). In this thesis, a resource allocation idea is further supported by transgenic lines e-*AtCGA1* 14 and e-*AtPDV1/PDV2* 8, which displayed the largest chloroplast sizes, accompanied by the lowest chloroplast numbers per cell. This potential trade-off mirrors the classic *arc* mutant phenotype, where larger chloroplasts are associated with a reduction in number (Pyke et al., 1994; Pyke & Leech, 1992).

Assessing the fraction of cellular volume occupied by chloroplasts also revealed an increase in the plastid compartment size in both e-*BpMADS* and e-*AtCGA1* transgenic lines. The approximately 1.3- to 1.8-fold increase in plastid coverage size observed in pericarp cells of different e-*BpMADS* and e-*AtCGA1* lines may be linked to the increase in chlorophyll and carotenoid levels. In contrast, there was no significant change in plastid coverage in the e-*AtPDV1/PDV2* overexpression lines. Although plastid division genes perform similar roles in Arabidopsis, tobacco, and tomato, it is possible that the effect of transgene expression is stage- and tissue-dependent. For example, transgene effects were more pronounced in young Arabidopsis leaves (Okazaki et al., 2009), moderate in fully expanded tobacco leaves (Głowacka et al., 2023), and in the present study led to significant results in two transgenic tomato lines. Moreover, the hypothesis of tissue specificity is further supported by the lack of differences between chloroplast number and volume between guard cell and mesophyll chloroplasts (Knoblauch et al., 2024).

Taken together, the observations of increased plastid compartment with the early overexpression of *BpMADS* and *AtCGA1* highlight a novel strategy to enhance pigment accumulation. This is particularly relevant in fruits, where chloroplast coverage is substantially lower than in mesophyll cells. For instance, it has been reported that pericarp cells of *Ailsa Craig* contain a chloroplast

coverage of approximately 15% of the mesophyll cells, offering considerable potential for further improvement (Cookson et al., 2003).

7.3 Plastid Compartment Size Is Closely Associated With Pigment Accumulation

The increase in chloroplast compartment observed in mature green fruits of early-specific *BpMADS* and *AtCGA1* lines was accompanied by changes in pigmentation that were apparent in the developing and ripening fruits. Increases in chlorophyll content in transgenic lines were substantial, ranging from approximately 40% to 90% in e-*BpMADS* lines and 45% to 78% in e-*AtCGA1* lines, relative to both wild-type and azygous controls. These increases were closely linked to the increases in total chloroplast coverage (e-*BpMADS* R^2: 0.86; e-*AtCGA1* R^2: 0.89), reinforcing the close association between plastid size and pigment accumulation. Notably, there was a clear association between chlorophyll and carotenoid levels in e-*BpMADS* and e-*AtCGA1* mature green fruits, reflecting the role of photosynthetic membranes in accumulating both pigments within the thylakoid membranes (Jarvis & López-Juez, 2013; Simkin et al., 2022). Previous research has shown similar increases in leaf chlorophyll by the overexpression of *BpMADS* in tobacco (ranging from 55% to 80%). In addition, *OsGATA11* (*CGA1*) overexpression in rice led to nearly a two-fold increase in chlorophyll under both sufficient and limiting nitrogen conditions (Hudson, 2010). Therefore, the mechanism by which both transcription factors drive pigment accumulation may be conserved across species. Although *CGA1* is a well-characterised regulator of chlorophyll biosynthesis (Chiang et al., 2012; Hudson et al., 2011), the relationship between *AP1*-like genes and chloroplast development remains elusive to date. Previous research suggests that the phenotypes observed could be a byproduct of the overexpression of *BpMADS* (Qu et al., 2013), as MADS-box genes act by recruiting additional transcriptional regulators to regulate a cascade of gene expression.

The results obtained here provide further evidence regarding the connection between plastid area and pigment accumulation. Pigment levels are determined by both biosynthetic rates and storage capacity, and thylakoid biogenesis increases membrane area, providing sites for both chlorophyll and carotenoid synthesis and sequestration in green fruit (Li & Yuan, 2013). In fact, improving plastid storage, alongside enhancements in biosynthetic rates, is at the forefront of agricultural research as a novel and successful strategy for biofortification. This technique has the potential to also enhance the concentration of other compounds of nutritional interest accumulated in

plastids, such as tocopherols (Morelli et al., 2023). The application of this strategy could represent an effective tool to increase pigment levels in chloroplasts, photochemical capacity in green fruits and total carotenoid content as the fruit ripens. Previous research has shown that *high pigment 3 (hp3)* tomato has plastids that are 30% larger and contain 30% more carotenoids in the ripe fruit (Galpaz et al., 2008). These results are also similar to the effects of tomato *GLK2* overexpression, in which an increase in the chloroplast compartment was associated with higher chlorophyll, lycopene and β-carotene levels (Nguyen et al., 2014).

Despite these promising outcomes, the relationship between pigments in green and ripe fruits is not straightforward. While an increase in chlorophyll content was observed at the mature green stage and subsequent lycopene and β-carotene accumulation in ripe fruits for some e-*BpMADS* and e-*AtCGA1* lines, this effect was not consistent across all lines. Some lines exhibited increases only in β-carotene levels, with lycopene levels remaining unaffected. The same trend was also observed in some *BpMADS* lines driven by the ripening promoter *CaFIB*. Moreover, a decrease in lycopene was observed in some e-*AtGNC* lines. These results are consistent with previous studies by Shi et al. (2021), who highlighted that chlorophyll levels during the green stage and carotenoid levels at the ripe stage are not necessarily interdependent (Barry et al., 2008; Shi et al., 2021). In addition, overexpression of *APRR2-like* in tomato, a regulator of pigment accumulation, resulted in transgenic fruits with an approximately 5-fold increase in chlorophyll, whereas the rise in carotenoid content at ripening was more modest, around 20%. (Pan et al., 2013). While the work here has focused on chlorophyll and carotenoids, it's expected that boosting the chloroplast compartment (and potentially chromoplast compartment) could also lead to increased tocopherol levels, as they also accumulate in plastids (Morelli et al., 2023). In fact, previous research has shown that wild-type plants harbouring *SlGLK2* (wild-type allele) contain significantly more chlorophyll at the green stage and tocopherols at the ripe stage compared to *Slglk2* (mutant allele) (Lupi et al., 2019). An important aspect for future research is quantifying the size of chromoplast compartments, which can provide valuable data for this project, as well as gathering information on the accumulation of other compounds stored in plastids.

Tocopherols, carotenoids, and the phytol tail of chlorophyll all share the common precursor geranylgeranyl diphosphate (GGPP), meaning these pathways may compete for substrate availability, which could partially explain some of the phenotypes observed in ripe fruits (Rodríguez-Concepción & Boronat, 2002). Furthermore, increased chlorophyll levels may provide

an additional supply of phytol during chlorophyll breakdown, which can be redirected into tocopherol biosynthesis. Tocopherols are subsequently stored within the plastoglobuli of chromoplasts (Morelli et al., 2023). Moreover, in tomatoes, the ripening process is normally associated with a reduction in the expression of lycopene β-cyclase, which converts lycopene into β-carotene, and as a result, the fruit accumulates large amounts of lycopene, the main carotenoid accumulated in tomatoes (Pecker et al., 1996). Previous research on tomato plants overexpressing a lycopene β-cyclase gene (*LCYB*) from *Nicotiana tabacum* resulted in transgenic fruits with increased levels of β-carotene despite no changes in lycopene (Ralley et al., 2016).

Therefore, at this stage, one possibility is that increased photosynthetic capacity may have enhanced the demand for photoprotective carotenoids in the thylakoid membranes. Here, the evidence shows that the increase in chlorophyll content was associated with an increase in total carotenoids in green fruits, which are primarily composed of β-carotene, lutein, and violaxanthin (Dharmapuri et al., 2002). This indicates an enhanced metabolic flux of both the ε- and β-branches of the carotenoid pathway during chloroplast development. It is possible that this pre-existing enhancement of the β-branch (responsible for β-carotene) and ε-branch (responsible for lutein) could also have an effect in the ripe fruit, maintaining or even increasing β-carotene levels (and lutein to some extent) at the expense of lycopene. It is important to note that although lutein levels are greatly reduced during ripening, red tomato fruit still contains trace amounts of this pigment (Dharmapuri et al., 2002), and that the spectrophotometric method used for the quantification of β-carotene in this study may overestimate its concentration due to spectral overlap with lutein.

Moving forward, it will also be important to consider not only transcriptional control but also post-translational regulation of plastid enzymes. For example, the stability of *PSY* is maintained by chaperones such as *OR*, which stabilise the enzyme and promote its accumulation, thereby maintaining efficient carotenoid biosynthesis (D'Andrea et al., 2018). A similar principle applies to photosynthetic enzymes such as RuBisCO, where engineering efforts have long been limited by the requirement for accessory factors within the chloroplast. Correct assembly and folding of RuBisCO are often hindered without compatible chaperones, reinforcing the need for co-expression strategies to ensure optimal protein activity (Wilson et al., 2018). Taken together, these findings reveal the need to evaluate gene overexpression not only at the transcriptional level but also from a post-translational perspective, where protein stability and chaperone activity impact the phenotypes observed.

7.4 Chloroplast Engineering in Tomato Fruits: Opportunities and Limitations for Photochemical Efficiency

The manipulation of chloroplast development and photosynthetic pigment content in green fruits translated into significant increases in photochemical capacity. The overexpression of both *BpMADS* and *AtCGA1* led to enhanced light absorption and utilisation, as evidenced by the higher effective PSII quantum yield (ΦPSII). The increase in the chloroplast storage capacity is tightly linked to an increase in photosynthetic pigment content, since both chlorophyll and carotenoid are stored in thylakoid membranes. Previous studies with Arabidopsis *arc* mutants have shown that a 4-fold increase in chloroplast size in mutant lines was accompanied by an increase in the degree of thylakoid stacking (Austin II and Webber, 2005). Therefore, in this study, it is expected that moderate increases in chloroplast plan area, approximately 1.5 to 2-fold, would also lead to an increase in thylakoid stacking, providing more surface area for energy transfer, without the detrimental effects caused by extremely large chloroplasts. This was further evidenced by the faster electron transport rates observed in most engineered lines of both transcription factors. Nevertheless, characterisation of chloroplast ultrastructure via transmission electron microscopy (TEM) would be necessary to fully characterise chloroplast thylakoid organisation and elucidate the impact of the overexpression of the transgenes at a deeper level.

The reduced coefficient of non-photochemical quenching (qN) in the engineered lines indicates a higher capacity for light utilisation in photochemistry, rather than dissipating it as heat. At low light, photosynthesis has been shown to function efficiently in both plants adapted to low-light and high-light conditions, with higher light intensities being limiting to photochemical capacity (Austin II and Webber, 2005). Moreover, in field crop canopies, lighting rarely remains at a steady state because of continuous fluctuations in light (De Souza et al., 2020). Here, the use of light curves has demonstrated the potential of the transgenic lines studied to manage excess light more efficiently as light intensity increases. This may be due to the combination of factors mentioned previously, such as increased photosynthetic pigment content, antioxidant carotenoids, and possibly thylakoid stacking, which produce a more robust photosynthetic apparatus. Previously, one of the main concerns of increasing active chloroplasts was related to photodamage, in which fruits could become overheated under high light. However, the increased antioxidant capacity of transgenic fruits in this study was shown to protect the plastids. The higher accumulation of carotenoids in the thylakoid membrane of e-*BpMADS* and e-*AtCGA1* may have also contributed to the stabilisation of lipid membranes and photoprotection against reactive

oxygen species (ROS) at higher light intensities (Li & Yuan, 2013; Nisar et al., 2015; Simkin, 2021). In contrast, simultaneous overexpression of *AtPDV1/PDV2* resulted in either no improvement or even a reduction in photochemical capacity. This finding aligns with previous reports in tobacco, where the overexpression of *PDV1/PDV2* under a RuBisCO promoter reduced performance in field conditions (Głowacka et al., 2023). Similarly, overexpression of *PDV1/PDV2* driven by the constitutive *35S* promoter in Arabidopsis resulted in no improvements in photosynthetic efficiency or photoprotection (Dutta et al., 2017). Moreover, recent work characterising *35S-PDV1/PDV2* Arabidopsis mesophyll and guard cell chloroplasts reported no significant differences in chloroplast size or number compared with the wild type (Knoblauch et al., 2024).

Throughout this study, a common observation was that the engineered lines with the largest chloroplast area were not the most photochemically efficient. While a larger chloroplast size can provide additional surface area for light harvesting and electron transport, the increase in size can also carry detrimental effects that may jeopardise photosynthetic efficiency. For instance, a larger chloroplast size can affect the surface area to volume ratio, possibly limiting the rates of metabolite exchange, such as the import of nutrients and export of assimilated carbon (Egea et al., 2011). Chloroplast movement has also been suggested to be affected by the size of chloroplasts (Dutta et al., 2017; Kasahara et al., 2002). Finally, the engineered lines with the largest chloroplast area did not display the highest chlorophyll content. A possible explanation is a dilution effect, where plastid expansion was not matched by a proportional increase in pigments and photosynthetic complexes in lines such as e-*AtCGA1* 14 and e-*AtPDV1/PDV2* 8. This dilution effect would mean that, despite an increase in the plastid compartment and overall chlorophyll content, the increase in pigment did not correspond proportionally to the new storage capacity, thereby reducing pigment density and limiting photochemical capacity. Taken together, the evidence suggests that increased plastid size alone does not necessarily guarantee enhanced photochemical efficiency and that additional analysis, such as of thylakoid organisation, may also be necessary to address the challenge of enhancing photochemical capacity more efficiently.

Although the evaluation of photochemical capacity in non-foliar tissues has traditionally been performed via chlorophyll fluorescence measurements (Carrara et al., 2001; Hetherington et al., 1998; Smillie et al., 1999), the analysis of downstream processes could provide valuable insights into how processed energy and reducing power are employed. In this study, we developed and optimised a protocol for the evaluation of gas exchange rates in tomato fruit using a custom

chamber adapted for non-foliar tissues. The analysis of respiration rates in the fruit of the tomato provides an indirect measurement of how carbon is being used internally. There is evidence that fruits possess part of a C_4 photosynthetic machinery capable of recycling respired carbon. This is evidenced by the high levels of malic enzyme (ME) and malate dehydrogenase (MDH) in fruit tissue, compared to leaves, indicating that CO_2 is fixed by PEPC into oxaloacetate (OAA), and reduced to malate via NAD-dependent malate dehydrogenase (MDH) (Willmer & Johnston, 1976). In our work, increasing light intensity in controlled conditions led to a reduction in CO_2 efflux, which suggests that the respired carbon was being used internally. Similarly, providing the system with increasing ambient CO_2 also led to a decrease in CO_2 release, indicating stimulation of the photosynthetic apparatus. Together, both CO_2 and light response results shed light on the unique features and limitations of photosynthesis performed by fruits. Among them, the contribution of atmospheric CO_2 uptake by the bulky pericarp tissue, the extent to which epidermal cuticle diffusion allows carbon diffusion to inner tissues and how internal CO_2 availability can limit photosynthetic rates (Cocaliadis et al., 2014; Garrido et al., 2023). Although these processes remain elusive, this study adds to the literature by providing quantitative evidence that respiration and the stimulation of the photosynthetic apparatus are tightly interconnected in fruit tissues.

7.5 Future Directions for Enhancing Fruit Photosynthesis

A growing concern related to increasing carbon fixation in crops is the balance between carbon and nitrogen metabolism. Elevated atmospheric CO_2 levels may lead to increased carbon but decreased nitrogen concentrations within the leaf, particularly in C_3 crops, which could have an impact on the nutrient content of crops (Taub & Wang, 2008; Walsh et al., 2024). Moreover, fruits are strong sink tissues, relying on mature leaves for nitrogen to maintain protein turnover (White et al., 2016), which will support the assembly and maintenance of their photosynthetic machinery. Increasing the fruit's capacity to contribute to its own growth and development could help reduce the fruit’s carbon sink, despite a potential rise in nitrogen requirements. Nevertheless, plants have already developed strategies to ripen fruits without completely draining resources from leaves (Barja et al., 2021). Regardless, any potential increases in the photosynthetic capacity of fruits should be assessed against the potential costs. The potential benefits of enhanced fruit photochemical capacity would have more impact if combining both genetic engineering and non-GM strategies.

Among non-GM approaches, the use of plant growth-promoting rhizobacteria (PGPR) can improve the physiological responses of crops under limiting conditions, such as salt, drought, heavy metals, high or low temperature (Pajuelo et al., 2023). The latest advances in biotechnology regarding the wide variety of PGPR in the rhizosphere, together with their colonisation capacity and mechanisms of action, have turned these rhizobacteria into a promising tool for agricultural management and a reliable component to overcome the challenge of climate change (Bhattacharyya & Jha, 2012). The use of genetic engineering could also be combined with traditional breeding. Different varieties exhibit varying photosynthetic efficiencies, particularly under stress conditions. For instance, leaf area, stomata aperture and water use efficiency can contribute to improved photosynthesis (Khan et al., 2023) and influence resource partitioning to fruits, ultimately contributing to the maximisation of fruit photosynthesis.

Moreover, the application of quantitative trait loci (QTLs) to exploit photosynthetic natural diversity can provide improvement to photosynthesis and yield without requiring genetic modification (Fahad et al., 2017; Soares et al., 2019; Walsh et al., 2024) The advent of intersection lines (IL) provides a powerful resource that can be used in tandem with QTLS, as it allows single specific regions to be analysed. Mining natural diversity represents a promising avenue as wild tomato relatives represent a large genetic pool. Several genetic resources are available for studying tomato genomics, including germplasm collections (TGRC, UC Davis) and the SOL Genomics Network, an online database for the tomato genome. Together, these strategies represent a powerful tool to optimise the use of genetic variation in nature (Bai & Lindhout, 2007).

Recent advances, including the development of a CRISPR-Cas9 system, represent a remarkable tool for delivering targeted improvement in commercial crops (Tiwari et al., 2023; Wang et al., 2019). While the narrow genetic base of modern tomato varieties makes it difficult for traditional breeding to introduce new traits (Tiwari et al., 2023), the tomato is an excellent candidate for investigating genetic improvements to photosynthesis due to its relatively short growth cycle and comprehensive genome annotation (The Tomato Genome Consortium, 2012). In fact, CRISPR has been recently extensively applied in tomatoes, with effects ranging from increasing sugar content (Kawaguchi et al., 2021), carotenoid levels (Hunziker et al., 2020), and shelf life (Yu et al., 2017) .

Improving agricultural productivity in the future decades represents a challenge to ensuring food security and fighting hidden hunger. This is of particular concern in the global south, in which are located many of the countries most heavily affected by agricultural failures and extreme weather events, as well as intense population (Alexandratos & Bruinsma, 2012). Therefore, providing

alternatives to ensure sustainable tomato production has become increasingly crucial to guarantee the vital dietary contribution that tomatoes can offer to these countries' growing population. Moreover, in the previous decades, the industry's focus on yield to the detriment of flavour and nutritional value caused a decline in the overall quality of tomato fruits (Cocaliadis et al., 2014; Klee & Resende, 2020). Moving forward, it would also be pertinent to collect data on fruit flavour as higher photosynthetic rates are known to contribute to the sugar profile of fruits (Garrido et al., 2023; Hiratsuka et al., 2012). Thus, approaches that target solutions to both fruit productivity and quality represent an opportunity for the industry sector and agricultural biotechnology research.

The use of biotechnology to increase photosynthetic efficiency in crops has been at the forefront of agricultural research for many years (Driever et al., 2017; Heyno et al., 2022; Simkin et al., 2015, 2017). More recently, the study of non-foliar photosynthesis (and particularly fruit) has gained traction (Carrara et al., 2001; Hetherington et al., 1998; Simkin et al., 2020; Smillie, 1992; Smillie et al., 1999). This thesis demonstrates both the potential and the limitations of manipulating chloroplast development to enhance photosynthetic performance and pigment accumulation in tomato fruits. Across multiple genetic strategies targeting plastid development, the results show that fruit chloroplasts can be reinforced to improve photochemical efficiency, but that these gains are constrained by developmental trade-offs, tissue specificity, and line-dependent effects. The use of genetic engineering represents an important milestone that can be applied to traditional breeding to enhance photosynthesis in tomato fruit, potentially leading to improvements in multiple traits that have been difficult to improve simultaneously via traditional methods alone. The short-term impact delivered as part of this project is relevant to the UK fruit and berry industry, providing a basis for future research. In the long term, the impact relating to land use, crop productivity and dietary contributions is relevant on a global scale moving forward, particularly in the context of climate resilience and sustainable diets.

Chapter 8 References

Ainsworth, E.A. and Long, S.P. (2005) 'What have we learned from 15 years of free-air CO_2 enrichment (FACE)? A meta-analytic review of the responses of photosynthesis, canopy properties and plant production to rising CO_2', *New Phytologist*, 165(2), pp. 351–372. https://doi.org/10.1111/j.1469-8137.2004.01224.x

Ainsworth, E.A. and Long, S.P. (2021) '30 years of free-air carbon dioxide enrichment (FACE): what have we learned about future crop productivity and its potential for adaptation?', *Global Change Biology*, 27(1), pp. 27–49. https://doi.org/10.1111/gcb.15375

Albertsson, P.Å. (2001) 'A quantitative model of the domain structure of the photosynthetic membrane', *Trends in Plant Science*, 6(8), pp. 349–354. https://doi.org/10.1016/S1360-1385(01)02021-0

Alexander, L. and Grierson, D. (2002) 'Ethylene biosynthesis and action in tomato: a model for climacteric fruit ripening', *Journal of Experimental Botany*, 53(377), pp. 2039–2055. https://doi.org/10.1093/jxb/erf072

Alexandratos, N. and Bruinsma, J. (2012) *World agriculture towards 2030/2050: the 2012 revision*. Rome: FAO. Available at: https://www.fao.org/4/ap106e/ap106e.pdf (Accessed: 26 July 2025).

An, Y., Zhou, Y., Han, X., Shen, C., Wang, S., Liu, C., Yin, W. and Xia, X. (2020) 'The GATA transcription factor GNC plays an important role in photosynthesis and growth in poplar', *Journal of Experimental Botany*, 71(6), pp. 1969–1984. https://doi.org/10.1093/jxb/erz564

Anthon, G.E. and Barrett, D.M. (2007) 'Standardization of a rapid spectrophotometric method for lycopene analysis', *Acta Horticulturae*, 758, pp. 111–128. https://doi.org/10.17660/ActaHortic.2007.758.12

Aschan, G. and Pfanz, H. (2003) 'Non-foliar photosynthesis – a strategy of additional carbon acquisition', *Flora – Morphology, Distribution, Functional Ecology of Plants*, 198(2), pp. 81–97. https://doi.org/10.1078/0367-2530-00080

Austin II, J. and Webber, A.N. (2005) 'Photosynthesis in Arabidopsis thaliana mutants with reduced chloroplast number', *Photosynthesis Research*, 85, pp. 373–384. https://doi.org/10.1007/s11120-005-7708-x

Bai, Y. and Lindhout, P. (2007) 'Domestication and breeding of tomatoes: what have we gained and what can we gain in the future?', *Annals of Botany*, 100(5), pp. 1085–1094. https://doi.org/10.1093/aob/mcm150

Barry, C.S., McQuinn, R.P., Chung, M.Y., Besuden, A. and Giovannoni, J.J. (2008) 'Amino acid substitutions in homologs of the STAY-GREEN protein are responsible for the green-flesh and chlorophyll retainer mutations of tomato and pepper', *Plant Physiology*, 147(1), pp. 179–187. https://doi.org/10.1104/pp.108.118430

Barsan, C., Sanchez-Bel, P., Rombaldi, C., Egea, I., Rossignol, M., Kuntz, M., Zouine, M., Latché, A., Bouzayen, M. and Pech, J.C. (2010) 'Characteristics of the tomato chromoplast revealed by proteomic analysis', *Journal of Experimental Botany*, 61(9), pp. 2413–2431. https://doi.org/10.1093/jxb/erq070

Barsan, C., Zouine, M., Maza, E., Bian, W., Egea, I., Rossignol, M., Bouyssie, D., Pichereaux, C., Purgatto, E., Bouzayen, M. and Latché, A. (2012) 'Proteomic analysis of chloroplast-to-chromoplast transition in tomato reveals metabolic shifts coupled with disrupted thylakoid biogenesis machinery and elevated energy-production components', *Plant Physiology*, 160(2), pp. 708–725. https://doi.org/10.1104/pp.112.203679

Beale, S.I. (1999) 'Enzymes of chlorophyll biosynthesis', *Photosynthesis Research*, 60(1), pp. 43–73. https://doi.org/10.1023/A:1006297731456

Behringer, C. and Schwechheimer, C. (2015) 'B-GATA transcription factors – insights into their structure, regulation, and role in plant development', *Frontiers in Plant Science*, 6, Article 90. https://doi.org/10.3389/fpls.2015.00090

Bemer, M., Karlova, R., Ballester, A.R., Tikunov, Y.M., Bovy, A.G., Wolters-Arts, M., Rossetto, P.D.B., Angenent, G.C. and de Maagd, R.A. (2012) 'The tomato FRUITFULL homologs TDR4/FUL1 and MBP7/FUL2 regulate ethylene-independent aspects of fruit ripening', *The Plant Cell*, 24(11), pp. 4437–4451. https://doi.org/10.1105/tpc.112.103283

Bergougnoux, V. (2014) ‘The history of tomato: from domestication to biopharming’, *Biotechnology Advances*, 32(1), pp. 170–189. https://doi.org/10.1016/j.biotechadv.2013.11.003

Bhattacharyya, P.N. and Jha, D.K. (2012) ‘Plant growth-promoting rhizobacteria (PGPR): emergence in agriculture’, *World Journal of Microbiology and Biotechnology*, 28(4), pp. 1327–1350. https://doi.org/10.1007/s11274-011-0979-9

Bi, Y.M., Zhang, Y., Signorelli, T., Zhao, R., Zhu, T. and Rothstein, S.J. (2005) ‘Genetic analysis of *Arabidopsis* GATA transcription factor gene family reveals a nitrate-inducible member important for chlorophyll synthesis and glucose sensitivity’, *The Plant Journal*, 44(4), pp. 680–692. https://doi.org/10.1111/j.1365-313X.2005.02568.x

Bian, W., Barsan, C., Egea, I., Purgatto, E., Chervin, C., Zouine, M., Latché, A., Bouzayen, M. and Pech, J.C. (2011) ‘Metabolic and molecular events occurring during chromoplast biogenesis’, *Journal of Botany*, 2011, Article 289859. https://doi.org/10.1155/2011/289859

Blanke, M.M. and Lenz, F. (1989) ‘Fruit photosynthesis’, *Plant, Cell and Environment*, 12(1), pp. 31–46. https://doi.org/10.1111/j.1365-3040.1989.tb01914.x

Blanke, M.M. (1992) ‘Photosynthesis of avocado fruit’, in Lovatt, C.J., Holthe, P.A. and Arpaia, M.L. (eds.) *Proceedings of the Second World Avocado Congress*. Vol. 1. Riverside, CA: University of California, pp. 179–189.

Blankenship, R.E. (2021) *Molecular mechanisms of photosynthesis*. 3rd edn. Chichester: John Wiley & Sons. https://doi.org/10.1002/9780470758472

Block, M.A., Douce, R., Joyard, J. and Rolland, N. (2007) ‘Chloroplast envelope membranes: a dynamic interface between plastids and the cytosol’, *Photosynthesis Research*, 92(2), pp. 225–244. https://doi.org/10.1007/s11120-007-9195-8

Bouis, H.E., Hotz, C., McClafferty, B., Meenakshi, J.V. and Pfeiffer, W.H. (2011) ‘Biofortification: a new tool to reduce micronutrient malnutrition’, *Food and Nutrition Bulletin*, 32(1 Suppl. 1), pp. S31–S40. https://doi.org/10.1177/15648265110321S105

Bouis, H.E. and Saltzman, A. (2017) ‘Improving nutrition through biofortification: a review of evidence from HarvestPlus (2003–2016)’, *Global Food Security*, 12, pp. 49–58. https://doi.org/10.1016/j.gfs.2017.01.009

Branthôme, F.X. (2020) *Global consumption of tomato products 2018/2019 edition*. Tomato News.

Büker, M., Schünemann, D. and Borchert, S. (1998) 'Enzymic properties and capacities of developing tomato (*Lycopersicon esculentum* L.) fruit plastids', *Journal of Experimental Botany*, 49(321), pp. 681–691. https://doi.org/10.1093/jxb/49.321.681

Burko, Y., Shleizer-Burko, S., Yanai, O., Shwartz, I., Zelnik, I.D., Jacob-Hirsch, J., Kela, I., Eshed-Williams, L. and Ori, N. (2013) 'A role for APETALA1/FRUITFULL transcription factors in tomato leaf development', *The Plant Cell*, 25(6), pp. 2070–2083. https://doi.org/10.1105/tpc.113.113035

Burney, J.A., Davis, S.J. and Lobell, D.B. (2010) 'Greenhouse gas mitigation by agricultural intensification', *Proceedings of the National Academy of Sciences of the United States of America*, 107(26), pp. 12052–12057. https://doi.org/10.1073/pnas.0914216107

Busi, M.V., Bustamante, C., D'Angelo, C., Hidalgo-Cuevas, M., Boggio, S.B., Valle, E.M. and Zabaleta, E. (2003) 'MADS-box genes expressed during tomato seed and fruit development', *Plant Molecular Biology*, 52(4), pp. 801–815. https://doi.org/10.1023/A:1025001402838

Cackett, L., Luginbuehl, L.H., Schreier, T.B., Lopez-Juez, E. and Hibberd, J.M. (2022) 'Chloroplast development in green plant tissues: the interplay between light, hormone, and transcriptional regulation', *New Phytologist*, 233(5), pp. 2000–2016. https://doi.org/10.1111/nph.17839

Camara, B., Hugueney, P., Bouvier, F., Kuntz, M. and Monéger, R. (1995) 'Biochemistry and molecular biology of chromoplast development', *International Review of Cytology*, 163, pp. 175–247. https://doi.org/10.1016/S0074-7696(08)62211-1

Chamovitz, D., Sandmann, G. and Hirschberg, J. (1993) 'Molecular and biochemical characterization of herbicide-resistant mutants of cyanobacteria reveals that phytoene desaturation is a rate-limiting step in carotenoid biosynthesis', *Journal of Biological Chemistry*, 268(23), pp. 17348–17353. https://doi.org/10.1016/S0021-9258(19)85341-3

Chan, K.X., Phua, S.Y., Crisp, P., McQuinn, R. and Pogson, B.J. (2016) 'Learning the languages of the chloroplast: retrograde signaling and beyond', *Annual Review of Plant Biology*, 67(1), pp. 25–53. https://doi.org/10.1146/annurev-arplant-043015-111854

Chen, H.C., Klein, A., Xiang, M., Backhaus, R.A. and Kuntz, M. (1998) 'Drought- and wound-induced expression in leaves of a gene encoding a chromoplast carotenoid-associated protein', *The Plant Journal*, 14(3), pp. 317–326. https://doi.org/10.1046/j.1365-313X.1998.00127.x

Chetty, V.J., Ceballos, N., Garcia, D., Narváez-Vásquez, J., Lopez, W. and Orozco-Cárdenas, M.L. (2013) 'Evaluation of four *Agrobacterium tumefaciens* strains for the genetic transformation of tomato (*Solanum lycopersicum* L.) cultivar Micro-Tom', *Plant Cell Reports*, 32(2), pp. 239–247. https://doi.org/10.1007/s00299-012-1358-1

Chi, W., Feng, P., Ma, J. and Zhang, L. (2015) 'Metabolites and chloroplast retrograde signaling', *Current Opinion in Plant Biology*, 25, pp. 32–38. https://doi.org/10.1016/j.pbi.2015.04.006

Chiang, Y.H., Zubo, Y.O., Tapken, W., Kim, H.J., Lavanway, A.M., Howard, L., Pilon, M., Kieber, J.J. and Schaller, G.E. (2012) 'Functional characterization of the GATA transcription factors GNC and CGA1 reveals their key role in chloroplast development, growth, and division in *Arabidopsis*', *Plant Physiology*, 160(1), pp. 332–348. https://doi.org/10.1104/pp.112.198705

Chida, H., Nakazawa, A., Akazaki, H., Hirano, T., Suruga, K., Ogawa, M., Satoh, T., Kadokura, K., Yamada, S., Hakamata, W. and Isobe, K. (2007) 'Expression of the algal cytochrome c_6 gene in *Arabidopsis* enhances photosynthesis and growth', *Plant and Cell Physiology*, 48(7), pp. 948–957. https://doi.org/10.1093/pcp/pcm064

Choi, S.W., Hoshikawa, K., Fujita, S., Thi, D.P., Mizoguchi, T., Ezura, H. and Ito, E. (2018) 'Evaluation of internal control genes for quantitative real-time PCR analyses for studying fruit development of dwarf tomato cultivar "Micro-Tom"', *Plant Biotechnology*, 35(3), pp. 225–235. https://doi.org/10.5511/plantbiotechnology.18.0525a

Chung, M.Y., Naing, A.H., Vrebalov, J., Shanmugam, A., Lee, D.J., Park, I.H., Kim, C.K. and Giovannoni, J.J. (2020) 'The use of SlAdh2 promoter as a novel fruit-specific promoter in transgenic tomato', *Journal of Plant Biotechnology*, 47(2), pp. 172–178. https://doi.org/10.5010/jpb.2020.47.2.172

Cocaliadis, M.F., Fernández-Muñoz, R., Pons, C., Orzaez, D. and Granell, A. (2014) 'Increasing tomato fruit quality by enhancing fruit chloroplast function: a double-edged sword?', *Journal of Experimental Botany*, 65(16), pp. 4589–4598. https://doi.org/10.1093/jxb/eru165

Cole, M.B., Augustin, M.A., Robertson, M.J. and Manners, J.M. (2018) 'The science of food security', *npj Science of Food*, 2(1), Article 14. https://doi.org/10.1038/s41538-018-0021-9

Conner, T. (1997) *Fruit specific promoters*. United States Patent 5,608,150. Available at: https://lens.org/080-376-008-373-168

Cookson, P.J., Kiano, J.W., Shipton, C.A., Fraser, P.D., Römer, S., Schuch, W., Bramley, P.M. and Pyke, K.A. (2003) 'Increases in cell elongation, plastid compartment size and phytoene synthase activity underlie the phenotype of the high pigment-1 mutant of tomato', *Planta*, 217(6), pp. 896–903. https://doi.org/10.1007/s00425-003-1065-9

Cortleven, A. and Schmülling, T. (2015) 'Regulation of chloroplast development and function by cytokinin', *Journal of Experimental Botany*, 66(16), pp. 4999–5013. https://doi.org/10.1093/jxb/erv132

Costa, J.M. and Heuvelink, E.J.T.B. (2018) 'The global tomato industry', in Heuvelink, E. (ed.) *Tomatoes*. Wallingford: CABI, pp. 1–26. https://doi.org/10.1079/9781780641935.0001

Cruz-Mendívil, A., Rivera-López, J., Germán-Báez, L.J., López-Meyer, M., Hernández-Verdugo, S., López-Valenzuela, J.A., Reyes-Moreno, C. and Valdez-Ortiz, A. (2011) 'A simple and efficient protocol for plant regeneration and genetic transformation of tomato cv. Micro-Tom from leaf explants', *HortScience*, 46(12), pp. 1655–1660. https://doi.org/10.21273/hortsci.46.12.1655

Dan, Y., Yan, H., Munyikwa, T., Dong, J., Zhang, Y. and Armstrong, C.L. (2006) 'Micro-Tom: a high-throughput model transformation system for functional genomics', *Plant Cell Reports*, 25(5), pp. 432–441. https://doi.org/10.1007/s00299-005-0084-3

D'Andrea, L., Simon-Moya, M., Llorente, B., Llamas, E., Marro, M., Loza-Alvarez, P., Li, L. and Rodriguez-Concepcion, M. (2018) 'Interference with Clp protease impairs carotenoid accumulation during tomato fruit ripening', *Journal of Experimental Botany*, 69(7), pp. 1557–1568. https://doi.org/10.1093/jxb/erx491

Davies, J.W. and Cocking, E.C. (1965) 'Changes in carbohydrates, proteins and nucleic acids during cellular development in tomato fruit locule tissue', *Planta*, 67(3), pp. 242–253. https://doi.org/10.1007/BF00385654

Davuluri, G.R., Van Tuinen, A., Fraser, P.D., Manfredonia, A., Newman, R., Burgess, D., Brummell, D.A., King, S.R., Palys, J., Uhlig, J. and Bramley, P.M. (2005) 'Fruit-specific RNAi-

mediated suppression of DET1 enhances carotenoid and flavonoid content in tomatoes', *Nature Biotechnology*, 23(7), pp. 890–895. https://doi.org/10.1038/nbt1108

Díaz de la Garza, R.I., Gregory III, J.F. and Hanson, A.D. (2007) 'Folate biofortification of tomato fruit', *Proceedings of the National Academy of Sciences of the United States of America*, 104(10), pp. 4218–4222. https://doi.org/10.1073/pnas.070040910

De Souza, A.P., Wang, Y., Orr, D.J., Carmo-Silva, E. and Long, S.P. (2020) 'Photosynthesis across African cassava germplasm is limited by Rubisco and mesophyll conductance at steady state, but by stomatal conductance in fluctuating light', *New Phytologist*, 225(6), pp. 2498–2512. https://doi.org/10.1111/nph.16142

Dekker, J.P. and Boekema, E.J. (2005) 'Supramolecular organization of thylakoid membrane proteins in green plants', *Biochimica et Biophysica Acta (BBA) – Bioenergetics*, 1706(1–2), pp. 12–39. https://doi.org/10.1016/j.bbabio.2004.09.009

Dharmapuri, S., Rosati, C., Pallara, P., Aquilani, R., Bouvier, F., Camara, B. and Giuliano, G. (2002) 'Metabolic engineering of xanthophyll content in tomato fruits', *FEBS Letters*, 519(1–3), pp. 30–34. https://doi.org/10.1016/S0014-5793(02)02699-6

de la Garza, R.D., Quinlivan, E.P., Klaus, S.M., Basset, G.J., Gregory III, J.F. and Hanson, A.D. (2004) 'Folate biofortification in tomatoes by engineering the pteridine branch of folate synthesis', *Proceedings of the National Academy of Sciences of the United States of America*, 101(38), pp. 13720–13725. https://doi.org/10.1073/pnas.0404208101

Doddrell, N.H., Lawson, T., Raines, C.A., Wagstaff, C. and Simkin, A.J. (2023) 'Feeding the world: impacts of elevated [CO_2] on nutrient content of greenhouse grown fruit crops and options for future yield gains', *Horticulture Research*, 10(4), Article uhad026. https://doi.org/10.1093/hr/uhad026

Döll, P., Müller Schmied, H., Schuh, C., Portmann, F.T. and Eicker, A. (2014) 'Global-scale assessment of groundwater depletion and related groundwater abstractions: combining hydrological modeling with information from well observations and GRACE satellites', *Water Resources Research*, 50(7), pp. 5698–5720. https://doi.org/10.1002/2014WR015595

Donnarumma, F., Paffetti, D., Fladung, M., Biricolti, S., Dieter, E., Altosaar, I. and Vettori, C. (2011) 'Transgene copy number estimation and analysis of gene expression levels in *Populus*

spp. transgenic lines', *BMC Proceedings*, 5(Suppl. 7), Article P152. https://doi.org/10.1186/1753-6561-5-S7-P152

de Boer, A.D. and Weisbeek, P.J. (1991) 'Chloroplast protein topogenesis: import, sorting and assembly', *Biochimica et Biophysica Acta (BBA) – Reviews on Biomembranes*, 1071(3), pp. 221–253. https://doi.org/10.1016/0304-4157(91)90015-O

Driever, S.M., Simkin, A.J., Alotaibi, S., Fisk, S.J., Madgwick, P.J., Sparks, C.A., Jones, H.D., Lawson, T., Parry, M.A.J. and Raines, C.A. (2017) 'Increased SBPase activity improves photosynthesis and grain yield in wheat grown in greenhouse conditions', *Philosophical Transactions of the Royal Society B: Biological Sciences*, 372(1730), Article 20160384. https://doi.org/10.1098/rstb.2016.0384

Du, K., Xia, Y., Zhan, D., Xu, T., Lu, T., Yang, J. and Kang, X. (2022) 'Genome-wide identification of the *Eucalyptus urophylla* GATA gene family and its diverse roles in chlorophyll biosynthesis', *International Journal of Molecular Sciences*, 23(9), Article 5251. https://doi.org/10.3390/ijms23095251

Dutta, S., Cruz, J.A., Imran, S.M., Chen, J., Kramer, D.M. and Osteryoung, K.W. (2017) 'Variations in chloroplast movement and chlorophyll fluorescence among chloroplast division mutants under light stress', *Journal of Experimental Botany*, 68(13), pp. 3541–3555. https://doi.org/10.1093/jxb/erx203

Eberhard, S., Finazzi, G. and Wollman, F.A. (2008) 'The dynamics of photosynthesis', *Annual Review of Genetics*, 42(1), pp. 463–515. https://doi.org/10.1146/annurev.genet.42.110807.091452

Edwards, K., Johnstone, C. and Thompson, C. (1991) 'A simple and rapid method for the preparation of plant genomic DNA for PCR analysis', *Nucleic Acids Research*, 19(6), p. 1349. https://doi.org/10.1093/nar/19.6.1349

Egea, I., Barsan, C., Bian, W., Purgatto, E., Latché, A., Chervin, C., Bouzayen, M. and Pech, J.C. (2010) 'Chromoplast differentiation: current status and perspectives', *Plant and Cell Physiology*, 51(10), pp. 1601–1611. https://doi.org/10.1093/pcp/pcq136

Egea, I., Bian, W., Barsan, C., Jauneau, A., Pech, J.C., Latché, A., Li, Z. and Chervin, C. (2011) 'Chloroplast to chromoplast transition in tomato fruit: spectral confocal microscopy analyses of

carotenoids and chlorophylls in isolated plastids and time-lapse recording on intact live tissue', *Annals of Botany*, 108(2), pp. 291–297. https://doi.org/10.1093/aob/mcr140

Ellul, P., Garcia-Sogo, B., Pineda, B., Rios, G., Roig, L. and Moreno, V. (2003) 'The ploidy level of transgenic plants in *Agrobacterium*-mediated transformation of tomato cotyledons (*Lycopersicon esculentum* L. Mill.) is genotype and procedure dependent', *Theoretical and Applied Genetics*, 106(2), pp. 231–238. https://doi.org/10.1007/s00122-002-0928-y

Elo, A., Lemmetyinen, J., Turunen, M.L., Tikka, L. and Sopanen, T. (2001) 'Three MADS-box genes similar to APETALA1 and FRUITFULL from silver birch (*Betula pendula*)', *Physiologia Plantarum*, 112(1), pp. 95–103. https://doi.org/10.1034/j.1399-3054.2001.1120113.x

Engler, C., Gruetzner, R., Kandzia, R. and Marillonnet, S. (2009) 'Golden gate shuffling: a one-pot DNA shuffling method based on type IIs restriction enzymes', *PLoS ONE*, 4(5), Article e5553. https://doi.org/10.1371/journal.pone.0005553

Engler, C. and Marillonnet, S. (2013) 'Golden gate cloning', in Valla, S. and Lale, R. (eds.) *DNA cloning and assembly methods*. Totowa, NJ: Humana Press, pp. 119–131. https://doi.org/10.1007/978-1-62703-764-8_9

Ermakova, M., Woodford, R., Taylor, Z., Furbank, R.T., Belide, S. and von Caemmerer, S. (2023) 'Faster induction of photosynthesis increases biomass and grain yield in glasshouse-grown transgenic *Sorghum bicolor* overexpressing Rieske FeS', *Plant Biotechnology Journal*, 21(6), pp. 1206–1216. https://doi.org/10.1111/tpj.14562

Escobar, M.A. and Dandekar, A.M. (2003) '*Agrobacterium tumefaciens* as an agent of disease', *Trends in Plant Science*, 8(8), pp. 380–386. https://doi.org/10.1016/S1360-1385(03)00162-6

Evans, J.R. (2013) 'Improving photosynthesis', *Plant Physiology*, 162(4), pp. 1780–1793. https://doi.org/10.1104/pp.113.219006

FAO, IFAD, UNICEF, WFP and WHO (2021) *The state of food security and nutrition in the world 2021*. Rome: FAO. https://doi.org/10.4060/cb4474en

FAO (2023) *FAOSTAT – Quality, Crops and Livestock (QCL)*. Rome: Food and Agriculture Organization of the United Nations. Available at: https://www.fao.org/faostat/en/#data/QCL (Accessed: 10 September 2025).

Feng, P., Guo, H., Chi, W., Chai, X., Sun, X., Xu, X., Ma, J., Rochaix, J.D., Leister, D., Wang, H. and Lu, C. (2016) 'Chloroplast retrograde signal regulates flowering', *Proceedings of the National Academy of Sciences of the United States of America*, 113(38), pp. 10708–10713. https://doi.org/10.1073/pnas.1521599113

Foley, J.A., Ramankutty, N., Brauman, K.A., Cassidy, E.S., Gerber, J.S., Johnston, M., Mueller, N.D., O'Connell, C., Ray, D.K., West, P.C. and Balzer, C. (2011) 'Solutions for a cultivated planet', *Nature*, 478(7369), pp. 337–342. https://doi.org/10.1038/nature10452

Forth, D. and Pyke, K.A. (2006) 'The suffulta mutation in tomato reveals a novel method of plastid replication during fruit ripening', *Journal of Experimental Botany*, 57(9), pp. 1971–1979. https://doi.org/10.1093/jxb/erj144

Fraser, P.D., Römer, S., Shipton, C.A., Mills, P.B., Kiano, J.W., Misawa, N., Drake, R.G., Schuch, W. and Bramley, P.M. (2002) 'Evaluation of transgenic tomato plants expressing an additional phytoene synthase in a fruit-specific manner', *Proceedings of the National Academy of Sciences of the United States of America*, 99(2), pp. 1092–1097. https://doi.org/10.1073/pnas.241374598

Friedland, N., Negi, S., Vinogradova-Shah, T., Wu, G., Ma, L., Flynn, S., Kumssa, T., Lee, C.H. and Sayre, R.T. (2019) 'Fine-tuning the photosynthetic light harvesting apparatus for improved photosynthetic efficiency and biomass yield', *Scientific Reports*, 9(1), Article 13028. https://doi.org/10.1038/s41598-019-49545-8

Fuglie, K., Gautam, M., Goyal, A. and Maloney, W.F. (2019) *Harvesting prosperity: technology and productivity growth in agriculture*. Washington, DC: World Bank. https://doi.org/10.1596/978-1-4648-1393-1

Fuglie, K., Morgan, S. and Jelliffe, J. (2024) *World agricultural production, resource use, and productivity, 1961–2020*. Washington, DC: United States Department of Agriculture. https://doi.org/10.22004/ag.econ.341638

Galpaz, N., Wang, Q., Menda, N., Zamir, D. and Hirschberg, J. (2008) 'Abscisic acid deficiency in the tomato mutant high-pigment 3 leading to increased plastid number and higher fruit lycopene content', *The Plant Journal*, 53(5), pp. 717–730. https://doi.org/10.1111/j.1365-313X.2007.03362.x

Gannon, B., Kaliwile, C., Arscott, S.A., Schmaelzle, S., Chileshe, J., Kalungwana, N., Mosonda, M., Pixley, K., Masi, C. and Tanumihardjo, S.A. (2014) 'Biofortified orange maize is as efficacious as a vitamin A supplement in Zambian children even in the presence of high liver reserves of vitamin A: a community-based, randomized placebo-controlled trial', *The American Journal of Clinical Nutrition*, 100(6), pp. 1541–1550. https://doi.org/10.3945/ajcn.114.087379

Gao, J., Wang, H., Yuan, Q. and Feng, Y. (2018) 'Structure and function of the photosystem supercomplexes', *Frontiers in Plant Science*, 9, Article 357. https://doi.org/10.3389/fpls.2018.00357

Garrido, A., Conde, A., Serôdio, J., De Vos, R.C.H. and Cunha, A. (2023) 'Fruit photosynthesis: more to know about where, how and why', *Plants*, 12(13), Article 2393. https://doi.org/10.3390/plants12132393

Garruña-Hernández, R., Monforte-González, M., Canto-Aguilar, A., Vázquez-Flota, F. and Orellana, R. (2013) 'Enrichment of carbon dioxide in the atmosphere increases the capsaicinoids content in Habanero peppers (*Capsicum chinense* Jacq.)', *Journal of the Science of Food and Agriculture*, 93(6), pp. 1385–1388. https://doi.org/10.1002/jsfa.5904

Gerszberg, A. and Grzegorczyk-Karolak, I. (2019) 'Influence of selected antibiotics on tomato regeneration in in vitro cultures', *Notulae Botanicae Horti Agrobotanici Cluj-Napoca*, 47(3), pp. 858–865. https://doi.org/10.15835/nbha47311401

Gray, S.B., Dermody, O., Klein, S.P., Locke, A.M., McGrath, J.M., Paul, R.E., Rosenthal, D.M., Ruiz-Vera, U.M., Siebers, M.H., Strellner, R., Ainsworth, E.A., Bernacchi, C.J., Long, S.P., Ort, D.R. and Leakey, A.D.B. (2016) 'Intensifying drought eliminates the expected benefits of elevated carbon dioxide for soybean', *Nature Plants*, 2, Article 16132. https://doi.org/10.1038/nplants.2016.132

Giménez, E., Pineda, B., Capel, J., Antón, M.T., Atarés, A., Pérez-Martín, F., García-Sogo, B., Angosto, T., Moreno, V. and Lozano, R. (2010) 'Functional analysis of the Arlequin mutant corroborates the essential role of the ARLEQUIN/TAGL1 gene during reproductive development of tomato', *PLoS ONE*, 5(12), Article e14427. https://doi.org/10.1371/journal.pone.0014427

Głowacka, K., Kromdijk, J., Salesse-Smith, C.E., Smith, C., Driever, S.M. and Long, S.P. (2023) 'Is chloroplast size optimal for photosynthetic efficiency?', *New Phytologist*, 239(6), pp. 2197–2211. https://doi.org/10.1111/nph.19091

Gray, J., Picton, S., Shabbeer, J., Schuch, W. and Grierson, D. (1992) 'Molecular biology of fruit ripening and its manipulation with antisense genes', *Plant Molecular Biology*, 19(1), pp. 69–87. https://doi.org/10.1007/BF00015609

Gray, M.W. (1989) 'The evolutionary origins of organelles', *Trends in Genetics*, 5, pp. 294–299. https://doi.org/10.1016/0168-9525(89)90111-X

Gray, S.B., Dermody, O., Klein, S.P., Locke, A.M., McGrath, J.M., Paul, R.E., Rosenthal, D.M., Ruiz-Vera, U.M., Siebers, M.H., Strellner, R., Ainsworth, E.A., Bernacchi, C.J., Long, S.P., Ort, D.R. and Leakey, A.D.B. (2016) 'Intensifying drought eliminates the expected benefits of elevated carbon dioxide for soybean', *Nature Plants*, 2, Article 16132. https://doi.org/10.1038/nplants.2016.132

Grimplet, J., Martínez-Zapater, J.M. and Carmona, M.J. (2016) 'Structural and functional annotation of the MADS-box transcription factor family in grapevine', *BMC Genomics*, 17(1), Article 80. https://doi.org/10.1186/s12864-016-2398-7

Gurrieri, L., Fermani, S., Zaffagnini, M., Sparla, F. and Trost, P. (2021) 'Calvin–Benson cycle regulation is getting complex', *Trends in Plant Science*, 26(9), pp. 898–912. https://doi.org/10.1016/j.tplants.2021.03.008

Hanson, M.R., Lin, M.T., Carmo-Silva, A.E. and Parry, M.A.J. (2016) 'Towards engineering carboxysomes into C_3 plants', *The Plant Journal*, 87(1), pp. 38–50. https://doi.org/10.1111/tpj.13139

Hernández-Verdeja, T. and Lundgren, M.R. (2024) 'GOLDEN2-LIKE transcription factors: a golden ticket to improve crops?', *Plants, People, Planet*, 6(1), pp. 79–93. https://doi.org/10.1002/ppp3.10412

Hetherington, S.E., Smillie, R.M. and Davies, W.J. (1998) 'Photosynthetic activities of vegetative and fruiting tissues of tomato', *Journal of Experimental Botany*, 49(324), pp. 1173–1181. https://doi.org/10.1093/jxb/49.324.1173

Heyno, E., Ermakova, M., Lopez-Calcagno, P.E., Woodford, R., Brown, K.L., Matthews, J.S.A., Osmond, B., Raines, C.A. and von Caemmerer, S. (2022) 'Rieske FeS overexpression in tobacco provides increased abundance and activity of cytochrome b_6f', *Physiologia Plantarum*, 174(6), Article e13803. https://doi.org/10.1111/ppl.13803

Hu, W. and Phillips, G.C. (2001) 'A combination of overgrowth-control antibiotics improves *Agrobacterium tumefaciens*-mediated transformation efficiency for cultivated tomato (*L. esculentum*)', *In Vitro Cellular and Developmental Biology – Plant*, 37, pp. 12–18. https://doi.org/10.1079/IVP2000130

Hudson, D. (2010) *CGA1 and GNC are key controllers modulating chlorophyll content, chloroplast number and starch*. PhD thesis. University of Guelph.

Hudson, D., Guevara, D., Yaish, M.W., Hannam, C., Long, N., Clarke, J.D., Bi, Y.M. and Rothstein, S.J. (2011) 'GNC and CGA1 modulate chlorophyll biosynthesis and glutamate synthase (GLU1/FD-GOGAT) expression in *Arabidopsis*', *PLoS ONE*, 6(11), Article e26765. https://doi.org/10.1371/journal.pone.0026765

Hunziker, J., Nishida, K., Kondo, A., Kishimoto, S., Ariizumi, T. and Ezura, H. (2020) 'Multiple gene substitution by Target-AID base-editing technology in tomato', *Scientific Reports*, 10(1), Article 20471. https://doi.org/10.1038/s41598-020-77379-2

Iizumi, T., Shiogama, H., Imada, Y., Hanasaki, N., Takikawa, H. and Nishimori, M. (2018) 'Crop production losses associated with anthropogenic climate change for 1981–2010 compared with preindustrial levels', *International Journal of Climatology*, 38(14), pp. 5405–5417. https://doi.org/10.1002/joc.5818

Intergovernmental Panel on Climate Change (IPCC) (2022) *Climate change 2022: impacts, adaptation and vulnerability*. Cambridge: Cambridge University Press. https://doi.org/10.1017/9781009325844

Irish, V. (2017) 'The ABC model of floral development', *Current Biology*, 27(17), pp. R887–R890. https://doi.org/10.1016/j.cub.2017.08.045

Islam, M.S., Matsui, T. and Yoshida, Y. (1996) 'Effect of carbon dioxide enrichment on physico-chemical and enzymatic changes in tomato fruits at various stages of maturity', *Scientia Horticulturae*, 65(2–3), pp. 137–149. https://doi.org/10.1016/0304-4238(95)00867-5

Jaggard, K.W., Qi, A. and Ober, S. (2010) 'Possible changes to arable crop yields by 2050', *Philosophical Transactions of the Royal Society B: Biological Sciences*, 365(1554), pp. 2835–2851. https://doi.org/10.1098/rstb.2010.0153

Jarvis, P. and López-Juez, E. (2013) 'Biogenesis and homeostasis of chloroplasts and other plastids', *Nature Reviews Molecular Cell Biology*, 14(12), pp. 787–802. https://doi.org/10.1038/nrm3702

Hibberd, J.M. and Quick, W.P. (2002) 'Characteristics of C_4 photosynthesis in stems and petioles of C_3 flowering plants', *Nature*, 415(6870), pp. 451–454. https://doi.org/10.1038/415451a

Hills, A.C., Khan, S. and López-Juez, E. (2015) 'Chloroplast biogenesis-associated nuclear genes: control by plastid signals evolved prior to their regulation as part of photomorphogenesis', *Frontiers in Plant Science*, 6, Article 1078. https://doi.org/10.3389/fpls.2015.01078

Hiwasa-Tanase, K., Kuroda, H., Hirai, T., Aoki, K., Takane, K. and Ezura, H. (2012) 'Novel promoters that induce specific transgene expression during the green to ripening stages of tomato fruit development', *Plant Cell Reports*, 31(8), pp. 1415–1424. https://doi.org/10.1007/s00299-012-1257-5

Ho, Q.T., Verboven, P., Verlinden, B.E., Lammertyn, J., Vandewalle, S. and Nicolaï, B.M. (2008) 'A continuum model for metabolic gas exchange in pear fruit', *PLoS Computational Biology*, 4(3), Article e1000023. https://doi.org/10.1371/journal.pcbi.1000023

Hoeberichts, F.A., Van der Plas, L.H.W. and Woltering, E.J. (2002) 'Ethylene perception is required for the expression of tomato ripening-related genes and associated physiological changes even at advanced stages of ripening', *Postharvest Biology and Technology*, 26, pp. 125–133. https://doi.org/10.1016/S0925-5214(02)00016-1

Horsch, R.B., Fraley, R.T., Rogers, S.G., Sanders, P.R., Lloyd, A. and Hoffmann, N. (1984) 'Inheritance of functional foreign genes in plants', *Science*, 223(4635), pp. 496–498. https://doi.org/10.1126/science.223.4635.496

Hu, Q., Zhang, H., Song, Y., Song, L., Zhu, L., Kuang, H. and Larkin, R.M. (2024) 'REDUCED CHLOROPLAST COVERAGE proteins are required for plastid proliferation and carotenoid accumulation in tomato', *Plant Physiology*, 196(1), pp. 511–534. https://doi.org/10.1093/plphys/kiae275

Jiang, X., Lubini, G., Hernandes-Lopes, J., Rijnsburger, K., Veltkamp, V., de Maagd, R.A., Angenent, G.C. and Bemer, M. (2022) 'FRUITFULL-like genes regulate flowering time and inflorescence architecture in tomato', *The Plant Cell*, 34(3), pp. 1002–1019. https://doi.org/10.1093/plcell/koab298

Jin, H., Li, M., Duan, S., Fu, M., Dong, X., Liu, B., Feng, D., Wang, J. and Wang, H.B. (2016) 'Optimization of light-harvesting pigment improves photosynthetic efficiency', *Plant Physiology*, 172(3), pp. 1720–1731. https://doi.org/10.1104/pp.16.00698

Johns, T. and Eyzaguirre, P.B. (2007) 'Biofortification, biodiversity and diet: a search for complementary applications against poverty and malnutrition', *Food Policy*, 32(1), pp. 1–24. https://doi.org/10.1016/j.foodpol.2006.03.014

Juniper, B.E. and Clowes, F.A.L. (1965) 'Cytoplasmic organelles and cell growth in root caps', *Nature*, 208(5013), pp. 864–865. https://doi.org/10.1038/208864a0

Kahlau, S. and Bock, R. (2008) 'Plastid transcriptomics and translatomics of tomato fruit development and chloroplast-to-chromoplast differentiation: chromoplast gene expression largely serves the production of a single protein', *The Plant Cell*, 20(4), pp. 856–874. https://doi.org/10.1105/tpc.107.055202

Kasahara, M., Kagawa, T., Oikawa, K., Suetsugu, N., Miyao, M. and Wada, M. (2002) 'Chloroplast avoidance movement reduces photodamage in plants', *Nature*, 420(6917), pp. 829–832. https://doi.org/10.1038/nature01202

Kato, Y., Sun, X., Zhang, L. and Sakamoto, W. (2012) 'Cooperative D1 degradation in the photosystem II repair mediated by chloroplastic proteases in *Arabidopsis*', *Plant Physiology*, 159(4), pp. 1428–1439. https://doi.org/10.1104/pp.112.199042

Kawaguchi, K., Takei-Hoshi, R., Yoshikawa, I., Nishida, K., Kobayashi, M., Kusano, M., Lu, Y., Ariizumi, T., Ezura, H., Otagaki, S., Matsumoto, S. and Shiratake, K. (2021) 'Functional disruption of cell wall invertase inhibitor by genome editing increases sugar content of tomato fruit without decrease fruit weight', *Scientific Reports*, 11(1), Article 20483. https://doi.org/10.1038/s41598-021-00966-4

Khan, I., Azam, A. and Mahmood, A. (2013) 'The impact of enhanced atmospheric carbon dioxide on yield, proximate composition, elemental concentration, fatty acid and vitamin C

contents of tomato (*Lycopersicon esculentum*)', *Environmental Monitoring and Assessment*, 185(1), pp. 205–214. https://doi.org/10.1007/s10661-012-2544-x

Kim, W., Iizumi, T. and Nishimori, M. (2019) 'Global patterns of crop production losses associated with droughts from 1983 to 2009', *Journal of Applied Meteorology and Climatology*, 58(6), pp. 1233–1244. https://doi.org/10.1175/JAMC-D-18-0174.1

Kirchhoff, H. (2019) 'Chloroplast ultrastructure in plants', *New Phytologist*, 223(2), pp. 565–574. https://doi.org/10.1111/nph.15730

Klee, H.J. and Giovannoni, J.J. (2011) 'Genetics and control of tomato fruit ripening and quality attributes', *Annual Review of Genetics*, 45, pp. 41–59. https://doi.org/10.1146/annurev-genet-110410-132507

Klee, H.J. and Resende, M.F.R. (2020) 'Plant domestication: reconstructing the route to modern tomatoes', *Current Biology*, 30(8), pp. R359–R361. https://doi.org/10.1016/j.cub.2020.02.072

Klimaszewska, K., Lachance, D., Bernier-Cardou, M. and Rutledge, R.G. (2003) 'Transgene integration patterns and expression levels in transgenic tissue lines of *Picea mariana*, *P. glauca* and *P. abies*', *Plant Cell Reports*, 21(11), pp. 1080–1087. https://doi.org/10.1007/s00299-003-0626-5

Knoblauch, J., Waadt, R., Cousins, A.B. and Kunz, H.H. (2024) 'Probing the in situ volumes of *Arabidopsis* leaf plastids using three-dimensional confocal and scanning electron microscopy', *The Plant Journal*, 117(2), pp. 332–341. https://doi.org/10.1111/tpj.16554

Krause, G.H. and Weis, E. (1991) 'Chlorophyll fluorescence and photosynthesis: the basics', *Annual Review of Plant Physiology and Plant Molecular Biology*, 42, pp. 313–362.

Kuntz, M., Chen, H.C., Simkin, A.J., Römer, S., Shipton, C.A., Drake, R., Schuch, W. and Bramley, P.M. (1998) 'Upregulation of two ripening-related genes from a non-climacteric plant (pepper) in a transgenic climacteric plant (tomato)', *The Plant Journal*, 13(3), pp. 351–361. https://doi.org/10.1046/j.1365-313x.1998.00355.x

Langenkämper, G., Manac'h, N., Broin, M., Cuiné, S., Becuwe, N., Kuntz, M. and Rey, P. (2001) 'Accumulation of plastid lipid-associated proteins (fibrillin/CDSP34) upon oxidative stress, ageing and biotic stress in *Solanaceae* and in response to drought in other species', *Journal of Experimental Botany*, 52(360), pp. 1545–1554. https://doi.org/10.1093/jexbot/52.360.1545

Larkin, R.M., Stefano, G., Ruckle, M.E., Stavoe, A.K., Sinkler, C.A., Brandizzi, F., Malmstrom, C.M., Osteryoung, K.W. and Chory, J. (2016) 'REDUCED CHLOROPLAST COVERAGE genes from *Arabidopsis thaliana* help to establish the size of the chloroplast compartment', *Proceedings of the National Academy of Sciences of the United States of America*, 113(8), pp. E1116–E1125. https://doi.org/10.1073/pnas.1515741113

Laval-Martin, D. (1977) 'Light versus dark carbon metabolism in cherry tomato fruits: I. Occurrence of photosynthesis. Study of the intermediates', *Plant Physiology*, 60(6), pp. 872–876.

Leclère, D., Obersteiner, M., Barrett, M., Butchart, S.H.M., Chaudhary, A., De Palma, A., DeClerck, F.A.J., Di Marco, M., Doelman, J.C., Dürauer, M., Freeman, R., Harfoot, M., Hasegawa, T., Hellweg, S., Hilbers, J.P., Hill, S.L.L., Humpenöder, F., Jennings, N., Krisztin, T. and Young, L. (2020) 'Bending the curve of terrestrial biodiversity needs an integrated strategy', *Nature*, 585(7826), pp. 551–556. https://doi.org/10.1038/s41586-020-2705-y

Lefebvre, S., Lawson, T., Zakhleniuk, O.V., Lloyd, J.C. and Raines, C.A. (2005) 'Increased sedoheptulose-1,7-bisphosphatase activity in transgenic tobacco plants stimulates photosynthesis and growth from an early stage in development', *Plant Physiology*, 138(1), pp. 451–460. https://doi.org/10.1104/pp.104.055046

Li, C., Lu, X., Xu, J. and Liu, Y. (2023) 'Regulation of fruit ripening by MADS-box transcription factors', *Scientia Horticulturae*, 314, Article 111950. https://doi.org/10.1016/j.scienta.2023.111950

Li, F., Wang, J., Chen, Y., Zou, Z., Wang, X. and Yue, M. (2007) 'Combined effects of enhanced ultraviolet-B radiation and doubled CO_2 concentration on growth, fruit quality and yield of tomato in winter plastic greenhouse', *Frontiers of Biology in China*, 2(4), pp. 414–418. https://doi.org/10.1007/s11515-007-0063-x

Li, L. and Yuan, H. (2013) 'Chromoplast biogenesis and carotenoid accumulation', *Archives of Biochemistry and Biophysics*, 539(2), pp. 102–109. https://doi.org/10.1016/j.abb.2013.07.002

Liang, G., Liu, J., Zhang, J. and Guo, J. (2020) 'Effects of drought stress on photosynthetic and physiological parameters of tomato', *Journal of the American Society for Horticultural Science*, 145(1), pp. 12–17. https://doi.org/10.21273/jashs04725-19

Liu, H. (2015) *Comparing Welch ANOVA, a Kruskal-Wallis test, and traditional ANOVA in case of heterogeneity of variance*. PhD thesis. Virginia Commonwealth University.

Long, S.P., Humphries, S. and Falkowski, P.G. (1994) 'Photoinhibition of photosynthesis in nature', *Annual Review of Plant Physiology and Plant Molecular Biology*, 45(1), pp. 633–662.

Long, S.P., Marshall-Colon, A. and Zhu, X.-G. (2015) 'Meeting the global food demand of the future by engineering crop photosynthesis and yield potential', *Cell*, 161(1), pp. 56–66. https://doi.org/10.1016/j.cell.2015.03.019

Long, S.P., Zhu, X.-G., Naidu, S.L. and Ort, D.R. (2006) 'Can improvement in photosynthesis increase crop yields?', *Plant, Cell and Environment*, 29(3), pp. 315–330. https://doi.org/10.1111/j.1365-3040.2005.01493.x

Long, S.P., Zhu, X.-G., Portis Jr, A.R. and Ort, D.R. (2004) 'Would transformation of C_3 crop plants with foreign Rubisco increase productivity? A computational analysis extrapolating from kinetic properties to canopy photosynthesis', *Plant, Cell and Environment*, 27, pp. 155–165. https://doi.org/10.1111/j.1365-3040.2003.01322.x

Lopez, A.B., Van Eck, J., Conlin, B.J., Paolillo, D.J., O'Neill, J. and Li, L. (2008) 'Effect of the cauliflower transgene on carotenoid accumulation and chromoplast formation in transgenic potato tubers', *Journal of Experimental Botany*, 59(2), pp. 213–223. https://doi.org/10.1093/jxb/erm299

Lopez-Juez, E. and Pyke, K.A. (2005) 'Plastids unleashed: their development and their integration in plant development', *International Journal of Developmental Biology*, 49(5–6), pp. 557–577. https://doi.org/10.1387/ijdb.051997el

Lu, G., Casaretto, J.A., Ying, S., Mahmood, K., Liu, F., Bi, Y.M. and Rothstein, S.J. (2017) 'Overexpression of *OsGATA12* regulates chlorophyll content, delays plant senescence and improves rice yield under high density planting', *Plant Molecular Biology*, 94(1–2), pp. 215–227. https://doi.org/10.1007/s11103-017-0604-x

Lu, S. and Li, L. (2008) 'Carotenoid metabolism: biosynthesis, regulation, and beyond', *Journal of Integrative Plant Biology*, 50(7), pp. 778–785. https://doi.org/10.1111/j.1744-7909.2008.00708.x

Lu, S., Van Eck, J., Zhou, X., Lopez, A.B., O'Halloran, D.M., Cosman, K.M., Conlin, B.J., Paolillo, D.J., Garvin, D.F., Vrebalov, J., Kochian, L.V., Küpper, H., Earle, E.D., Cao, J. and Li, L. (2006) 'The cauliflower *Or* gene encodes a DnaJ cysteine-rich domain-containing protein that mediates high levels of β-carotene accumulation', *The Plant Cell*, 18(12), pp. 3594–3605. https://doi.org/10.1105/tpc.106.046417

Lupi, A.C.D.L., Silvestre Lira, B., Gramegna, G., Trench, B., Rocha, F., Alves, R., Demarco, D., Eustáquio, L., Peres, P., Purgatto, E., Freschi, L. and Rossi, M. (2019) '*Solanum lycopersicum* GOLDEN2-LIKE 2 transcription factor affects fruit quality in a light- and auxin-dependent manner', *PLoS ONE*, 14(2), Article e0212224. https://doi.org/10.1371/journal.pone.0212224

Lytovchenko, A., Eickmeier, I., Pons, C., Osorio, S., Szecowka, M., Lehmberg, K., Arrivault, S., Tohge, T., Pineda, B., Anton, M.T., Hedtke, B., Lu, Y., Fisahn, J., Bock, R., Stitt, M., Grimm, B., Granell, A. and Fernie, A.R. (2011) 'Tomato fruit photosynthesis is seemingly unimportant in primary metabolism and ripening but plays a considerable role in seed development', *Plant Physiology*, 157(4), pp. 1650–1663. https://doi.org/10.1104/pp.111.186874

Manac'h, N. and Kuntz, M. (1999) 'Stress induction of a nuclear gene encoding for a plastid protein is mediated by photo-oxidative events', *Plant Physiology and Biochemistry*, 37(11), pp. 859–868. https://doi.org/10.1016/S0981-9428(99)00112-6

Mandel, M.A. and Yanofsky, M.F. (1995) 'A gene triggering flower formation in *Arabidopsis*', *Nature*, 377, pp. 522–524. https://doi.org/10.1038/377522a0

Maple, J. and Møller, S.G. (2007) 'Plastid division coordination across a double-membraned structure', *FEBS Letters*, 581(11), pp. 2162–2167. https://doi.org/10.1016/j.febslet.2007.02.062

Mariem, S.B., Soba, D., Zhou, B., Loladze, I., Morales, F. and Aranjuelo, I. (2021) 'Climate change, crop yields, and grain quality of C_3 cereals: a meta-analysis of [CO_2], temperature, and drought effects', *Plants*, 10(6), Article 1052. https://doi.org/10.3390/plants10061052

Marrison, J.L., Rutherford, S.M., Robertson, E.J., Lister, C., Dean, C. and Leech, R.M. (1999) 'The distinctive roles of five different ARC genes in the chloroplast division process in *Arabidopsis*', *The Plant Journal*, 18(6), pp. 651–662. https://doi.org/10.1046/j.1365-313x.1999.00500.x

Mayer, J.E., Pfeiffer, W.H. and Beyer, P. (2008) 'Biofortified crops to alleviate micronutrient malnutrition', *Current Opinion in Plant Biology*, 11(2), pp. 166–170. https://doi.org/10.1016/j.pbi.2008.01.007

McCarl, B.A., Fei, C., Mu, J. and Wang, X. (2022) 'Managing land carrying capacity: key to achieving sustainable production systems for food security', *Land*, 11(4), Article 484. https://doi.org/10.3390/land11040484

McCormick, S., Niedermeyer, J., Fry, J., Barnason, A., Horsch, R. and Fraley, R. (1986) 'Leaf disc transformation of cultivated tomato (*L. esculentum*) using *Agrobacterium tumefaciens*', *Plant Cell Reports*, 5, pp. 1–8. https://doi.org/10.1007/BF00269248

Meng, L., Fan, Z., Zhang, Q., Wang, C., Gao, Y., Deng, Y., Zhu, B., Zhu, H., Chen, J., Shan, W., Yin, X., Zhong, S., Grierson, D., Jiang, C.Z., Luo, Y. and Fu, D.Q. (2018) 'BEL1-LIKE HOMEODOMAIN 11 regulates chloroplast development and chlorophyll synthesis in tomato fruit', *The Plant Journal*, 94(6), pp. 1126–1140. https://doi.org/10.1111/tpj.13924

Mielecki, J., Gawroński, P. and Karpiński, S. (2020) 'Retrograde signaling: understanding the communication between organelles', *International Journal of Molecular Sciences*, 21(17), Article 6173. https://doi.org/10.3390/ijms21176173

Milhet, Y. and Costes, C. (1975) 'Effects of CO_2 nutrition on growth and yield of muskmelon (*Cucumis melo* L.), egg-plant (*Solanum melongena* L.) and sweet-pepper (*Capsicum annuum* L.)', *Acta Horticulturae*, 51, pp. 201–212. https://doi.org/10.17660/actahortic.1975.51.21

Mirkovic, T., Ostroumov, E.E., Anna, J.M., Van Grondelle, R., Govindjee and Scholes, G.D. (2017) 'Light absorption and energy transfer in the antenna complexes of photosynthetic organisms', *Chemical Reviews*, 117(2), pp. 249–293. https://doi.org/10.1021/acs.chemrev.6b00002

Mirzabaev, A., Bezner Kerr, R., Hasegawa, T., Pradhan, P., Wreford, A., Cristina Tirado von der Pahlen, M. and Gurney-Smith, H. (2023) 'Severe climate change risks to food security and nutrition', *Climate Risk Management*, 39, Article 100473. https://doi.org/10.1016/j.crm.2022.100473

Miyagishima, S.-Y., Froehlich, J.E. and Osteryoung, K.W. (2006) 'PDV1 and PDV2 mediate recruitment of the dynamin-related protein ARC5 to the plastid division site', *The Plant Cell*, 18(10), pp. 2517–2530. https://doi.org/10.1105/tpc.106.045484

Miyawaki, K., Matsumoto-Kitano, M. and Kakimoto, T. (2004) 'Expression of cytokinin biosynthetic isopentenyltransferase genes in *Arabidopsis*: tissue specificity and regulation by auxin, cytokinin, and nitrate', *The Plant Journal*, 37(1), pp. 128–138. https://doi.org/10.1046/j.1365-313x.2003.01945.x

Molesini, B., Dusi, V., Pennisi, F. and Pandolfini, T. (2020) 'How hormones and MADS-box transcription factors are involved in controlling fruit set and parthenocarpy in tomato', *Genes*, 11(12), Article 1441. https://doi.org/10.3390/genes11121441

Molotoks, A., Smith, P. and Dawson, T.P. (2021) 'Impacts of land use, population, and climate change on global food security', *Food and Energy Security*, 10(1), Article e261. https://doi.org/10.1002/fes3.261

Morelli, L., García Romañach, L., Glauser, G., Shanmugabalaji, V., Kessler, F. and Rodriguez-Concepcion, M. (2023) 'Nutritional enrichment of plant leaves by combining genes promoting tocopherol biosynthesis and storage', *Metabolites*, 13(2), Article 193. https://doi.org/10.3390/metabo13020193

Munaweera, T.I.K., Jayawardana, N.U., Rajaratnam, R. and Dissanayake, N. (2022) 'Modern plant biotechnology as a strategy in addressing climate change and attaining food security', *Agriculture and Food Security*, 11(1), Article 69. https://doi.org/10.1186/s40066-022-00369-2

Murchie, E.H. and Lawson, T. (2013) 'Chlorophyll fluorescence analysis: a guide to good practice and understanding some new applications', *Journal of Experimental Botany*, 64(13), pp. 3983–3998. https://doi.org/10.1093/jxb/ert208

Murchie, E.H. and Ruban, A.V. (2020) 'Dynamic non-photochemical quenching in plants: from molecular mechanism to productivity', *The Plant Journal*, 101(4), pp. 885–896. https://doi.org/10.1111/tpj.14601

Nagaya, S., Kawamura, K., Shinmyo, A. and Kato, K. (2010) 'The HSP terminator of *Arabidopsis thaliana* increases gene expression in plant cells', *Plant and Cell Physiology*, 51(2), pp. 328–332. https://doi.org/10.1093/pcp/pcp188

Naito, T., Kiba, T., Koizumi, N., Yamashino, T. and Mizuno, T. (2007) 'Characterization of a unique GATA family gene that responds to both light and cytokinin in *Arabidopsis thaliana*',

Bioscience, Biotechnology and Biochemistry, 71(6), pp. 1557–1560. https://doi.org/10.1271/bbb.60692

Nakano, T., Kimbara, J., Fujisawa, M., Kitagawa, M., Ihashi, N., Maeda, H., Kasumi, T. and Ito, Y. (2012) 'MACROCALYX and JOINTLESS interact in the transcriptional regulation of tomato fruit abscission zone development', *Plant Physiology*, 158(1), pp. 439–450. https://doi.org/10.1104/pp.111.183731

Naqvi, S., Zhu, C., Farré, G., Ramessar, K., Bassie, L., Breitenbach, J., Conesa, D.P., Ros, G., Sandmann, G., Capell, T. and Christou, P. (2009) 'Transgenic multivitamin corn through biofortification of endosperm with three vitamins representing three distinct metabolic pathways', *Proceedings of the National Academy of Sciences of the United States of America*, 106(19), pp. 7762–7767. https://doi.org/10.1073/pnas.0901412106

Nasir, M.U., Hussain, S. and Jabbar, S. (2015) 'Tomato processing, lycopene and health benefits: a review', *Science Letters*, 3(1), pp. 1–5.

Nelson, N. and Yocum, C.F. (2006) 'Structure and function of photosystems I and II', *Annual Review of Plant Biology*, 57(1), pp. 521–565. https://doi.org/10.1146/annurev.arplant.57.032905.105350

Nezhdanova, A.V., Slugina, M.A., Dyachenko, E.A., Kamionskaya, A.M., Kochieva, E.Z. and Shchennikova, A.V. (2021) 'Analysis of the structure and function of the tomato *Solanum lycopersicum* L. MADS-box gene *SlMADS5*', *Vavilov Journal of Genetics and Breeding*, 25(5), pp. 492–500. https://doi.org/10.18699/vj21.056

Ng, M. and Yanofsky, M.F. (2001) 'Function and evolution of the plant MADS-box gene family', *Nature Reviews Genetics*, 2, pp. 186–195. https://doi.org/10.1038/35056041

Nguyen, C.V., Vrebalov, J.T., Gapper, N.E., Zheng, Y., Zhong, S., Fei, Z. and Giovannoni, J.J. (2014) 'Tomato GOLDEN2-LIKE transcription factors reveal molecular gradients that function during fruit development and ripening', *The Plant Cell*, 26(2), pp. 585–601. https://doi.org/10.1105/tpc.113.118794

Nisar, N., Li, L., Lu, S., Khin, N.C. and Pogson, B.J. (2015) 'Carotenoid metabolism in plants', *Molecular Plant*, 8(1), pp. 68–82. https://doi.org/10.1016/j.molp.2014.12.007

Ohnishi, A., Wada, H. and Kobayashi, K. (2018) 'Improved photosynthesis in *Arabidopsis* roots by activation of GATA transcription factors', *Photosynthetica*, 56(1), pp. 433–444. https://doi.org/10.1007/s11099-018-0785-9

Okazaki, K., Kabeya, Y., Suzuki, K., Mori, T., Ichikawa, T., Matsui, M., Nakanishi, H. and Miyagishima, S.-Y. (2009) 'The PLASTID DIVISION1 and 2 components of the chloroplast division machinery determine the rate of chloroplast division in land plant cell differentiation', *The Plant Cell*, 21(6), pp. 1769–1783. https://doi.org/10.1105/tpc.109.067785

Orr, D.J., Alcântara, A., Kapralov, M.V., Andralojc, P.J., Carmo-Silva, E. and Parry, M.A.J. (2016) 'Surveying Rubisco diversity and temperature response to improve crop photosynthetic efficiency', *Plant Physiology*, 172(2), pp. 707–717. https://doi.org/10.1104/pp.16.00750

Osteryoung, K.W., Stokes, K.D., Rutherford, S.M., Percival, A.L. and Lee, W.Y. (1998) 'Chloroplast division in higher plants requires members of two functionally divergent gene families with homology to bacterial ftsZ', *The Plant Cell*, 10(12), pp. 1991–2004. https://doi.org/10.1105/tpc.10.12.1991

Pajuelo, E., Carrasco, J.A., Flores-Duarte, N.J., Rodríguez-Llorente, I.D., Mesa-Marín, J., Mateos-Naranjo, E., Redondo-Gómez, S. and Navarro-Torre, S. (2023) 'Designing tailored bioinoculants for sustainable agrobiology in multi-stressed environments', in Egamberdieva, D. and Ahmad, P. (eds.) *Microorganisms for Sustainability*, 43, pp. 359–397. https://doi.org/10.1007/978-981-19-9570-5_16

Pan, Y., Bradley, G., Pyke, K., Ball, G., Lu, C., Fray, R., Marshall, A., Jayasuta, S., Baxter, C., van Wijk, R., Boyden, L., Cade, R., Chapman, N.H., Fraser, P.D., Hodgman, C. and Seymour, G.B. (2013) 'Network inference analysis identifies an APRR2-like gene linked to pigment accumulation in tomato and pepper fruits', *Plant Physiology*, 161(3), pp. 1476–1485. https://doi.org/10.1104/pp.112.212654

Pařenicová, L., De Folter, S., Kieffer, M., Horner, D.S., Favalli, C., Busscher, J., Cook, H.E., Ingram, R.M., Kater, M.M., Davies, B., Angenent, G.C. and Colombo, L. (2003) 'Molecular and phylogenetic analyses of the complete MADS-box transcription factor family in *Arabidopsis*: new openings to the MADS world', *The Plant Cell*, 15(7), pp. 1538–1551. https://doi.org/10.1105/tpc.011544

Park, S., Kim, H.S., Jung, Y.J., Kim, S.H., Ji, C.Y., Wang, Z., Jeong, J.C., Lee, H.S., Lee, S.Y. and Kwak, S.S. (2016) 'Orange protein has a role in phytoene synthase stabilization in sweetpotato', *Scientific Reports*, 6(1), Article 33563. https://doi.org/10.1038/srep33563

Parry, M.A.J., Andralojc, P.J., Scales, J.C., Salvucci, M.E., Carmo-Silva, A.E., Alonso, H. and Whitney, S.M. (2013) 'Rubisco activity and regulation as targets for crop improvement', *Journal of Experimental Botany*, 64(3), pp. 717–730. https://doi.org/10.1093/jxb/ers336

Pawar, B.D., Jadhav, A.S., Kale, A.A., Chimote, V.P. and Pawar, S.V. (2013) 'Effect of explants, bacterial cell density and overgrowth-control antibiotics on transformation efficiency in tomato (*Solanum lycopersicum* L.)', *Journal of Applied Horticulture*, 15(2), pp. 95–99.

Pecker, I., Gabbay, R., Cunningham, F.X. and Hirschberg, J. (1996) 'Cloning and characterization of the cDNA for lycopene β-cyclase from tomato reveals decrease in its expression during fruit ripening', *Plant Molecular Biology*, 30(4), pp. 807–819. https://doi.org/10.1007/BF00019013

Pei, Y., He, X., Xue, Q., Deng, H., Xu, W., Yang, C., Wu, M., Wang, W., Tang, W., Niu, W., Huang, Y., Gong, R., Bouzayen, M., Hong, Y. and Liu, M. (2025) 'The bifunctional transcription factor DEAR1 oppositely regulates chlorophyll biosynthesis and degradation in tomato fruits', *The Plant Cell*, 37(7), Article koaf167. https://doi.org/10.1093/plcell/koaf167

Perrine, Z., Negi, S. and Sayre, R.T. (2012) 'Optimization of photosynthetic light energy utilization by microalgae', *Algal Research*, 1(2), pp. 134–142. https://doi.org/10.1016/j.algal.2012.07.002

Petrillo, E., Godoy Herz, M.A., Fuchs, A., Reifer, D., Fuller, J., Yanovsky, M.J., Simpson, C., Brown, J.W., Barta, A., Kalyna, M. and Kornblihtt, A.R. (2014) 'A chloroplast retrograde signal regulates nuclear alternative splicing', *Science*, 344(6182), pp. 424–427. https://doi.org/10.1126/science.1247003

Piechulla, B., Glick, R.E., Bahl, H., Melis, A. and Gruissem, W. (1987) 'Changes in photosynthetic capacity and photosynthetic protein composition during tomato fruit development', *Plant Physiology*, 84(3), pp. 911–917. https://doi.org/10.1104/pp.84.3.911

Poorter, H., Fiorani, F., Pieruschka, R., Wojciechowski, T., van der Putten, W.H., Kleyer, M., Schurr, U. and Postma, J. (2016) 'Pampered inside, pestered outside? Differences and similarities between plants growing in controlled conditions and in the field', *New Phytologist*, 212(4), pp. 838–855. https://doi.org/10.1111/nph.14243

Porra, R.J., Thompson, W.A. and Kriedemann, P.E. (1989) 'Determination of accurate extinction coefficients and simultaneous equations for assaying chlorophylls a and b extracted with four different solvents: verification of the concentration of chlorophyll standards by atomic absorption spectroscopy', *Biochimica et Biophysica Acta (BBA) – Bioenergetics*, 975(3), pp. 384–394. https://doi.org/10.1016/S0005-2728(89)80347-0

Powell, A.L.T., Nguyen, C.V., Hill, T., Cheng, K.L.L., Figueroa-Balderas, R., Aktas, H., Ashrafi, H., Pons, C., Fernández-Muñoz, R., Vicente, A., Lopez-Baltazar, J., Barry, C.S., Liu, Y., Chetelat, R., Granell, A., Van Deynze, A., Giovannoni, J.J. and Bennett, A.B. (2012) 'Uniform ripening encodes a Golden 2-like transcription factor regulating tomato fruit chloroplast development', *Science*, 336(6089), pp. 1711–1715. https://doi.org/10.1126/science.1222218

Pyke, K. (2007) 'Plastid biogenesis and differentiation', in Bock, R. (ed.) *Topics in Current Genetics*, 19, pp. 1–28. https://doi.org/10.1007/4735_2007_0226

Pyke, K. (2011) 'Analysis of plastid number, size, and distribution in *Arabidopsis* plants by light and fluorescence microscopy', in Maliga, P. (ed.) *Methods in Molecular Biology*, 774, pp. 19–32. https://doi.org/10.1007/978-1-61779-234-2_2

Pyke, K.A. (1999) 'Plastid division and development', *The Plant Cell*, 11(4), pp. 549–556. https://doi.org/10.1105/tpc.11.4.549

Pyke, K.A. and Leech, R.M. (1991) 'Rapid image analysis screening procedure for identifying chloroplast number mutants in mesophyll cells of *Arabidopsis thaliana* (L.) Heynh.', *Plant Physiology*, 96(4), pp. 1193–1195. https://doi.org/10.1104/pp.96.4.1193

Pyke, K.A. and Leech, R.M. (1992) 'Chloroplast division and expansion is radically altered by nuclear mutations in *Arabidopsis thaliana*', *Plant Physiology*, 99(3), pp. 1005–1008. https://doi.org/10.1104/pp.99.3.1005

Pyke, K.A., Rutherford, S.M., Robertson, E.J. and Leech, R.M. (1994) 'arc6, a fertile *Arabidopsis* mutant with only two mesophyll cell chloroplasts', *Plant Physiology*, 106(3), pp. 1169–1177. https://doi.org/10.1104/pp.106.3.1169

Qiu, D., Ma, J. and Liu, T. (2015) 'Optimization of *Agrobacterium*-mediated transformation conditions for tomato (*Solanum lycopersicum* L.)', *Plant Omics Journal*, 8(6), pp. 460–467.

Qu, G.Z., Zheng, T., Liu, G., Wang, W., Zang, L., Liu, H. and Yang, C. (2013) 'Overexpression of a MADS-box gene from birch (*Betula platyphylla*) promotes flowering and enhances chloroplast development in transgenic tobacco', *PLoS ONE*, 8(5), Article e63398. https://doi.org/10.1371/journal.pone.0063398

Quinet, M., Angosto, T., Yuste-Lisbona, F.J., Blanchard-Gros, R., Bigot, S., Martinez, J.P. and Lutts, S. (2019) 'Tomato fruit development and metabolism', *Frontiers in Plant Science*, 10, Article 1554. https://doi.org/10.3389/fpls.2019.01554

Raines, C.A. (2003) 'The Calvin cycle revisited', *Photosynthesis Research*, 75(1), pp. 1–10. https://doi.org/10.1023/A:1022421515027

Rajeevkumar, S., Anunanthini, P. and Sathishkumar, R. (2015) 'Epigenetic silencing in transgenic plants', *Frontiers in Plant Science*, 6, Article 693. https://doi.org/10.3389/fpls.2015.00693

Ralley, L., Schuch, W., Fraser, P.D. and Bramley, P.M. (2016) 'Genetic modification of tomato with the tobacco lycopene β-cyclase gene produces high β-carotene and lycopene fruit', *Zeitschrift für Naturforschung C*, 71(9–10), pp. 295–301. https://doi.org/10.1515/znc-2016-0102

Ramankutty, N., Mehrabi, Z., Waha, K., Jarvis, L., Kremen, C., Herrero, M. and Rieseberg, L.H. (2018) 'Trends in global agricultural land use: implications for environmental health and food security', *Annual Review of Plant Biology*, 69, pp. 789–815. https://doi.org/10.1146/annurev-arplant-042817-040256

Rangani, J., Kumari, A., Patel, M., Brahmbhatt, H. and Parida, A.K. (2019) 'Phytochemical profiling, polyphenol composition, and antioxidant activity of the leaf extract from the medicinal halophyte *Thespesia populnea* reveal a potential source of bioactive compounds and nutraceuticals', *Journal of Food Biochemistry*, 43(2), Article e12731. https://doi.org/10.1111/jfbc.12731

Ray, D.K., Mueller, N.D., West, P.C. and Foley, J.A. (2013) 'Yield trends are insufficient to double global crop production by 2050', *PLoS ONE*, 8(6), Article e66428. https://doi.org/10.1371/journal.pone.0066428

Riechmann, J.L. and Meyerowitz, E.M. (1997) 'MADS domain proteins in plant development', *Biological Chemistry*, 378(10), pp. 1079–1101.

Rodríguez-Concepción, M. and Boronat, A. (2002) 'Elucidation of the methylerythritol phosphate pathway for isoprenoid biosynthesis in bacteria and plastids: a metabolic milestone achieved through genomics', *Plant Physiology*, 130(3), pp. 1079–1089. https://doi.org/10.1104/pp.007138

Römer, S., Fraser, P.D., Kiano, J.W., Shipton, C.A., Misawa, N., Schuch, W. and Bramley, P.M. (2000) 'Elevation of the provitamin A content of transgenic tomato plants', *Nature Biotechnology*, 18(6), pp. 666–669. https://doi.org/10.1038/76523

Ruuska, S.A., Schwender, J. and Ohlrogge, J.B. (2004) 'The capacity of green oilseeds to utilize photosynthesis to drive biosynthetic processes', *Plant Physiology*, 136(1), pp. 2700–2709. https://doi.org/10.1104/pp.104.047977

Sagar, M., Chervin, C., Mila, I., Hao, Y., Roustan, J.P., Benichou, M., Gibon, Y., Biais, B., Maury, P., Latché, A., Pech, J.C., Bouzayen, M. and Zouine, M. (2013) '*SlARF4*, an auxin response factor involved in the control of sugar metabolism during tomato fruit development', *Plant Physiology*, 161(3), pp. 1362–1374. https://doi.org/10.1104/pp.113.213843

Sakamoto, W., Miyagishima, S. and Jarvis, P. (2008) 'Chloroplast biogenesis: control of plastid development, protein import, division and inheritance', *The Arabidopsis Book*, 6, Article e0110. https://doi.org/10.1199/tab.0110

Sambrook, J. and Russell, D.W. (2001) *Molecular cloning: a laboratory manual*. 3rd edn. Cold Spring Harbor, NY: Cold Spring Harbor Laboratory Press.

Sánchez, C., Fischer, G. and Sanjuanelo, D.W. (2013) 'Stomatal behavior in fruits and leaves of the purple passion fruit (*Passiflora edulis* Sims) and fruits and cladodes of the yellow pitaya [*Hylocereus megalanthus* (K. Schum. ex Vaupel) Ralf Bauer]', *Agronomía Colombiana*, 31, pp. 38–47.

Santino, C.G., Stanford, G.L. and Conner, T.W. (1997) 'Developmental and transgenic analysis of two tomato fruit enhanced genes', *Plant Molecular Biology*, 33(2), pp. 405–416. https://doi.org/10.1023/A:1005770319014

Sarker, R.H., Islam, K. and Hoque, M.I. (2009) 'In vitro regeneration and *Agrobacterium*-mediated genetic transformation of tomato (*Lycopersicon esculentum* Mill.)', *Plant Tissue Culture and Biotechnology*, 19(1), pp. 101–111.

Sauer, K. (1978) ‘Photosynthetic membranes’, *Accounts of Chemical Research*, 11(7), pp. 257–264. https://doi.org/10.1021/ar50127a003

Scarpeci, T.E., Marro, M.L., Bortolotti, S., Boggio, S.B. and Valle, E.M. (2007) ‘Plant nutritional status modulates glutamine synthetase levels in ripe tomatoes (*Solanum lycopersicum* cv. Micro-Tom)’, *Journal of Plant Physiology*, 164(2), pp. 137–145. https://doi.org/10.1016/j.jplph.2006.01.003

Schauberger, B., Ben-Ari, T., Makowski, D., Kato, T., Kato, H. and Ciais, P. (2018) ‘Yield trends, variability and stagnation analysis of major crops in France over more than a century’, *Scientific Reports*, 8(1), Article 16865. https://doi.org/10.1038/s41598-018-35351-1

Senge, M.O., Ryan, A.A., Letchford, K.A., MacGowan, S.A. and Mielke, T. (2014) ‘Chlorophylls, symmetry, chirality, and photosynthesis’, *Symmetry*, 6(3), pp. 781–843. https://doi.org/10.3390/sym6030781

Seymour, G.B., Chapman, N.H., Chew, B.L. and Rose, J.K.C. (2013) ‘Regulation of ripening and opportunities for control in tomato and other fruits’, *Plant Biotechnology Journal*, 11(3), pp. 269–278. https://doi.org/10.1111/j.1467-7652.2012.00738.x

Sharkey, T.D. (2019) ‘Discovery of the canonical Calvin–Benson cycle’, *Photosynthesis Research*, 140(2), pp. 235–252. https://doi.org/10.1007/s11120-018-0600-2

Sharma, P., Aggarwal, P. and Kaur, A. (2017) ‘Biofortification: a new approach to eradicate hidden hunger’, *Food Reviews International*, 33(1), pp. 1–21. https://doi.org/10.1080/87559129.2015.1137309

Shi, Y., Pang, X., Liu, W., Wang, R., Su, D., Gao, Y., Wu, M., Deng, W., Liu, Y. and Li, Z. (2021) ‘*SlZHD17* is involved in the control of chlorophyll and carotenoid metabolism in tomato fruit’, *Horticulture Research*, 8(1), Article 196. https://doi.org/10.1038/s41438-021-00696-8

Shikata, M. and Ezura, H. (2016) ‘Micro-Tom tomato as an alternative plant model system: mutant collection and efficient transformation’, in Ezura, H., Ariizumi, T. and García-Mas, J. (eds.) *Methods in Molecular Biology*, 1363, pp. 47–55. https://doi.org/10.1007/978-1-4939-3115-6_5

Shore, P. and Sharrocks, A.D. (1995) ‘The MADS-box family of transcription factors’, *European Journal of Biochemistry*, 229(1), pp. 1–13. https://doi.org/10.1111/j.1432-1033.1995.tb20430.x

Simkin, A.J. (2019) ‘Genetic engineering for global food security: photosynthesis and biofortification’, *Plants*, 8(12), Article 586. https://doi.org/10.3390/plants8120586

Simkin, A.J. (2021) ‘Carotenoids and apocarotenoids in planta: their role in plant development, contribution to the flavour and aroma of fruits and flowers, and their nutraceutical benefits’, *Plants*, 10(11), Article 2321. https://doi.org/10.3390/plants10112321

Simkin, A.J., Faralli, M., Ramamoorthy, S. and Lawson, T. (2020) ‘Photosynthesis in non-foliar tissues: implications for yield’, *The Plant Journal*, 101(4), pp. 1001–1015. https://doi.org/10.1111/tpj.14633

Simkin, A.J., Kapoor, L., Doss, C.G.P., Hofmann, T.A., Lawson, T. and Ramamoorthy, S. (2022) ‘The role of photosynthesis-related pigments in light harvesting, photoprotection and enhancement of photosynthetic yield in planta’, *Photosynthesis Research*, 152(1), pp. 23–42. https://doi.org/10.1007/s11120-021-00892-6

Simkin, A.J., López-Calcagno, P.E. and Raines, C.A. (2019) ‘Feeding the world: improving photosynthetic efficiency for sustainable crop production’, *Journal of Experimental Botany*, 70(4), pp. 1119–1140. https://doi.org/10.1093/jxb/ery445

Simkin, A.J., McAusland, L., Headland, L.R., Lawson, T. and Raines, C.A. (2015) ‘Multigene manipulation of photosynthetic carbon assimilation increases CO_2 fixation and biomass yield in tobacco’, *Journal of Experimental Botany*, 66(13), pp. 4075–4090. https://doi.org/10.1093/jxb/erv204

Simkin, A.J., McAusland, L., Lawson, T. and Raines, C.A. (2017) ‘Overexpression of the Rieske FeS protein increases electron transport rates and biomass yield’, *Plant Physiology*, 175(1), pp. 134–145. https://doi.org/10.1104/pp.17.00622

Smil, V. (2001) *Feeding the world: a challenge for the twenty-first century*. Cambridge, MA: MIT Press.

Smillie, R.M. (1992) ‘Calvin cycle activity in fruit and the effect of heat stress’, *Scientia Horticulturae*, 51(1–2), pp. 83–95. https://doi.org/10.1016/0304-4238(92)90133-F

Smillie, R.M., Hetherington, S.E. and Davies, W.J. (1999) ‘Photosynthetic activity of the calyx, green shoulder, pericarp, and locular parenchyma of tomato fruit’, *Journal of Experimental Botany*, 50(334), pp. 707–718. https://doi.org/10.1093/jxb/50.334.707

Smirnova, O.G. and Kochetov, A.V. (2020) 'Choice of the promoter for tissue- and developmental stage-specific gene expression', in Orzaez, D. and Granell, A. (eds.) *Methods in Molecular Biology*, 2124, pp. 69–106. https://doi.org/10.1007/978-1-0716-0356-7_4

Steinhauser, M.C., Steinhauser, D., Koehl, K., Carrari, F., Gibon, Y., Fernie, A.R. and Stitt, M. (2010) 'Enzyme activity profiles during fruit development in tomato cultivars and *Solanum pennellii*', *Plant Physiology*, 153(1), pp. 80–98. https://doi.org/10.1104/pp.110.154336

Stephenson, P.G., Fankhauser, C. and Terry, M.J. (2009) 'PIF3 is a repressor of chloroplast development', *Proceedings of the National Academy of Sciences of the United States of America*, 106(18), pp. 7654–7659. https://doi.org/10.1073/pnas.0811684106

Sudhakar, K. and Mamat, R. (2019) 'Artificial leaves: towards bio-inspired solar energy converters', in Sayigh, A. (ed.) *Comprehensive Renewable Energy*. Amsterdam: Elsevier. https://doi.org/10.1016/B978-0-12-409548-9.11799-3

Sun, A.Z. and Guo, F.Q. (2016) 'Chloroplast retrograde regulation of heat stress responses in plants', *Frontiers in Plant Science*, 7, Article 398. https://doi.org/10.3389/fpls.2016.00398

Sun, B., Zhang, Q.Y., Yuan, H., Gao, W., Han, B. and Zhang, M. (2020) 'PDV1 and PDV2 differentially affect remodeling and assembly of the chloroplast DRP5B RING1 complex', *Plant Physiology*, 182(4), pp. 1966–1978. https://doi.org/10.1104/pp.19.01490

Sun, H.J., Uchii, S., Watanabe, S. and Ezura, H. (2006) 'A highly efficient transformation protocol for Micro-Tom, a model cultivar for tomato functional genomics', *Plant and Cell Physiology*, 47(3), pp. 426–431. https://doi.org/10.1093/pcp/pci251

Sun, T. (2010) 'Gibberellin–GID1–DELLA: a pivotal regulatory module for plant growth and development', *Plant Physiology*, 154(2), pp. 567–570. https://doi.org/10.1104/pp.110.161554

Sun, T., Yuan, H., Cao, H., Yazdani, M., Tadmor, Y. and Li, L. (2018) 'Carotenoid metabolism in plants: the role of plastids', *Molecular Plant*, 11(1), pp. 58–74. https://doi.org/10.1016/j.molp.2017.09.010

Taiz, L., Zeiger, E., Møller, I.M. and Murphy, A. (2015) *Plant physiology and development*. 6th edn. Sunderland, MA: Sinauer Associates.

Takahashi, S. and Badger, M.R. (2011) ‘Photoprotection in plants: a new light on photosystem II damage’, *Trends in Plant Science*, 16(1), pp. 53–60. https://doi.org/10.1016/j.tplants.2010.10.001

Takei, K., Sakakibara, H., Taniguchi, M. and Sugiyama, T. (2001) ‘Nitrogen-dependent accumulation of cytokinins in root and the translocation to leaf: implication of cytokinin species that induces gene expression of maize response regulator’, *Plant and Cell Physiology*, 42(1), pp. 85–93. https://doi.org/10.1093/pcp/pce009

Tanaka, A., Fujita, K. and Kikuchi, K. (1974) ‘Nutrio-physiological studies on the tomato plant III. Photosynthetic rate of individual leaves in relation to the dry matter production of plants’, *Soil Science and Plant Nutrition*, 20(2), pp. 173–183. https://doi.org/10.1080/00380768.1974.10433240

Taub, D.R. and Wang, X. (2008) ‘Why are nitrogen concentrations in plant tissues lower under elevated CO_2? A critical examination of the hypotheses’, *Journal of Integrative Plant Biology*, 50(11), pp. 1365–1374. https://doi.org/10.1111/j.1744-7909.2008.00754.x

The Tomato Genome Consortium (2012) ‘The tomato genome sequence provides insights into fleshy fruit evolution’, *Nature*, 485(7400), pp. 635–641. https://doi.org/10.1038/nature11119

Tigchelaar, E.C., McGlasson, W.B. and Buescher, R.W. (1978) ‘Genetic regulation of tomato fruit ripening’, *HortScience*, 13(5), pp. 508–513. https://doi.org/10.21273/hortsci.13.5.508

Tilman, D., Cassman, K.G., Matson, P.A., Naylor, R. and Polasky, S. (2002) ‘Agricultural sustainability and intensive production practices’, *Nature*, 418(6898), pp. 671–677. https://doi.org/10.1038/nature01014

Tiwari, J.K., Singh, A.K. and Behera, T.K. (2023) ‘CRISPR/Cas genome editing in tomato improvement: advances and applications’, *Frontiers in Plant Science*, 14, Article 1121209. https://doi.org/10.3389/fpls.2023.1121209

United Nations (2019) *World population prospects 2019: data booklet*. New York: United Nations. Available at: https://www.un.org/development/desa/pd/content/world-population-prospects-2019-data-booklet (Accessed: 26 January 2026).

Verma, V. (2022) ‘Global status of genetically modified crops’, in [Editor(s) unknown] (eds.) *Agricultural biotechnology: latest research and trends*, pp. 305–322.

Vogg, G., Fischer, S., Leide, J., Emmanuel, E., Jetter, R., Levy, A.A. and Riederer, M. (2004) 'Tomato fruit cuticular waxes and their effects on transpiration barrier properties: functional characterization of a mutant deficient in a very-long-chain fatty acid β-ketoacyl-CoA synthase', *Journal of Experimental Botany*, 55(401), pp. 1401–1410. https://doi.org/10.1093/jxb/erh149

Vrebalov, J., Pan, I.L., Arroyo, A.J.M., McQuinn, R., Chung, M., Poole, M., Rose, J., Seymour, G., Grandillo, S., Giovannoni, J. and Irish, V.F. (2009) 'Fleshy fruit expansion and ripening are regulated by the tomato SHATTERPROOF gene TAGL1', *The Plant Cell*, 21(10), pp. 3041–3062. https://doi.org/10.1105/tpc.109.066936

Vrebalov, J., Ruezinsky, D., Padmanabhan, V., White, R., Medrano, D., Drake, R., Schuch, W. and Giovannoni, J. (2002) 'A MADS-box gene necessary for fruit ripening at the tomato ripening-inhibitor (rin) locus', *Science*, 296(5566), pp. 343–346. https://doi.org/10.1126/science.1068181

Walsh, C.A., Lundgren, M.R. and Lundgren, C.R.M. (2024) 'Nutritional quality of photosynthetically diverse crops under future climates', *Plants, People, Planet*, 6(6), pp. 1272–1283. https://doi.org/10.1002/ppp3.10544

Wang, H., Schauer, N., Usadel, B., Frasse, P., Zouine, M., Hernould, M., Latché, A., Pech, J.C., Fernie, A.R. and Bouzayen, M. (2009) 'Regulatory features underlying pollination-dependent and independent tomato fruit set revealed by transcript and primary metabolite profiling', *The Plant Cell*, 21(5), pp. 1428–1452. https://doi.org/10.1105/tpc.108.060830

Wang, Q., Zhang, Q.D., Zhu, X.G., Lu, C.M., Kuang, T.Y. and Li, C.Q. (2002) 'PSII photochemistry and xanthophyll cycle in two super-high-yield rice hybrids, Liangyoupeijiu and Hua-an 3 during photoinhibition and subsequent restoration', *Acta Botanica Sinica*, 44, pp. 1297–1302.

Wang, S., Liu, J., Feng, Y., Niu, X., Giovannoni, J. and Liu, Y. (2008) 'Altered plastid levels and potential for improved fruit nutrient content by downregulation of the tomato DDB1-interacting protein CUL4', *The Plant Journal*, 55(1), pp. 89–103. https://doi.org/10.1111/j.1365-313x.2008.03489.x

Wang, S., Lu, G., Hou, Z., Luo, Z., Wang, T., Li, H., Zhang, J. and Ye, Z. (2014) 'Members of the tomato FRUITFULL MADS-box family regulate style abscission and fruit ripening', *Journal of Experimental Botany*, 65(12), pp. 3005–3014. https://doi.org/10.1093/jxb/eru137

Wang, T., Zhang, H. and Zhu, H. (2019) ‘CRISPR technology is revolutionizing the improvement of tomato and other fruit crops’, *Horticulture Research*, 6(1), Article 77. https://doi.org/10.1038/s41438-019-0159-x

Wang, Y., Tian, C., Na, Q., Zhu, C., Cao, H., Zhang, M. and Meng, L. (2024) ‘The role of *SlCHRC* in carotenoid biosynthesis and plastid development in tomato fruit’, *International Journal of Biological Macromolecules*, 281, Article 136354. https://doi.org/10.1016/j.ijbiomac.2024.136354

Wang, Z., Shen, Y., Yang, X., Pan, Q., Ma, G., Bao, M., Zheng, B., Duanmu, D., Lin, R., Larkin, R.M. and Ning, G. (2019) ‘Overexpression of particular MADS-box transcription factors in heat-stressed plants induces chloroplast biogenesis in petals’, *Plant, Cell and Environment*, 42(5), pp. 1545–1560. https://doi.org/10.1111/pce.13472

Weber, E., Engler, C., Gruetzner, R., Werner, S. and Marillonnet, S. (2011) ‘A modular cloning system for standardized assembly of multigene constructs’, *PLoS ONE*, 6(2), Article e16765. https://doi.org/10.1371/journal.pone.0016765

Weise, S.E., Carr, D.J., Bourke, A.M., Hanson, D.T., Swarthout, D. and Sharkey, T.D. (2015) ‘The arc mutants of *Arabidopsis* with fewer large chloroplasts have a lower mesophyll conductance’, *Photosynthesis Research*, 124(1), pp. 117–126. https://doi.org/10.1007/s11120-015-0110-4

Wieczorek, P., Wrzesińska, B. and Obrepalska-Steplowska, A. (2013) ‘Assessment of reference gene stability influenced by extremely divergent disease symptoms in *Solanum lycopersicum* L.’, *Journal of Virological Methods*, 194(1–2), pp. 161–168. https://doi.org/10.1016/j.jviromet.2013.08.010

Williams, K., Koch, G.W. and Mooney, H.A. (1985) ‘The carbon balance of flowers of *Diplacus aurantiacus* (Scrophulariaceae)’, *Oecologia*, 66(4), pp. 530–535. https://doi.org/10.1007/BF00379333

Willmer, C.M. and Johnston, W.R. (1976) ‘Carbon dioxide assimilation in some aerial plant organs and tissues’, *Planta*, 130(1), pp. 33–37. https://doi.org/10.1007/BF00390841

Wilson, R.H., Martin-Avila, E., Conlan, C. and Whitney, S.M. (2018) ‘An improved *Escherichia coli* screen for Rubisco identifies a protein–protein interface that can enhance CO_2-fixation

kinetics', *Journal of Biological Chemistry*, 293(1), pp. 18–27. https://doi.org/10.1074/jbc.M117.810861

Wohlfahrt, Y., Smith, J.P., Tittmann, S., Honermeier, B. and Stoll, M. (2018) 'Primary productivity and physiological responses of *Vitis vinifera* L. cvs. under free-air carbon dioxide enrichment (FACE)', *European Journal of Agronomy*, 101, pp. 149–162. https://doi.org/10.1016/j.eja.2018.09.005

Wu, M., Xu, X., Hu, X., Liu, Y., Cao, H., Chan, H., Gong, Z., Yuan, Y., Luo, Y., Feng, B., Li, Z. and Deng, W. (2020) '*SlMYB72* regulates the metabolism of chlorophylls, carotenoids, and flavonoids in tomato fruit', *Plant Physiology*, 183(3), pp. 854–868. https://doi.org/10.1104/pp.20.00156

Xiong, D., Huang, J., Peng, S. and Li, Y. (2017) 'A few enlarged chloroplasts are less efficient in photosynthesis than a large population of small chloroplasts in *Arabidopsis thaliana*', *Scientific Reports*, 7(1), Article 5782. https://doi.org/10.1038/s41598-017-06460-0

Yamori, W. (2016) 'Photosynthetic response to fluctuating environments and photoprotective strategies under abiotic stress', *Journal of Plant Research*, 129(3), pp. 379–395. https://doi.org/10.1007/s10265-016-0816-1

Yamori, W., Evans, J.R. and von Caemmerer, S. (2010) 'Effects of growth and measurement light intensities on temperature dependence of CO_2 assimilation rate in tobacco leaves', *Plant, Cell and Environment*, 33(3), pp. 332–343. https://doi.org/10.1111/j.1365-3040.2009.02067.x

Yang, Y., Tilman, D., Jin, Z., Smith, P., Barrett, C.B., Zhu, Y.G., Burney, J., D'Odorico, P., Fantke, P., Fargione, J., Finlay, J.C., Rulli, M.C., Sloat, L., van Groenigen, K.J., West, P.C., Ziska, L., Michalak, A.M., Lobell, D.B., Clark, M. and Zhuang, M. (2024) 'Climate change exacerbates the environmental impacts of agriculture', *Science*, 385(6713), Article eadn3747. https://doi.org/10.1126/science.adn3747

Yazdani, M., Sun, Z., Yuan, H., Zeng, S., Thannhauser, T.W., Vrebalov, J., Ma, Q., Xu, Y., Fei, Z., Van Eck, J., Tian, S., Tadmor, Y., Giovannoni, J.J. and Li, L. (2019) 'Ectopic expression of ORANGE promotes carotenoid accumulation and fruit development in tomato', *Plant Biotechnology Journal*, 17(1), pp. 33–49. https://doi.org/10.1111/pbi.12945

Yu, Q.H., Wang, B., Li, N., Tang, Y., Yang, S., Yang, T., Xu, J., Guo, C., Yan, P., Wang, Q. and Asmutola, P. (2017) 'CRISPR/Cas9-induced targeted mutagenesis and gene replacement to generate long-shelf life tomato lines', *Scientific Reports*, 7(1), Article 11874. https://doi.org/10.1038/s41598-017-12262-1

Zhang, C., Liu, J., Zhang, Y., Cai, X., Gong, P., Zhang, J., Wang, T., Li, H. and Ye, Z. (2011) 'Overexpression of *SlGMEs* leads to ascorbate accumulation with enhanced oxidative stress, cold, and salt tolerance in tomato', *Plant Cell Reports*, 30(3), pp. 389–398. https://doi.org/10.1007/s00299-010-0939-0

Zhang, M., Schmitz, A.J., Kadirjan-Kalbach, D.K., TerBush, A.D. and Osteryoung, K.W. (2013) 'Chloroplast division protein ARC3 regulates chloroplast FtsZ-ring assembly and positioning in *Arabidopsis* through interaction with FtsZ2', *The Plant Cell*, 25(5), pp. 1787–1802. https://doi.org/10.1105/tpc.113.111047

Zhang, Z., Zou, W., Lin, P., Wang, Z., Chen, Y., Yang, X., Zhao, W., Zhang, Y., Wang, D., Que, Y. and Wu, Q. (2024) 'Evolution and function of MADS-box transcription factors in plants', *International Journal of Molecular Sciences*, 25(24), Article 13278. https://doi.org/10.3390/ijms252413278

Zhong, C., Jian, S.F., Huang, J., Jin, Q.Y. and Cao, X.C. (2019) 'Trade-off of within-leaf nitrogen allocation between photosynthetic nitrogen-use efficiency and water deficit stress acclimation in rice (*Oryza sativa* L.)', *Plant Physiology and Biochemistry*, 135, pp. 41–50. https://doi.org/10.1016/j.plaphy.2018.11.021

Zhu, X.G., Long, S.P. and Ort, D.R. (2010) 'Improving photosynthetic efficiency for greater yield', *Annual Review of Plant Biology*, 61, pp. 235–261. https://doi.org/10.1146/annurev-arplant-042809-112206